

The “ β -cell Hippo pathway” under physiological and pathological conditions

Dissertation

zur Erlangung des Grades eines Doktors der Naturwissenschaften im
Fachbereich Biologie/Chemie der Universität Bremen

vorgelegt von

Karthika Annamalai , M.Sc.

Bremen, 25.02.2021

Datum des Dissertationskolloquiums: 12. April 2021 14:00 Uhr

1. Gutachter: Prof. Dr. Kathrin Maedler

2. Gutachter: Prof. Dr. Cristina Aguayo-Mazzucato

Versicherung an Eides Statt

Ich, Karthika Annamalai,

versichere an Eides Statt durch meine Unterschrift, dass ich die vorstehende Arbeit selbständig und ohne fremde Hilfe angefertigt und alle Stellen, die ich wörtlich dem Sinne nach aus Veröffentlichungen entnommen habe, als solche kenntlich gemacht habe, mich auch keiner anderen als der angegebenen Literatur oder sonstiger Hilfsmittel bedient habe.

Ich versichere an Eides Statt, dass ich die vorgenannten Angaben nach bestem Wissen und Gewissen gemacht habe und dass die Angaben der Wahrheit entsprechen und ich nichts verschwiegen habe.

Die Strafbarkeit einer falschen eidesstattlichen Versicherung ist mir bekannt, namentlich die Strafandrohung gemäß § 156 StGB bis zu drei Jahren Freiheitsstrafe oder Geldstrafe bei vorsätzlicher Begehung der Tat bzw. gemäß § 161 Abs. 1 StGB bis zu einem Jahr Freiheitsstrafe oder Geldstrafe bei fahrlässiger Begehung.

Ort, Datum Unterschrift

I SUMMARY

Diabetes mellitus is a complex metabolic disorder characterized by insulin deficiency, typically resulting from an inadequate dysfunctional β -cell mass. One of the major hallmarks for the tremendous decline in the functional β -cell mass is β -cell apoptosis, namely the loss of β -cell through apoptotic cell death.

The Hippo signaling pathway is a prominent regulator of organ size and tissue homeostasis which is indispensable for the regulation of both β -cell dysfunction and apoptosis. My lab identified that the core component of the Hippo pathway, mammalian sterile 20-like 1 (MST1) kinase, is chronically activated in human and rodent β -cells under multiple experimental models of diabetes as well as in pathological specimen. Genetic inhibition of MST1 restored β -cell viability and function. Consequently, MST1 inhibition could be a promising approach for β -cell protective therapy in diabetes.

In the first part of my thesis, I showed that neratinib, a well-known irreversible pan-HER/EGFR tyrosine kinase inhibitor, could potently inhibit MST1, its downstream signaling and subsequent apoptosis in β -cells under diabetogenic conditions and also restored functional β -cell mass in models of both autoimmune associated type 1 diabetes and obesity associated type 2 diabetes.

In the second part, I investigated the downstream target of MST1, namely the large tumor suppressor homolog 1/2 (LATS1/2) kinase in the regulation of stress-responsive signaling pathways and β -cell apoptosis. Endogenous LATS1/2 activity was highly upregulated in β -cells/islets under diabetic conditions. LATS2 deficiency in both isolated rodent and human islets was sufficient to rescue β -cells from apoptosis. Moreover, *in vivo* data revealed the potential β -cell protective phenotype of β -cell specific LATS2-KO mice (β -LATS2-KO) during high fat/ high sugar-induced β -cell decompensation and failure as well as in a model of severe β -cell destruction.

Mechanistically, I determined the mutual crosstalk between Hippo-LATS2, mTORC1 and the intracellular recycling system of autophagy. LATS2 worked upstream of mTORC1 in mediating β -cell apoptosis under diabetic conditions and LATS2-induced mTORC1 activation mediated autophagic impairment and exacerbated β -cell apoptosis. My data also show that the macroautophagy machinery regulates LATS2's protein turnover in β -cells at the basal level. Altogether, my work highlights the existence of a bidirectional crosstalk between autophagy and Hippo-LATS2 in pancreatic β -cells.

Hence, targeting the Hippo components MST1 and LATS2 might be a potent therapeutic strategy for β -cell protection in diabetes.

II ZUSAMMENFASSUNG

Diabetes mellitus ist eine komplexe Stoffwechselerkrankung, gekennzeichnet durch einen Mangel an Insulin, der typischerweise aus einem Zusammenspiel unzureichender β -Zellen und deren Dysfunktion resultiert. Eines der Hauptmerkmale für den enormen Rückgang der funktionellen β -Zellmasse ist die β -Zell-Apoptose, also der Verlust der β -Zellen durch Zelltod.

Der Hippo-Signalweg ist ein prominenter Regulator von Organgröße und -homöostase, der sowohl für die Regulation der β -Zelldysfunktion als auch der Apoptose unabdingbar ist. Mein Labor hat herausgefunden, dass die Kernkomponente des Hippo-Signalwegs, die Mammalian sterile 20-like 1 (MST1) Kinase, sowohl in humanen β -Zellen als auch in denen von Mäusen in allen getesteten experimentellen Diabetes-Modellen sowie in pathologischen Diabetes-Proben chronisch aktiviert ist. Die genetische Hemmung von MST1 stellte die Lebensfähigkeit und die Funktion von β -Zellen wieder her. Folglich ist die MST1-Inhibierung ein vielversprechender Ansatz für eine β -Zellschutztherapie im Diabetes.

Im ersten Teil meiner Arbeit habe ich gezeigt, dass Neratinib, ein bereits bekannter irreversibler pan-HER/EGFR-Tyrosinkinase-Inhibitor, MST1, seine nachgeschaltete Signalübertragung und die nachfolgende Apoptose in β -Zellen unter diabetogenen Bedingungen wirksam hemmen kann und auch die funktionelle β -Zellmasse sowohl in Modellen des autoimmunen Typ-1-Diabetes als auch des übergewichtsassoziierten Typ-2-Diabetes wiederherstellt.

Im zweiten Teil untersuchte ich das regulatorische untergeordnete Target von MST1, nämlich die Large Tumorsuppressor-Homolog 1/2 (LATS1/2)-Kinasen und deren Regulation von Stress-Signalwegen und β -Zellapoptose. Genau wie bei MST1, fand ich auch die endogene LATS1/2-Aktivität in β -Zellen und in ganzen Inselzellen unter diabetischen Bedingungen stark hochreguliert. Dabei reichte ein Mangel an LATS2 aus, um β -Zellen vor Apoptose zu retten; sowohl in human Inseln als auch von Mäusen. Darüber hinaus zeigten *in vivo*-Daten den potentiell β -zellschützenden Phänotyp von β -zellspezifischen LATS2-KO-Mäusen (β -LATS2-KO) während Fett- und Zucker-induzierter β -Zelldekompensation und -versagen sowie in Modellen schwerer β -Zellzerstörung.

Mechanistisch identifizierte ich ein Zusammenspiel zwischen Hippo-LATS2, mTORC1 und dem intrazellulären Recyclingsystem, der Autophagie. LATS2 beeinflusst mTORC1 bei der Induktion von β -Zell-Apoptose unter diabetischen Bedingungen: die LATS2-induzierte mTORC1-Aktivierung verhinderte den Regelmechanismus der Autophagie und verstärkte damit die β -Zell-Apoptose. Meine Daten zeigen auch, dass die Makroautophagie den direkten Proteinumsatz von

LATS2 in β -Zellen auf basaler Ebene reguliert. Insgesamt unterstreicht meine Arbeit die Existenz eines bidirektionalen Crosstalks zwischen Autophagie und Hippo-LATS2 in β -Zellen des Pankreas.

Daher könnte eine gezielte Beeinflussung der Hippo-Komponenten MST1 und LATS2 eine wirksame therapeutische Strategie zum Schutz von β -Zellen im Diabetes sein.

III ABBREVIATIONS

ADP	Adenosine diphosphate
AMBRA1	Activating molecule in Beclin 1-regulated autophagy
AMP	Adenosine monophosphate
AMPK	AMP-activated protein kinase
ATP	Adenosine triphosphate
BAK	Bcl-2-antagonist/killer1
BAX	Bcl-2-associated X protein
BCL- _{xL}	B cell lymphoma-extra large
BCL-2	B cell lymphoma 2
BID	BH3 interacting domain death agonist
BIM	Bcl-2 like protein 11
CD8	Cluster of differentiation 8
CRL41	Cullin 4-RING ubiquitin ligase
CUX1	CUT-like homeobox 1
DEPTOR	DEP domain-containing mTOR interacting protein
DPP-4	Dipeptidyl peptidase 4
EF1- α	Elongation factor 1- α
EGFR	Epidermal growth factor receptor
EZH2	Enhancer of zeste homolog 2
FDA	Food and drug administration
FGFR	Fibroblast growth factor receptor
FKBP12	FK506-binding protein 12
FOXP3	Forkhead box P3
GABARAP	Gamma-aminobutyric acid type A receptor-associated protein
GCK	Glucokinase
GFAP	Glial fibrillary acidic protein
GLP-1	Glucagon-like peptide-1
GPCR	G protein-coupled receptors
GSIS	Glucose-stimulated insulin secretion
GSK	Glycogen synthase kinase
GTP	Guanosine triphosphate
H&E	Hematoxylin & Eosin
HER2	Human epidermal growth factor receptor 2
HES1	Hairy and enhancer of split 1
HOPS	Homotypic fusion and protein sorting
INS1-E	Rat Insulinoma cell line INS-1E
IRS 1/2	Insulin receptor substrate 1/2
ITCH / AIP1	Itchy E3 ubiquitin protein ligase
JNK	c-Jun N-terminal kinase
LATS	Large tumor suppressor kinase
LC3	Microtubule-associated protein 1A/1B-light chain 3
LIR	LC3 interacting region
LIMD1	LIM domain containing 1
MAP4K	Mitogen activated protein kinase kinase kinase kinase
MAPK	Mitogen-activated protein kinase
MIN6	Mouse insulinoma cell line MIN6

MOB1	Mps1-binder-related 1
MST1	mammalian sterile 20-like kinase-1
MyD88	Myeloid differentiation primary response protein 88
NADH	Nicotinamide adenine dinucleotide
NBR1	Neighbour of breast cancer 1
NDP52	Nuclear dot protein 52
NDR family	Nuclear Dbf2-related family
NEDD4	Neuronal precursor cell-expressed developmentally downregulated 4
NeuroD1	Neurogenic Differentiation 1
NKX6.1	Homeobox protein Nkx-6.1
PARP	Poly ADP ribose polymerase
PC1/3	Prohormone convertase 1/3
PDGFR	Platelet-derived growth factor receptor
PDX1	Pancreatic and Duodenal Homeobox 1
PHLPP 1/2	PH domain and leucine rich repeat protein phosphatase 1/2
PI3K	Phosphoinositide 3-kinase
PIP2	Phosphatidylinositol 4,5-biphosphate
PIP3	Phosphatidylinositol (3,4,5)-triphosphate
PKA	Protein kinase A
PKC	Protein kinase C
PLEKHM1	Pleckstrin homology domain containing family M member 1
PRAS40	Proline rich AKT substrate of 40kDa
PRC2	Polycomb repressive complex 2
PTF 1	Pancreas transcription factor 1
RIN	Rat insulinoma cell line RIN
RTK	Receptor tyrosine kinase
SGK1	Serum/Glucocorticoid regulated kinase 1
SMURF1	Smad ubiquitin regulatory factor 1
SNARE	Snap receptor
SREBP	Sterol regulatory element-binding protein 1
STK	Serine/threonine kinase
STX17	Syntaxin-17
STZ	Streptozotocin
TEAD	Transcriptional enhancer factor TEF-1
TFEB	Transcription factor EB
TGF	Tumor growth factor
TNFR1	Tumor necrosis factor receptor 1
β -TRCP	Beta-transducin repeats-containing proteins
TSC1/2	Tuberous sclerosis protein 1/2
UBA	Ubiquitin associated
ULK1/2	Unc-51 like autophagy activating kinase
UVRAG	Ultraviolet irradiation resistance-associated gene
VEGFR	Vascular endothelial growth factor
VMP1	Vacuole membrane protein 1
WIPI 1/2	WD-repeat protein interacting with phosphoinositides
YAP	Yes-associated protein

CONTENTS

I	SUMMARY	4
II	ZUSAMMENFASSUNG	5
III	ABBREVIATIONS	7
1	INTRODUCTION	11-42
	1. Diabetes Mellitus – The epidemic continues	
	2. Introduction to pancreas and β -cells 2.1. Insulin- the maker of pancreatic β -cells 2.2. Mechanisms of insulin secretion by β -cells 2.3. Insulin action	
	3. Apoptosis and β -cell failure 3.1. Mechanistical pathways of apoptosis 3.2. β -cell apoptosis – hallmark of reduced β -cell mass in diabetes	
	4. Major signaling pathways that regulate β -cell development, turnover and survival 4.1. mTOR signaling pathway 4.2. Autophagy and the Secretory pathway 4.3. mTOR as the regulator of autophagy 4.4. HIPPO signaling pathway : Basics 4.5. Role of Hippo pathway in Islet biology & diabetes	
	5. AIM OF MY THESIS	42
	REFERENCES	43
2	RESULTS	63
	2.1. Neratinib protects pancreatic beta cells in diabetes	63
	2.2. The Hippo kinase LATS2 impairs pancreatic β -cell survival in diabetes through the mTORC1-autophagy axis	95
3	DISCUSSION	144
	OUTLOOK	157
	CONCLUSIONS	158
	REFERENCES	159
4	APPENDIX	160-197

	4.1. Ageing potentiates diet-induced glucose intolerance, β-cell failure and tissue inflammation through TLR4	
	4.2. Loss of Deubiquitinase USP1 blocks pancreatic β-cell apoptosis by inhibiting DNA damage response	
	ACKNOWLEDGEMENTS	198

1 INTRODUCTION

1. Diabetes Mellitus – The epidemic continues

The existence of the crippling disease “Diabetes” was recorded in the third dynasty Egyptian papyrus in 1552 BC [1]. Later, this led the Greek Physician Apollonius of Memphis to coin the term “DIABETES” in 250 BC, which means “to pass through”. In the 11th century, “MELLITUS” the Latin word for honey was added to Diabetes as the urine of the diabetic patients determined to be very sweet [2]. For nearly thousands of years there was no treatment for this devastating disease. The approach for treating diabetes was started in 1797 and eventually, Langerhans discovered the cells that secrete the insulin hormone in 1869, which is the key secreted factor for the regulation of sugar levels in the blood. Later, he named the cells “Islets of Langerhans” [2]. This year we celebrate the discovery of insulin by Fredrick Banting and Charles Best in Toronto in 1921 [1]. Their efforts on injecting the pancreatic extracts to diabetic dogs lowered blood glucose levels. Later, the purification of insulin was performed by a biochemist, James Collip [3]. The story of insulin discovery was legendary. Although insulin administration is not a cure for diabetes, it is truly a life saver in the modern history awarded by the Nobel Prize in Physiology or Medicine in 1923 [4, 5].

The American Diabetes Association (ADA) classified diabetes into type 1 diabetes (T1D), type 2 diabetes (T2D), other types and gestational diabetes mellitus (GDM) [6]. The ninth edition of International Diabetes Federation (IDF 2019) highlights that approximately 463 million adults between the age group of 20 to 79 years are living with diabetes which will rise to 578 million by 2030 and 700 million by 2045. Nearly 1 in 11 adults (20-79 years) has impaired glucose tolerance which is around 450 million people globally. While T1D is defined as the chronic autoimmune disease where autoreactive T-cells induce the destruction of pancreatic β -cells resulting in absolute insulin deficiency, the most prevalent T2D is a complex metabolic disorder characterized by progressive loss of β -cell insulin secretion against a background of insulin resistance, which is due to an inadequate adaptation in β -cell mass [7, 8].

2. Introduction to pancreas and β -cells

2.1. Insulin- the maker of pancreatic β -cells

The pancreas is a major organ of human physiology that plays an essential role in digestion and metabolism. It is located behind the stomach and shares the shelter with other organs including spleen, liver and small intestine. The pancreas is composed of two morphologically and functionally distinct components, namely the endocrine and the exocrine. The exocrine part of pancreas contains acinar and ductal cells that produces digestive enzymes whereas the endocrine part of pancreas carries five different hormone secreting cells to form an aggregate called islets of Langerhans. The cell types of the islets of Langerhans include α -cells that secrete glucagon, β -cells that secrete insulin, δ cells that release somatostatin, ϵ cells that release ghrelin and PP-cells that secrete pancreatic polypeptide. The islets of Langerhans are connected with the intra-islet microvascular network in order to regulate blood glucose levels by directly secreting the hormones into the bloodstream as shown in Fig.1A [9]. Pancreatic β -cells are the major regulators of mammalian energy homeostasis and glucose metabolism [10].

Pancreatic β -cell identity is specialized by the expression of key transcription factors (TF) namely PDX1, MafA, NKX6.1 and NeuroD1 [11, 12]. These TFs play an inevitable role in the transcription of single insulin gene, *INS*, in humans and two different genes *ins1* and *ins2* in rodents (located on chromosome 11), specifically in response to glucose and autocrine signaling [13]. The special β -cell transcriptional machinery also regulates the components of β -cell secretory pathway such as glucose transporter 2 (GLUT2) and insulin processing enzyme PC1/3, emphasizing their contribution to the establishment and maintenance of β -cell identity [14].

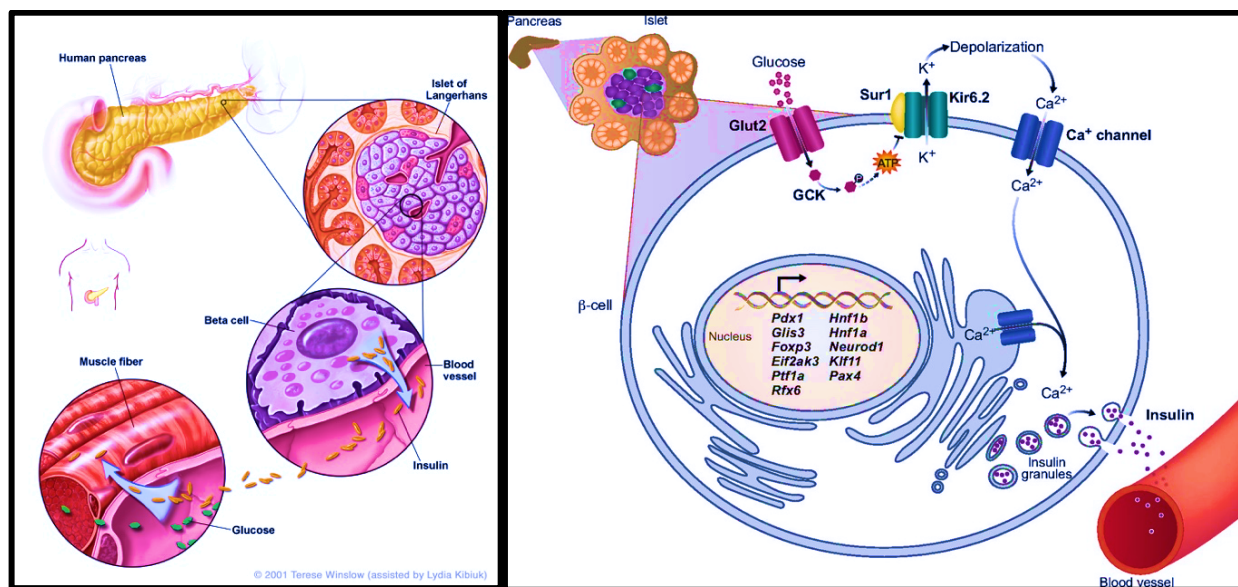


Fig.1: A) The islet of Langerhans, the endocrine part of the pancreas regulates blood glucose levels by secreting insulin into the bloodstream; B) Mechanism of insulin secretion by Pancreatic β -cells. From Pagliuca *et al* [10].

2.2. Mechanisms of insulin secretion by β -cells

Glucose serves as the major stimulator of insulin production and secretion. Increase in plasma glucose concentration is sensed by glucose transporters such as Glut1/2 that are expressed on the β -cell membrane. While the major glucose transporter in the rodent β -cells is Glut2, its principal counterpart in human β -cells is Glut1. The transported glucose is phosphorylated by glucokinase (GCK), initiate the glycolysis, the metabolic pathway that eventually generates ATP (adenosine triphosphate), NADH and pyruvate as the end products. The glycolytic product pyruvate is the substrate of TCA (tricarboxylic acid) cycle processed in the mitochondria. Additionally, the cytosolic NADH and the NADH generated via TCA cycle in the mitochondria stimulate the ETC (electron transport chain) resulting in (1) H^+ gradient dissipation that drives ATP production via ATP synthase and (2) matrix hyperpolarization that increases the mitochondrial Ca^{2+} , which further enhances the NADH and ATP production via TCA cycle. This process eventually results in the increase of cytosolic ATP levels and ATP/ADP ratio [15, 16]. The elevation of ATP/ADP ratio in the cytosol, closes K_{ATP} channels and initiates membrane depolarization by spontaneous opening of T type Ca^{2+} channels. The membrane depolarization further regenerates the activation of voltage-gated L type and P/Q type Ca^{2+} channels and Na^+ channels causing Action potentials firing. This triggers Ca^{2+} influx resulting in the exocytosis of insulin granules and thus hormone secretion (Fig.1B) [17]. The K_{ATP} channel in β -cells is in the structural form of a tetra-octamer which is composed of four sulfonylurea receptor 1 (SUR1) and rectifying K^+ channel 6.2 subunits (kir6.2) in the inward [18]. The process of insulin secretion is biphasic [19]. There is rapid insulin secretion at the first phase, followed by gradual increase for nearly 60 minutes in the second phase, which is also known as K_{ATP} channel independent Glucose Stimulated Insulin Secretion (GSIS) [20] [21].

Additionally, β -cells are primed by incretin hormones that are released from gut L cells such as GLP-1 (Glucagon like polypeptide-1) and glucose-dependent insulinotropic polypeptide (GIP) which enhance nutrient induced insulin secretion via 3',5'-cyclic adenosine monophosphate (cAMP) pathway in PKA dependent or independent manner [22] [23]. Excluding glucose, free fatty acid (FFA) also involved in the augmentation of insulin release, which is independent of K_{ATP} channel [24] [25]. Other stimulatory signals include parasympathetic nerves and neuropeptides, that causes acetylcholine release in the islets, leading to GSIS via activation of PKC [26].

2.3. Insulin action

The secreted insulin is delicately distributed and acts on different organs of the human body which is the paramount example of integrated cellular physiology. In the first pass, insulin is delivered to the liver via portal circulation and it undergoes the process called insulin clearance [27, 28]. The insulin that surpasses the clearance reaches the heart which is then pumped to the peripheral tissues by arterial circulation resulting in NO mediated vasodilation [29-32], in order to regulate the glucose uptake in the skeletal muscles [33, 34] and adipose tissue via Glut4 translocation. Besides acting on the insulin receptor (IR) of liver, muscle and fat, insulin also acts on neurons and glial cells of the brain to regulate appetite and energy expenditure. Insulin action in the brain also modulates cognition, memory and mood. Conversely, insulin enters the liver for the second pass clearance. The major action of insulin in the liver is to suppress gluconeogenesis and glycogenolysis. Finally, the journey of insulin ends by degradation in the kidney.

3. Apoptosis and β -cell failure

The Greek word '**Apoptosis**' is found in the notes of Hippocrates in 4th century BC, which means the falling of leaves in autumn. Here, Hippocrates of Cos used the term apoptosis in medicine to describe the gangrene development during treatment of fractures with bandages [35]. Ultimately, the term apoptosis was coined and defined in the paper published by Kerr, Wyllie, and Currie in 1972 [36]. The process of DNA degradation by endonucleases and formation of 'DNA ladder' was determined to be the first characteristic of apoptosis, the programmed cell death. Hence, DNA ladder was the first marker for apoptosis. The another major marker of apoptosis is the determination of phosphotidyl serine at the surface of dead cells [37]. Currently, there are several techniques available to determine the apoptotic cells, which includes TUNEL (terminal deoxy transferase mediated dUTP nick end-labeling), a method that labels both double and single stranded DNA breaks [38] and immunohistochemical or immunoblot analysis of apoptosis markers such as Caspase-3 or PARP cleavage, or other key components of the intrinsic and extrinsic pathway of apoptosis (see below) [39].

3.1. Mechanistical pathways of apoptosis

Apoptosis occurs by cascade activation of caspase proteases. Two distinct pathways of apoptosis are 1) the extrinsic pathway or death receptor mediated pathway and 2) the intrinsic pathway or mitochondria dependent pathway [40]. The extrinsic pathway is initiated by ligation of death receptors such as Fas, DR4, DR5 and TNFR1 with their respective ligands such as FasL, tumor necrosis factor-(TNF-) related apoptosis inducing ligand (TRAIL) and TNF- α . The above ligation induces the activation of initiator caspase-8 which directs the activation of executer caspase-3

and also could cleaves BID (BH3 interacting domain death agonist) resulting in mitochondrial destabilization and cytosolic relocalization of cytochrome-c leading to the initiation of apoptosome complex, which is required for the activation of downstream caspases such as caspase-9 and caspase-3 that promotes DNA fragmentation and cell death [41]. On the other hand, the intrinsic pathway is stimulated by the activation of BCL-2 family of mitochondrial death proteins. The BCL-2 family proteins pertain both anti-apoptotic and pro-apoptotic characteristics. Cellular stress initiates the apoptotic response by activating pro-apoptotic BH3-only factors such as BAX or BAK, which modulates the mitochondrial outer membrane to release cytochrome c into the cytosol [42, 43]. The pro-apoptotic actions of BAX and BAK are regulated by anti-apoptotic BCL-2 proteins such as BCL-2 and BCL-x_L. BAX and BAK similar to BID, cause alteration in mitochondrial membrane, mediate cytochrome-c release and form a macromolecular apoptosome which is a multimeric complex of cytochrome-c, dATP, the adaptor protein Apaf1 (apoptotic protease activating factor-1) and procaspase-9. The apoptosome facilitates the activation of apoptosis mediating executioner protease caspase-9, leading to caspase-3 activation and finally resulting in cell apoptosis [40]. The process of apoptosis is necessary for the development, ageing and for the proper maintenance of cell turnover in tissues. Under several pathological conditions, inappropriate apoptosis is triggered and the balance between the cell populations are lost leading to several disorders such as neurodegenerative diseases, cancer, autoimmune disorders and diabetes.

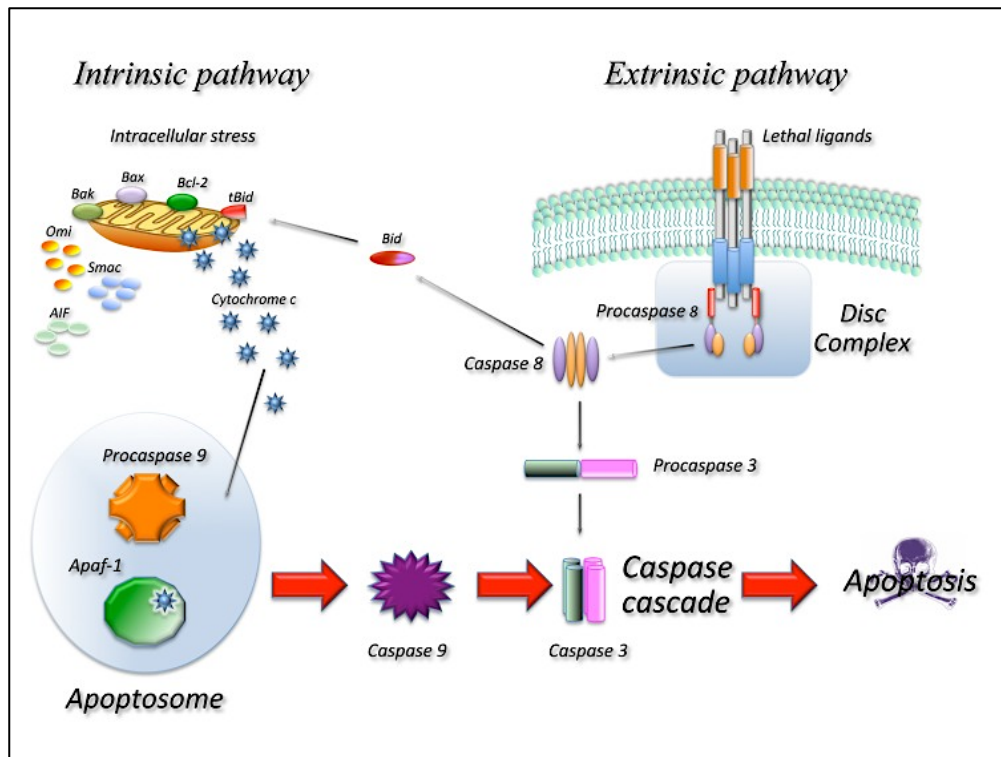


Fig.2: Representation of two main mechanistical pathways of apoptosis : death receptor-mediated or Extrinsic pathway and mitochondria-dependent or Intrinsic pathway; from Favaloro, B. et al. [44].

3.2. β -cell apoptosis – hallmark of reduced β -cell mass in diabetes

The critical factors that define the functional β -cell mass are β -cell number, β -cell size and their ability to secrete mature insulin in an appropriate well-controlled manner [45]. However, in the context of prolonged insulin resistance and consequential hyperglycemia, pancreatic β -cells elicit a compensatory response by β -cell expansion, and/or increase in β -cell function which ultimately lead to enhanced β -cell mass. Despite the compensatory role of β -cells, the existence of sustained metabolic stress, eventually cause β -cell failure which is characterized by β -cell dysfunction and progressive loss of β -cell mass [46-49]. Evidently, the autopsies of patients with T2D show a huge decrease (nearly 30-60%) in β -cell mass compared to non-diabetic patients. It is noted that the underlying mechanism for reduction of β -cell mass is most likely a tremendous increase in the rate of β -cell apoptosis, which is evident in islets from both lean and obese T2D patients as determined by multiple complementary approaches like *In situ* TUNEL & Caspase-3 staining as well as EM-based determination of apoptotic cells [46, 50, 51]. Butler *et al.* observed a significant increase in β -cell apoptosis with no change in the rate of β -cell replication or neogenesis in the pancreas of both lean and obese T2D patients [46, 47]. These findings strongly indicate the role

of apoptosis in reduced β -cell mass in T2D. Moreover, another proposed persuasive mechanism underlying β -cell deficit is β -cell dedifferentiation [52, 53] [54]. Notably, under prolonged stressed conditions, β -cells lose their differentiated phenotype and cellular identity, and subsequently adapt to a precursor-like state. The dedifferentiation process involves, (1) downregulation of β -cell enriched genes such as PDX1, Nkx6.1 and MafA, (2) concomitant upregulation of suppressed genes in the matured β -cells (β -cell forbidden or “disallowed” genes), and (3) the probable upregulation of progenitor cell genes such as Neurogenin3, Oct4, Nanog and L-Myc [52, 53]. This phenotypic reconfiguration of β -cells ultimately results in defective insulin secretion and exhibit impairment in the regulation of glucose homeostasis. Nevertheless, the contribution of β -cell dedifferentiation to reduced β -cell mass is still under debate and requires detailed mechanistical investigations [55-57].

In T1D, it is shown that the perinatal wave of β -cell apoptosis contributes to the presentation of auto-antigens subsequently promoting autoimmune response against β -cells [58-60]. Mechanistically, the ‘death receptors’ (Fas and TNFR and their respective ligands) that are activated by cytokines such as IL-1 β and the cytotoxic components such as perforin and granzyme B released by CD8+ T cells cause β -cell apoptosis in T1D [61].

However, T2D is a complex metabolic disorder which is substantiated by progressive insulin resistance, hyperlipidemia and chronic hyperglycemia further increasing the insulin secretory demand as mentioned above, subsequently triggering severe mitochondria stress [62-64] and ER stress [65, 66] and finally β -cell apoptosis. Moreover, tremendous increase in the amyloid deposition and disruption in the islet architecture are associated with T2D [67]. Despite the above discoveries, the external signaling pathways that mediate β -cell apoptosis are still obscure [45].

4. Major signaling pathways that regulate β -cell development, turnover and survival

4.1. mTOR signaling pathway

The discovery of TOR protein kinase was a mere serendipity in the biochemical and medical research world. Suren Sehgal, the father of rapamycin, realized that the compound has novel properties beyond its immunosuppressant activities and hence, encouraged the NCI (National Cancer Institute) to investigate the anti-tumor activity of rapamycin, which led to the finding of its target protein, therefore named mechanistic target of Rapamycin (mTOR) [68, 69]. mTOR exists as two homologs TOR1/DRR1 and TOR2/DRR2 and was initially identified and isolated by Michael N. Hall and George P. Livi independently in the mutant strains of *Saccharomyces*

cerevisiae [70-74], which was later determined to be conserved among eukaryotes [75-77]. Moreover, the mechanistic target of rapamycin (mTOR) was concurrently discovered by three individual groups David M. Sabatini, Stuart L. Schreiber and Robert T. Abraham in the mid 1990s, naming it RAFT1 (Rapamycin and FKBP12 Target1), FRAP (FKBP Rapamycin Associated Protein) and mTOR respectively, which is widely called as mTOR, as coined by Abraham [78-81]. mTOR (~289kDa) is a serine/threonine kinase and one of the members of phosphoinositide 3 kinase-related kinase (PIKK) pathway that plays a key role in cell proliferation, growth, differentiation and survival [82-86]. The vital physiological function of mTOR was demonstrated by the fact of embryonic lethality for mTOR knockout mice [87]. The primary structure of mTOR comprises 20 tandem Huntingtin-Elongation factor 3-regulatory subunit A of PP2A-TOR1 (HEAT) repeats at the N-terminal, followed by FKBP12- Rapamycin Binding (FRB) domain, the Focal Adhesion Targeting (FAT) domain, a catalytic Kinase (KIN) domain which is connected to another FAT domain at the C-terminal end (FATC) through Negative Regulatory Domain (NRD) which is important for the mTOR activity [85, 88-91].

mTOR functions in two structurally and functionally distinct protein complexes mTORC1 and mTORC2 [79]. The interacting proteins of mTOR in mTORC1 are Raptor, mLST8, PRAS40 and DEPTOR [90, 92-95], whereas in mTORC2, mTOR specifically associates with Rictor, mSin1 and Protor apart from the common interacting proteins mLST8 and DEPTOR [96, 97]. The macrolide rapamycin inhibits mTORC1 activity by forming a complex with intracellular receptor FKBP12 that directly binds to the FRB domain of mTORC1 [90, 98, 99]. Initially, rapamycin was observed to inhibit TORC1 but not TORC2 in yeast, However, further study in mammals showed that chronic treatment of rapamycin intensely inhibits mTORC1, as well as mTORC2 [100]. This inhibitory role of rapamycin is however resistant to 4E-BP1, another prominent substrate of mTORC1 [101, 102].

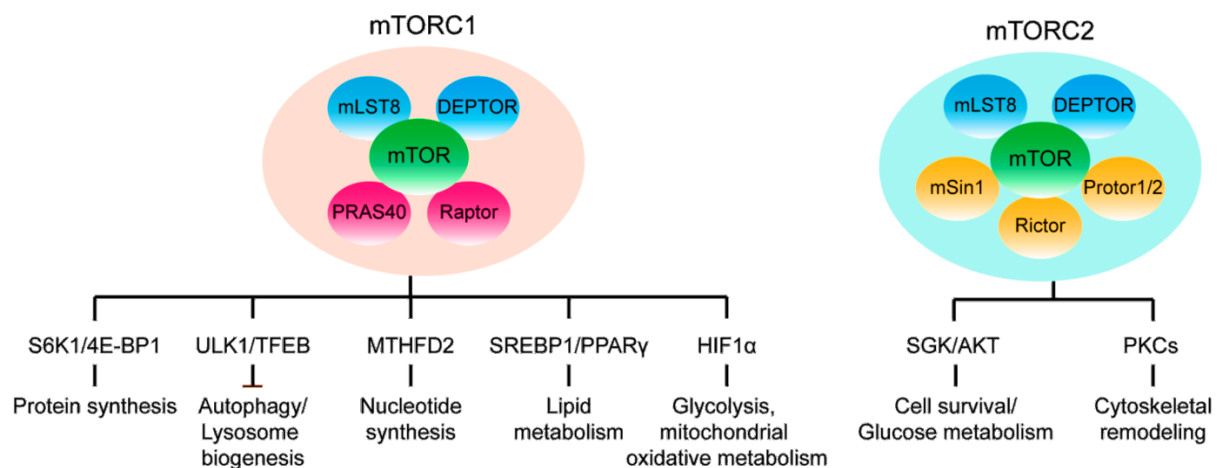


Fig.3. Illustration of the two distinct protein complexes mTORC1 and mTORC2 and their major downstream signaling pathways. mTORC1 regulates anabolic process that includes protein synthesis, nucleotide synthesis, lipogenesis and catabolic process glycolysis and by inhibiting autophagy and lysosomal pathways. Conversely, mTORC2 regulates glucose metabolism and cytoskeletal remodeling. From *Mao,Z. & W.Zhang et al* [103].

The mTOR signaling pathway is highly sensitive to the nutrients in the environment especially to the leucine and arginine amino acids in the lysosomes and in the cytosol [104]. The heterodimeric Rag GTPases localizes the mTORC1 to the lysosomes in response to the nutrients, furthermore mTORC1 kinase activity is stabilized by Rheb GTPases which functions in response to the insulin, growth factors and the energy levels [95, 105-107]. mTORC1 activation promotes most anabolic processes such as protein synthesis by phosphorylating the 70 kDa ribosomal protein S6 Kinase1 (P70S6K1) and the eukaryotic translation initiation factor 4E binding protein (4EBP) [108], lipid synthesis by modulating SREBP transcription factor [109] and nucleotide synthesis which is required for DNA replication and for ribosome synthesis [108, 110, 111]. Furthermore, mTORC1 represses the key catabolic process autophagy, in order to promote cell growth. The mechanistical role of mTOR in regulating autophagy is briefly explained in next section. On the other hand, the functional regulation of mTORC2 is not well-defined as mTORC1. The kinase mTORC2 is activated by growth factors like Insulin via PI3K signaling, where PI3K phosphorylates PIP2 into PIP3, in which PIP3 directly binds to the mSin1, the interacting partner of mTORC2 [112-114]. It is also known that TSC1/2 activates mTORC2 [115-117]. This activation enables mTORC2 to phosphorylate and activate AGC kinases that includes AKT/PKB, SGK1 and PKC α [118-120]. As a defined process, mTORC2 phosphorylates AKT at Ser473 [120]. The additional activation and phosphorylation of AKT at Ser473 apart from Thr308, modulates AKT for substrate specificity, leading to the activation of specific substrate like FOXOs transcription factors [121, 122]. Remarkably, mTORC2 is considered to play a central role in the whole body glucose and lipid metabolism, as loss of mTORC2 in the insulin responsive tissues deteriorates whole body glucose homeostasis [123].

4.1.1. Chronic mTORC1 hyperactivity: a hallmark of β -cell failure in T2D

mTORC1, the master regulator of cell growth and metabolism in response to nutrients and growth factors, is mainly dysregulated in several pathological conditions such as cancer, neurological diseases, obesity and T2D [124].

Normally, β -cells benefit from short-term acute mTORC1 activation by enhancing β -cell mass as an outcome of the increase in β -cell growth and proliferation. This was well understood by the 'loss of function' experiments performed in rodents for mTORC1 signaling. mTORC1 deficient

mice exhibit reduced β -cell mass, poor postnatal islet development, hypoinsulinemia and glucose intolerance [125-129]. Furthermore, mTORC1 plays an important role in β -cell survival. Islets isolated from β -cell specific mTOR knockout mice as well as the mTORC1 deficient β -cell line, showed increase in the expression of thioredoxin-interacting protein (TXNIP) and carbohydrate-response element-binding protein (ChREBP), which is also consistent with the islets from diabetic mice and from T2D patients [130]. TXNIP is transcriptionally activated by ChREBP to induce mitochondrial dysfunction and oxidative stress leading to β -cell apoptosis. This revealed the prominent role of mTOR in suppressing the transcriptional activity on TXNIP by forming a huge complex with ChREBP-Max protein and hence, reducing the oxidative stress and β -cell apoptosis [126, 131].

Conversely, long-term constitutive activation of mTORC1 in β -cells imparts the biphasic role of mTOR in glucose homeostasis [130]. Young mice with β -cell specific TSC2 deletion, an upstream inhibitor of mTORC1 which leads to prolonged activation of mTORC1, shows improved glucose tolerance, β -cell hypertrophy and hyperinsulinemia, whereas, old mice with sustained mTORC1 activation in β -cells, develop hyperglycemia by gradual loss in β -cell mass as a result of increase in β -cell apoptosis [132, 133]. Moreover, our lab determined that mTORC1 is upregulated in islets isolated from human T2D patients compared to the non-diabetic individuals contributing to impaired β -cell function and survival [130]. Genetic or chemical inhibition of mTORC1-S6K1 signaling in T2D human islets restores insulin secretion [134]. These findings are consistent with the sustained mTORC1 activation in the T2D animal models [130]. Also, chronic activation of mTORC1 causes impaired autophagy/mitophagy, ER stress and lipid accumulation [134, 135].

In contrast, mTORC2 activation is downregulated in mouse and human diabetic islets [136]. The decline in mTORC2 levels is due to the negative feedback loop of hyperactivated mTORC1 which phosphorylates and inactivates the mTORC2 subunits mSin1 and Rictor and ultimately deteriorates the activation of mTORC2 and subsequent AKT signaling [134, 136-139]. This suggests that mTORC1 improves β -cell mass and glucose metabolism in the short term, however, prolonged activation of mTORC1 is deleterious to the β -cells causing β -cell failure and dysfunction [130]. This makes one to understand that mTORC1 is a double-edged sword in the regulation of β -cell mass and function in response to nutrients [130].

4.2. Autophagy and the Secretory Pathway

“Life is an equilibrium state between synthesis and degradation of proteins”, an impressive statement quoted by Yoshinori Ohsumi, the Noble Prize winner of Physiology/Medicine in 2016, for his tremendous work on the discovery the process of autophagy and its underlying mechanisms. The name autophagy is derived from Greek, ‘Auto’ means Self and ‘Phagy’ means eating, which was first proposed by Christian de Duve in 1963, during his seminal work on the discovery of lysosomes. Duve named the terms ‘Autophagy’ and ‘Heterophagy’ to distinguish the degradation of intracellular components from uptake and the degradation of extracellular substances respectively [140-143]. Initially, Duve *et al.* morphologically observed the self-eating of mitochondria and other intracellular structures within the lysosomes of the rat liver infused with glucagon [144]. However, the molecular mechanism behind the glucagon induced autophagy in the liver was not clearly understood, except the utility of cyclic AMP induced activation of PKA in liver [145]. Later, in 1990s, autophagy was rediscovered by the scientific world, in delineating how autophagy is regulated and executed at the molecular level in yeast (*Saccharomyces cerevisiae*). Ohsumi *et al.* identified various autophagy related genes by performing a genetic screen in a yeast model, which also made Klionsky to name those genes as ATG (AuTophagy) genes which were then widely studied for their functions and for their interaction between the encoded proteins. Initially, there were at least 15 genes that regulate autophagy under nutrient deprivation in yeast, but subsequent intensive researches discovered nearly 41 Atg related genes in yeast which are conserved in slime mould, plants, worms, flies and mammals [140, 143, 146, 147]. Thus, autophagy is simply defined as the evolutionarily conserved catabolic process that digests the macromolecules or cellular organelles within the lysosomes for nutrient recycling to sustain through cellular stress and nutrient insufficiency.

Autophagy of intracellular macromolecules involves lysosomal degradation in mammalian cells and vacuolar degradation in yeast and plants [147]. Autophagy is not only limited to the maintenance of cellular homeostasis through the catabolism of proteins, lipids, carbohydrates and iron, it also plays an eminent role in the regulation of cell proliferation, differentiation and replicative senescence. The classical model of autophagy exists during starvation; however, basal autophagy is observed to function even under nutrient rich conditions to manage the house keeping function for the quality control of intracellular proteins and organelles in all cells [148-151]. There are three different pathways for the delivery of the target substrates into the lysosomes for degradation, namely, microautophagy, macroautophagy and chaperone mediated autophagy (CMA).

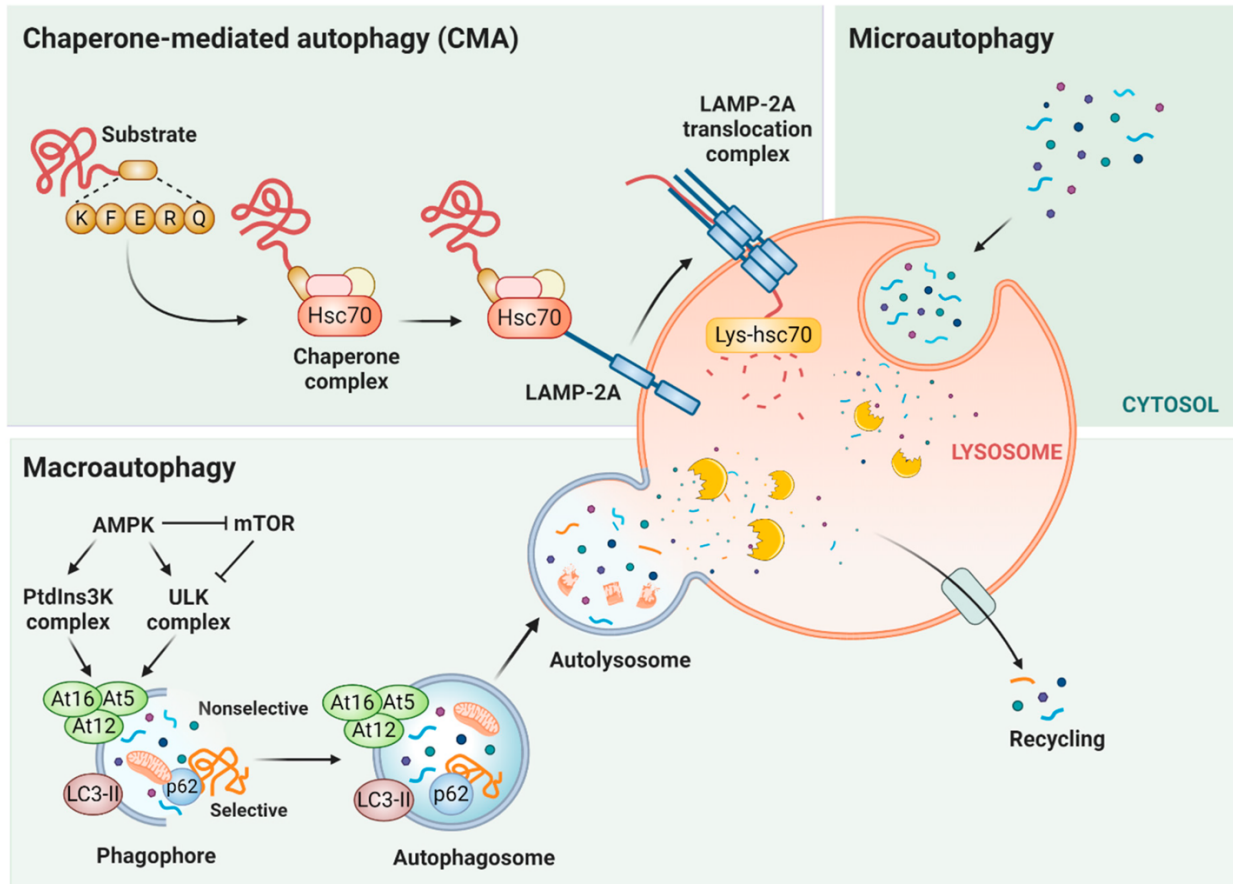


Fig.4. Three major types of autophagy: CMA (Chaperone mediated autophagy), microautophagy and macroautophagy. In CMA, the target proteins with KFERQ like motif are selectively recognized by HSC70 cytosolic chaperone, which are subsequently translocated via LAMP2A translocation complex inside the lysosome for degradation. In microautophagy, the cargo is directly captured by the lysosomal membrane invagination for degradative process. The most common macroautophagy can be both selective and non-selective. Macroautophagy is regulated by mTORC1 and AMPK signaling pathways, and macroautophagy pathway is processed by different stages where the cargo is surrounded by growing phagophore, which further nucleates and forms autophagosome, and subsequent fusion with lysosomes to form autolysosome and eventually cargo degradation. From *Andrade-Tomaz, M. et al.* [152].

4.2.1. The Macroautophagic machinery

Macroautophagy is the most extensively studied canonical or non-canonical pathway, which sequesters the macromolecules or a bulk of cytoplasm (cargo) in a double membrane vesicle termed autophagosome [153]. The formation of autophagosome occurs through a series of events which includes initiation, nucleation, elongation and maturation of a phagophore [154, 155]. This complex pathway of sequestration of the cargo is regulated by multiple protein kinases [156]. Eventually, the complete mature autophagosome fuses with an endo-lysosomal compartment to form the autophagolysosome (also known as autolysosome) for the degradation of the internal material by lysosomal proteolytic enzymes, which further supplies the nutrients to the cytoplasm

for the anabolic process and energy production. Macroautophagy functions constitutively at the basal level to maintain homeostatic balance in response to various stress signals or metabolic demand, substantiating its cytoprotective mechanism [157]. However, excessive or uncontrolled autophagy is detrimental to the cells [158]. The functional characterization of Atg related genes describe the molecular aspects of macroautophagy. Four sequential steps of macroautophagy are described in the following.

Initiation of macroautophagy: The initiation of the complex autophagic machinery is induced by numerous stimuli that includes hypoxia, growth factors, hormones, intracellular calcium levels, ATP levels, accumulation of misfolded proteins and infection by pathogens. The classical and well characterized stimuli are starvation and energy deprivation, where master metabolic regulators mTORC1 and AMPK are inhibited and activated respectively [157, 159]. AMPK positively regulates autophagy by phosphorylating both autophagy machinery components ULK1 and Beclin 1 complexes [160]. The phosphorylated and activated ULK1/2 associates with the regulatory proteins Atg13, FIP200 (also known as RB1CC1) and Atg101 in order to form the initial site of autophagosome formation [161-164].

Nucleation of autophagosome membrane: The responsible proteins and their functional roles involved in the origin and nucleation of the phagophore are still under investigation. However, the endoplasmic reticulum (ER), the interconnected site between ER and mitochondria as well as plasma membrane, Golgi apparatus and late endosomes serve as the major source of autophagosomal membrane [165-167]. Most of the study shows that the nucleation of the phagophore is triggered by Beclin-1 complex which is downstream to ULK1 complex [168, 169]. The Beclin-1 complex consists of the Beclin1, class III Phosphatidylinositol 3 Kinase (hVps34) and Atg14L which is essential for the production of phosphatidylinositol-3-phosphate (PI3P) [170, 171]. PI3P enriched membrane structure is called as omegasome, which detaches from the ER to further recruit autophagy machinery proteins for the expansion of phagophore [172]. One major role of PI3P is recruiting WIP1/2 (Atg18 in yeast) complex for the movement of Atg9L1 (Atg9 in yeast) transmembrane protein in order to expand the size of the phagophore [158, 173-175]. This Atg9L1 is observed to co-localize with LC3 and Rab7 proteins which are the well-known markers of autophagic vacuoles [164]. Correspondingly, the Beclin-1 complex (Beclin1:hVps34:Atg14L) is regulated by several factors such as VMP1, AMBRA1, MyD88 and Bcl-2 family proteins which serve as the checkpoints for the autophagosome formation [176-178].

Autophagosome elongation and maturation: The budding phagophore membrane further recruits two different ubiquitin-like conjugation systems for the expansion of autophagosome. In the first ubiquitylation-like reaction, Atg12 is activated by Atg7 (homologous to E1 ubiquitin

activating enzyme) and subsequently conjugated to Atg5 by Atg10 (homologous to E2 ubiquitin conjugating enzyme) to form Atg12-Atg5:Atg16L multimeric complex. The second ubiquitylation-like reaction is the lipidation of LC3 (Atg8 in yeast) [147, 179-181]. Initially, LC3 is processed by Atg4 protease to form cytosolic LC3-I which is further activated by Atg7 and conjugated by Atg3 at its C-terminal glycine to PE for the production of membrane bound LC3-II [182, 183]. While both the ubiquitylation-like reactions crosstalk for the expansion, Atg12-Atg5 conjugation is lost and LC3-II stays as remnant upon completion of the autophagosome [184, 185]. The presence of LC3-II determines the size of a complete autophagosome through its tethering and membrane hemi fusion activities. Moreover, LC3-II plays a crucial role in recognizing the autophagic cargoes selectively and in serving as a docking site for the adaptor proteins [186, 187].

Fusion of autophagosomes with endo-lysosomal compartment and degradation: The important phase of macroautophagy is the fusion of the matured and closed autophagosome with the lysosome. Initially, autophagosomes fuse with late endosomes to form an amphisome, which is a prerequisite for autophagosome and lysosome fusion [185]. The amphisomes subsequently fuse with lysosomes to generate autolysosomes. The fusion of outer autophagosomal membrane with the lysosome depends on various factors such as Rab GTPases, tethering factors, SNAREs and auxiliary proteins. In mammals, Atg8 family proteins encompass two subgroups namely, the LC3 family and GABARAP family. Although LC3 proteins are involved in the expansion and completion of autophagosome, the GABARAP subfamily is required for the later steps i.e. for fusion initiation [188, 189]. Likewise, the presence of PI4P on the autophagosomes activate Rab7 GTPases and recruit the tethers like HOPS complex and the SNAREs like STX17 complex [190, 191]. This event also requires an adaptor protein PLEKHM1 which associate with both GABARAP and other Atg8 proteins on the autophagosomes and RAB7 on the lysosomal membrane to form a bridge between both the organelles with HOPS complex. Eventually, the outer membranes of both the organelles merge and the autophagic body is released into the lumen of lysosome and degraded by the lysosomal proteases [188, 192, 193]. It is noted that ion and lipid compositions regulate the autophagosome and lysosome fusion [188].

Selective macroautophagy is mediated by LC3II and P62/SQSTM1: Macroautophagy occurs either in selective or in non-selective manner. In non-selective macroautophagy, the cargoes that are loaded into the autophagosomes are not bonded to the autophagosomal inner membrane, rather it occurs only by random engulfment leading to endo-lysosomal fusion and degradation. While selective macroautophagy is mediated by more than one autophagy receptors that carry an important LIR motif (consensus sequence WxxL) and UBA domain, for its interaction with the

conserved hydrophobic pockets of LC3-II protein (homolog of Atg8) of the growing phagophore membrane and for the interaction with ubiquitylated substrates or cargoes respectively [194].

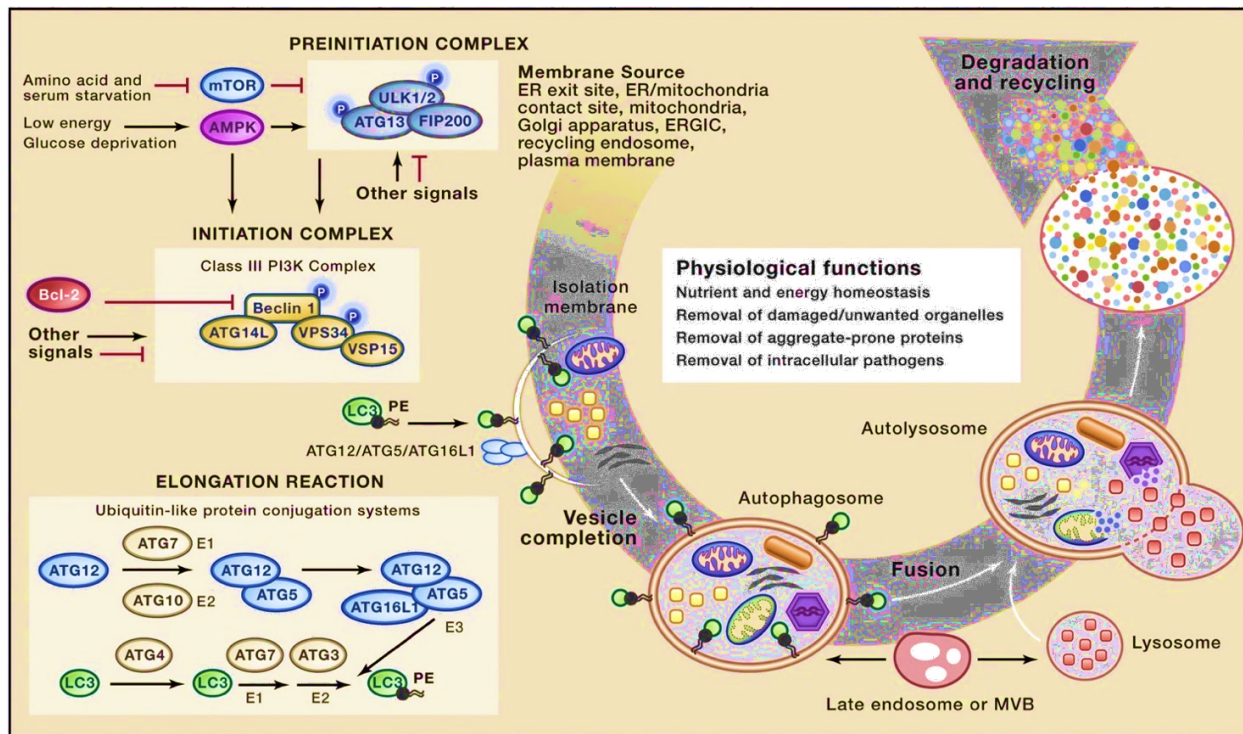


Fig.5. Schematic representation of the macroautophagy pathway. A pre-initiation complex, also called as ULK1/2 complex is regulated by kinases such as mTORC1 and AMPK which results in inhibitory or stimulatory phosphorylations of ULK1/2 proteins. Firstly, the pre-initiation complex activates class III PI3K complex (initiation complex) which subsequently generates PI3P that further recruits PI3P binding proteins and proteins responsible for phagophore elongation resulting in formation of double membrane structure autophagosome, which surrounds the cargo material. LC3-PE is alone stably associate with the mature autophagosome, where the autophagosome fuses with lysosome to form autolysosome and subsequent degradation of cargo proteins. From Green, D.R. et al. [195].

The firstly identified autophagy receptor was p62/SQSTM1 (sequestosome 1) which further extended with the identification of NBR1, NDP52, Tax1BP1, and Optineurin [196-201]. Currently, these autophagy receptors are known as Sequestosome 1-like receptors (SLRs) [202]. The SLRs have specificity towards the ubiquitinated cargoes. For example, the well-characterized p62 which has both LIR motif and UBA domain, specifically defines the fate of several misfolded proteins, damaged organelles, intracellular bacteria, viral capsids and various signaling proteins or complexes [203, 204]. Eventually, The SLRs degrade with their cargo within the autolysosomes.

4.2.2. Chaperone Mediated Autophagy (CMA): a unique mechanistical pathway

The selective delivery of cytosolic proteins into the lysosomes was initially proposed by J.Fred Dice, which was later embraced by cell biologists after the rediscovery of autophagy [205]. The

detailed characterization of macroautophagy led to the strong understanding that there are several ways for a cell to carry out autophagy. Dice determined that introduction of a mixture of radiolabeled proteins through red blood cell 'ghosts' into the serum free fibroblasts culture accelerated lysosomal degradation [206, 207]. His team later resolved this process by uncovering the novel motif which corresponds to the residue sequence KFERQ in the protein substrate, as a selective factor for lysosomal degradation [208, 209]. Nearly 40% of proteins carry a canonical KFERQ motif in a mammalian proteome [210]. However, the susceptibility of the protein substrate for degradation is based on the physical properties of the amino acid residues rather than the specific amino acids KFERQ, i.e. Glu residue at one end carrying one positively charged, one hydrophobic, one negatively charged residue and a fifth residue that can be either positive or hydrophobic [205]. Moreover, a protein that lacks the KFERQ like motif undergoes post translational modifications such as acetylation and phosphorylation in order to generate one such motif [211, 212]. The pentapeptide KFERQ in a protein is recognized by a cytosolic chaperone called HSC70 (Heat shock cognate 70), a constitutive member of heat shock protein 70 family, suggesting that HSC70 chaperone guides the KFERQ containing protein substrate to the lysosomal membrane for degradation [213]. This specific engagement of a chaperone for lysosomal degradation of a selective protein substrate is then renamed as CMA. However, the HSC70 chaperone is not limited to CMA, it is also involved in the delivery of KFERQ containing cytosolic proteins to late endosomes for endosomal microautophagy (eMI) and it also leads the massive protein aggregates to lysosomal degradation through a complex macroautophagy process called Chaperone assisted selective autophagy (CASA) [214]. The substrate protein that binds to the HSC70 chaperone in CMA, interacts with the lysosomal membrane through cytosolic tail of single span membrane protein LAMP2A (lysosome-associated membrane protein type 2A) [215]. The protein receptor LAMP2A is one of the three splice variants of *LAMP2* gene, which is indispensable for CMA but not for macroautophagy and microautophagy [216]. Initially, LAMP2A is in the form of a monomer at the lysosomal membrane, which gradually forms a multimer complex upon binding with the CMA substrate [212]. Interestingly, the protein substrate that bound to the LAMP2A receptor protein undergoes unfolding from the folded state for its translocation across the lysosomal membrane, which is mediated by several cochaperones along with HSC70. The multimerization of the LAMP2A is stabilized by a lysosomal variant of HSC90 that acts at the luminal side of the membrane [217]. Once the substrate is translocated into the lysosomal lumen, the multimer complex of LAMP2A disassembles rapidly in a GTP dependent manner with the help of GFAF and EF1 α [218]. Eventually, change in the lipid composition of the lysosomal membrane

alter LAMP2A multimerization, leading to its recruitment to specific membrane microdomains where LAMP2A is degraded [219, 220].

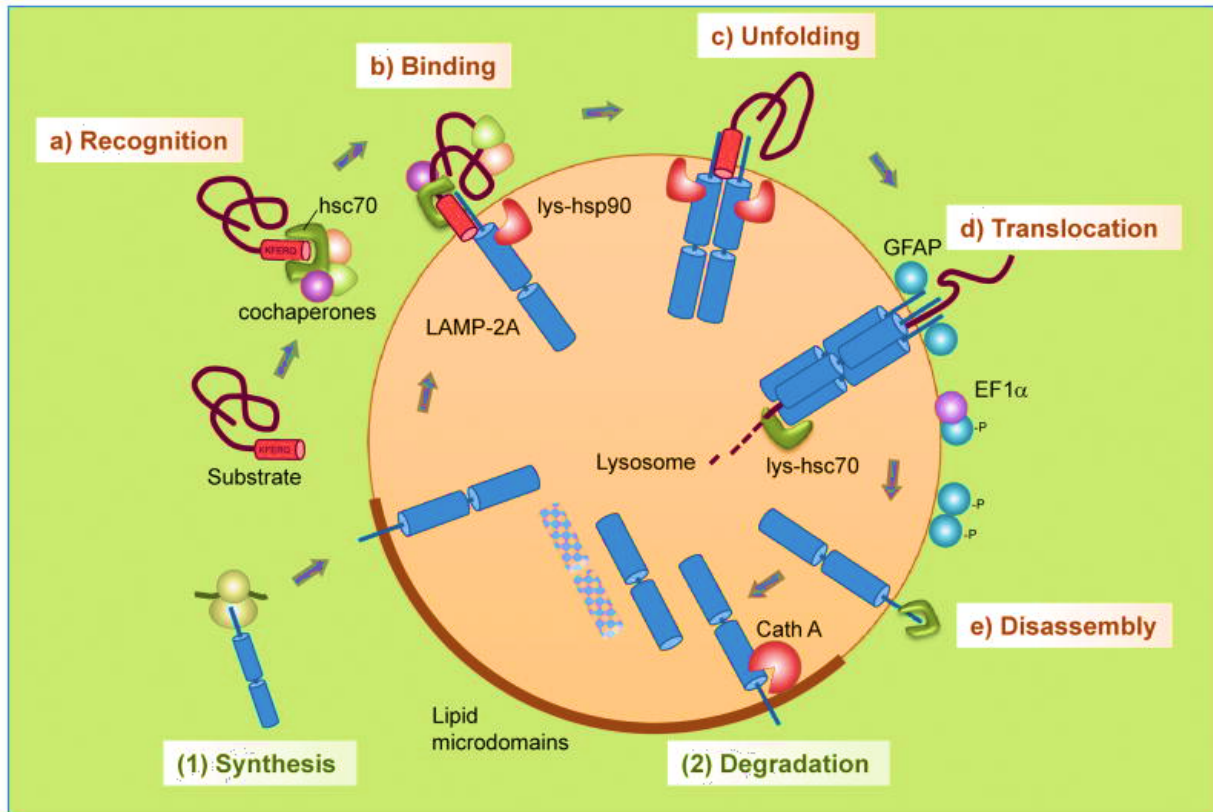


Fig. 6. Schematic representation of Chaperone Mediated Autophagy pathway(CMA). The steps in CMA include a) recognition of KFERQ like motif carrying proteins by hsc70 cochaperones, b) binding of hsc70 cochaperones to LAMP2A , c) unfolding of the protein substrate, d) translocation of the substrate via LAMP2A complex and subsequent degradation, e) disassembly of the LAMP2A complex. The regulation of LAMP2A is by 1. *de novo* synthesis and 2. degradation within the lysosome. From Kaushik, S. *et al.* [214].

4.2.3. Impaired autophagy is a hallmark of β -cell failure and T2D

The central role of autophagy in the maintenance of β -cell survival and function is undeniable as dysregulation in autophagy causes β -cell dysfunction, β -cell death and abnormal insulin sensitivity in the insulin target tissues. Firstly, the physiological role of autophagy in β -cells was studied by two different research groups using β -cell specific *Atg7*-deficient mice as *in vivo* model of defective autophagy in β -cells [221, 222]. Here, the islets of *Atg7*-deficient mice that were subjected to H&E and toluidine-blue staining show cyst like structures and ‘balloon-like’ cells with pale stained cytoplasm respectively. Electron microscopy (EM) data revealed that the ‘balloon-like’ cells present in the islets of *Atg7* deficient cells were the degenerating β -cells with a remarkably smaller number of insulin granules and with high number of morphologically abnormal mitochondria and

ER [223-225]. Also, it was reported that *Atg7*-deficient mice were glucose intolerant which is due to the reduction in glucose stimulated insulin secretion. The accumulation of structurally abnormal and dysfunctional mitochondria in the β -cells trigger impaired glucose stimulated ATP production, contributing to the defective insulin secretion. Moreover, *Atg7*-deficient mice showed progressive β -cell degeneration where the cellular hypertrophy is accompanied by degeneration and depletion of insulin immunoreactivity. These degenerative changes were triggered by the increased accumulation of polyubiquitinated proteins aggregates and overexpression of LC3 binding protein p62 [222, 226, 227]. These findings suggest that basal autophagy is indispensable for constitutive protein turnover in β -cells and for the maintenance of normal islet architecture and function. Secondly and importantly, the role of autophagy in β -cells under pathological conditions is contentious, as it is cytoprotective in most of the studies which is further explained below. Also, failure in the autophagic machinery causes cytotoxicity to the cells [228]. Predominantly, there is a significant increase in the levels of autophagosomes in β -cells in an obesity associated environment, e.g. in INS-1 β -cells treated with free fatty acids (FFAs; especially palmitate) and in pancreatic islets isolated from insulin-resistant leptin- or leptin receptor- deficient *ob/ob* and *db/db* diabetic mice as well as in high fat diet fed mice. This indicates the induction of autophagy under the state of insulin resistance and ER stress in β -cells. However, experiments performed with autophagy deficient diabetic mice models (β -*Atg7*-KO with HFD for 12 weeks) showed severely impaired glucose tolerance, lack of β -cell hyperplasia or β -cell compensation, increased β -cell apoptosis and reduced β -cell proliferation compared to the control diabetic mice (*Atg7*^{fl/fl} fed with HFD) [221, 225, 229]. This suggests that the induced autophagy acts as an adaptive response against insulin resistance and β -cell stress, whereas loss of autophagy under the same condition triggers β -cell dysfunction and inadequate β -cell mass, eventually leading to the development of β -cell failure and diabetes [223]. Moreover, one of the major cause of β -cell failure in stressed β -*Atg7*-KO mice is ER stress. The Unfolded Protein Response (UPR), as a key sign of ER stress, is insufficient under loss of autophagy in β -cells, deteriorating the adaptive response of UPR resulting in β -cell dysfunction [225, 230, 231]. Also, impaired autophagy can cause β -cell death by the accumulation of human islet amyloid polypeptide (hIAPP) oligomers which is prominently observed in human T2D islets [230]. Hence, autophagy protects the β -cells from chronic ER stress and cytotoxicity.

4.3. mTOR as the regulator of autophagy

Both mTORC1 and mTORC2 plays a pivotal role in regulating the lysosomal degradative autophagy pathway. The discovery of autophagy induction by either genetic or pharmacologic inhibition of mTORC1 was first confirmed in yeast and thereafter in *Drosophila* [232, 233]. However, the finding of mechanistical regulation of autophagy by mTORC1 in mammalian cells was fairly recent [234] and it startlingly regulates all the sequential steps of macroautophagy (Fig.7). Initially, three different groups independently unveiled that under nutrient rich-conditions, mTORC1 directly phosphorylates ULK1/2 at Ser758 and Ser638 and also phosphorylates Atg13 at Ser258 and subsequently inhibits the initiation of autophagy prompted by ULK1 complex [161-163]. This phosphorylation inhibition of ULK1 complex by mTORC1 prevents ULK1/2 from interacting with AMPK. It is shown that both mTORC1 and AMPK reciprocally regulate autophagy initiation, while AMPK is activated under nutrient or energy deprivation and it specifically phosphorylates and activates ULK1 at Ser317 and Ser777, leading to autophagy induction [160, 235]. Moreover, mTORC1 negatively regulates the nucleation of phagophore which is a prerequisite for autophagosome formation. Here, mTORC1 phosphorylates the key components of class III phosphatidylinositol 3-kinase (PI3KC3) complex namely, ATG14L, AMBRA1 and NRBF2, eventually inhibiting the Vps34 lipid kinase activity of PI3KC3 complex and its recruitment at the ER [236-238]. Additionally, mTORC1 inhibits autophagosome expansion by phosphorylating WIPI2 at Ser395 preventing it from facilitating LC3 lipidation, and also by phosphorylating p300 acetyltransferase which acetylates LC3 and prevents LC3-Atg7 interaction [239, 240]. Lastly, mTORC1 regulates the final stages of macroautophagy by phosphorylating UVRAG at Ser498 and Pacer at Ser157 respectively. This action of mTORC1 disrupts UVRAG interaction with HOPS complex and Pacer interaction with HOPS and Stx17, resulting in the inhibition of autophagosome maturation and fusion with lysosomes [241, 242].

Apart from the above regulating process, mTORC1 also regulates autophagy at the transcriptional level by targeting TFEB transcription factor which initiates the expression of genes critical for lysosomal biogenesis and autophagy machinery. mTORC1 phosphorylates TFEB at Ser211 to facilitate 14-3-3 binding and subsequent cytoplasmic sequestration, eventually preventing TFEB from its cytoplasmic to nucleus shuttling [243, 244]. The mechanistical role of mTORC2 in the regulation of autophagy is not well defined. However, mTORC2 indirectly regulates autophagy by phosphorylating AKT at the hydrophobic motif site Ser473 and activating AKT/mTORC1 axis, leading to the subsequent activation of mTORC1 and inhibition of autophagy [235]. Interestingly, mTORC2 is also confirmed to negatively regulate another unique pathway of autophagy, CMA [245]. In contrast, mTORC2 stimulates autophagy under nutrient deprivation condition [246]. This

shows that mTORC2 functions in two different ways for autophagy regulation based on the cellular environment and the type of autophagy [130].

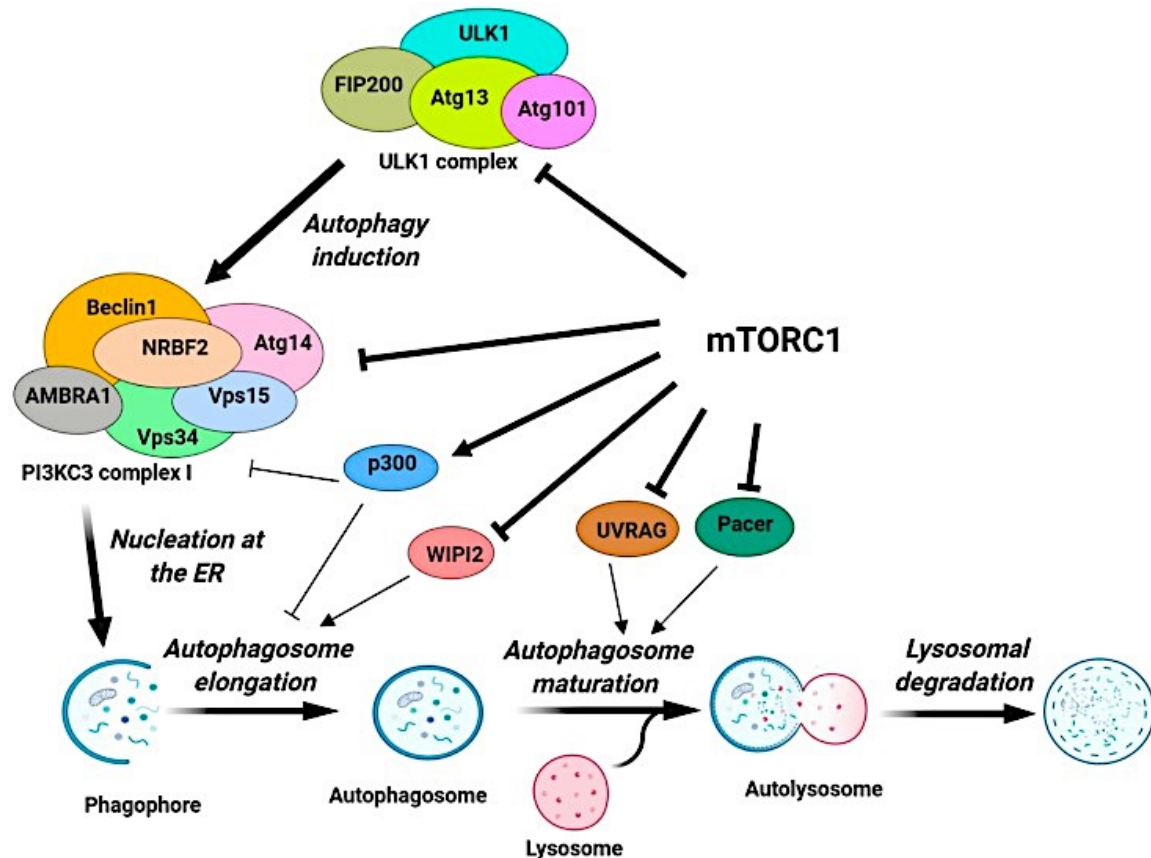


Fig.7. Representation of mTOR regulation in all sequential steps of macro autophagy. 1. mTORC1 phosphorylates ULK1 and Atg13 and inhibits their activity in autophagy initiation. 2. mTORC1 inhibits the nucleation step by phosphorylating PI3KC3 complex I, 3. mTORC1 regulates the autophagosome elongation by phosphorylating p300 and WIPI2, 4. Finally, mTORC1 regulates the fusion of autophagosome with lysosome by phosphorylating UVRAG and Pacer. From *Dossou, A.S. et al.* [247]

4.3.1. The mTORC1-autophagy axis in T2D

As described above, there is an opposite correlation between mTORC1 and autophagic flux in β -cells under diabetic conditions where mTORC1 and autophagy are activated and impaired, respectively. Thus, attempts to stimulate autophagy by inhibition of mTORC1 might be an efficient tool to preserve β -cell viability and function. In MIN6 β -cells, loss of mTORC1 activity significantly restores β -cells from apoptosis [130, 248]. Similarly, autophagy stimulation by pharmacological inhibition of mTORC1 using rapamycin in the ER stress induced diabetes mouse model (Akita mice), improved β -cell survival and function [130, 249]. This suggests that autophagy stimulation

either by mTORC1 inhibition or by AMPK activation, might be an effective approach to protect β -cells from its dysfunction and apoptosis.

In this work, I identified the connection of important signaling pathways for growth and metabolic adaptation in the β -cells, namely mTORC1 and Hippo signaling pathway. Thus, the story of Hippo pathway is described in detail below.

4.4. HIPPO signaling pathway: Basics

The mystery behind the control of organ size during development and regeneration was first ploughed by Twitty and Schwind in 1931, demonstrating that an organ must possess intrinsic signals in order to determine its size, which was corroborated by Michalopoulos while determining the factors responsible for liver regeneration [250, 251]. This knowledge was later developed by Metcalf suggesting that both internal and external signals operate in organ size control [252, 253]. Multiple model organisms and intensive research over two decades strongly substantiated that the Hippo pathway plays an imperative role in the regulation of organ size and in maintaining tissue homeostasis, as the major evolutionarily conserved components of the Hippo pathway and their functions [250]. The core components of the Hippo pathway were first discovered in *Drosophila* by genetic screening, although few components of the pathway were already known for their independent functions in mammals and other species [254]. The chronological order in the discovery of the core Hippo components in *Drosophila* is as follows: the kinase Warts (*wts*) which encodes NDR family kinases, was initially identified as tumor suppressor gene, as a result of mosaic based screening in a *Drosophila* imaginal disc in 1995 [255, 256]. Later, the gene Salvador (*Sav*) was identified by two research groups [250, 257] and subsequently Hippo (*Hpo*) that encodes the family of Ste-20 protein kinase was identified by using similar genetic screens, paving the way for the establishment of Hippo pathway in 2003 [258-261]. The pathway was named based on the tremendous overgrowth observed in the phenotype of *Drosophila* ('big-headed', reminiscent of the hippopotamus) as a result of loss of function mutations in the genes *Wts*, *Sav* and *Hpo* [254]. Furthermore, the gene *Mats* whose mutation caused massive tissue growth as that of *Hpo*, *Wts* and *Sav*, was identified and added to the signaling cascade of the Hippo pathway [262, 263]. Mutant cells grew faster than normal cells and were resistant to pro-apoptotic signals. Interestingly, Hariharan *et al.* showed that the physical interaction of *Sav* with *Wts* limits cell proliferation by transcriptionally regulating *Cylin E* and *Diap* [258]. This led to the understanding that the signal cascade of Hippo pathway links to the transcriptional regulator(s) that switches 'on' and 'off' the genes responsible for cell proliferation and growth. In relation to this understanding, Huang *et al.* found a transcriptional activator using yeast two hybrid screens

with Wts as bait and eventually identified *Yorkie* (Yki) (also known as YAP and its paralog TAZ in mammals) as the downstream transcriptional regulators of Hippo pathway [264]. Evidence for this was provided by many independent groups in deciphering the mechanistical role of highly conserved core kinases in *Drosophila*. In mammals, the direct homologs of all core components of the Hippo pathway, namely, Hpo, Sav, Wts, Mats and Yki are Mammalian sterile 20-like 1/2 (MST1/2 a.k.a. STK3/4) [265, 266], Salvador (SAV1), Large tumor suppressor homolog 1/2 (LATS1/2) [267, 268], MOB kinase activator1 A/B (MOB1A/B) [269-271] and Yes associated protein (YAP) /Transcriptional co-activator with PDZ binding motif (TAZ) [272, 273] respectively. The mechanistical actions of the mammalian Hippo pathway is similar as in *Drosophila*. Several extracellular upstream signals control the core components which includes GPCR (G protein-coupled receptors), cell junction, Extracellular matrix (ECM) proteins, hormonal and metabolic cues as well as soluble factors like amphiregulin that binds EGFR [274]. The pathway is switched 'on' when MST1/2 forms a complex with Sav1 and undergoes activation phosphorylation. Sav1 contains WW-domain that enables it to integrate with the upstream signals bringing light to the cascade activation [275]. However, MST1/2 kinases can be activated without any upstream signals, by undergoing dimerization and phosphorylating Sav1 [276]. The phosphorylated MST1/2-Sav1 complex phosphorylates MOB1 and LATS1/2 at its hydrophobic motifs (LATS1 at T1079 and LATS2 at T1041) in a canonical manner and consequently, activated LATS1/2 phosphorylates the transcriptional activator(s) YAP/TAZ at multiple sites [274, 277, 278]. Correspondingly, NF2 (Merlin) regulate both MST1/2 and LATS1/2 kinases in the upstream level.

Also, it has been shown that that NF2 directly binds to LATS1/2 and foster its activation independent of MST1/2 [278]. Notably, apart from MST1/2 kinases, LATS1/2 are phosphorylated at their hydrophobic motifs and activated by two different forms of MAP4Ks (MAP4K1/2/3/5 and MAP4K4/6/7) [279, 280]. Eventually, YAP phosphorylation at S127 and TAZ at S89 promote their binding with 14-3-3 and subsequent cytoplasmic retention, while additional phosphorylation of YAP at S381 and TAZ at S311 respectively, primes YAP/TAZ to undergo further phosphorylation by CK1 δ/ϵ kinase, which subsequently activates the phosphodegron motif of YAP/TAZ resulting in the recruitment of β -TRCP, following polyubiquitylation and degradation of YAP/TAZ [281-283]. The above process is silent when Hippo is switched 'off', enabling unphosphorylated YAP/TAZ to translocate into the nucleus and bind with several transcriptional factors, especially, TEAD1-4 (TEA/ATTS domain) transcription factor family proteins in order to regulate the expression of genes responsible for cell proliferation, survival and migration, and tissue growth [284-287]. This suggests that the Hippo pathway limits cell proliferation and promotes apoptosis simultaneously.

Although several signaling pathways, namely Wnt/ β -Catenin, Notch, TGF- β and mTOR signaling pathways are involved in determining cell number and cell size in metazoans, the Hippo pathway functions as key regulator in determining the organ size by directing both cell proliferation and apoptosis instantaneously and it also acts as a signal hub in integrating all the above mentioned signaling pathways [250].

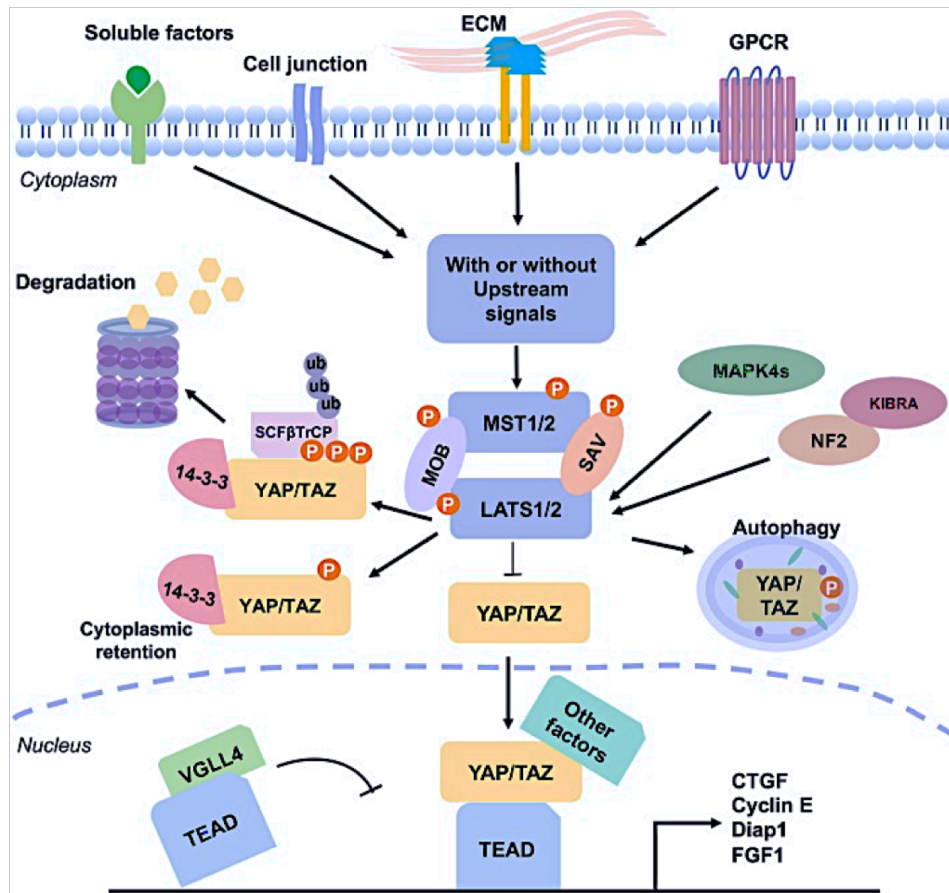


Fig.8. Schematic representation of the mechanical role of mammalian Hippo signaling pathway. The Hippo pathway is switched ON, upon phosphorylation and activation of MST1/2 kinases which is stimulated by upstream signals such as GPCRs, ECM proteins, cell junction and soluble factors. MST1/2 activation regulates LATS1/2 activity, which subsequently phosphorylates YAP/TAZ and inhibit the activity of YAP/TAZ engagement in gene expression for cell proliferation and growth. On the other hand, Kibra associate with NF2 and MAPK4s to directly activate Hippo core kinase LATS1/2 which is independent of the upstream signals. From *Chen, Y.A. et al.* [274].

4.4.1. The Hippo MST1/2 kinase: Structure, Function and Regulation

The MST family is known as one of the subfamilies (GCK subfamily) of STE superfamily which was named after the yeast Sterile20 Kinase [266]. There are five different MST kinases in

mammals, which can be subdivided into two groups, namely, MST1/2 (STK4/3) and MST3/4/YSK1 (STK24/26/25), which is conserved in all metazoans [288, 289].

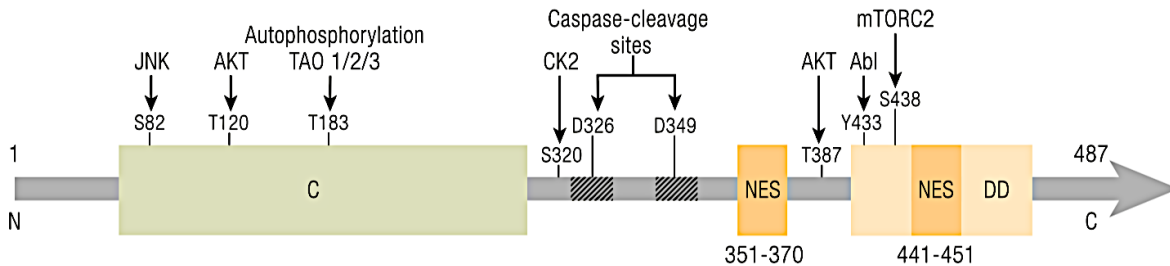


Fig. 9. Secondary structure of Hippo kinase MST1: N-terminal of MST1 is composed of a kinase catalytic domain; and the non-catalytic domain consists of two caspase cleavage sites, two nuclear export sites (NES) and a dimerization domain (DD) or Salvador-Rassf-Hippo(SARAH) domain which is from 431 to 487 aa residue at the C-terminal. From *Ardestani et al.* [290].

The kinases MST1 and MST2 are homologous by sequence and are identical in their structural organization, with the polypeptides of 487 and 491 amino acids respectively [291]. MST1 kinase consists of an N-terminal catalytic domain and a C-terminal regulatory region encompassing an autoinhibitory domain (331 to 391 aa residue), two caspase cleavage sites, two nuclear export signals and a unique coiled-coil structure known as Salvador-Rassf-Hippo or SARAH domain (431 to 487 aa residue) [292, 293]. Remarkably, the unique characteristic of MST1/2 kinases is forming homodimers via the SARAH domain for their stability and activity [294]. The SARAH domain of two monomers (MST1-MST1 and MST2-MST2) interact with each other by forming antiparallel helices via non-covalent interactions namely hydrophobic, electrostatic and hydrogen bonds [295]. Moreover, MST1/2 kinases undergo heterodimerization with other SARAH domain containing proteins such as, Ras association domain family (RASSF1-6) proteins and SAV1 or WW45 scaffold protein for their activation and regulation [296].

The MST1 kinase is activated by autophosphorylation at the region T183 of the activation loop in response to external signals [276, 297]. This activation loop phosphorylation at the region T183 is also regulated by TAO1/2/3 kinases [298, 299]. Additionally, MST1 activity is regulated by other protein kinases by transphosphorylation such as AKT at T120 and T387 residues [300-302], JNK at S82 residue [303], c-Abl at Y433 residue [304], mTORC2 at S438 residue [305] and CK2 at S320 residue [306]. Although the transphosphorylation by the kinases JNK, c-Abl and CK2 activates MST1 kinase, the phosphorylation initiated by AKT and mTORC2 inhibits the MST1 kinase activity. Interestingly, the metal dependent protein phosphatase (PPM) family members,

PHLPP1/2 also regulate the MST1 kinase activation. PHLPP1/2 dephosphorylate MST1 kinase at the AKT target phosphorylation site T387 residue, resulting in the activation of MST1 kinase [307, 308]. Moreover, the two caspase cleavage sites at D326 and D349 which separates the regulatory region (autoinhibitory domain and SARAH domain) from the catalytic domain, is essential to elevate the MST1 activity. During apoptosis, the cleaved form of MST1 kinase (N-terminal catalytic domain, 36-38kDa) is translocated into the nucleus to target nuclear substrates, as it is free from the NES (nuclear export signals) located at the regulatory region of the protein [309].

The cleaved MST1 kinase triggers apoptosis by phosphorylating Histone-H2B at Ser14 resulting DNA fragmentation and chromatin degradation [310]. Although MST1/2 kinases phosphorylate and activate LATS1/2 kinases and mediate cell apoptosis by inactivating the downstream transcriptional activators YAP/TAZ, it is also involved in the regulation of FOXO1 and FOXO3 transcription factors which notably triggers neuronal cell death [311]. Furthermore, MST1/2 kinases regulate Ets family member GABP transcription factor activity by inhibiting GABP mediated YAP gene expression [312].

Formerly, global knockout of both MST1 and MST2 in mice embryos developed early lethality, while single knockout (MST1^{-/-} or MST2^{-/-}) was indistinguishable from the wildtype as they were viable, fertile and developed normally [313]. It is apparent from the above study that both MST1 and MST2 Kinase function redundantly and are critical for early mouse development [314]. Moreover, conditional MST1/2 knockout in the liver and colon of mice, confirmed the conserved significant role of MST1/2 kinases as the organ size regulator and as a potent tumor suppressor [315]. Unlike *Drosophila*, MST1/2 kinases carry several regulatory and functional roles in mammals deviating from its conserved role in Hippo pathway. Recently, MST1/2 role in the regulation of both innate and adaptive immunity is unveiled as it is showed that MST1 kinase activate non-canonical Hippo signaling pathway via MOB1A/B or NDR1/2 or crosstalk with many other signaling pathways for the regulation process [316]. Particularly, the core kinases MST1/2 play a critical role in the regulation of T cell proliferation, migration, homing and differentiation [316].

4.4.2. The Hippo LATS1/2 Kinase

Another putative Ser/Thr Kinase in the Hippo signaling cascade with broad regulatory functions is LATS1/2 which belongs to the NDR family of kinases under the subgroup of AGC protein kinase family [317]. As mentioned above, *Lats* gene was first discovered in *Drosophila* in 1995, which later determined to be the evolutionarily conserved gene with homologs in other species such as,

yeast (*dbf2*, *cbk1*, *orb6*), *C.elegans* (*cLats*), mice (*Lats1*, *Lats2*) and humans (*NDR1*, *NDR2*, *LATS1*, *LATS2*) [267, 268, 318]. The sequence database search located the human *LATS1* and *LATS2* genes to chromosome 6q24-51 and 13q11-q12 regions respectively, exhibiting loss of heterozygosity in primary cancers, indicating that *LATS1* and *LATS2* are tumor suppressor genes [268, 319]. However, downregulation of *LATS1/2* kinases were spotted in tumor development rather *LATS1/2* mutations which is seldom [320].

Unlike other AGC kinases, human *LATS1* and *LATS2* kinases are almost homologous to each other (Fig.10), sharing conserved domains that includes C-terminal Ser/Thr Kinase or catalytic domain (708-1130 residue for *LATS1* and 670-1108 residue for *LATS2*), a Protein Binding Domain (PBD), two *LATS* conserved domains and an Ubiquitin binding domain (UBA) in the N-terminal of the *LATS1/2* kinase. As a significant factor, *LATS1/2* contain more than one PPxY motifs (two in *LATS1* and one in *LATS2*) which specifically interacts with WW-domain containing proteins for protein-protein interaction, particularly, *LATS1/2* interacts with WW-domains of YAP/TAZ and one of the NEDD4 E3 ubiquitin ligase ITCH via PPxY motifs. One of the distinct features in *LATS1* and *LATS2* structure is the presence of P-stretch (aa.236-266) in *LATS1* and PA (proline Alanine) repeat in *LATS2*. The proteins MOB1, ZYXIN, LIMD1 bind within the PBD domain for regulation of *LATS* activity and localization [317, 320].

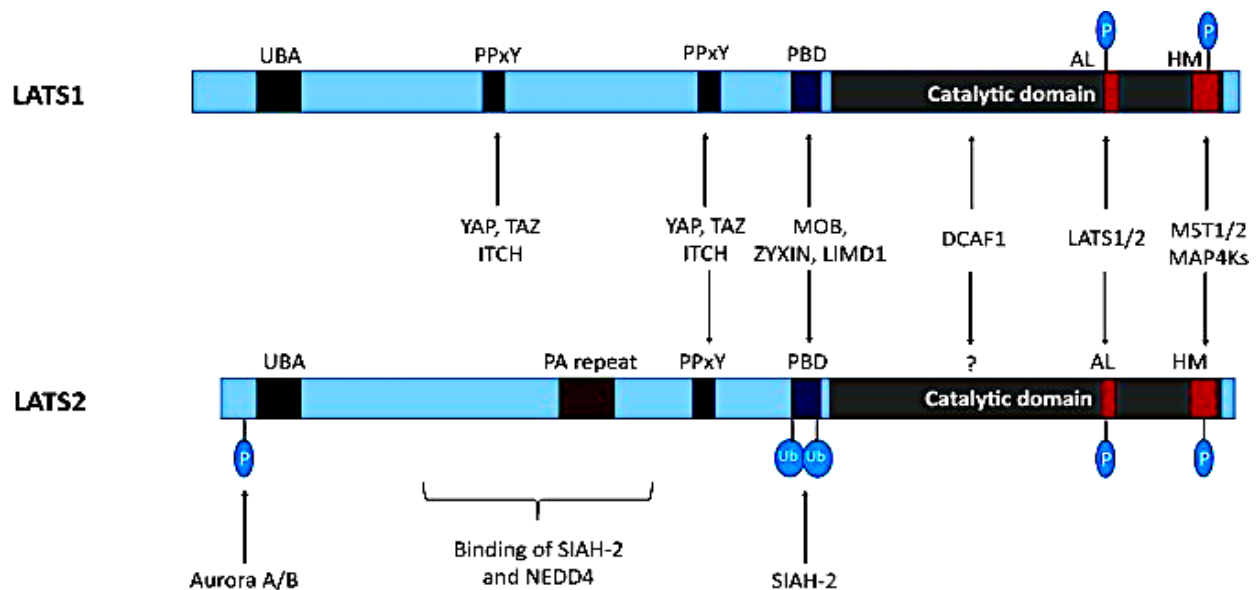


Fig.10. Hippo Kinase LATS1/2 domain structure and protein interaction: LATS1/2 contains hydrophobic motif (HM) at the C-terminal, is regulated by MST1/2 and MAP4Ks by phosphorylation, which is followed by autophosphorylation of LATS1/2 at the activation loop (AL); There is a ubiquitin associated domain (UBA) in the N-terminal and a protein binding domain (PBD) that regulates LATS1/2 activity and availability, the transcriptional co-activators YAP/TAZ interacts with LATS1/2 via PPxY motifs; there is an additional PA repeat and also an Aurora A/B phosphorylation site which is distinct in LATS2. From Meng,Z. et al. [317].

Regulation of LATS1/2 kinase turnover: LATS1/2 kinases are regulated at both transcriptional and post-transcriptional levels. Notably, the regulation of LATS1/2 by post-translational modifications is beyond phosphorylation. First and foremost, LATS1/2 activity is tightly regulated by phosphorylation at two conserved regulatory motifs, namely the catalytic domain and the hydrophobic motif at the C-terminal end [321]. MST1/2 kinases and MAP4Ks phosphorylate LATS1/2 at their hydrophobic motifs, LATS1 at Thr1079 and LATS2 at Thr1041 respectively, as deletion of both MST1/2 and MAP4Ks result in the destruction of hydrophobic motif phosphorylation and LATS1/2 activation [279, 280, 322]. Furthermore, binding of LATS1/2 with MOB1-SAV1-MST1/2 complex stimulates the phosphorylated MOB1A/1B to trigger LATS1/2-MOB1A/1B complex dissociation from MST1/2 and undergo autophosphorylation in the activation loop of LATS1/2 (LATS1 at S909 and LATS2 at S871), eventually resulting in the activation of LATS kinases [323]. This shows the regulation of LATS1/2 activation by MST1/2 and MAP4Ks, and an acute role of MOB1A/1B as a scaffolding protein. As a contrary, PP2A phosphatase determined to negatively modulate LATS1/2 activity by dephosphorylation, as it was shown that PP2A inhibitor okadaic acid, promotes LATS1/2 activation [324, 325]. Remarkably, LATS2 is phosphorylated by Aurora-A kinase at the residue Ser83 for LATS2 mobilization to the centrosomes during mitosis [326]. Additionally, while the kinase Nuak1 which is a part of AMPK family, impairs LATS1 stability by direct Ser464 phosphorylation, H-Ras increases the stability of LATS2 via signaling cascade that includes ATR kinase and Chk1 [327, 328]. Another important post-translational modification for LATS1/2 regulation is ubiquitination. As mentioned earlier, the NEDD4-like family of E3 ubiquitin ligases such as NEDD4, ITCH/AIP1, WWP1, WWP2, SMURF1 and SMURF2, contain WW domains which directly interacts with the PPxY motifs of LATS1/2, resulting in destabilization via ubiquitination and degradation of LATS kinases [320, 329]. The E3 ubiquitin ligase CRL4 (DCAF1) ubiquitinates and inhibits LATS1/2 in NF2 deficient tumor cells [330]. Interestingly, SIAH2, a hypoxia-mediated E3 ubiquitin ligase, ubiquitinates and destabilizes LATS2, resulting in YAP activation under hypoxia indicating the role of LATS1/2 in stress response and differentiation [331]. Recently, it is reported that LATS2 is also regulated by O-GlcNAcylation post-translational modification which is mediated by O-GlcNAc transferase (OGT) in cancer cells. LATS2 O-GlcNAcylation at the residue Thr436 blocks further activation of LATS and dysregulates the Hippo pathway, subsequently resulting in YAP hyperactivation and tumorigenesis [332]. Likewise, the transcriptional regulation of both LATS1 and LATS2 were studied widely. The kinase LATS1 expression is identified to be regulated by the transcription factor CUX1, whereas, the transcription factors P53 and FOXP3 are determined to regulate the

expression of LATS2 [333-335]. Surprisingly, LATS2 transactivation is regulated by YAP/TAZ activity, as it is proved that YAP-TEAD complex bind *LATS2* promoter for LATS2 transcription, contributing to the negative feedback mechanism of the Hippo pathway, which demonstrates the functional difference between LATS1 and LATS2, and is also evolutionarily conserved in *Drosophila* [336]. Moreover, LATS2 mRNA levels are regulated by miRNAs and mRNA binding proteins, as miRNA-224-3p, miRNA-372, miRNA-373 and miRNA-31 shown to downregulate LATS2 expression [337-340]. Also, Tristetrapolin (TTP), an ARE binding protein shown to bind the 3'UTR of LATS2 mRNA to destabilize and downregulate LATS2 protein expression [341]. These findings enrich the understanding that LATS1/2 kinases are regulated by several mechanisms for maintenance of homeostasis in cell proliferation and tumor development.

Redundant and divergent functions of LATS1 and LATS2 kinases:

As mentioned earlier, LATS1/2 kinases broadly function as the tumor suppressors by negatively regulating YAP/TAZ, which can occur either by canonical or by non-canonical Hippo signaling pathway, based on the stimuli and cell type. Notably, LATS1/2 also function via Hippo independent pathways. Initially, it was proved that loss of *Drosophila* Warts (homolog of mammalian LATS1/2) is larval lethal [255, 256]. However, this functional understanding is twisted in mammals, as LATS1 knockout mice are viable but develop tumors, while LATS2 knock out mice exhibit embryonal lethality [325, 342, 343]. Also, LATS2 deficient mouse embryonic fibroblasts (MEFs) display loss of contact inhibition as cellular homeostatic response to over proliferation [325, 342]. LATS2 determined to play a significant role in centrosome duplication and in maintenance of mitotic fidelity and genomic stability during embryogenesis, nevertheless both LATS1 and LATS2 kinases are crucial for early embryonic development as they distinguish between inner cell mass (ICM) and trophectoderm in preimplantation embryos [344]. Moreover, LATS1/2 play a critical role in heart development, as heart specific deletion of LATS1/2 instigated heart abnormalities [345, 346]. Although both LATS1 and LATS2 regulate G2/M transition of cell cycle, LATS2 additionally regulates G1/S transition phase of cell cycle by promoting activation of P53-dependent checkpoint, eventually arresting cell cycle progression and inhibiting cell proliferation [320, 347]. Apparently, overexpression of both LATS1 and LATS2 induce apoptosis with divergent mechanistical action. LATS1 preferentially upregulates the pro-apoptotic proteins Bax and P53 whereas LATS2 downregulates anti-apoptotic protein Bcl-X_L and Bcl-2 under mitotic stress and oncogene activation [348, 349]. Also, LATS2 induce apoptosis via the P73-YAP complex in leukemic cells [350, 351]. Furthermore, LATS1/2 can be directly modulated by upstream GPCRs for either activation or inactivation of YAP based on the nature and type of the

G proteins [352-354]. LATS1/2 regulate both Epithelial to Mesenchymal Transition (EMT) and migration during development and oncogenic transformation [351]. LATS2 unique functions are attributed to its nuclear localization, as it binds with several nuclear proteins within the nucleus. LATS2 stabilizes the activity of P53 tumor suppressor [327, 333, 355]. Moreover, LATS2 regulates chromatin dynamics by directly binding to Polycomb repressive complex 2 (PRC2) in the chromatin and positively regulating the histone methyltransferase activity of PRC2 at the mRNA and protein levels [356]. LATS2 also binds the chromatin and negatively regulates β -catenin induced transcription [357]. Interestingly, LATS2 plays an important role in the metabolic homeostasis, as it suppresses the hepatic cholesterol accumulation by regulating the transcriptional activity of SREBP1 and SREBP2 transcriptional factors [358].

These findings show (1) the exclusive role of LATS1/2 kinases which act beyond the Hippo pathway and (2) while LATS1/2 may function redundantly, they have their own specific substrates in different cell types or cellular context.

4.5. Role of Hippo pathway in Islet biology and diabetes

Hippo pathway in pancreas development

Although the transcription factors that define the identity of pancreas cell subsets are widely known, the signaling pathways that tightly regulate growth, proliferation and survival of pancreatic cell subsets by their integration still needs clarity. As Hippo pathway plays a prominent role in regulating organ size and tissue homeostasis, it is undoubtedly crucial for pancreas development and architecture, especially in the regulation of stem and progenitor cells [359-362]. The mouse pancreas undergoes two different stages during its complete development, namely primary and secondary transitions that occur between E9.5 to E12.5 and E13.5 to E16.5, respectively [363, 364]. At the primary transition, the absolute numbers of transcription factor PDX1 expressing progenitor cells define the size of pancreas by bringing forth ductal, acinar and endocrine compartments, whereas the secondary transition is characterized by robust proliferation and differentiation in the pancreatic epithelium. The acinar compartment is dependent on the expression of PTF1a, while the endocrine progenitor cells express Neurogenin-3 (Ngn3) transcription factor and the ductal epithelium express SOX9 transcription factor during differentiation [365-369]. Crucially, Ngn3 expressing endocrine compartment are mitotically quiescent [365, 368], and a study on pancreas specific MST1/2 knockout mice during mouse pancreas development showed that the expression of YAP transcriptional activator is totally

repressed following the endocrine fate specification although it is transiently active in the exocrine cells [370, 371]. This finding is consistent with the experiments performed using human cadaveric islets, which unveiled that YAP is downregulated and undetectable in the endocrine progenitor cells, and the onset of Ngn3 expression is adequate to extinguish YAP expression at the mRNA levels [372-374]. Consequently, the YAP-dependent role of Hippo MST1/2 kinase is minimal in endocrine islet cells, as YAP is selectively repressed and named as 'disallowed' gene in all developing islet cells (rodent/human islets and in β -cell lines) [290]. Further investigation of endocrine specification from bipotent pancreatic progenitors derived from human embryonic stem cells at a single cell level revealed that YAP1 functions as the gatekeeper in determining the fate of pancreatic progenitors in the developing pancreas [375]. Mamidi *et al.* show that the progenitor state in the bipotent pancreatic progenitors is maintained by expression of YAP1-TEAD4-HES1 that responds to fibronectin-integrin α 5 β 1 signaling, however, the enrichment of the ECM proteins such as laminin and collagen diminishes the fibronectin-integrin α 5 β 1-YAP1 axis expression and enhances the expression of Ngn3 for endocrine specification [375]. In line with this understanding, Melton's group also showed the significance of YAP inhibition for the differentiation of stem cell derived insulin producing β -cells (SC- β -cells) [376]. Chemical or genetic inhibition of YAP increases the generation of endocrine differentiation and SC- β -cells, whereas, sustained activation of YAP impairs β -cell differentiation [376]. However, TAZ expression levels are detectable and extremely low in the adult mouse and human islets [290, 377, 378]. Hence, it is apparent that the genetic ablation of MST1/2 kinases are not sufficient to retrieve β -cells from its quiescence state and to induce β -cell proliferation under physiological conditions [290].

The Hippo pathway regulates β -cell survival and function in diabetes

As described above the Hippo cascade kinases are functional but minimal in mature and functional β -cells under normal physiological conditions. In 2014, my lab showed that that the core component of the Hippo pathway, MST1 kinase, is chronically activated in pure β -cells as well as in rodent and human islets under multiple diverse diabetic conditions. Activated MST1 in the form of both full length auto phosphorylated MST1 at T183 (pMST1-T183) and cleaved MST1 (cMST1) is abundant in isolated islets from diabetic mice (HFD and db/db mice) as well as from human individuals with T2D [379, 380]. The hyperactivation of MST1 kinase is not only confined to β -cells but is also activated in the kidney of hyperglycemic IRS2KO mice, epididymal fats of HFD mice, cardiomyocytes and podocytes of rodents under high glucose conditions, signifying the pathologic activation of MST1 kinase in several tissues during diabetes progression [290, 379, 381-384].

Further work show that the activated MST1 induces β -cell apoptosis via the mitochondrial dependent pathway by the activation of pro-apoptotic BCL-2 family member protein BIM. The upregulation of BIM elevates the pro-apoptotic BAX / antiapoptotic BCL-2 ratio, resulting in cytochrome C release and subsequent caspases activation (Caspase 9 and caspase 3) causing β -cell apoptosis [290]. Apart from triggering apoptotic signals, MST1 phosphorylates and destabilizes PDX1 transcription factor by promoting ubiquitin mediated PDX1 degradation and subsequently, resulting in β -cell dysfunction [379].

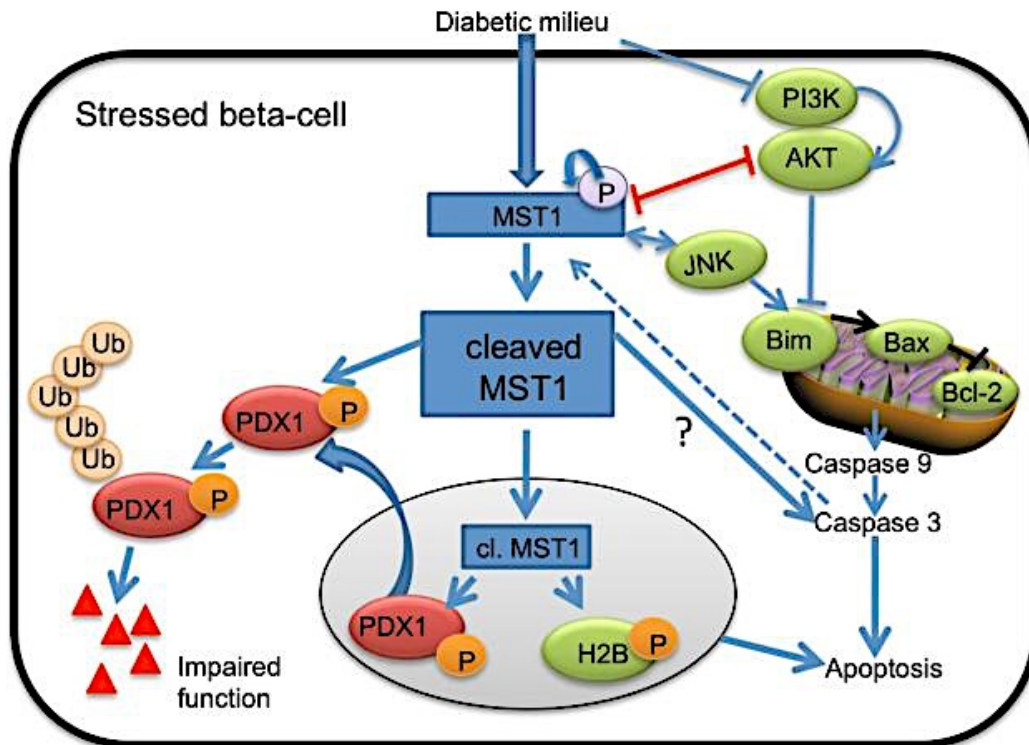


Fig.11. The mechanistical action of MST1 kinase in stressed pancreatic β -cell: Activated MST1 kinase triggers mitochondria mediated β -cell apoptosis via JNK/AKT signaling. The acceleration of β -cell apoptosis is increased by Caspase3 mediated cleavage of MST1 into a constitutive active form by a positive feedback mechanism. Also cl.MST1 kinase translocate into the nucleus and destabilizes PDX1 resulting in β -cell dysfunction. Additionally, cl.MST1 phosphorylates Histone H2B and induces chromatin condensation, eventually leading to β -cell apoptosis. From Ardestani *et al.* [379].

Conversely, genetic inhibition of MST1 in both rodent and human islets as well as in β -cell cell line could rescue the β -cells from apoptosis and restore β -cell function under diabetic conditions [379]. Likewise, Merlin, an upstream component of Hippo pathway, plays a significant role in β -cell survival as the loss of Merlin in INS1-E β -cell line and human islets protects the β -cells from apoptosis under diabetic conditions [385, 386]. Furthermore, my lab identified that the overexpression of LATS2 which acts downstream to MST1 kinase, is sufficient to trigger β -cell

apoptosis and impair β -cell function in rodent INS-1E cells and human islets [290]. Altogether, the Hippo pathway plays a crucial role in β -cells under diabetic conditions by regulating β -cell viability and function.

5. AIM OF MY THESIS

The major aim of diabetes research is to find a definite and eternal solution for the cure of this chronic metabolic disorder. The absolute and/or relative insulin deficiency in diabetes is the results of an inadequate functional β -cell mass which occurs through β -cell dysfunction and/or loss of β -cells via apoptosis or dedifferentiation. As described above, the Hippo kinase MST1 plays an indispensable role in triggering both β -cell dysfunction and apoptosis.

The 1st aim of my PhD thesis was to determine efficacy and functional significance of a small molecule inhibitor of MST1 for restoration of β -cell function and survival in several experimental models of diabetes *in vitro*, *ex vivo* and *in vivo*.

The 2nd part of my thesis work was absolutely focused on investigating the role of LATS2 kinase in the regulation of stress-responsive signaling pathways and β -cell apoptosis. The initial findings that were already achieved in my lab in relation to LATS2 are that

- (1) LATS2 overexpression is sufficient to impair β -cell function and trigger β -cell apoptosis.
- (2) Loss of LATS2 kinase rescues β -cells from apoptosis under diabetic conditions in INS1-E cells and human islets.
- (3) β -cell specific LATS2 ablation protects from STZ-induced β -cell destruction and diabetes, and
- (4) LATS2 induces β -cell apoptosis via regulation of mTORC1 and autophagy pathways.

To complete the full picture of LATS2's regulation and action in pancreatic β -cells under physiological conditions and at a diabetic state, I aimed to address the following remaining questions, whether

- a) the endogenous LATS1/2 is activated in β -cells/islets under diabetic conditions,
- b) LATS2 deficiency in both isolated mice and human islets is sufficient to rescue β -cells from apoptosis using complementary approaches and
- c) β -cell specific LATS-KO mice (β -LATS2-KO) may have a β -cell protective phenotype during HFD-induced β -cell decompensation and failure.

Mechanistically, I hypothesized a dynamic mutual cross-talk between Hippo kinase LATS2, mTORC1 and the important degradative pathway autophagy.

With my work, I can provide further insights into the regulation and function of the complex “ β -cell Hippo pathway” at both physiological and disease states.

REFERENCES

1. Karamanou, M., et al., *Milestones in the history of diabetes mellitus: The main contributors*. World J Diabetes, 2016. **7**(1): p. 1-7.
2. Ramirez-Dominguez, M., *Historical Background of Pancreatic Islet Isolation*. Adv Exp Med Biol, 2016. **938**: p. 1-9.
3. Lakhtakia, R., *The history of diabetes mellitus*. Sultan Qaboos Univ Med J, 2013. **13**(3): p. 368-70.
4. Alpert, J.S., *An Amazing Story: The Discovery of Insulin*. Am J Med, 2016. **129**(3): p. 231-2.
5. Karamitsos, D.T., *The story of insulin discovery*. Diabetes Res Clin Pract, 2011. **93 Suppl 1**: p. S2-8.
6. American Diabetes, A., *Diagnosis and classification of diabetes mellitus*. Diabetes Care, 2014. **37 Suppl 1**: p. S81-90.
7. Cohrs, C.M., et al., *Dysfunction of Persisting beta Cells Is a Key Feature of Early Type 2 Diabetes Pathogenesis*. Cell Rep, 2020. **31**(1): p. 107469.
8. Mezza, T., et al., *beta-Cell Fate in Human Insulin Resistance and Type 2 Diabetes: A Perspective on Islet Plasticity*. Diabetes, 2019. **68**(6): p. 1121-1129.
9. Zhong, F. and Y. Jiang, *Endogenous Pancreatic beta Cell Regeneration: A Potential Strategy for the Recovery of beta Cell Deficiency in Diabetes*. Front Endocrinol (Lausanne), 2019. **10**: p. 101.
10. Pagliuca, F.W. and D.A. Melton, *How to make a functional beta-cell*. Development, 2013. **140**(12): p. 2472-83.
11. Matsuoka, T.A., et al., *Members of the large Maf transcription family regulate insulin gene transcription in islet beta cells*. Mol Cell Biol, 2003. **23**(17): p. 6049-62.
12. Vanhooose, A.M., et al., *MafA and MafB regulate Pdx1 transcription through the Area II control region in pancreatic beta cells*. J Biol Chem, 2008. **283**(33): p. 22612-9.
13. Andrali, S.S., et al., *Glucose regulation of insulin gene expression in pancreatic beta-cells*. Biochem J, 2008. **415**(1): p. 1-10.
14. Gao, T., et al., *Pdx1 maintains beta cell identity and function by repressing an alpha cell program*. Cell Metab, 2014. **19**(2): p. 259-71.
15. Komatsu, M., et al., *Glucose-stimulated insulin secretion: A newer perspective*. J Diabetes Investig, 2013. **4**(6): p. 511-6.
16. MacDonald, P.E., J.W. Joseph, and P. Rorsman, *Glucose-sensing mechanisms in pancreatic beta-cells*. Philos Trans R Soc Lond B Biol Sci, 2005. **360**(1464): p. 2211-25.

17. Ashcroft, F.M. and P. Rorsman, *Diabetes mellitus and the beta cell: the last ten years*. Cell, 2012. **148**(6): p. 1160-71.
18. Inagaki, N., et al., *Reconstitution of IKATP: an inward rectifier subunit plus the sulfonylurea receptor*. Science, 1995. **270**(5239): p. 1166-70.
19. Grodsky, G.M., *A threshold distribution hypothesis for packet storage of insulin and its mathematical modeling*. J Clin Invest, 1972. **51**(8): p. 2047-59.
20. Hosker, J.P., et al., *Similar reduction of first- and second-phase B-cell responses at three different glucose levels in type II diabetes and the effect of gliclazide therapy*. Metabolism, 1989. **38**(8): p. 767-72.
21. Gembal, M., et al., *Mechanisms by which glucose can control insulin release independently from its action on adenosine triphosphate-sensitive K⁺ channels in mouse B cells*. J Clin Invest, 1993. **91**(3): p. 871-80.
22. Leech, C.A., et al., *Molecular physiology of glucagon-like peptide-1 insulin secretagogue action in pancreatic beta cells*. Prog Biophys Mol Biol, 2011. **107**(2): p. 236-47.
23. Yajima, H., et al., *cAMP enhances insulin secretion by an action on the ATP-sensitive K⁺ channel-independent pathway of glucose signaling in rat pancreatic islets*. Diabetes, 1999. **48**(5): p. 1006-12.
24. Itoh, Y., et al., *Free fatty acids regulate insulin secretion from pancreatic beta cells through GPR40*. Nature, 2003. **422**(6928): p. 173-6.
25. Komatsu, M. and G.W. Sharp, *Palmitate and myristate selectively mimic the effect of glucose in augmenting insulin release in the absence of extracellular Ca²⁺*. Diabetes, 1998. **47**(3): p. 352-7.
26. Gilon, P. and J.C. Henquin, *Mechanisms and physiological significance of the cholinergic control of pancreatic beta-cell function*. Endocr Rev, 2001. **22**(5): p. 565-604.
27. Meier, J.J., J.D. Veldhuis, and P.C. Butler, *Pulsatile insulin secretion dictates systemic insulin delivery by regulating hepatic insulin extraction in humans*. Diabetes, 2005. **54**(6): p. 1649-56.
28. Jung, S.H., et al., *Adapting to insulin resistance in obesity: role of insulin secretion and clearance*. Diabetologia, 2018. **61**(3): p. 681-687.
29. Barrett, E.J., et al., *The vascular actions of insulin control its delivery to muscle and regulate the rate-limiting step in skeletal muscle insulin action*. Diabetologia, 2009. **52**(5): p. 752-64.
30. Palmer, R.M., D.S. Ashton, and S. Moncada, *Vascular endothelial cells synthesize nitric oxide from L-arginine*. Nature, 1988. **333**(6174): p. 664-6.
31. Zeng, G., et al., *Roles for insulin receptor, PI3-kinase, and Akt in insulin-signaling pathways related to production of nitric oxide in human vascular endothelial cells*. Circulation, 2000. **101**(13): p. 1539-45.
32. Vincent, M.A., et al., *Skeletal muscle microvascular recruitment by physiological hyperinsulinemia precedes increases in total blood flow*. Diabetes, 2002. **51**(1): p. 42-8.
33. Vincent, M.A., et al., *Inhibiting NOS blocks microvascular recruitment and blunts muscle glucose uptake in response to insulin*. Am J Physiol Endocrinol Metab, 2003. **285**(1): p. E123-9.

34. Bradley, E.A., et al., *Local NOS inhibition impairs vascular and metabolic actions of insulin in rat hindleg muscle in vivo*. Am J Physiol Endocrinol Metab, 2013. **305**(6): p. E745-50.
35. Andre, N., *Hippocrates of Cos and apoptosis*. Lancet, 2003. **361**(9365): p. 1306.
36. Kerr, J.F., A.H. Wyllie, and A.R. Currie, *Apoptosis: a basic biological phenomenon with wide-ranging implications in tissue kinetics*. Br J Cancer, 1972. **26**(4): p. 239-57.
37. Diamantis, A., et al., *A brief history of apoptosis: from ancient to modern times*. Onkologie, 2008. **31**(12): p. 702-6.
38. Gorczyca, W., J. Gong, and Z. Darzynkiewicz, *Detection of DNA strand breaks in individual apoptotic cells by the in situ terminal deoxynucleotidyl transferase and nick translation assays*. Cancer Res, 1993. **53**(8): p. 1945-51.
39. Archana, M., et al., *Various methods available for detection of apoptotic cells--a review*. Indian J Cancer, 2013. **50**(3): p. 274-83.
40. Dorn, G.W., 2nd, *Molecular mechanisms that differentiate apoptosis from programmed necrosis*. Toxicol Pathol, 2013. **41**(2): p. 227-34.
41. Loreto, C., et al., *The role of intrinsic pathway in apoptosis activation and progression in Peyronie's disease*. Biomed Res Int, 2014. **2014**: p. 616149.
42. Kharbanda, S., et al., *Role for Bcl-xL as an inhibitor of cytosolic cytochrome C accumulation in DNA damage-induced apoptosis*. Proc Natl Acad Sci U S A, 1997. **94**(13): p. 6939-42.
43. Kluck, R.M., et al., *The release of cytochrome c from mitochondria: a primary site for Bcl-2 regulation of apoptosis*. Science, 1997. **275**(5303): p. 1132-6.
44. Favalaro, B., et al., *Role of apoptosis in disease*. Aging (Albany NY), 2012. **4**(5): p. 330-49.
45. Johnson, J.D. and D.S. Luciani, *Mechanisms of pancreatic beta-cell apoptosis in diabetes and its therapies*. Adv Exp Med Biol, 2010. **654**: p. 447-62.
46. Butler, A.E., et al., *Beta-cell deficit and increased beta-cell apoptosis in humans with type 2 diabetes*. Diabetes, 2003. **52**(1): p. 102-10.
47. Butler, A.E., et al., *Increased beta-cell apoptosis prevents adaptive increase in beta-cell mass in mouse model of type 2 diabetes: evidence for role of islet amyloid formation rather than direct action of amyloid*. Diabetes, 2003. **52**(9): p. 2304-14.
48. Lee, J.H., et al., *Protection from beta-cell apoptosis by inhibition of TGF-beta/Smad3 signaling*. Cell Death Dis, 2020. **11**(3): p. 184.
49. Rhodes, C.J., *Type 2 diabetes-a matter of beta-cell life and death?* Science, 2005. **307**(5708): p. 380-4.
50. Masini, M., et al., *Autophagy in human type 2 diabetes pancreatic beta cells*. Diabetologia, 2009. **52**(6): p. 1083-6.
51. Tomita, T., *Immunocytochemical localisation of caspase-3 in pancreatic islets from type 2 diabetic subjects*. Pathology, 2010. **42**(5): p. 432-7.
52. Bensellam, M., J.C. Jonas, and D.R. Laybutt, *Mechanisms of beta-cell dedifferentiation in diabetes: recent findings and future research directions*. J Endocrinol, 2018. **236**(2): p. R109-R143.
53. Chen, C., et al., *Human beta cell mass and function in diabetes: Recent advances in knowledge and technologies to understand disease pathogenesis*. Mol Metab, 2017. **6**(9): p. 943-957.

54. Accili, D., et al., *When beta-cells fail: lessons from dedifferentiation*. *Diabetes Obes Metab*, 2016. **18 Suppl 1**: p. 117-22.
55. Butler, A.E., et al., *beta-Cell Deficit in Obese Type 2 Diabetes, a Minor Role of beta-Cell Dedifferentiation and Degranulation*. *J Clin Endocrinol Metab*, 2016. **101**(2): p. 523-32.
56. Cinti, F., et al., *Evidence of beta-Cell Dedifferentiation in Human Type 2 Diabetes*. *J Clin Endocrinol Metab*, 2016. **101**(3): p. 1044-54.
57. Md Moin, A.S., et al., *Increased Frequency of Hormone Negative and Polyhormonal Endocrine Cells in Lean Individuals With Type 2 Diabetes*. *J Clin Endocrinol Metab*, 2016. **101**(10): p. 3628-3636.
58. Liadis, N., et al., *Caspase-3-dependent beta-cell apoptosis in the initiation of autoimmune diabetes mellitus*. *Mol Cell Biol*, 2005. **25**(9): p. 3620-9.
59. Mathis, D., L. Vence, and C. Benoist, *beta-Cell death during progression to diabetes*. *Nature*, 2001. **414**(6865): p. 792-8.
60. Trudeau, J.D., et al., *Neonatal beta-cell apoptosis: a trigger for autoimmune diabetes?* *Diabetes*, 2000. **49**(1): p. 1-7.
61. Thomas, H.E., et al., *Beta cell apoptosis in diabetes*. *Apoptosis*, 2009. **14**(12): p. 1389-404.
62. Federici, M., et al., *High glucose causes apoptosis in cultured human pancreatic islets of Langerhans: a potential role for regulation of specific Bcl family genes toward an apoptotic cell death program*. *Diabetes*, 2001. **50**(6): p. 1290-301.
63. Kaneto, H., et al., *Oxidative stress and pancreatic beta-cell dysfunction*. *Am J Ther*, 2005. **12**(6): p. 529-33.
64. Robertson, R.P., et al., *Beta-cell glucose toxicity, lipotoxicity, and chronic oxidative stress in type 2 diabetes*. *Diabetes*, 2004. **53 Suppl 1**: p. S119-24.
65. Eizirik, D.L., A.K. Cardozo, and M. Cnop, *The role for endoplasmic reticulum stress in diabetes mellitus*. *Endocr Rev*, 2008. **29**(1): p. 42-61.
66. Laybutt, D.R., et al., *Endoplasmic reticulum stress contributes to beta cell apoptosis in type 2 diabetes*. *Diabetologia*, 2007. **50**(4): p. 752-63.
67. Haataja, L., et al., *Islet amyloid in type 2 diabetes, and the toxic oligomer hypothesis*. *Endocr Rev*, 2008. **29**(3): p. 303-16.
68. Garber, K., *Rapamycin's resurrection: a new way to target the cancer cell cycle*. *J Natl Cancer Inst*, 2001. **93**(20): p. 1517-9.
69. Seto, B., *Rapamycin and mTOR: a serendipitous discovery and implications for breast cancer*. *Clin Transl Med*, 2012. **1**(1): p. 29.
70. Cafferkey, R., et al., *Dominant missense mutations in a novel yeast protein related to mammalian phosphatidylinositol 3-kinase and VPS34 abrogate rapamycin cytotoxicity*. *Mol Cell Biol*, 1993. **13**(10): p. 6012-23.
71. Heitman, J., N.R. Movva, and M.N. Hall, *Targets for cell cycle arrest by the immunosuppressant rapamycin in yeast*. *Science*, 1991. **253**(5022): p. 905-9.
72. Helliwell, S.B., et al., *TOR1 and TOR2 are structurally and functionally similar but not identical phosphatidylinositol kinase homologues in yeast*. *Mol Biol Cell*, 1994. **5**(1): p. 105-18.

73. Koltin, Y., et al., *Rapamycin sensitivity in Saccharomyces cerevisiae is mediated by a peptidyl-prolyl cis-trans isomerase related to human FK506-binding protein*. Mol Cell Biol, 1991. **11**(3): p. 1718-23.
74. Kunz, J., et al., *Target of rapamycin in yeast, TOR2, is an essential phosphatidylinositol kinase homolog required for G1 progression*. Cell, 1993. **73**(3): p. 585-96.
75. Alvarez-Ponce, D., M. Aguade, and J. Rozas, *Network-level molecular evolutionary analysis of the insulin/TOR signal transduction pathway across 12 Drosophila genomes*. Genome Res, 2009. **19**(2): p. 234-42.
76. Janus, A., T. Robak, and P. Smolewski, *The mammalian target of the rapamycin (mTOR) kinase pathway: its role in tumourigenesis and targeted antitumour therapy*. Cell Mol Biol Lett, 2005. **10**(3): p. 479-98.
77. Jiang, B.H. and L.Z. Liu, *Role of mTOR in anticancer drug resistance: perspectives for improved drug treatment*. Drug Resist Updat, 2008. **11**(3): p. 63-76.
78. Brown, E.J., et al., *A mammalian protein targeted by G1-arresting rapamycin-receptor complex*. Nature, 1994. **369**(6483): p. 756-8.
79. Sabatini, D.M., et al., *RAFT1: a mammalian protein that binds to FKBP12 in a rapamycin-dependent fashion and is homologous to yeast TORs*. Cell, 1994. **78**(1): p. 35-43.
80. Sabers, C.J., et al., *Isolation of a protein target of the FKBP12-rapamycin complex in mammalian cells*. J Biol Chem, 1995. **270**(2): p. 815-22.
81. Sabatini, D.M., *Twenty-five years of mTOR: Uncovering the link from nutrients to growth*. Proc Natl Acad Sci U S A, 2017. **114**(45): p. 11818-11825.
82. Lench, N.J., R. Macadam, and A.F. Markham, *The human gene encoding FKBP-rapamycin associated protein (FRAP) maps to chromosomal band 1p36.2*. Hum Genet, 1997. **99**(4): p. 547-9.
83. Takai, H., et al., *Tel2 regulates the stability of PI3K-related protein kinases*. Cell, 2007. **131**(7): p. 1248-59.
84. Martelli, A.M., F. Buontempo, and J.A. McCubrey, *Drug discovery targeting the mTOR pathway*. Clin Sci (Lond), 2018. **132**(5): p. 543-568.
85. Asnaghi, L., et al., *mTOR: a protein kinase switching between life and death*. Pharmacol Res, 2004. **50**(6): p. 545-9.
86. Hay, N. and N. Sonenberg, *Upstream and downstream of mTOR*. Genes Dev, 2004. **18**(16): p. 1926-45.
87. Murakami, M., et al., *mTOR is essential for growth and proliferation in early mouse embryos and embryonic stem cells*. Mol Cell Biol, 2004. **24**(15): p. 6710-8.
88. Andrade, M.A. and P. Bork, *HEAT repeats in the Huntington's disease protein*. Nat Genet, 1995. **11**(2): p. 115-6.
89. Bosotti, R., A. Isacchi, and E.L. Sonnhammer, *FAT: a novel domain in PIK-related kinases*. Trends Biochem Sci, 2000. **25**(5): p. 225-7.
90. Peterson, R.T., et al., *FKBP12-rapamycin-associated protein (FRAP) autophosphorylates at serine 2481 under translationally repressive conditions*. J Biol Chem, 2000. **275**(10): p. 7416-23.
91. Sekulic, A., et al., *A direct linkage between the phosphoinositide 3-kinase-AKT signaling pathway and the mammalian target of rapamycin in mitogen-stimulated and transformed cells*. Cancer Res, 2000. **60**(13): p. 3504-13.

92. Hara, K., et al., *Raptor, a binding partner of target of rapamycin (TOR), mediates TOR action*. Cell, 2002. **110**(2): p. 177-89.
93. Kim, D.H., et al., *GbetaL, a positive regulator of the rapamycin-sensitive pathway required for the nutrient-sensitive interaction between raptor and mTOR*. Mol Cell, 2003. **11**(4): p. 895-904.
94. Peterson, T.R., et al., *DEPTOR is an mTOR inhibitor frequently overexpressed in multiple myeloma cells and required for their survival*. Cell, 2009. **137**(5): p. 873-86.
95. Sancak, Y., et al., *PRAS40 is an insulin-regulated inhibitor of the mTORC1 protein kinase*. Mol Cell, 2007. **25**(6): p. 903-15.
96. Sarbassov, D.D., et al., *Rictor, a novel binding partner of mTOR, defines a rapamycin-insensitive and raptor-independent pathway that regulates the cytoskeleton*. Curr Biol, 2004. **14**(14): p. 1296-302.
97. Bononi, A., et al., *Protein kinases and phosphatases in the control of cell fate*. Enzyme Res, 2011. **2011**: p. 329098.
98. Inoki, K., *mTOR signaling in autophagy regulation in the kidney*. Semin Nephrol, 2014. **34**(1): p. 2-8.
99. Yang, H., et al., *mTOR kinase structure, mechanism and regulation*. Nature, 2013. **497**(7448): p. 217-23.
100. Sarbassov, D.D., et al., *Prolonged rapamycin treatment inhibits mTORC2 assembly and Akt/PKB*. Mol Cell, 2006. **22**(2): p. 159-68.
101. Efeyan, A. and D.M. Sabatini, *mTOR and cancer: many loops in one pathway*. Curr Opin Cell Biol, 2010. **22**(2): p. 169-76.
102. Soliman, G.A., et al., *mTOR Ser-2481 autophosphorylation monitors mTORC-specific catalytic activity and clarifies rapamycin mechanism of action*. J Biol Chem, 2010. **285**(11): p. 7866-79.
103. Mao, Z. and W. Zhang, *Role of mTOR in Glucose and Lipid Metabolism*. Int J Mol Sci, 2018. **19**(7).
104. Hara, K., et al., *Amino acid sufficiency and mTOR regulate p70 S6 kinase and eIF-4E BP1 through a common effector mechanism*. J Biol Chem, 1998. **273**(23): p. 14484-94.
105. Menon, S., et al., *Spatial control of the TSC complex integrates insulin and nutrient regulation of mTORC1 at the lysosome*. Cell, 2014. **156**(4): p. 771-85.
106. Sancak, Y., et al., *Ragulator-Rag complex targets mTORC1 to the lysosomal surface and is necessary for its activation by amino acids*. Cell, 2010. **141**(2): p. 290-303.
107. Sancak, Y., et al., *The Rag GTPases bind raptor and mediate amino acid signaling to mTORC1*. Science, 2008. **320**(5882): p. 1496-501.
108. Saxton, R.A. and D.M. Sabatini, *mTOR Signaling in Growth, Metabolism, and Disease*. Cell, 2017. **168**(6): p. 960-976.
109. Porstmann, T., et al., *SREBP activity is regulated by mTORC1 and contributes to Akt-dependent cell growth*. Cell Metab, 2008. **8**(3): p. 224-36.
110. Ben-Sahra, I., et al., *Stimulation of de novo pyrimidine synthesis by growth signaling through mTOR and S6K1*. Science, 2013. **339**(6125): p. 1323-8.
111. Ben-Sahra, I., et al., *mTORC1 induces purine synthesis through control of the mitochondrial tetrahydrofolate cycle*. Science, 2016. **351**(6274): p. 728-733.

112. Gaubitz, C., et al., *TORC2 Structure and Function*. Trends Biochem Sci, 2016. **41**(6): p. 532-545.
113. Liu, P., et al., *PtdIns(3,4,5)P3-Dependent Activation of the mTORC2 Kinase Complex*. Cancer Discov, 2015. **5**(11): p. 1194-209.
114. Saxton, R.A. and D.M. Sabatini, *mTOR Signaling in Growth, Metabolism, and Disease*. Cell, 2017. **169**(2): p. 361-371.
115. Huang, J., et al., *The TSC1-TSC2 complex is required for proper activation of mTOR complex 2*. Mol Cell Biol, 2008. **28**(12): p. 4104-15.
116. Huang, J. and B.D. Manning, *A complex interplay between Akt, TSC2 and the two mTOR complexes*. Biochem Soc Trans, 2009. **37**(Pt 1): p. 217-22.
117. Huang, J., et al., *Signaling events downstream of mammalian target of rapamycin complex 2 are attenuated in cells and tumors deficient for the tuberous sclerosis complex tumor suppressors*. Cancer Res, 2009. **69**(15): p. 6107-14.
118. Garcia-Martinez, J.M. and D.R. Alessi, *mTOR complex 2 (mTORC2) controls hydrophobic motif phosphorylation and activation of serum- and glucocorticoid-induced protein kinase 1 (SGK1)*. Biochem J, 2008. **416**(3): p. 375-85.
119. Manning, B.D. and A. Toker, *AKT/PKB Signaling: Navigating the Network*. Cell, 2017. **169**(3): p. 381-405.
120. Sarbassov, D.D., et al., *Phosphorylation and regulation of Akt/PKB by the rictor-mTOR complex*. Science, 2005. **307**(5712): p. 1098-101.
121. Guertin, D.A., et al., *Ablation in mice of the mTORC components raptor, rictor, or mLST8 reveals that mTORC2 is required for signaling to Akt-FOXO and PKCalpha, but not S6K1*. Dev Cell, 2006. **11**(6): p. 859-71.
122. Jacinto, E., et al., *SIN1/MIP1 maintains rictor-mTOR complex integrity and regulates Akt phosphorylation and substrate specificity*. Cell, 2006. **127**(1): p. 125-37.
123. Kennedy, B.K. and D.W. Lamming, *The Mechanistic Target of Rapamycin: The Grand Conductor of Metabolism and Aging*. Cell Metab, 2016. **23**(6): p. 990-1003.
124. Condon, K.J. and D.M. Sabatini, *Nutrient regulation of mTORC1 at a glance*. J Cell Sci, 2019. **132**(21).
125. Blandino-Rosano, M., et al., *Loss of mTORC1 signalling impairs beta-cell homeostasis and insulin processing*. Nat Commun, 2017. **8**: p. 16014.
126. Chau, G.C., et al., *mTOR controls ChREBP transcriptional activity and pancreatic beta cell survival under diabetic stress*. J Cell Biol, 2017. **216**(7): p. 2091-2105.
127. Elghazi, L., et al., *Role of nutrients and mTOR signaling in the regulation of pancreatic progenitors development*. Mol Metab, 2017. **6**(6): p. 560-573.
128. Ni, Q., et al., *Raptor regulates functional maturation of murine beta cells*. Nat Commun, 2017. **8**: p. 15755.
129. Sinagoga, K.L., et al., *Distinct roles for the mTOR pathway in postnatal morphogenesis, maturation and function of pancreatic islets*. Development, 2017. **144**(13): p. 2402-2414.
130. Ardestani, A., et al., *mTORC1 Signaling: A Double-Edged Sword in Diabetic beta Cells*. Cell Metab, 2018. **27**(2): p. 314-331.
131. Maedler, K. and A. Ardestani, *mTORC in beta cells: more Than Only Recognizing Comestibles*. J Cell Biol, 2017. **216**(7): p. 1883-1885.

132. Bartolome, A., et al., *Pancreatic beta-cell failure mediated by mTORC1 hyperactivity and autophagic impairment*. Diabetes, 2014. **63**(9): p. 2996-3008.
133. Rachdi, L., et al., *Disruption of Tsc2 in pancreatic beta cells induces beta cell mass expansion and improved glucose tolerance in a TORC1-dependent manner*. Proc Natl Acad Sci U S A, 2008. **105**(27): p. 9250-5.
134. Yuan, T., et al., *Reciprocal regulation of mTOR complexes in pancreatic islets from humans with type 2 diabetes*. Diabetologia, 2017. **60**(4): p. 668-678.
135. Varshney, R., et al., *Kaempferol alleviates palmitic acid-induced lipid stores, endoplasmic reticulum stress and pancreatic beta-cell dysfunction through AMPK/mTOR-mediated lipophagy*. J Nutr Biochem, 2018. **57**: p. 212-227.
136. Yuan, T., et al., *mTORC2 Signaling: A Path for Pancreatic beta Cell's Growth and Function*. J Mol Biol, 2018. **430**(7): p. 904-918.
137. Gu, Y., et al., *Rictor/mTORC2 is essential for maintaining a balance between beta-cell proliferation and cell size*. Diabetes, 2011. **60**(3): p. 827-37.
138. Julien, L.A., et al., *mTORC1-activated S6K1 phosphorylates Rictor on threonine 1135 and regulates mTORC2 signaling*. Mol Cell Biol, 2010. **30**(4): p. 908-21.
139. Liu, P., et al., *Author Correction: Sin1 phosphorylation impairs mTORC2 complex integrity and inhibits downstream Akt signalling to suppress tumorigenesis*. Nat Cell Biol, 2019. **21**(5): p. 662-663.
140. Glick, D., S. Barth, and K.F. Macleod, *Autophagy: cellular and molecular mechanisms*. J Pathol, 2010. **221**(1): p. 3-12.
141. Harnett, M.M., et al., *From Christian de Duve to Yoshinori Ohsumi: More to autophagy than just dining at home*. Biomed J, 2017. **40**(1): p. 9-22.
142. Sheng, R. and Z.H. Qin, *History and Current Status of Autophagy Research*. Adv Exp Med Biol, 2019. **1206**: p. 3-37.
143. Yu, L., Y. Chen, and S.A. Tooze, *Autophagy pathway: Cellular and molecular mechanisms*. Autophagy, 2018. **14**(2): p. 207-215.
144. Deter, R.L. and C. De Duve, *Influence of glucagon, an inducer of cellular autophagy, on some physical properties of rat liver lysosomes*. J Cell Biol, 1967. **33**(2): p. 437-49.
145. Yin, X.M., W.X. Ding, and W. Gao, *Autophagy in the liver*. Hepatology, 2008. **47**(5): p. 1773-85.
146. Klionsky, D.J., *Autophagy: from phenomenology to molecular understanding in less than a decade*. Nat Rev Mol Cell Biol, 2007. **8**(11): p. 931-7.
147. Nakatogawa, H., et al., *Dynamics and diversity in autophagy mechanisms: lessons from yeast*. Nat Rev Mol Cell Biol, 2009. **10**(7): p. 458-67.
148. Decuyper, J.P., G. Bultynck, and J.B. Parys, *A dual role for Ca(2+) in autophagy regulation*. Cell Calcium, 2011. **50**(3): p. 242-50.
149. Hara, T., et al., *Suppression of basal autophagy in neural cells causes neurodegenerative disease in mice*. Nature, 2006. **441**(7095): p. 885-9.
150. Jia, G. and J.R. Sowers, *Autophagy: a housekeeper in cardiorenal metabolic health and disease*. Biochim Biophys Acta, 2015. **1852**(2): p. 219-24.
151. Kaur, J. and J. Debnath, *Autophagy at the crossroads of catabolism and anabolism*. Nat Rev Mol Cell Biol, 2015. **16**(8): p. 461-72.

152. Andrade-Tomaz, M., et al., *The Role of Chaperone-Mediated Autophagy in Cell Cycle Control and Its Implications in Cancer*. Cells, 2020. **9**(9).
153. Al-Bari, M.A.A. and P. Xu, *Molecular regulation of autophagy machinery by mTOR-dependent and -independent pathways*. Ann N Y Acad Sci, 2020.
154. Antonioli, M., et al., *Emerging Mechanisms in Initiating and Terminating Autophagy*. Trends Biochem Sci, 2017. **42**(1): p. 28-41.
155. Mizushima, N. and M. Komatsu, *Autophagy: renovation of cells and tissues*. Cell, 2011. **147**(4): p. 728-41.
156. Xiang, H., et al., *Targeting autophagy-related protein kinases for potential therapeutic purpose*. Acta Pharm Sin B, 2020. **10**(4): p. 569-581.
157. Galluzzi, L., T. Yamazaki, and G. Kroemer, *Linking cellular stress responses to systemic homeostasis*. Nat Rev Mol Cell Biol, 2018. **19**(11): p. 731-745.
158. Klionsky, D.J. and P. Codogno, *The mechanism and physiological function of macroautophagy*. J Innate Immun, 2013. **5**(5): p. 427-33.
159. Laplante, M. and D.M. Sabatini, *mTOR signaling in growth control and disease*. Cell, 2012. **149**(2): p. 274-93.
160. Kim, J., et al., *AMPK and mTOR regulate autophagy through direct phosphorylation of Ulk1*. Nat Cell Biol, 2011. **13**(2): p. 132-41.
161. Ganley, I.G., et al., *ULK1.ATG13.FIP200 complex mediates mTOR signaling and is essential for autophagy*. J Biol Chem, 2009. **284**(18): p. 12297-305.
162. Hosokawa, N., et al., *Nutrient-dependent mTORC1 association with the ULK1-Atg13-FIP200 complex required for autophagy*. Mol Biol Cell, 2009. **20**(7): p. 1981-91.
163. Jung, C.H., et al., *ULK-Atg13-FIP200 complexes mediate mTOR signaling to the autophagy machinery*. Mol Biol Cell, 2009. **20**(7): p. 1992-2003.
164. Mehrpour, M., et al., *Overview of macroautophagy regulation in mammalian cells*. Cell Res, 2010. **20**(7): p. 748-62.
165. Ge, L., L. Wilz, and R. Schekman, *Biogenesis of autophagosomal precursors for LC3 lipidation from the ER-Golgi intermediate compartment*. Autophagy, 2015. **11**(12): p. 2372-4.
166. Pavel, M. and D.C. Rubinsztein, *Mammalian autophagy and the plasma membrane*. FEBS J, 2017. **284**(5): p. 672-679.
167. Shibutani, S.T. and T. Yoshimori, *A current perspective of autophagosome biogenesis*. Cell Res, 2014. **24**(1): p. 58-68.
168. Egan, D.F., et al., *Small Molecule Inhibition of the Autophagy Kinase ULK1 and Identification of ULK1 Substrates*. Mol Cell, 2015. **59**(2): p. 285-97.
169. Russell, R.C., et al., *ULK1 induces autophagy by phosphorylating Beclin-1 and activating VPS34 lipid kinase*. Nat Cell Biol, 2013. **15**(7): p. 741-50.
170. Itakura, E., et al., *Beclin 1 forms two distinct phosphatidylinositol 3-kinase complexes with mammalian Atg14 and UVRAG*. Mol Biol Cell, 2008. **19**(12): p. 5360-72.
171. Sun, Q., et al., *Identification of Barkor as a mammalian autophagy-specific factor for Beclin 1 and class III phosphatidylinositol 3-kinase*. Proc Natl Acad Sci U S A, 2008. **105**(49): p. 19211-6.
172. Ktistakis, N.T. and S.A. Tooze, *Digesting the Expanding Mechanisms of Autophagy*. Trends Cell Biol, 2016. **26**(8): p. 624-635.

173. Proikas-Cezanne, T., et al., *WIPI-1alpha (WIPI49), a member of the novel 7-bladed WIPI protein family, is aberrantly expressed in human cancer and is linked to starvation-induced autophagy*. *Oncogene*, 2004. **23**(58): p. 9314-25.
174. Longatti, A. and S.A. Tooze, *Vesicular trafficking and autophagosome formation*. *Cell Death Differ*, 2009. **16**(7): p. 956-65.
175. Young, A.R., et al., *Starvation and ULK1-dependent cycling of mammalian Atg9 between the TGN and endosomes*. *J Cell Sci*, 2006. **119**(Pt 18): p. 3888-900.
176. Cecconi, F. and B. Levine, *The role of autophagy in mammalian development: cell makeover rather than cell death*. *Dev Cell*, 2008. **15**(3): p. 344-57.
177. Pattingre, S. and B. Levine, *Bcl-2 inhibition of autophagy: a new route to cancer?* *Cancer Res*, 2006. **66**(6): p. 2885-8.
178. Simonsen, A. and S.A. Tooze, *Coordination of membrane events during autophagy by multiple class III PI3-kinase complexes*. *J Cell Biol*, 2009. **186**(6): p. 773-82.
179. Kabeya, Y., et al., *LC3, a mammalian homologue of yeast Apg8p, is localized in autophagosome membranes after processing*. *EMBO J*, 2000. **19**(21): p. 5720-8.
180. Mizushima, N., et al., *Mouse Apg16L, a novel WD-repeat protein, targets to the autophagic isolation membrane with the Apg12-Apg5 conjugate*. *J Cell Sci*, 2003. **116**(Pt 9): p. 1679-88.
181. Mizushima, N., et al., *A new protein conjugation system in human. The counterpart of the yeast Apg12p conjugation system essential for autophagy*. *J Biol Chem*, 1998. **273**(51): p. 33889-92.
182. Hanada, T., et al., *The Atg12-Atg5 conjugate has a novel E3-like activity for protein lipidation in autophagy*. *J Biol Chem*, 2007. **282**(52): p. 37298-302.
183. Ohsumi, Y. and N. Mizushima, *Two ubiquitin-like conjugation systems essential for autophagy*. *Semin Cell Dev Biol*, 2004. **15**(2): p. 231-6.
184. Nemoto, T., et al., *The mouse APG10 homologue, an E2-like enzyme for Apg12p conjugation, facilitates MAP-LC3 modification*. *J Biol Chem*, 2003. **278**(41): p. 39517-26.
185. Ravikumar, B., et al., *Mammalian macroautophagy at a glance*. *J Cell Sci*, 2009. **122**(Pt 11): p. 1707-11.
186. Weidberg, H., et al., *LC3 and GATE-16 N termini mediate membrane fusion processes required for autophagosome biogenesis*. *Dev Cell*, 2011. **20**(4): p. 444-54.
187. Wild, P., D.G. McEwan, and I. Dikic, *The LC3 interactome at a glance*. *J Cell Sci*, 2014. **127**(Pt 1): p. 3-9.
188. Lorincz, P. and G. Juhasz, *Autophagosome-Lysosome Fusion*. *J Mol Biol*, 2020. **432**(8): p. 2462-2482.
189. Weidberg, H., et al., *LC3 and GATE-16/GABARAP subfamilies are both essential yet act differently in autophagosome biogenesis*. *EMBO J*, 2010. **29**(11): p. 1792-802.
190. Albanesi, J., et al., *GABARAP-mediated targeting of PI4K2A/PI4KIIalpha to autophagosomes regulates PtdIns4P-dependent autophagosome-lysosome fusion*. *Autophagy*, 2015. **11**(11): p. 2127-2129.
191. Kriegenburg, F., C. Ungermann, and F. Reggiori, *Coordination of Autophagosome-Lysosome Fusion by Atg8 Family Members*. *Curr Biol*, 2018. **28**(8): p. R512-R518.
192. Amaya, C., C.M. Fader, and M.I. Colombo, *Autophagy and proteins involved in vesicular trafficking*. *FEBS Lett*, 2015. **589**(22): p. 3343-53.

193. Nakamura, S. and T. Yoshimori, *New insights into autophagosome-lysosome fusion*. J Cell Sci, 2017. **130**(7): p. 1209-1216.
194. Lamark, T., S. Svenning, and T. Johansen, *Regulation of selective autophagy: the p62/SQSTM1 paradigm*. Essays Biochem, 2017. **61**(6): p. 609-624.
195. Green, D.R. and B. Levine, *To be or not to be? How selective autophagy and cell death govern cell fate*. Cell, 2014. **157**(1): p. 65-75.
196. Bjorkoy, G., et al., *p62/SQSTM1 forms protein aggregates degraded by autophagy and has a protective effect on huntingtin-induced cell death*. J Cell Biol, 2005. **171**(4): p. 603-14.
197. Kirkin, V., et al., *A role for NBR1 in autophagosomal degradation of ubiquitinated substrates*. Mol Cell, 2009. **33**(4): p. 505-16.
198. Newman, A.C., et al., *TBK1 kinase addiction in lung cancer cells is mediated via autophagy of Tax1bp1/Ndp52 and non-canonical NF-kappaB signalling*. PLoS One, 2012. **7**(11): p. e50672.
199. Pankiv, S., et al., *p62/SQSTM1 binds directly to Atg8/LC3 to facilitate degradation of ubiquitinated protein aggregates by autophagy*. J Biol Chem, 2007. **282**(33): p. 24131-45.
200. Thurston, T.L., et al., *The TBK1 adaptor and autophagy receptor NDP52 restricts the proliferation of ubiquitin-coated bacteria*. Nat Immunol, 2009. **10**(11): p. 1215-21.
201. Wild, P., et al., *Phosphorylation of the autophagy receptor optineurin restricts Salmonella growth*. Science, 2011. **333**(6039): p. 228-33.
202. Deretic, V., *Autophagy as an innate immunity paradigm: expanding the scope and repertoire of pattern recognition receptors*. Curr Opin Immunol, 2012. **24**(1): p. 21-31.
203. Johansen, T. and T. Lamark, *Selective autophagy mediated by autophagic adapter proteins*. Autophagy, 2011. **7**(3): p. 279-96.
204. Rogov, V., et al., *Interactions between autophagy receptors and ubiquitin-like proteins form the molecular basis for selective autophagy*. Mol Cell, 2014. **53**(2): p. 167-78.
205. Cuervo, A.M., *Chaperone-mediated autophagy: Dice's 'wild' idea about lysosomal selectivity*. Nat Rev Mol Cell Biol, 2011. **12**(8): p. 535-41.
206. Auteri, J.S., et al., *Regulation of intracellular protein degradation in IMR-90 human diploid fibroblasts*. J Cell Physiol, 1983. **115**(2): p. 167-74.
207. Neff, N.T., et al., *Degradation of proteins microinjected into IMR-90 human diploid fibroblasts*. J Cell Biol, 1981. **91**(1): p. 184-94.
208. Backer, J.M. and J.F. Dice, *Covalent linkage of ribonuclease S-peptide to microinjected proteins causes their intracellular degradation to be enhanced during serum withdrawal*. Proc Natl Acad Sci U S A, 1986. **83**(16): p. 5830-4.
209. Chiang, H.L. and J.F. Dice, *Peptide sequences that target proteins for enhanced degradation during serum withdrawal*. J Biol Chem, 1988. **263**(14): p. 6797-805.
210. Kaushik, S. and A.M. Cuervo, *The coming of age of chaperone-mediated autophagy*. Nat Rev Mol Cell Biol, 2018. **19**(6): p. 365-381.
211. Cuervo, A.M., et al., *Selective binding and uptake of ribonuclease A and glyceraldehyde-3-phosphate dehydrogenase by isolated rat liver lysosomes*. J Biol Chem, 1994. **269**(42): p. 26374-80.

212. Cuervo, A.M. and E. Wong, *Chaperone-mediated autophagy: roles in disease and aging*. Cell Res, 2014. **24**(1): p. 92-104.
213. Chiang, H.L., et al., *A role for a 70-kilodalton heat shock protein in lysosomal degradation of intracellular proteins*. Science, 1989. **246**(4928): p. 382-5.
214. Kaushik, S. and A.M. Cuervo, *Chaperone-mediated autophagy: a unique way to enter the lysosome world*. Trends Cell Biol, 2012. **22**(8): p. 407-17.
215. Cuervo, A.M. and J.F. Dice, *A receptor for the selective uptake and degradation of proteins by lysosomes*. Science, 1996. **273**(5274): p. 501-3.
216. Massey, A.C., et al., *Consequences of the selective blockage of chaperone-mediated autophagy*. Proc Natl Acad Sci U S A, 2006. **103**(15): p. 5805-10.
217. Bandyopadhyay, U., et al., *The chaperone-mediated autophagy receptor organizes in dynamic protein complexes at the lysosomal membrane*. Mol Cell Biol, 2008. **28**(18): p. 5747-63.
218. Bandyopadhyay, U., et al., *Identification of regulators of chaperone-mediated autophagy*. Mol Cell, 2010. **39**(4): p. 535-47.
219. Kaushik, S., A.C. Massey, and A.M. Cuervo, *Lysosome membrane lipid microdomains: novel regulators of chaperone-mediated autophagy*. EMBO J, 2006. **25**(17): p. 3921-33.
220. Rodriguez-Navarro, J.A., et al., *Inhibitory effect of dietary lipids on chaperone-mediated autophagy*. Proc Natl Acad Sci U S A, 2012. **109**(12): p. E705-14.
221. Ebato, C., et al., *Autophagy is important in islet homeostasis and compensatory increase of beta cell mass in response to high-fat diet*. Cell Metab, 2008. **8**(4): p. 325-32.
222. Jung, H.S., et al., *Loss of autophagy diminishes pancreatic beta cell mass and function with resultant hyperglycemia*. Cell Metab, 2008. **8**(4): p. 318-24.
223. Chen, Z.F., et al., *The double-edged effect of autophagy in pancreatic beta cells and diabetes*. Autophagy, 2011. **7**(1): p. 12-6.
224. Hoshino, A., et al., *Inhibition of p53 preserves Parkin-mediated mitophagy and pancreatic beta-cell function in diabetes*. Proc Natl Acad Sci U S A, 2014. **111**(8): p. 3116-21.
225. Quan, W., et al., *Autophagy deficiency in beta cells leads to compromised unfolded protein response and progression from obesity to diabetes in mice*. Diabetologia, 2012. **55**(2): p. 392-403.
226. Fujitani, Y., R. Kawamori, and H. Watada, *The role of autophagy in pancreatic beta-cell and diabetes*. Autophagy, 2009. **5**(2): p. 280-2.
227. Komatsu, M., et al., *Homeostatic levels of p62 control cytoplasmic inclusion body formation in autophagy-deficient mice*. Cell, 2007. **131**(6): p. 1149-63.
228. Hur, K.Y., H.S. Jung, and M.S. Lee, *Role of autophagy in beta-cell function and mass*. Diabetes Obes Metab, 2010. **12 Suppl 2**: p. 20-6.
229. Sheng, Q., et al., *Autophagy protects pancreatic beta cell mass and function in the setting of a high-fat and high-glucose diet*. Sci Rep, 2017. **7**(1): p. 16348.
230. Lee, Y.H., et al., *beta-cell autophagy: Mechanism and role in beta-cell dysfunction*. Mol Metab, 2019. **27S**: p. S92-S103.
231. Scheuner, D., et al., *Control of mRNA translation preserves endoplasmic reticulum function in beta cells and maintains glucose homeostasis*. Nat Med, 2005. **11**(7): p. 757-64.

232. Noda, T. and Y. Ohsumi, *Tor, a phosphatidylinositol kinase homologue, controls autophagy in yeast*. J Biol Chem, 1998. **273**(7): p. 3963-6.
233. Scott, R.C., O. Schuldiner, and T.P. Neufeld, *Role and regulation of starvation-induced autophagy in the Drosophila fat body*. Dev Cell, 2004. **7**(2): p. 167-78.
234. Russell, R.C., H.X. Yuan, and K.L. Guan, *Autophagy regulation by nutrient signaling*. Cell Res, 2014. **24**(1): p. 42-57.
235. Kim, Y.C. and K.L. Guan, *mTOR: a pharmacologic target for autophagy regulation*. J Clin Invest, 2015. **125**(1): p. 25-32.
236. Ma, X., et al., *MTORC1-mediated NRBF2 phosphorylation functions as a switch for the class III PtdIns3K and autophagy*. Autophagy, 2017. **13**(3): p. 592-607.
237. Nazio, F., et al., *mTOR inhibits autophagy by controlling ULK1 ubiquitylation, self-association and function through AMBRA1 and TRAF6*. Nat Cell Biol, 2013. **15**(4): p. 406-16.
238. Yuan, H.X., R.C. Russell, and K.L. Guan, *Regulation of PIK3C3/VPS34 complexes by MTOR in nutrient stress-induced autophagy*. Autophagy, 2013. **9**(12): p. 1983-95.
239. Wan, W., et al., *mTORC1 Phosphorylates Acetyltransferase p300 to Regulate Autophagy and Lipogenesis*. Mol Cell, 2017. **68**(2): p. 323-335 e6.
240. Wan, W., et al., *mTORC1-Regulated and HUWE1-Mediated WIPI2 Degradation Controls Autophagy Flux*. Mol Cell, 2018. **72**(2): p. 303-315 e6.
241. Cheng, X., et al., *Pacer Is a Mediator of mTORC1 and GSK3-TIP60 Signaling in Regulation of Autophagosome Maturation and Lipid Metabolism*. Mol Cell, 2019. **73**(4): p. 788-802 e7.
242. Kim, Y.M., et al., *mTORC1 phosphorylates UVRAG to negatively regulate autophagosome and endosome maturation*. Mol Cell, 2015. **57**(2): p. 207-18.
243. Martina, J.A., et al., *MTORC1 functions as a transcriptional regulator of autophagy by preventing nuclear transport of TFEB*. Autophagy, 2012. **8**(6): p. 903-14.
244. Roczniak-Ferguson, A., et al., *The transcription factor TFEB links mTORC1 signaling to transcriptional control of lysosome homeostasis*. Sci Signal, 2012. **5**(228): p. ra42.
245. Arias, E., et al., *Lysosomal mTORC2/PHLPP1/Akt Regulate Chaperone-Mediated Autophagy*. Mol Cell, 2015. **59**(2): p. 270-84.
246. Vlahakis, A., et al., *TOR complex 2-Ypk1 signaling is an essential positive regulator of the general amino acid control response and autophagy*. Proc Natl Acad Sci U S A, 2014. **111**(29): p. 10586-91.
247. Dossou, A.S. and A. Basu, *The Emerging Roles of mTORC1 in Macromanaging Autophagy*. Cancers (Basel), 2019. **11**(10).
248. Mir, S.U., et al., *Inhibition of autophagic turnover in beta-cells by fatty acids and glucose leads to apoptotic cell death*. J Biol Chem, 2015. **290**(10): p. 6071-85.
249. Bachar-Wikstrom, E., et al., *Stimulation of autophagy improves endoplasmic reticulum stress-induced diabetes*. Diabetes, 2013. **62**(4): p. 1227-37.
250. Kim, W. and E.H. Jho, *The history and regulatory mechanism of the Hippo pathway*. BMB Rep, 2018. **51**(3): p. 106-118.
251. Michalopoulos, G.K. and M.C. DeFrances, *Liver regeneration*. Science, 1997. **276**(5309): p. 60-6.

252. Metcalf, D., *The Autonomous Behaviour of Normal Thymus Grafts*. Aust J Exp Biol Med Sci, 1963. **41**: p. SUPPL437-47.
253. Metcalf, D., *Restricted Growth Capacity of Multiple Spleen Grafts*. Transplantation, 1964. **2**: p. 387-92.
254. Snigdha, K., et al., *Hippo Signaling in Cancer: Lessons From Drosophila Models*. Front Cell Dev Biol, 2019. **7**: p. 85.
255. Justice, R.W., et al., *The Drosophila tumor suppressor gene warts encodes a homolog of human myotonic dystrophy kinase and is required for the control of cell shape and proliferation*. Genes Dev, 1995. **9**(5): p. 534-46.
256. Xu, T., et al., *Identifying tumor suppressors in genetic mosaics: the Drosophila lats gene encodes a putative protein kinase*. Development, 1995. **121**(4): p. 1053-63.
257. Kango-Singh, M., et al., *Shar-pei mediates cell proliferation arrest during imaginal disc growth in Drosophila*. Development, 2002. **129**(24): p. 5719-30.
258. Harvey, K.F., C.M. Pflieger, and I.K. Hariharan, *The Drosophila Mst ortholog, hippo, restricts growth and cell proliferation and promotes apoptosis*. Cell, 2003. **114**(4): p. 457-67.
259. Jia, J., et al., *The Drosophila Ste20 family kinase dMST functions as a tumor suppressor by restricting cell proliferation and promoting apoptosis*. Genes Dev, 2003. **17**(20): p. 2514-9.
260. Pantalacci, S., N. Tapon, and P. Leopold, *The Salvador partner Hippo promotes apoptosis and cell-cycle exit in Drosophila*. Nat Cell Biol, 2003. **5**(10): p. 921-7.
261. Udan, R.S., et al., *Hippo promotes proliferation arrest and apoptosis in the Salvador/Warts pathway*. Nat Cell Biol, 2003. **5**(10): p. 914-20.
262. Lai, Z.C., et al., *Control of cell proliferation and apoptosis by mob as tumor suppressor, mats*. Cell, 2005. **120**(5): p. 675-85.
263. Wei, X., T. Shimizu, and Z.C. Lai, *Mob as tumor suppressor is activated by Hippo kinase for growth inhibition in Drosophila*. EMBO J, 2007. **26**(7): p. 1772-81.
264. Huang, J., et al., *The Hippo signaling pathway coordinately regulates cell proliferation and apoptosis by inactivating Yorkie, the Drosophila Homolog of YAP*. Cell, 2005. **122**(3): p. 421-34.
265. Creasy, C.L. and J. Chernoff, *Cloning and characterization of a human protein kinase with homology to Ste20*. J Biol Chem, 1995. **270**(37): p. 21695-700.
266. Creasy, C.L. and J. Chernoff, *Cloning and characterization of a member of the MST subfamily of Ste20-like kinases*. Gene, 1995. **167**(1-2): p. 303-6.
267. Tao, W., et al., *Human homologue of the Drosophila melanogaster lats tumour suppressor modulates CDC2 activity*. Nat Genet, 1999. **21**(2): p. 177-81.
268. Yabuta, N., et al., *Structure, expression, and chromosome mapping of LATS2, a mammalian homologue of the Drosophila tumor suppressor gene lats/warts*. Genomics, 2000. **63**(2): p. 263-70.
269. Bichsel, S.J., et al., *Mechanism of activation of NDR (nuclear Dbf2-related) protein kinase by the hMOB1 protein*. J Biol Chem, 2004. **279**(34): p. 35228-35.
270. Chow, A., Y. Hao, and X. Yang, *Molecular characterization of human homologs of yeast MOB1*. Int J Cancer, 2010. **126**(9): p. 2079-89.

271. Stavridi, E.S., et al., *Crystal structure of a human Mob1 protein: toward understanding Mob-regulated cell cycle pathways*. *Structure*, 2003. **11**(9): p. 1163-70.
272. Halder, G. and R.L. Johnson, *Hippo signaling: growth control and beyond*. *Development*, 2011. **138**(1): p. 9-22.
273. Kanai, F., et al., *TAZ: a novel transcriptional co-activator regulated by interactions with 14-3-3 and PDZ domain proteins*. *EMBO J*, 2000. **19**(24): p. 6778-91.
274. Chen, Y.A., et al., *WW Domain-Containing Proteins YAP and TAZ in the Hippo Pathway as Key Regulators in Stemness Maintenance, Tissue Homeostasis, and Tumorigenesis*. *Front Oncol*, 2019. **9**: p. 60.
275. Callus, B.A., A.M. Verhagen, and D.L. Vaux, *Association of mammalian sterile twenty kinases, Mst1 and Mst2, with hSalvador via C-terminal coiled-coil domains, leads to its stabilization and phosphorylation*. *FEBS J*, 2006. **273**(18): p. 4264-76.
276. Glantschnig, H., G.A. Rodan, and A.A. Reszka, *Mapping of MST1 kinase sites of phosphorylation. Activation and autophosphorylation*. *J Biol Chem*, 2002. **277**(45): p. 42987-96.
277. Hergovich, A., D. Schmitz, and B.A. Hemmings, *The human tumour suppressor LATS1 is activated by human MOB1 at the membrane*. *Biochem Biophys Res Commun*, 2006. **345**(1): p. 50-8.
278. Yin, F., et al., *Spatial organization of Hippo signaling at the plasma membrane mediated by the tumor suppressor Merlin/NF2*. *Cell*, 2013. **154**(6): p. 1342-55.
279. Meng, Z., et al., *MAP4K family kinases act in parallel to MST1/2 to activate LATS1/2 in the Hippo pathway*. *Nat Commun*, 2015. **6**: p. 8357.
280. Zheng, Y., et al., *Identification of Happyhour/MAP4K as Alternative Hpo/Mst-like Kinases in the Hippo Kinase Cascade*. *Dev Cell*, 2015. **34**(6): p. 642-55.
281. Liu, C.Y., et al., *The hippo tumor pathway promotes TAZ degradation by phosphorylating a phosphodegron and recruiting the SCF{beta}-TrCP E3 ligase*. *J Biol Chem*, 2010. **285**(48): p. 37159-69.
282. Nguyen, T.H. and J.M. Kugler, *Ubiquitin-Dependent Regulation of the Mammalian Hippo Pathway: Therapeutic Implications for Cancer*. *Cancers (Basel)*, 2018. **10**(4).
283. Zhao, B., et al., *A coordinated phosphorylation by Lats and CK1 regulates YAP stability through SCF(beta-TRCP)*. *Genes Dev*, 2010. **24**(1): p. 72-85.
284. Galli, G.G., et al., *YAP Drives Growth by Controlling Transcriptional Pause Release from Dynamic Enhancers*. *Mol Cell*, 2015. **60**(2): p. 328-37.
285. Stein, C., et al., *YAP1 Exerts Its Transcriptional Control via TEAD-Mediated Activation of Enhancers*. *PLoS Genet*, 2015. **11**(8): p. e1005465.
286. Vassilev, A., et al., *TEAD/TEF transcription factors utilize the activation domain of YAP65, a Src/Yes-associated protein localized in the cytoplasm*. *Genes Dev*, 2001. **15**(10): p. 1229-41.
287. Zanconato, F., et al., *Genome-wide association between YAP/TAZ/TEAD and AP-1 at enhancers drives oncogenic growth*. *Nat Cell Biol*, 2015. **17**(9): p. 1218-27.
288. Thompson, B.J. and E. Sahai, *MST kinases in development and disease*. *J Cell Biol*, 2015. **210**(6): p. 871-82.
289. Pombo, C.M., et al., *MST Kinases and Metabolism*. *Endocrinology*, 2019. **160**(5): p. 1111-1118.

290. Ardestani, A. and K. Maedler, *The Hippo Signaling Pathway in Pancreatic beta-Cells: Functions and Regulations*. *Endocr Rev*, 2018. **39**(1): p. 21-35.
291. Galan, J.A. and J. Avruch, *MST1/MST2 Protein Kinases: Regulation and Physiologic Roles*. *Biochemistry*, 2016. **55**(39): p. 5507-5519.
292. Hergovich, A., et al., *NDR kinases regulate essential cell processes from yeast to humans*. *Nat Rev Mol Cell Biol*, 2006. **7**(4): p. 253-64.
293. Ling, P., et al., *Biosignaling of mammalian Ste20-related kinases*. *Cell Signal*, 2008. **20**(7): p. 1237-47.
294. Khokhlatchev, A., et al., *Identification of a novel Ras-regulated proapoptotic pathway*. *Curr Biol*, 2002. **12**(4): p. 253-65.
295. Hwang, E., et al., *Structural insight into dimeric interaction of the SARA domains from Mst1 and RASSF family proteins in the apoptosis pathway*. *Proc Natl Acad Sci U S A*, 2007. **104**(22): p. 9236-41.
296. Avruch, J., et al., *Protein kinases of the Hippo pathway: regulation and substrates*. *Semin Cell Dev Biol*, 2012. **23**(7): p. 770-84.
297. Praskova, M., et al., *Regulation of the MST1 kinase by autophosphorylation, by the growth inhibitory proteins, RASSF1 and NORE1, and by Ras*. *Biochem J*, 2004. **381**(Pt 2): p. 453-62.
298. Boggiano, J.C., P.J. Vanderzalm, and R.G. Fehon, *Tao-1 phosphorylates Hippo/MST kinases to regulate the Hippo-Salvador-Warts tumor suppressor pathway*. *Dev Cell*, 2011. **21**(5): p. 888-95.
299. Poon, C.L., et al., *The sterile 20-like kinase Tao-1 controls tissue growth by regulating the Salvador-Warts-Hippo pathway*. *Dev Cell*, 2011. **21**(5): p. 896-906.
300. Collak, F.K., et al., *Threonine-120 phosphorylation regulated by phosphoinositide-3-kinase/Akt and mammalian target of rapamycin pathway signaling limits the antitumor activity of mammalian sterile 20-like kinase 1*. *J Biol Chem*, 2012. **287**(28): p. 23698-709.
301. Jang, S.W., et al., *Akt phosphorylates Mst1 and prevents its proteolytic activation, blocking FOXO3 phosphorylation and nuclear translocation*. *J Biol Chem*, 2007. **282**(42): p. 30836-44.
302. Yuan, Z., et al., *Phosphoinositide 3-kinase/Akt inhibits MST1-mediated pro-apoptotic signaling through phosphorylation of threonine 120*. *J Biol Chem*, 2016. **291**(43): p. 22858.
303. Bi, W., et al., *c-Jun N-terminal kinase enhances MST1-mediated pro-apoptotic signaling through phosphorylation at serine 82*. *J Biol Chem*, 2010. **285**(9): p. 6259-64.
304. Xiao, L., et al., *The c-Abl-MST1 signaling pathway mediates oxidative stress-induced neuronal cell death*. *J Neurosci*, 2011. **31**(26): p. 9611-9.
305. Sciarretta, S., et al., *mTORC2 regulates cardiac response to stress by inhibiting MST1*. *Cell Rep*, 2015. **11**(1): p. 125-36.
306. Servas, C., et al., *The mammalian STE20-like kinase 1 (MST1) is a substrate for the apoptosis inhibiting protein kinase CK2*. *Cell Signal*, 2017. **36**: p. 163-175.
307. Jung, S., et al., *PHLPP1 regulates contact inhibition by dephosphorylating Mst1 at the inhibitory site*. *Biochem Biophys Res Commun*, 2014. **443**(4): p. 1263-9.
308. Qiao, M., et al., *Mst1 is an interacting protein that mediates PHLPPs' induced apoptosis*. *Mol Cell*, 2010. **38**(4): p. 512-23.

309. Ura, S., et al., *Caspase cleavage of MST1 promotes nuclear translocation and chromatin condensation*. Proc Natl Acad Sci U S A, 2001. **98**(18): p. 10148-53.
310. Lu, C., et al., *MAPKs and Mst1/Caspase-3 pathways contribute to H2B phosphorylation during UVB-induced apoptosis*. Sci China Life Sci, 2010. **53**(6): p. 663-8.
311. Chen, S., et al., *Mammalian Sterile20-like Kinases: Signalings and Roles in Central Nervous System*. Aging Dis, 2018. **9**(3): p. 537-552.
312. Wu, H., et al., *The Ets transcription factor GABP is a component of the hippo pathway essential for growth and antioxidant defense*. Cell Rep, 2013. **3**(5): p. 1663-77.
313. Oh, S., et al., *Crucial role for Mst1 and Mst2 kinases in early embryonic development of the mouse*. Mol Cell Biol, 2009. **29**(23): p. 6309-20.
314. Song, H., et al., *Mammalian Mst1 and Mst2 kinases play essential roles in organ size control and tumor suppression*. Proc Natl Acad Sci U S A, 2010. **107**(4): p. 1431-6.
315. Zhou, D., et al., *Mst1 and Mst2 protein kinases restrain intestinal stem cell proliferation and colonic tumorigenesis by inhibition of Yes-associated protein (Yap) overabundance*. Proc Natl Acad Sci U S A, 2011. **108**(49): p. E1312-20.
316. Hong, L., et al., *Role of Hippo signaling in regulating immunity*. Cell Mol Immunol, 2018. **15**(12): p. 1003-1009.
317. Meng, Z., T. Moroishi, and K.L. Guan, *Mechanisms of Hippo pathway regulation*. Genes Dev, 2016. **30**(1): p. 1-17.
318. Hori, T., et al., *Molecular cloning of a novel human protein kinase, kpm, that is homologous to warts/lats, a Drosophila tumor suppressor*. Oncogene, 2000. **19**(27): p. 3101-9.
319. Nishiyama, Y., et al., *A human homolog of Drosophila warts tumor suppressor, h-warts, localized to mitotic apparatus and specifically phosphorylated during mitosis*. FEBS Lett, 1999. **459**(2): p. 159-65.
320. Visser, S. and X. Yang, *LATS tumor suppressor: a new governor of cellular homeostasis*. Cell Cycle, 2010. **9**(19): p. 3892-903.
321. Pearce, L.R., D. Komander, and D.R. Alessi, *The nuts and bolts of AGC protein kinases*. Nat Rev Mol Cell Biol, 2010. **11**(1): p. 9-22.
322. Li, Q., et al., *The conserved misshapen-warts-Yorkie pathway acts in enteroblasts to regulate intestinal stem cells in Drosophila*. Dev Cell, 2014. **31**(3): p. 291-304.
323. Ni, L., et al., *Structural basis for Mob1-dependent activation of the core Mst-Lats kinase cascade in Hippo signaling*. Genes Dev, 2015. **29**(13): p. 1416-31.
324. Chan, E.H., et al., *The Ste20-like kinase Mst2 activates the human large tumor suppressor kinase Lats1*. Oncogene, 2005. **24**(12): p. 2076-86.
325. Yabuta, N., et al., *Lats2 is an essential mitotic regulator required for the coordination of cell division*. J Biol Chem, 2007. **282**(26): p. 19259-71.
326. Toji, S., et al., *The centrosomal protein Lats2 is a phosphorylation target of Aurora-A kinase*. Genes Cells, 2004. **9**(5): p. 383-97.
327. Aylon, Y., et al., *Silencing of the Lats2 tumor suppressor overrides a p53-dependent oncogenic stress checkpoint and enables mutant H-Ras-driven cell transformation*. Oncogene, 2009. **28**(50): p. 4469-79.
328. Humbert, N., et al., *Regulation of ploidy and senescence by the AMPK-related kinase NUAK1*. EMBO J, 2010. **29**(2): p. 376-86.

329. Chen, C. and L.E. Matesic, *The Nedd4-like family of E3 ubiquitin ligases and cancer*. *Cancer Metastasis Rev*, 2007. **26**(3-4): p. 587-604.
330. Li, W., et al., *Merlin/NF2 loss-driven tumorigenesis linked to CRL4(DCAF1)-mediated inhibition of the hippo pathway kinases Lats1 and 2 in the nucleus*. *Cancer Cell*, 2014. **26**(1): p. 48-60.
331. Ma, B., et al., *Hypoxia regulates Hippo signalling through the SIAH2 ubiquitin E3 ligase*. *Nat Cell Biol*, 2015. **17**(1): p. 95-103.
332. Kim, E., et al., *O-GlcNAcylation on LATS2 disrupts the Hippo pathway by inhibiting its activity*. *Proc Natl Acad Sci U S A*, 2020. **117**(25): p. 14259-14269.
333. Aylon, Y., et al., *A positive feedback loop between the p53 and Lats2 tumor suppressors prevents tetraploidization*. *Genes Dev*, 2006. **20**(19): p. 2687-700.
334. Siam, R., et al., *Transcriptional activation of the Lats1 tumor suppressor gene in tumors of CUX1 transgenic mice*. *Mol Cancer*, 2009. **8**: p. 60.
335. Li, W., et al., *Identification of a tumor suppressor relay between the FOXP3 and the Hippo pathways in breast and prostate cancers*. *Cancer Res*, 2011. **71**(6): p. 2162-71.
336. Park, G.S., et al., *An evolutionarily conserved negative feedback mechanism in the Hippo pathway reflects functional difference between LATS1 and LATS2*. *Oncotarget*, 2016. **7**(17): p. 24063-75.
337. Cho, W.J., et al., *miR-372 regulates cell cycle and apoptosis of ags human gastric cancer cell line through direct regulation of LATS2*. *Mol Cells*, 2009. **28**(6): p. 521-7.
338. Lee, K.H., et al., *MicroRNA-373 (miR-373) post-transcriptionally regulates large tumor suppressor, homolog 2 (LATS2) and stimulates proliferation in human esophageal cancer*. *Exp Cell Res*, 2009. **315**(15): p. 2529-38.
339. Song, L., et al., *Downregulation of microRNA-224-3p Hampers Retinoblastoma Progression via Activation of the Hippo-YAP Signaling Pathway by Increasing LATS2*. *Invest Ophthalmol Vis Sci*, 2020. **61**(3): p. 32.
340. Voorhoeve, P.M., et al., *A genetic screen implicates miRNA-372 and miRNA-373 as oncogenes in testicular germ cell tumors*. *Cell*, 2006. **124**(6): p. 1169-81.
341. Lee, H.H., et al., *Stability of the LATS2 tumor suppressor gene is regulated by tristetraprolin*. *J Biol Chem*, 2010. **285**(23): p. 17329-37.
342. McPherson, J.P., et al., *Lats2/Kpm is required for embryonic development, proliferation control and genomic integrity*. *EMBO J*, 2004. **23**(18): p. 3677-88.
343. St John, M.A., et al., *Mice deficient of Lats1 develop soft-tissue sarcomas, ovarian tumours and pituitary dysfunction*. *Nat Genet*, 1999. **21**(2): p. 182-6.
344. Nishioka, N., et al., *The Hippo signaling pathway components Lats and Yap pattern Tead4 activity to distinguish mouse trophectoderm from inner cell mass*. *Dev Cell*, 2009. **16**(3): p. 398-410.
345. Heallen, T., et al., *Hippo pathway inhibits Wnt signaling to restrain cardiomyocyte proliferation and heart size*. *Science*, 2011. **332**(6028): p. 458-61.
346. Matsui, Y., et al., *Lats2 is a negative regulator of myocyte size in the heart*. *Circ Res*, 2008. **103**(11): p. 1309-18.
347. Hergovich, A. and B.A. Hemmings, *Hippo signalling in the G2/M cell cycle phase: lessons learned from the yeast MEN and SIN pathways*. *Semin Cell Dev Biol*, 2012. **23**(7): p. 794-802.

348. Ke, H., et al., *Putative tumor suppressor Lats2 induces apoptosis through downregulation of Bcl-2 and Bcl-x(L)*. *Exp Cell Res*, 2004. **298**(2): p. 329-38.
349. Yang, X., et al., *Human homologue of Drosophila lats, LATS1, negatively regulate growth by inducing G(2)/M arrest or apoptosis*. *Oncogene*, 2001. **20**(45): p. 6516-23.
350. Kawahara, M., et al., *Kpm/Lats2 is linked to chemosensitivity of leukemic cells through the stabilization of p73*. *Blood*, 2008. **112**(9): p. 3856-66.
351. Furth, N. and Y. Aylon, *The LATS1 and LATS2 tumor suppressors: beyond the Hippo pathway*. *Cell Death Differ*, 2017. **24**(9): p. 1488-1501.
352. Miller, E., et al., *Identification of serum-derived sphingosine-1-phosphate as a small molecule regulator of YAP*. *Chem Biol*, 2012. **19**(8): p. 955-62.
353. Mo, J.S., et al., *Regulation of the Hippo-YAP pathway by protease-activated receptors (PARs)*. *Genes Dev*, 2012. **26**(19): p. 2138-43.
354. Yu, F.X., et al., *Regulation of the Hippo-YAP pathway by G-protein-coupled receptor signaling*. *Cell*, 2012. **150**(4): p. 780-91.
355. Aylon, Y., et al., *The Lats2 tumor suppressor augments p53-mediated apoptosis by promoting the nuclear proapoptotic function of ASPP1*. *Genes Dev*, 2010. **24**(21): p. 2420-9.
356. Torigata, K., et al., *LATS2 Positively Regulates Polycomb Repressive Complex 2*. *PLoS One*, 2016. **11**(7): p. e0158562.
357. Li, J., et al., *LATS2 suppresses oncogenic Wnt signaling by disrupting beta-catenin/BCL9 interaction*. *Cell Rep*, 2013. **5**(6): p. 1650-63.
358. Aylon, Y., et al., *The LATS2 tumor suppressor inhibits SREBP and suppresses hepatic cholesterol accumulation*. *Genes Dev*, 2016. **30**(7): p. 786-97.
359. Lian, I., et al., *The role of YAP transcription coactivator in regulating stem cell self-renewal and differentiation*. *Genes Dev*, 2010. **24**(11): p. 1106-18.
360. Mo, J.S., H.W. Park, and K.L. Guan, *The Hippo signaling pathway in stem cell biology and cancer*. *EMBO Rep*, 2014. **15**(6): p. 642-56.
361. Robertson, A., et al., *Genetic ablation of the mammalian sterile-20 like kinase 1 (Mst1) improves cell reprogramming efficiency and increases induced pluripotent stem cell proliferation and survival*. *Stem Cell Res*, 2017. **20**: p. 42-49.
362. Tamm, C., N. Bower, and C. Anneren, *Regulation of mouse embryonic stem cell self-renewal by a Yes-YAP-TEAD2 signaling pathway downstream of LIF*. *J Cell Sci*, 2011. **124**(Pt 7): p. 1136-44.
363. Pictet, R.L., et al., *An ultrastructural analysis of the developing embryonic pancreas*. *Dev Biol*, 1972. **29**(4): p. 436-67.
364. Bastidas-Ponce, A., et al., *Cellular and molecular mechanisms coordinating pancreas development*. *Development*, 2017. **144**(16): p. 2873-2888.
365. Desgraz, R. and P.L. Herrera, *Pancreatic neurogenin 3-expressing cells are unipotent islet precursors*. *Development*, 2009. **136**(21): p. 3567-74.
366. Gradwohl, G., et al., *neurogenin3 is required for the development of the four endocrine cell lineages of the pancreas*. *Proc Natl Acad Sci U S A*, 2000. **97**(4): p. 1607-11.
367. Krapp, A., et al., *The bHLH protein PTF1-p48 is essential for the formation of the exocrine and the correct spatial organization of the endocrine pancreas*. *Genes Dev*, 1998. **12**(23): p. 3752-63.

368. Pan, F.C. and C. Wright, *Pancreas organogenesis: from bud to plexus to gland*. Dev Dyn, 2011. **240**(3): p. 530-65.
369. Stanger, B.Z., A.J. Tanaka, and D.A. Melton, *Organ size is limited by the number of embryonic progenitor cells in the pancreas but not the liver*. Nature, 2007. **445**(7130): p. 886-91.
370. Gao, T., et al., *Hippo signaling regulates differentiation and maintenance in the exocrine pancreas*. Gastroenterology, 2013. **144**(7): p. 1543-53, 1553 e1.
371. George, N.M., et al., *Hippo signaling regulates pancreas development through inactivation of Yap*. Mol Cell Biol, 2012. **32**(24): p. 5116-28.
372. Cebola, I., et al., *TEAD and YAP regulate the enhancer network of human embryonic pancreatic progenitors*. Nat Cell Biol, 2015. **17**(5): p. 615-626.
373. George, N.M., et al., *Exploiting Expression of Hippo Effector, Yap, for Expansion of Functional Islet Mass*. Mol Endocrinol, 2015. **29**(11): p. 1594-607.
374. Zhang, Z.W., et al., *miR-375 inhibits proliferation of mouse pancreatic progenitor cells by targeting YAP1*. Cell Physiol Biochem, 2013. **32**(6): p. 1808-17.
375. Mamidi, A., et al., *Mechanosignalling via integrins directs fate decisions of pancreatic progenitors*. Nature, 2018. **564**(7734): p. 114-118.
376. Rosado-Olivieri, E.A., et al., *YAP inhibition enhances the differentiation of functional stem cell-derived insulin-producing beta cells*. Nat Commun, 2019. **10**(1): p. 1464.
377. Benner, C., et al., *The transcriptional landscape of mouse beta cells compared to human beta cells reveals notable species differences in long non-coding RNA and protein-coding gene expression*. BMC Genomics, 2014. **15**: p. 620.
378. Blodgett, D.M., et al., *Novel Observations From Next-Generation RNA Sequencing of Highly Purified Human Adult and Fetal Islet Cell Subsets*. Diabetes, 2015. **64**(9): p. 3172-81.
379. Ardestani, A., et al., *MST1 is a key regulator of beta cell apoptosis and dysfunction in diabetes*. Nat Med, 2014. **20**(4): p. 385-397.
380. Ardestani, A. and K. Maedler, *MST1: a promising therapeutic target to restore functional beta cell mass in diabetes*. Diabetologia, 2016. **59**(9): p. 1843-9.
381. Carew, R.M., et al., *Deletion of Irs2 causes reduced kidney size in mice: role for inhibition of GSK3beta?* BMC Dev Biol, 2010. **10**: p. 73.
382. Kawano, Y., et al., *Loss of Pdk1-Foxo1 signaling in myeloid cells predisposes to adipose tissue inflammation and insulin resistance*. Diabetes, 2012. **61**(8): p. 1935-48.
383. Wu, W., et al., *Early protective role of MST1 knockdown in response to experimental diabetic nephropathy*. Am J Transl Res, 2016. **8**(3): p. 1397-411.
384. Zhang, M., et al., *MST1 coordinately regulates autophagy and apoptosis in diabetic cardiomyopathy in mice*. Diabetologia, 2016. **59**(11): p. 2435-2447.
385. Yuan, T., et al., *Loss of Merlin/NF2 protects pancreatic beta-cells from apoptosis by inhibiting LATS2*. Cell Death Dis, 2016. **7**: p. e2107.
386. Yuan, T., K. Maedler, and A. Ardestani, *Pancreatic beta-cell rescue in diabetes by targeting Merlin*. Expert Rev Endocrinol Metab, 2017. **12**(2): p. 97-99.

2 Results

Manuscript I

2.1 Neratinib Protects pancreatic beta cells in diabetes

Amin Ardestani*, Sijia Li*, Karthika Annamalai*, Blaz Lypse* *et al.*

*These authors contributed equally

Published in Nature communications. 2019 Nov 1;10(1):5015. doi: 10.1038/s41467-019-12880-5.

My contribution:

Designed, performed experiments, analysed data and assembled the figures for:

Figures: 3C,D ; 4A-E ; 7C ; 8G,H,I,K ; 9F (partially contributed)



Supplementary Figures: 8A,B; 9.

ARTICLE

<https://doi.org/10.1038/s41467-019-12880-5>

OPEN

Neratinib protects pancreatic beta cells in diabetes

Amin Ardestani^{1,5,6*}, Sijia Li^{2,5}, Karthika Annamalai^{1,5}, Blaz Lupse^{1,5}, Shirin Geravandi¹, Aleksandra Dobrowolski¹, Shan Yu², Siying Zhu², Tyler D. Baguley², Murali Surakattula², Janina Oetjen ^{1,3,4}, Lena Hauberg-Lotte³, Raquel Herranz¹, Sushil Awal¹, Delsi Altenhofen¹, Van Nguyen-Tran², Sean Joseph², Peter G. Schultz², Arnab K. Chatterjee², Nikki Rogers², Matthew S. Tremblay^{2,6*}, Weijun Shen^{2,6*} & Kathrin Maedler ^{1,6*}

The loss of functional insulin-producing β -cells is a hallmark of diabetes. Mammalian sterile 20-like kinase 1 (MST1) is a key regulator of pancreatic β -cell death and dysfunction; its deficiency restores functional β -cells and normoglycemia. The identification of MST1 inhibitors represents a promising approach for a β -cell-protective diabetes therapy. Here, we identify neratinib, an FDA-approved drug targeting HER2/EGFR dual kinases, as a potent MST1 inhibitor, which improves β -cell survival under multiple diabetogenic conditions in human islets and INS-1E cells. In a pre-clinical study, neratinib attenuates hyperglycemia and improves β -cell function, survival and β -cell mass in type 1 (streptozotocin) and type 2 (obese *Lepr^{db/db}*) diabetic mouse models. In summary, neratinib is a previously unrecognized inhibitor of MST1 and represents a potential β -cell-protective drug with proof-of-concept in vitro in human islets and in vivo in rodent models of both type 1 and type 2 diabetes.

¹Centre for Biomolecular Interactions Bremen, University of Bremen, Bremen, Germany. ²Calibr at Scripps Research, La Jolla, CA, USA. ³Center for Industrial Mathematics, University of Bremen, Bremen, Germany. ⁴MALDI Imaging Lab, University of Bremen, Bremen, Germany. ⁵These authors contributed equally: Amin Ardestani, Sijia Li, Karthika Annamalai, Blaz Lupse. ⁶These authors jointly supervised this work: Amin Ardestani, Matthew S. Tremblay, Weijun Shen, Kathrin Maedler. *email: ardestani.amin@gmail.com; mtremblay@scripps.edu; wshen@scripps.edu; kmaedler@uni-bremen.de

Loss of function and/or mass of pancreatic β -cells is a critical pathogenic hallmark of both type 1 and 2 diabetes (T1D/T2D)^{1–5}. Pancreatic β -cell apoptosis contributes to the loss of insulin-producing β -cells in diabetes, rapidly induced by the activation of the immune system in T1D and slowly progressing in T2D^{1–4,6–11}. In addition, β -cell dedifferentiation^{12–14} and failure of adaptive expansion due to impaired proliferation^{15,16} are other proposed mechanisms for the loss of functional β -cell mass in diabetes. The mechanisms of β -cell failure are complex; multiple triggering factors have been identified, which initiate signaling cascades that affect the expression of apoptotic genes. The development of novel agents that can selectively block β -cell apoptosis together with the restoration of β -cell function with safety profiles commensurate with the treatment of chronic disease is urgently needed. Current therapies for the treatment of diabetes are directed toward alleviating only the symptoms, i.e., the normalization of glycemia through enhanced insulin secretion from the remaining β -cells, and the improvement of insulin sensitivity in T2D, and through tightly controlled exogenous insulin therapy in T1D. None of the currently used antidiabetic agents target the maintenance of endogenous β -cell mass, although it has been demonstrated that even a small amount of preserved endogenous insulin secretory function has great clinical benefits¹⁷.

In our previous work, we identified mammalian sterile 20-like kinase 1 (MST1, also known as STK4, KRS2) as a critical regulator of pancreatic β -cell death and dysfunction¹¹. MST1 is a ubiquitously expressed serine/threonine kinase, the major upstream signaling kinase in the Hippo pathway, involved in multiple cellular processes, such as morphogenesis, proliferation, stress response, and apoptosis^{18,19}. MST1 is a direct target as well as an activator of caspases, forming a feed-forward loop that drives the apoptotic signaling pathway^{20,21}. MST1 promotes cell death through regulation of multiple downstream targets, such as LATS1/2, histone H2B, FOXO family members, the intrinsic mitochondrial proapoptotic pathway, stress kinase c-Jun-N-terminal kinase (JNK), and caspase-3 activation^{19,22,23}. MST1 is strongly activated in β -cells under diabetogenic conditions and its activity correlates with β -cell apoptosis and degradation of PDX1^{11,24}, a β -cell transcription factor highly important for β -cell identity, survival, and function²⁵. MST1 deficiency markedly restores β -cell function and survival and leads to protection of β -cell mass and normoglycemia in mouse models of diabetes¹¹. The identification and elaboration of MST1 inhibitors represents a promising approach to β -cell-protective drugs for the treatment of diabetes.

Several series of MST1 inhibitors have been reported, demonstrating the feasibility of generating potent, selective small-molecule inhibitors^{26–29}. Through a biochemical MST1 inhibition screen across a highly privileged collection of 641 drug-like kinase inhibitors, we identified neratinib as a potent MST1 inhibitor. Neratinib is a covalent, irreversible ATP-competitive dual inhibitor of HER2/EGFR. The epidermal growth factor receptor (EGFR, also named ErbB-1/HER1) and human epidermal growth factor receptor 2 (HER2, also named ErbB-2) are tyrosine kinases of the ErbB family and involved in organ development and growth, as well as in the pathogenesis of various tumors³⁰. FDA approved for the treatment of breast cancer^{31–33}, neratinib is also in clinical trials for lung, colorectal, and bladder cancers. Via its acrylamide moiety, neratinib forms a covalent interaction with the conserved cysteine residue (Cys-773 in EGFR and Cys-805 in HER2), resulting in tight engagement of the ATP-binding site and robust inhibition of the activation of the EGFR signaling pathway and cell proliferation³⁴. However, this conserved cysteine is not present in MST1.

In this study, we report neratinib as a β -cell-protective kinase inhibitor in proof-of-concept experiments in a widely used β -cell

line, in human islets, as well as in both T1D and T2D rodent models. Specifically, the goal of this work was to evaluate neratinib's efficacy to prevent apoptosis in human islets and to restore normoglycemia in the streptozotocin (STZ)-induced and in the obese *Lepr^{db/db}* diabetic mouse models.

Results

Neratinib was identified as MST1 inhibitor. To identify novel MST1 inhibitors, we developed a high-throughput LanthaScreen Eu kinase binding assay platform in 1536-well format. A focused library of 641 annotated kinase inhibitor compounds was screened at 5 concentrations (1, 0.2, 0.04, 0.008, and 0.0016 μ M). With staurosporine as the positive control, we chose hits with $\geq 75\%$ inhibition of binding at 1 μ M and $\geq 50\%$ inhibition at 0.2 μ M compared with staurosporine, which exhibited 100% inhibition at 1 μ M. A total of 39 hits were selected for 9-point dose response confirmation in triplicate, starting at 1 μ M followed by 1:5 serial dilution. Neratinib was identified as a potent inhibitor of MST1 ($IC_{50} = 37.7$ nM for the binding assay) (Fig. 1a, b).

We then re-profiled neratinib in a representative panel of 50 serine, threonine, and tyrosine kinases, which revealed inhibition of 16 serine/threonine and tyrosine kinases with $>50\%$ of inhibition at 10 μ M, including 98% MST1 inhibition by neratinib (Fig. 1c). Following the above results, we expanded the kinase assay panel to 250 kinases, which revealed inhibition of 59 serine/threonine and tyrosine kinases with 50% of inhibition at 3 μ M, reconfirming 97% MST1 inhibition by neratinib ($IC_{50} = 91.4$ nM for the activity-based assay; Supplementary Fig. 1a). We further evaluated these targets in dose-response experiments to 38 kinases in the panel, including EGFR, MAP4K4, MST1, and MST2, which showed consistent potency of neratinib on these four kinases, as well as potent inhibition on LOK, MAP4K5, and YES (Supplementary Fig. 1b). Further expanded dose-response experiments revealed neratinib's IC_{50} values of 1.79 nM for the well-known EGFR inhibition, 33.48 nM for MAP4K4, and 87.81 nM for MST2, indicating only a limited activity of neratinib toward MST2 (Supplementary Fig. 2).

Neratinib blocks MST1 activation and apoptosis in β -cells. To identify whether neratinib can inhibit MST1 activation and restore β -cell survival under chronic diabetogenic conditions, we exposed the INS-1E cells to various stress conditions in vitro (oxidative stress: H_2O_2 , increasing glucose concentrations alone: glucotoxicity or in combination with palmitic acid: glucolipotoxicity, and ER stress: thapsigargin). As shown previously¹¹, MST1 was highly upregulated by all diabetic conditions upon chronic exposure, shown by its autophosphorylation (pMST1-T183; Fig. 2). In contrast, neratinib potently inhibited H_2O_2 - and high glucose/palmitate-induced MST1 activation and apoptosis as represented by caspase-3 and PARP cleavage in β -cells (Fig. 2a–c). Also, neratinib restored PDX1 expression in β -cells, which was reduced by elevated glucose concentrations (Fig. 2c).

Caspase-3 activation induced by the ER stressor thapsigargin was dose-dependently abolished by neratinib, as determined by the NucView 488 caspase-3 assay (Supplementary Fig. 3a) confirming our previous data showing MST1 and caspase-3 activation by thapsigargin in β -cells, and the prevention of thapsigargin-induced apoptosis by caspase-3 inhibition¹¹. Similarly, caspase-3 activation induced by the complex mixture of inflammatory cytokines (TNF α /IFN γ) and high glucose (33 mM; Supplementary Fig. 3b) as well as lipooligosaccharide (LPS)-induced expression of inflammatory cytokines TNF α , IL-1 β , and IL-6 was largely inhibited by neratinib (Supplementary Fig. 3c). Neratinib treatment showed no evidence of interference on basal

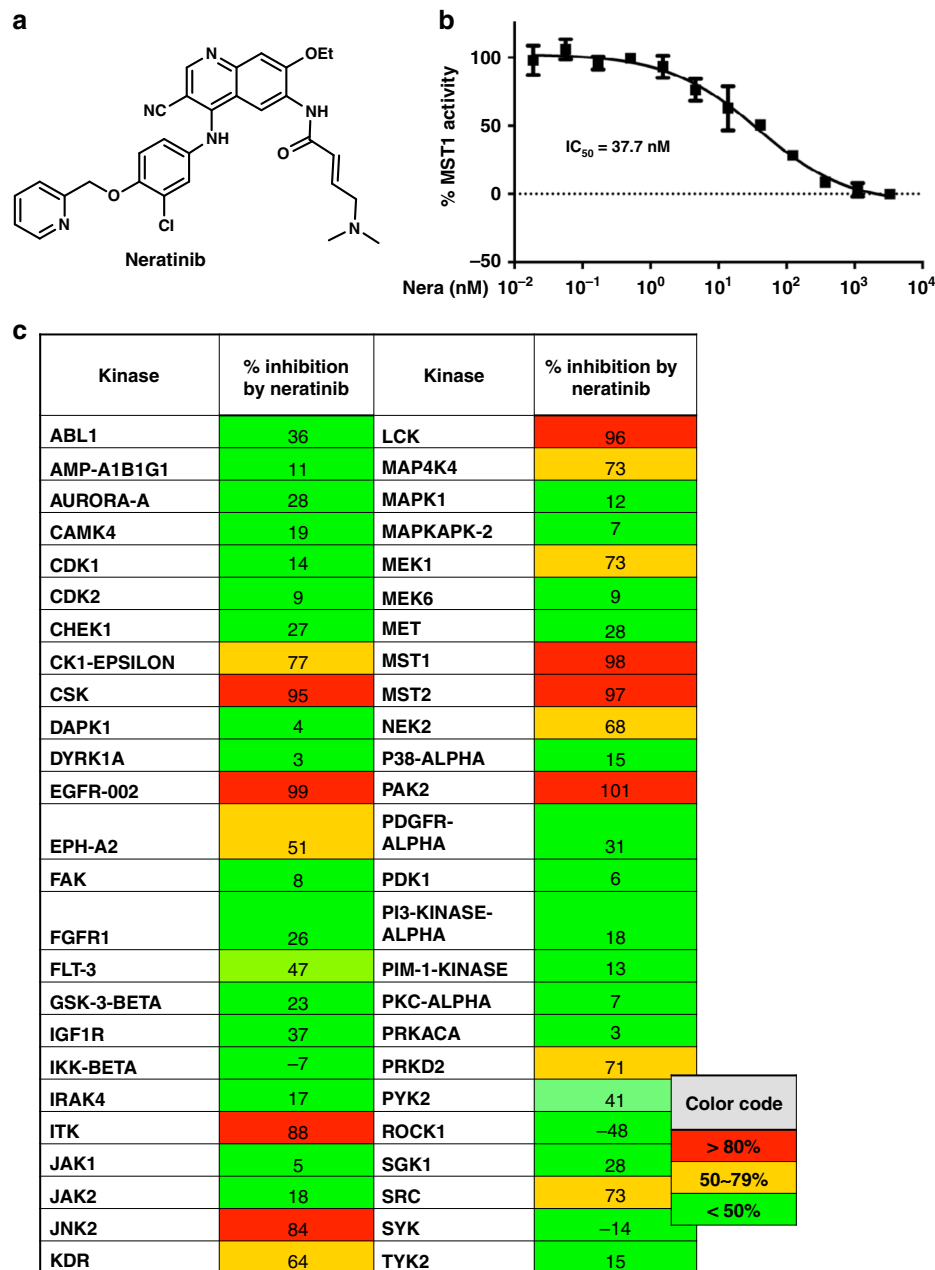


Fig. 1 Neratinib, a kinase inhibitor with MST1 efficacy. **a** Chemical structure of neratinib. **b** Biochemical dose response confirmation of MST1 inhibition. Data show means \pm SEM from three independent experiments ($n = 3$). **c** Kinase profiling showing % kinase inhibition at $10 \mu\text{M}$ neratinib with a panel of 50 kinases, means of duplicates are shown. Source data for **(b)** are provided as a Source Data file

cell viability as determined by steady-state ATP concentrations in INS-1E β -cells at all tested concentrations (Supplementary Fig. 3d).

Neratinib blocks MST1 activation and apoptosis in islets. The efficacy of neratinib to restore β -cell survival under multiple diabetogenic conditions was confirmed in six independent experiments by using human islet preparations from six different organ donors. Human islets were plated in a monolayer-like culture, and due to the complexity of the islet tissue culture, we also tested the higher concentration of $25 \mu\text{M}$ neratinib, which did not result in any detectable toxicity at basal control levels. Again, neratinib potently and significantly inhibited pro-inflammatory cytokine- as well as high glucose/palmitate-induced MST1 activation and caspase-3 activation in human

islets (Fig. 3a, b). Further analysis of TUNEL/insulin co-positivity in isolated human (Fig. 3c, d) as well as in mouse islets (Fig. 4f, g) confirmed the anti-apoptotic action of neratinib indicating its β -cell-specific protective effect against diabetogenic condition-induced apoptosis in both primary human and mouse isolated islets.

Neratinib blocks MST1 signaling and β -cell apoptosis. Further analyses in INS-1E β -cells (Fig. 4a-c), human (Fig. 4d, e), and mouse islets (Fig. 4f, g) confirmed that the protective effect of neratinib on β -cell apoptosis was dependent on MST1. As we observed a parallel restoration of β -cell survival and MST1 inhibition, we aimed to identify whether neratinib can specifically interfere with MST1 downstream signaling and block MST1-induced apoptosis.

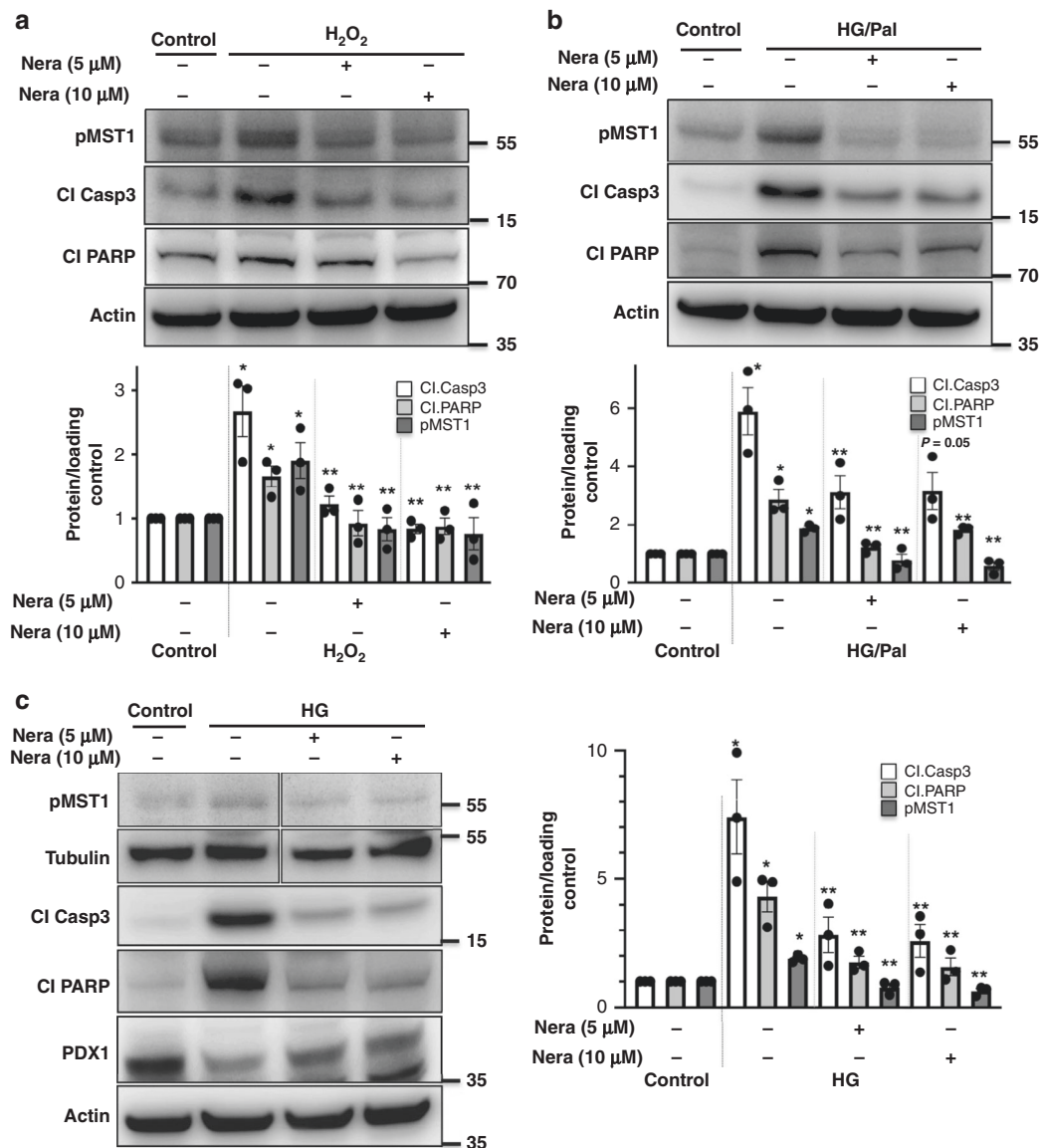


Fig. 2 Neratinib blocks MST1 activation and apoptosis in INS-1E β -cells. INS-1E cells were exposed to diabetogenic conditions (**a** H₂O₂, **b**, **c** 22.2 mM glucose or the mixture of 22.2 mM glucose and 0.5 mM palmitate (HG/Palm)) \pm neratinib for 72 h. Phospho-MST1 (pMST1; pThr183), caspase-3 and PARP cleavage, PDX1, tubulin, and actin were analyzed by western blotting. Representative Western blots and pooled quantitative densitometry analysis are shown from three independent cell line experiments ($n = 3$). Results shown are means \pm SEM. * $p < 0.05$ H₂O₂ or HG or HG/Pal to control, ** $p < 0.05$ neratinib to vehicle-treated β -cells under the same diabetogenic conditions; all by Student's t tests. Source data are provided as a Source Data file

Recently, a highly sensitive and reproducible bioluminescence-based biosensor (LATS-BS) that monitors the specific activity of MST1 and its downstream substrate LATS kinase in vitro in real time was developed³⁵. Both MST1 and LATS2 are core kinases of Hippo signaling pathway, which act together to induce β -cell apoptosis³⁶, and the specific MST1–LATS2 signaling activation can therefore be analyzed by this assay. LATS1/2 kinases phosphorylate their own established target Hippo transcriptional coactivator yes-associated protein (YAP) on S127 that exposes the docking site for binding of 14-3-3 proteins and leads to YAP cytoplasmic sequestration. Therefore a LATS-BS construct has been generated with fusion of YAP fragment and 14-3-3 with N-terminal and C-terminal firefly luciferase fragments (N-luc and C-luc), respectively that assesses LATS kinase activity by measuring the interaction between pS127-YAP and 14-3-3³⁵ in a MST1–LATS2-phosphorylation-dependent manner (Fig. 4a). Adenoviral overexpression of MST1/LATS2 in YAP-deficient

INS-1E³⁷ β -cells transfected with LATS-BS induced strong bioluminescence-based induction of luciferase activity (represents YAP-14-3-3 final interaction; Fig. 4b) as well as YAP-S127 phosphorylation as determined by YAP-S127 phospho-specific antibody (Fig. 4c), both which was strongly inhibited by neratinib indicating its potent inhibitory action against MST1–LATS2 signaling, while canertinib, a related acrylamide-based covalent EGFR inhibitor with a similar structure to neratinib but without MST family inhibitory activity³⁸ added at the same conditions had no inhibitory effect.

Consistent with our previous observations that MST1 overexpression alone was sufficient to induce β -cell apoptosis¹¹, adenoviral overexpression of MST1 induced a dramatic induction of β -cell apoptosis in isolated human islets, which was significantly blocked by neratinib (Fig. 4d, e and Supplementary Fig. 4) suggesting a direct interference of neratinib with proapoptotic MST1 or its downstream signaling. To see whether

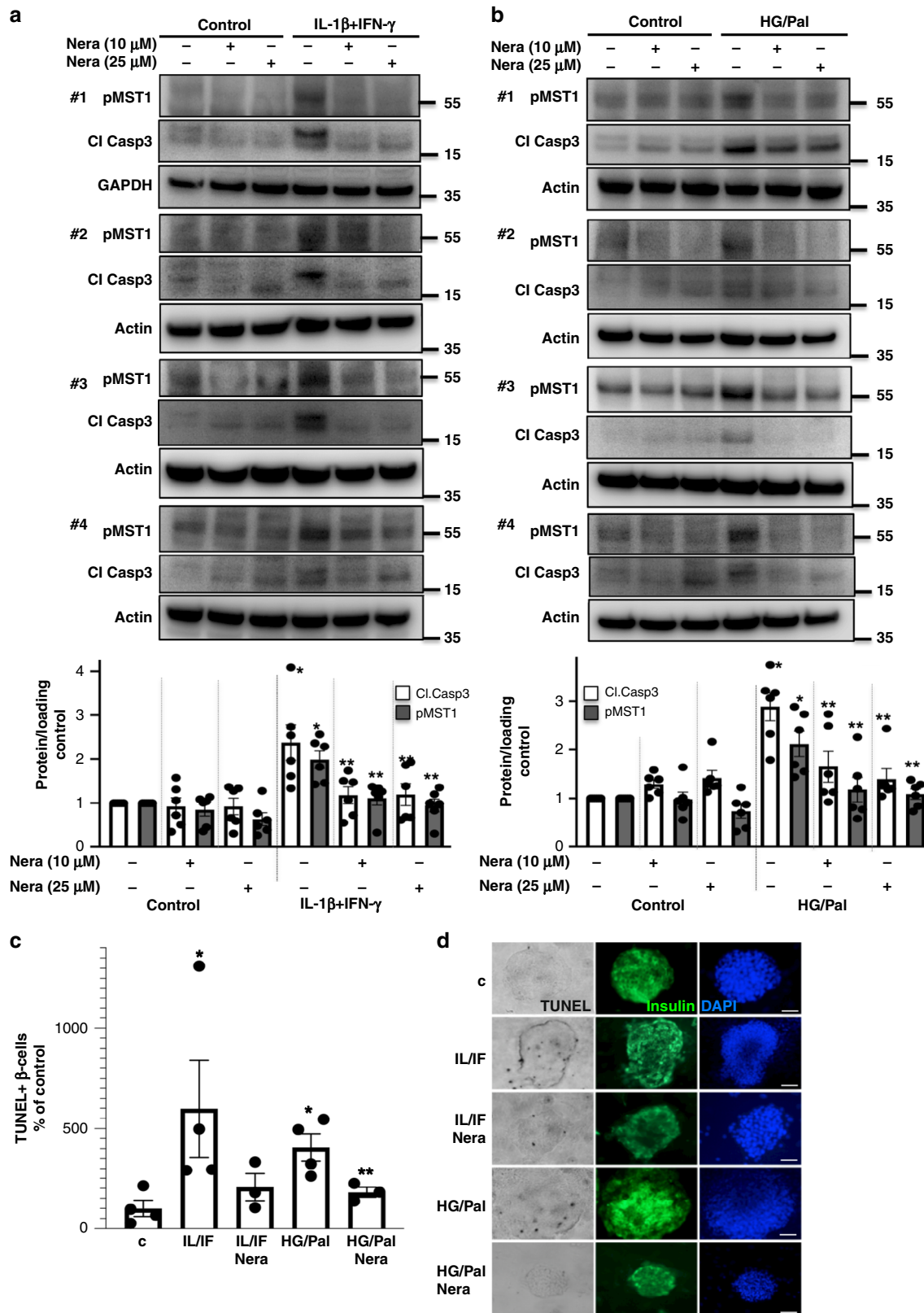
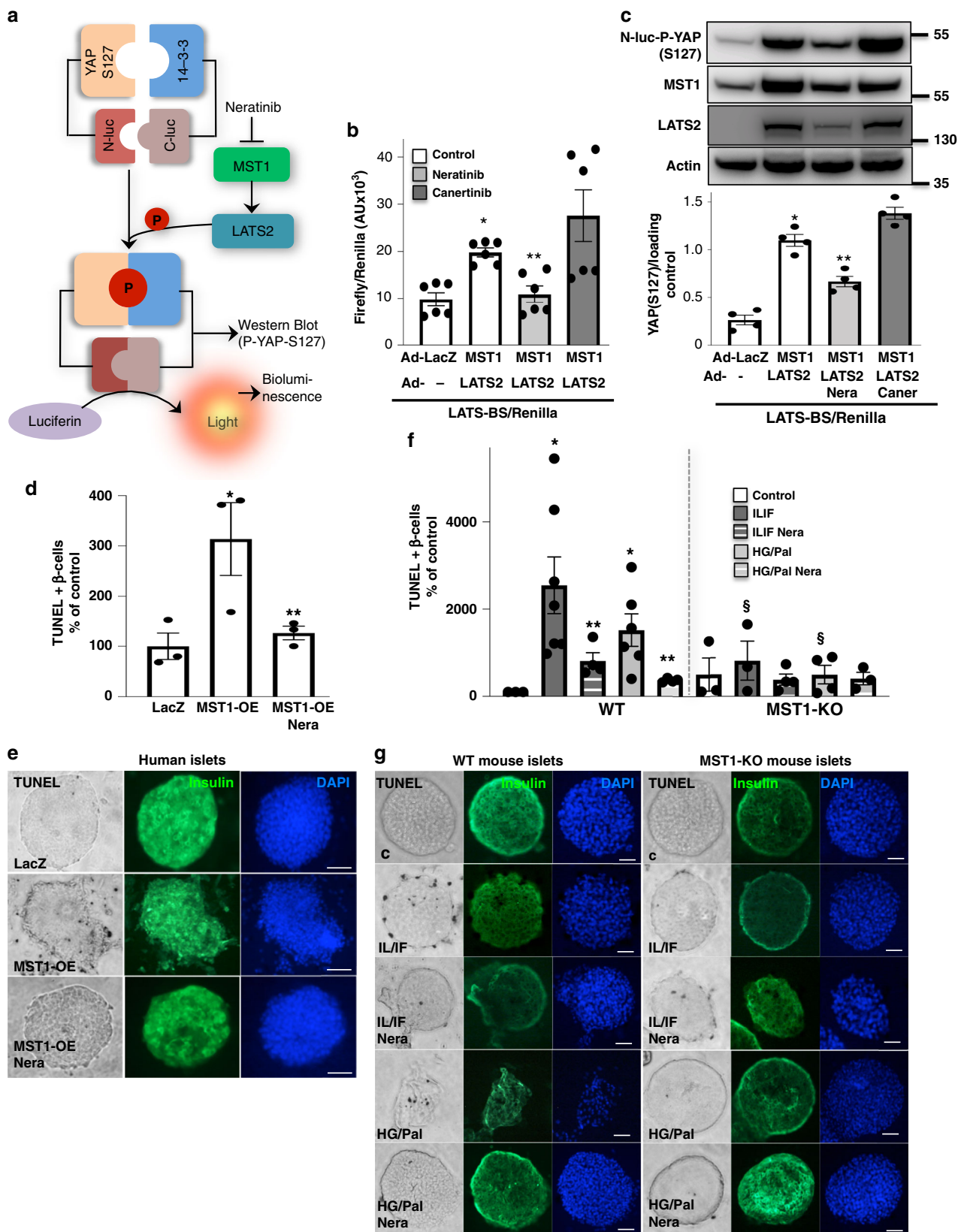


Fig. 3 Neratinib blocks MST1 activation and apoptosis in human islets. Human islets were exposed to diabetogenic conditions (**a**, **c**, **d** IL-1 β /IFN γ , **b-d** mixture of 22.2 mM glucose and 0.5 mM palmitate (HG/Palm)) \pm neratinib for 72 h. **a**, **b** Phospho-MST1 (pMST1; pThr183), caspase-3 cleavage, and GAPDH or actin were analyzed by western blotting. Representative Western blots of four different human islet donors (**a**, **b**; upper panels) and pooled quantitative densitometry analysis (**a**, **b**; lower panels) of six different human islet donors are shown ($n = 6$). **c**, **d** β -cell apoptosis analyzed by triple staining of TUNEL (black nuclei), insulin (green), and dapi (blue). Scale bar, 100 μ m. An average number of 40,420 insulin-positive β -cell per condition was counted in 3-4 independent experiments from 3 to 4 different human islet donors ($n = 3-4$). Results shown are means \pm SEM. * $p < 0.05$ IL/IF or HG/Pal to control, ** $p < 0.05$ neratinib to vehicle-treated islets under the same diabetogenic conditions; all by Student's t tests. Source data are provided as a Source Data file



MST1 is the true target of neratinib in the context of β -cell protection from apoptosis, we evaluated its effect in isolated islets from global MST1-knockout (MST1-KO) mice and their wild-type (WT) littermates. While pro-inflammatory cytokines and glucolipototoxicity highly induced apoptosis in WT mice, their harmful effect on β -cell survival was almost gone in islets isolated

from MST1-KO mice (Fig. 4f, g), consistent with our previous observation¹¹. Similarly, neratinib reduced cytokine- and glucolipototoxicity-induced apoptosis in WT islets, but had no additive effect in MST1-KO mice, assuming that MST1 inhibition by neratinib is sufficient to restore β -cell survival. Neratinib had no significant effect in MST1-KO islets, neither on cytokine- nor

Fig. 4 Neratinib blocks MST1 signaling and MST1-induced β -cell apoptosis. **a** Domain structure and mechanism of action for the LATS-BS. At control condition, there is no interaction between YAP and 14-3-3 showing minimal bioluminescence activity for LATS-BS (N-luc-YAP15-S127 and C-luc-14-3-3)³⁵. Upon LATS activation induced by MST1, LATS-dependent phosphorylation of YAP15-S127 (analyzed by Western blotting in **(c)**) leads to 14-3-3 binding, luciferase complementation, and high biosensor signal corresponding to higher LATS activity (analyzed by bioluminescence in **(b)**). **b, c** Adenoviral overexpression of MST1/LATS2 or LacZ (control) in INS-1E cells, which had been transfected with the firefly luciferase reporter plasmids N-luc-YAP15-S127 and C-luc-14-3-3 as well as pRL-Renilla luciferase vector control 24 h before 10 μ M neratinib or canertinib was added for the last 24 h. Downstream YAP-S127 phosphorylation was determined by luciferase activity (normalized to the Renilla signal **(b)**). Western blotting for YAP-S127 phospho-specific antibody **(c)**; successful transfection was confirmed by LATS2 and MST1 analysis, and actin was used as housekeeping control. Data are means from six independent culture dishes ($n = 6$; **b**) or four independent cell line experiments ($n = 4$; **c**) \pm SEM. Representative Western blot is shown. **d, e** Human islets were infected with Ad-LacZ (control) or Ad-MST1 adenoviruses and exposed to 10 μ M neratinib for 48 h. **f, g** Isolated islets from MST1-KO mice and their WT littermates were recovered after isolation overnight and exposed to diabetogenic conditions (IL-1 β /IFN γ or the mixture of 22.2 mM glucose and 0.5 mM palmitate (HG/Pal)) \pm 10 μ M neratinib for 72 h. **d-g** β -cell apoptosis was analyzed by triple staining of TUNEL (black nuclei), insulin (green), and dapi (blue). Scale bar, 100 μ m. **d** An average number of 30,700 insulin-positive β -cell per condition was counted in three independent experiments from three different donors ($n = 3$) and **f** of 5942 insulin-positive β -cells per condition from three to seven mice/condition ($n = 3-7$). Results shown are means \pm SEM. * $p < 0.05$ MST1-OE, or IL/IF or HG/Pal to Lac-Z or control, ** $p < 0.05$ neratinib treated with MST1-OE or IL/IF or HG/Pal-treated islets to vehicle-treated islets under the same conditions; $^{\S}p < 0.05$ MST1-KO to WT islets under the same diabetogenic conditions; all by Student's *t* tests. Source data are provided as a Source Data file

in glucolipototoxicity-induced apoptosis; these results show that neratinib specifically blocks MST1 signaling and MST1-mediated β -cell apoptosis in islets under diabetogenic conditions.

Neratinib but not canertinib restores β -cell survival. To provide further incisive target validation data for MST1, cellular target engagement as well as functional studies were performed by using neratinib and a closely related EGFR inhibitor canertinib (a.k.a. CI-1033) that lacks MST1 inhibitory activity as a target control. Indeed, canertinib showed potent EGFR inhibition (IC₅₀ value of 0.21 nM), but no appreciable inhibition of MST1 or MST2 at concentrations up to 10 μ M in our biochemical kinase inhibition assays (Supplementary Fig. 5). Cellular target engagement assays such as the cellular thermal shift assay (CETSA) determine direct interactions between a drug and its protein target, based on drug- or ligand-induced thermal stabilization of target proteins in intact cells³⁹. In this case, CETSA has been applied to assess the direct interaction of neratinib or canertinib with MST1 in INS1-E cells. Consistent with their biochemical kinase inhibition profile, a specific binding of neratinib to MST1 in live cells is suggested by MST1 stabilization at 55 $^{\circ}$ C, while its degradation occurred at the same condition with canertinib or vehicle control (Fig. 5a).

We then compared the effect of neratinib and canertinib on MST1 activation, its downstream apoptotic target, and β -cell apoptosis in metabolically stressed β -cells. While neratinib, consistently with presented data (Figs. 2 and 3), strongly counteracted stress-induced MST1 activation and caspase-3 and PARP cleavage, the EGFR inhibitor canertinib was ineffective at a similar concentration (Fig. 5b, c). We have previously shown that MST1 activates the mitochondrial pathway of cell death in β -cells through regulating the BH3-only protein member BIM of Bcl-2 family proteins and that MST1-induced apoptosis requires BIM to trigger mitochondrial-mediated apoptosis in β -cells¹¹. Correspondingly, our data show that the EGFR/MST1 inhibitor neratinib but not the EGFR inhibitor canertinib significantly reduced downstream mitochondrial BIM induction under diabetic conditions (Fig. 5b, c). Unlike neratinib, canertinib showed a significant stimulatory effect on apoptotic effectors cleaved caspase-3, cleaved PARP, and BIM under basal conditions (Fig. 5b, c). These data suggest that EGFR signaling inhibition (as represented by canertinib) is dispensable for neratinib-induced MST1 inhibition and protection from apoptosis.

Neratinib restores glycemia in a T1D mouse model. Initial pharmacokinetic studies in mice (Supplementary Fig. 6a) were performed to determine the exposure and half-life of neratinib.

Mice were food-deprived overnight, and neratinib (5 mg/kg in 30% PEG400/0.5% Tween80/5% propylene glycol in saline; single i.p. dose) was given to the mice, and plasma samples were collected 30 min., 1, 3, and 7 h post dosing. Neratinib displayed a stable exposure profile in mice plasma and reached the maximum concentration at 306 ng/mL, on average 0.67 h post dosing (Supplementary Fig. 6a).

Multiple low-dose streptozotocin (MLD-STZ) injections induce severe diabetes through activation of cell-intrinsic apoptotic pathways as well as selective immune-mediated destruction of β -cells. Since neratinib blocked apoptosis in human islets and in β -cells, we tested its ability to restore normoglycemia in vivo in a mouse model of MLD-STZ-induced β -cell demise and T1D. Neratinib treatment had no influence on body weight (Supplementary Fig. 6b). By day 3 of post-STZ treatment, hyperglycemia was evident, with glucose levels progressively increasing throughout the 35-day study (Fig. 6a). This was accompanied with severely impaired glucose tolerance in the STZ-treated control mice (Fig. 6b). Neratinib-treated mice had lower glucose levels during the entire 35 days of the study and exhibited significantly improved glucose tolerance. Neratinib had no effect on glycemia in nondiabetic control mice (Fig. 6a, b).

Insulin tolerance tests demonstrated dramatically elevated glucose levels during a 4-h fast prior to insulin administration (Fig. 6c), but neither neratinib nor STZ had a significant effect on insulin sensitivity, shown by the analysis of normalized glucose levels (Fig. 6d). Indeed, impaired insulin secretion observed in STZ-treated mice during an intraperitoneal glucose-stimulated insulin secretion assay was significantly improved with neratinib treatment (Fig. 6e). Consistently, insulin-to-glucose ratios were significantly elevated in neratinib-treated STZ mice (Fig. 6f). These data suggest that glucoregulatory effects of neratinib are primarily mediated by improved β -cell function. Furthermore, islet architecture was disrupted, leading to significantly reduced β -cell mass, in STZ-treated mice compared with nondiabetic control mice (Fig. 6g), as a result of profound increase in β -cell apoptosis (Fig. 6h and Supplementary Fig. 7). Together with the increased β -cell apoptosis induced by STZ, β -cell proliferation was also induced, indicative of compensatory capacity in response to STZ-induced β -cell injury (Fig. 6i and as reported before¹¹). Neratinib restored β -cell mass and reduced β -cell apoptosis (Fig. 6g, h), with no effect on β -cell proliferation in either control or diabetic mice (Fig. 6i).

Neratinib restores PDX1, NKX6.1, and Glut2 expression. We next examined whether neratinib can also restore expression of

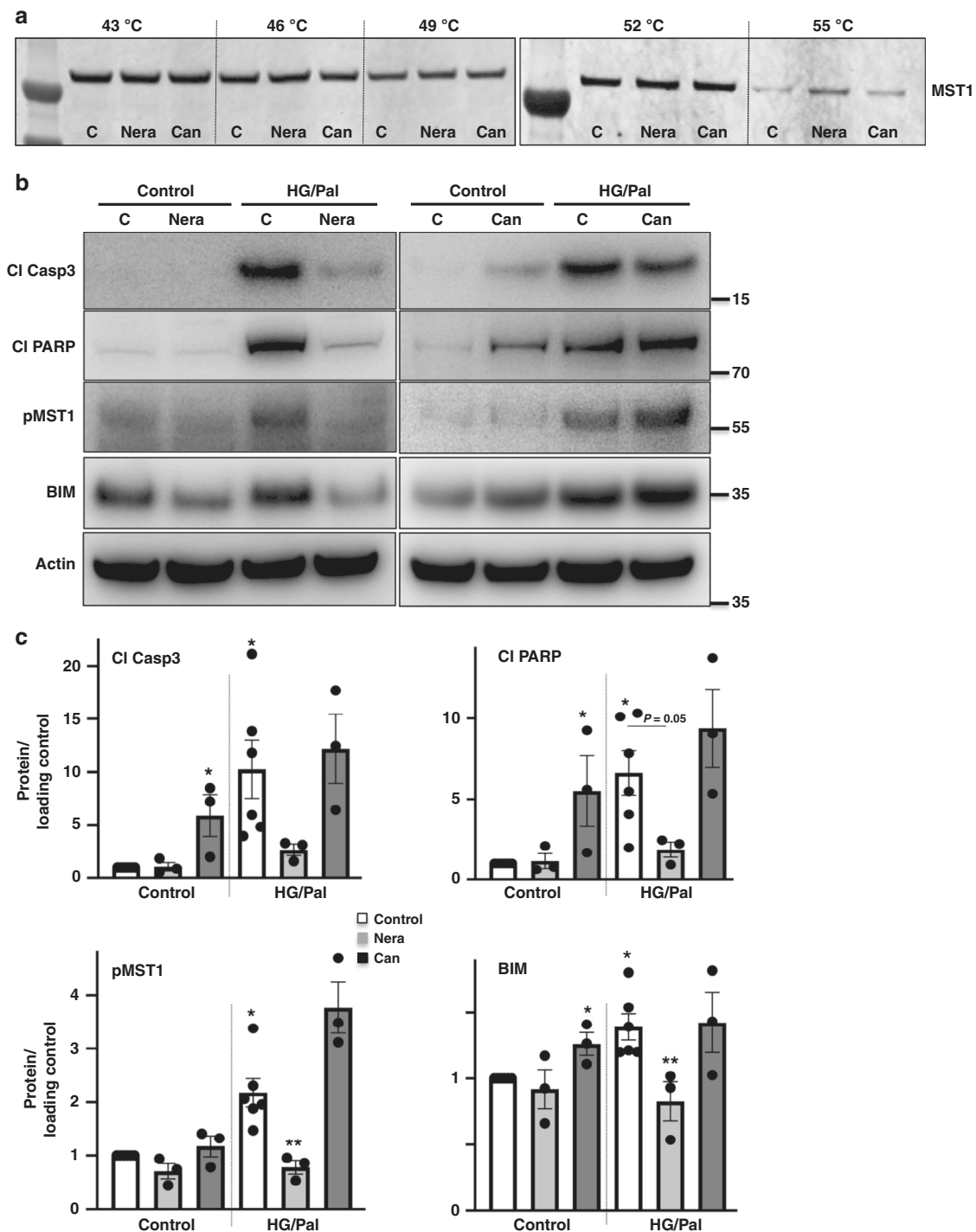
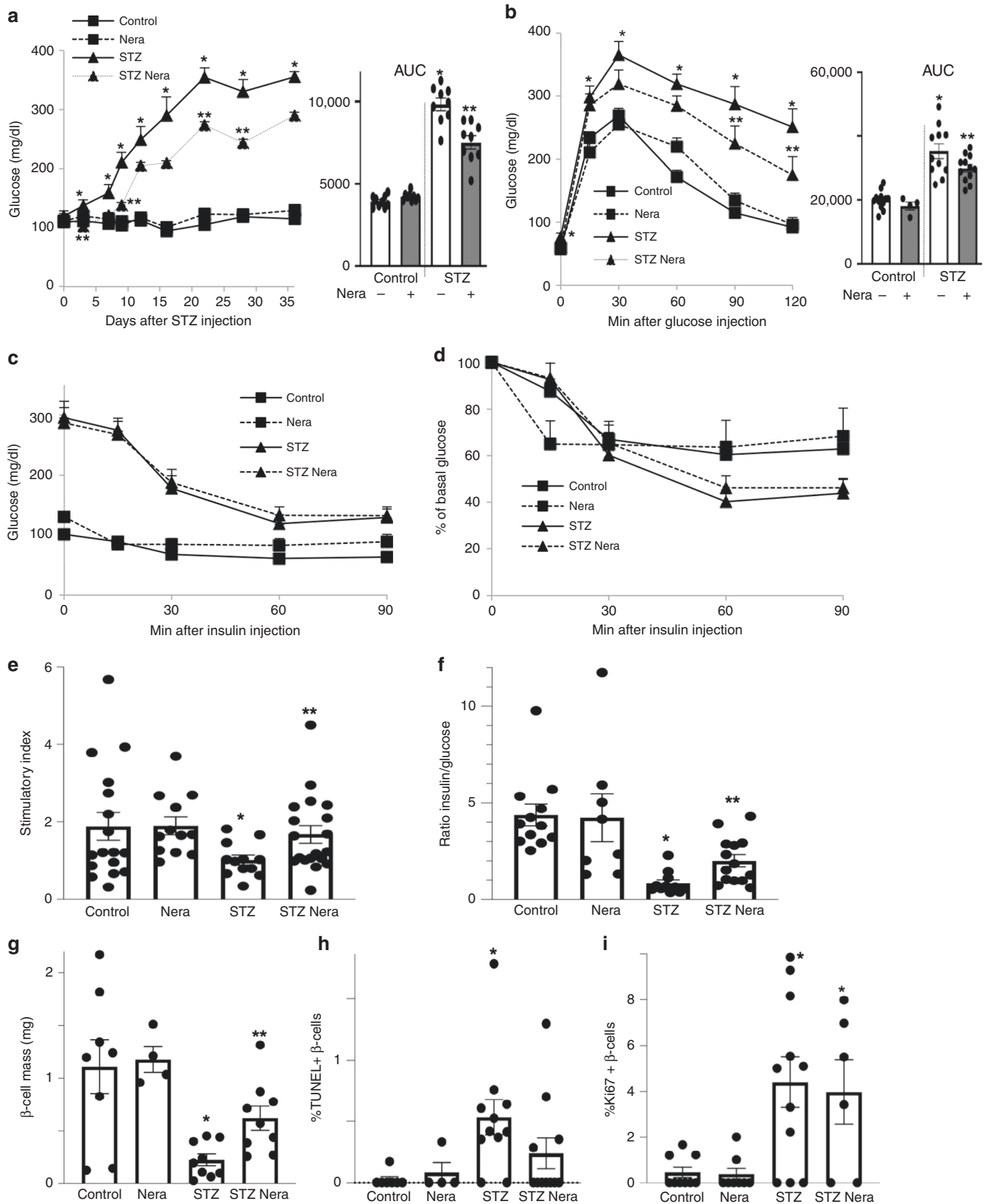


Fig. 5 Neratinib but not canertinib binds to MST1 and restores β -cell survival through MST1 inhibition. **a** CETSAs were performed in INS-1E cells pretreated with 5 μ M neratinib, canertinib, or vehicle control, followed by heating to denature and precipitate protein at different temperatures. The stabilized MST1 protein in the soluble fraction of the cell lysate was detected by using western blotting. **b, c** INS-1E cells were exposed to diabetogenic conditions (22.2 mM glucose and 0.5 mM palmitate (HG/Pal)) \pm 10 μ M neratinib or canertinib for 24 h. Phospho-MST1 (pMST1; pThr183), caspase-3 and PARP cleavage, and BIM and actin were analyzed by western blotting. Representative Western blots (**b**) and pooled quantitative densitometry analysis (**c**) are shown from 3–6 independent culture dishes ($n = 3–6$). Results shown are means \pm SEM. * $p < 0.05$ HG/Pal to control, ** $p < 0.05$ neratinib to vehicle + HG/Pal-treated β -cells under the same conditions; all by Student's *t* tests. Source data are provided as a Source Data file

three important markers for β -cell glucose metabolism and insulin production—the transcription factors PDX1 and NKX6.1 and the glucose transporter Glut2. MLD–STZ-treated mice showed impairment in the islet architecture with smaller islets and many insulin-negative cells together with reduced numbers and expression of nuclear PDX1- and NKX6.1-positive cells.

Many cells within the islets, which still express insulin, had lost their NKX6.1 expression. These effects were markedly attenuated by neratinib treatment (Fig. 7a, b). The PDX1 target gene Glut2 was largely preserved in β -cell membranes of control mice, while the disrupted islet architecture of diabetic mice was also apparent by Glut2 staining, which was barely detectable in the MLD–STZ-



treated mice (Fig. 7c). Neratinib treatment restored β -cell Glut2 expression (Fig. 7c). These effects of neratinib confirm previous results from MST1-KO mice, where PDX1 and Glut2 protein expression was greatly restored, and β -cell function and survival were highly preserved¹¹.

Neratinib restores glycemia in a T2D mouse model. Obese diabetic $Lepr^{db/db}$ mice (db/db, Fig. 8) become severely diabetic and exhibit β -cell apoptosis and dysfunction⁴⁰ together with islet upregulation of activated MST1¹¹ at the age of 10 weeks. To test whether MST1 inhibition by neratinib could affect glycemia in

Fig. 6 Neratinib improves glycemia, insulin secretion, and β -cell survival in the MLD-STZ-mouse model of type 1 diabetes. C57Bl/6J mice were injected with 40 mg/kg streptozotocin or citrate buffer for 5 consecutive days. Neratinib or vehicle was daily i.p. injected at a concentration of 5 mg/kg starting 3 h before the first STZ injection throughout the whole experiment of 35 days. **a** Random fed blood glucose measurements after the first STZ injection (day 0) over 35 days and **b** intraperitoneal glucose tolerance test (ipGTT); (respective area-under-the curve (AUC) analyses are shown in the right insets). **c, d** Intraperitoneal insulin tolerance test (ipITT). In **d**, basal glucose values were normalized to 100%. **e** Insulin secretion measured from retro-orbital blood draw during an ipGTT measured before (0 min) and 15 min after glucose injection; data are expressed as the ratio of secreted insulin at 15 min/0 min (stimulatory index). **f** The ratio of secreted insulin and glucose is calculated at fed state. **g-i** Mice were killed at day 35. **g** β -cell mass (given as percentage of the whole pancreatic section from ten sections spanning the width of the pancreas) and quantitative analyses from triple staining for **h** TUNEL or **i** Ki67, insulin, and DAPI expressed as percentage of TUNEL- or Ki67-positive β -cells \pm SEM. An average number of 2331 (**h**), or 26369 (**i**) β -cells were counted. $n = 9$ mice/group for (**a**); $n = 4-12$ for (**b**); $n = 5-15$ for (**c**) and (**d**); $n = 12-19$ for (**e**); $n = 8-14$ for (**f**); $n = 4-9$ for (**g**); $n = 4-11$ for (**h**); and $n = 6-11$ mice/group for (**i**); all from three independent experiments). Data show means \pm SEM. * $p < 0.05$ STZ compared with vehicle-injected mice, ** $p < 0.05$ STZ compared with STZ-Nera injected mice; by one-way ANOVA with Bonferroni corrections for (**a, b**); by Student's *t* tests for (**e-i**). Source data are provided as a Source Data file

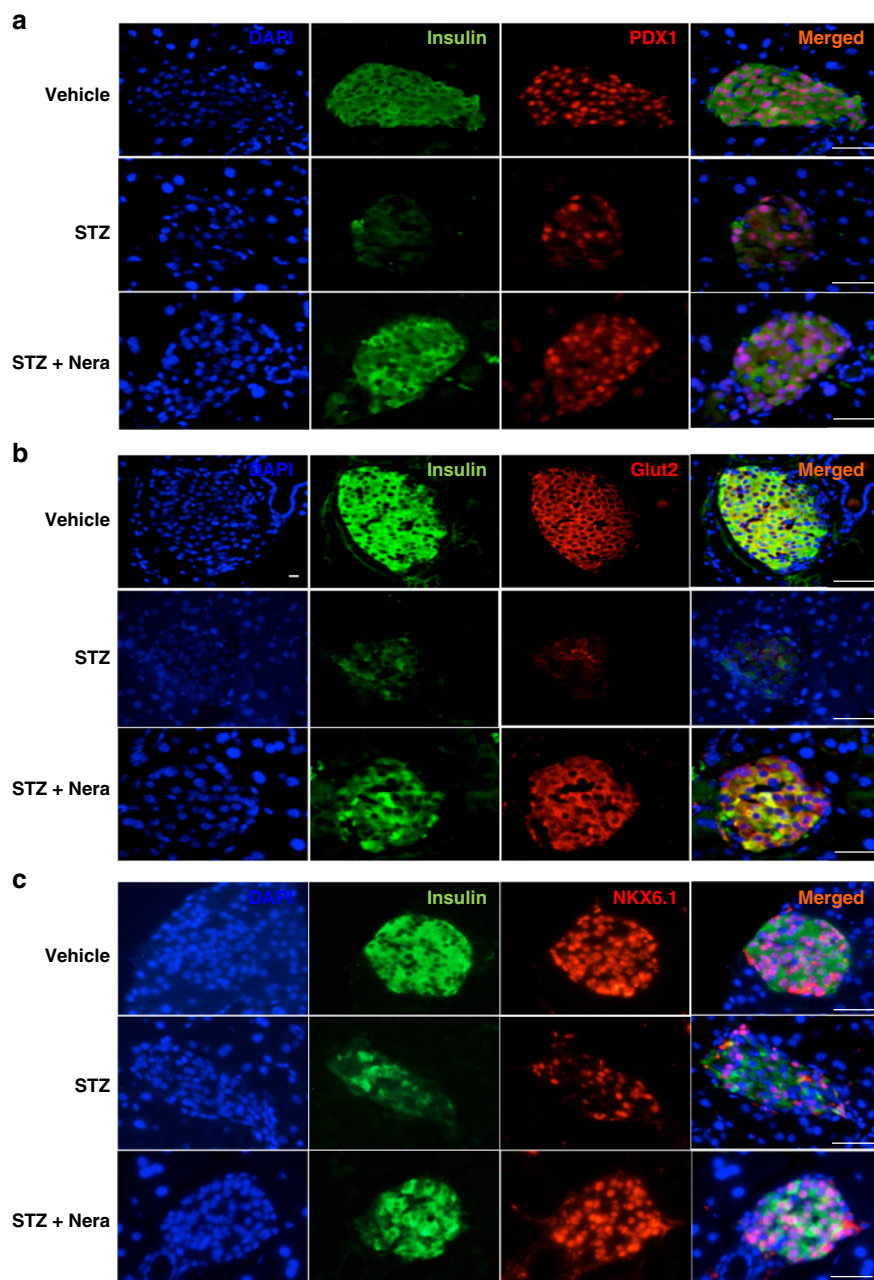


Fig. 7 Neratinib restores PDX1, NKX6.1, and Glut2 expression. Representative triple stainings for PDX1 (red, **a**), Glut2 (red, **b**), or NKX6.1 (red, **c**), insulin (green), and DAPI (blue) are shown from vehicle-, STZ-, and STZ/Nera-treated mice ($n = 8, 4, 9$ & 9 mice/group). Scale bar, 100 μ m

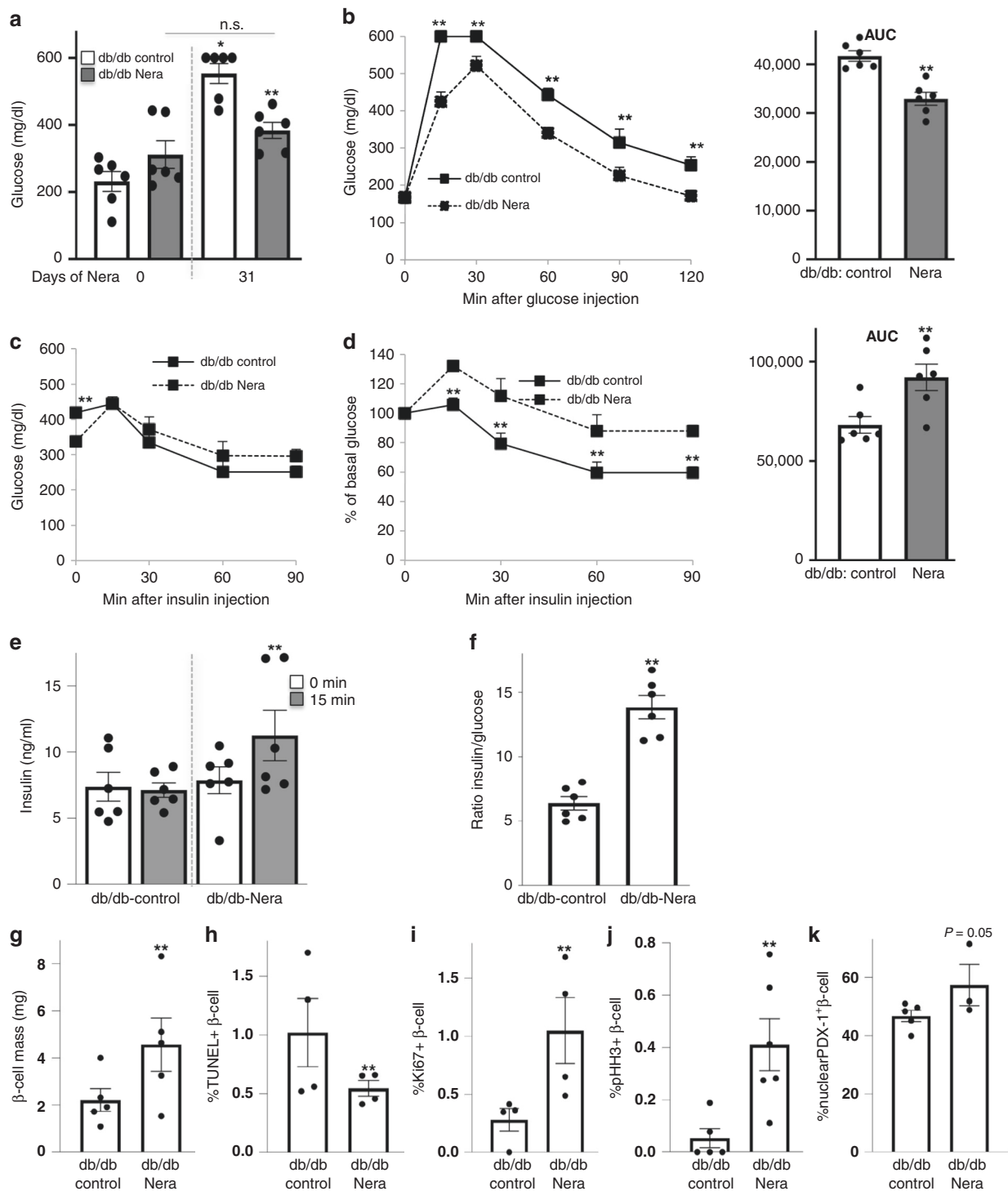


Fig. 8 Neratinib improves glycemia, insulin secretion, and β -cell survival in obese db/db mouse model of type 2 diabetes. Obese diabetic *Lep^{db/db}* mice on the C57BLKS/J background (db/db) were randomized in two groups at the age of 6 weeks, and then, neratinib or vehicle was daily i.p. injected at a concentration of 5 mg/kg throughout the whole experiment of 31 days. **a** Random fed blood glucose measurements before and after 31 days of Neratinib or vehicle injection (last day of the study). **b** Intraperitoneal glucose tolerance test (ipGTT). **c, d** Intraperitoneal insulin tolerance test (ipITT). In **d**, basal glucose values were normalized to 100% (respective area-under-the-curve (AUC) analyses for **b** and **d** are shown in the right insets). **e** Insulin secretion during an ipGTT measured before (0 min) and 15 min after glucose injection. **f** The ratio of secreted insulin and glucose is calculated at fed state. Data are representative of six mice per group ($n = 6$ for **(a-f)**). **g-j** Mice were killed at day 31. **g** β -cell mass (given as percentage of the whole pancreatic section from ten sections spanning the width of the pancreas; $n = 5$ mice/group) and quantitative analyses from triple stainings for **(h)** TUNEL, **(i)** Ki67, **(j)** pHH3, and **(k)** nuclear PDX1 expression, insulin, and DAPI expressed as percentage of TUNEL-, Ki67-, pHH3-, or nuclear PDX1-positive β -cells \pm SEM. An average number of 13667 (**h**), 5937 (**i**), 7108 (**j**), or 4330 (**k**) β -cells were counted from $n = 3-5$ (**h, i, k**) or $n = 5-6$ (**j**) mice/group. Data show means \pm SEM. * $p < 0.05$ vehicle control at the end (10.5 weeks of age) compared with the start of the study (6 weeks of age), ** $p < 0.05$ db/db compared with db/db-Nera injected mice; by one-way ANOVA with Bonferroni corrections for **(a)**; by Student's *t* tests for **(b-k)**. Source data are provided as a Source Data file

the db/db model, 6-week-old obese db/db mice were treated daily with neratinib or vehicle over a period of 31 days. Neratinib treatment had no influence on body weight (Supplementary Fig. 6c). While blood glucose levels remained stable and glucose levels did not significantly increase in the neratinib-treated db/db mice after 4 weeks, they predictably rose to severe hyperglycemia (>500 mg/dL) in the vehicle-treated db/db mice (Fig. 8a). Attenuation of hyperglycemia was also evident in the intraperitoneal glucose tolerance test, in which neratinib showed lower glucose levels at all time points measured (Fig. 8b), and enhanced insulin secretion and insulin-to-glucose ratios (Fig. 8e, f). Basal glucose levels were unchanged by neratinib treatment after an overnight fast (Fig. 8b), but 20% lower in the neratinib-treated mice after a short fast of 4 h (Fig. 8c). These differences in fasting glucose prompted us to conduct an intraperitoneal insulin tolerance test, which showed that neratinib-treated mice had a modestly reduced ability to lower their glucose levels in response to insulin challenge (Fig. 8c, d), despite neratinib's improvement in the overall restoration of glucose homeostasis. At the level of the β -cell, neratinib showed increased β -cell mass (Fig. 8g), which resulted from significantly reduced β -cell apoptosis (Fig. 8h and Supplementary Fig. 8a) and increased proliferation as determined by two markers Ki67 and phospho-Histone H3 (pHH3) immunolabeling (Fig. 8i, j and Supplementary Fig. 8b, c). While less than 50% of β -cells contained PDX1 in the nucleus, nuclear PDX1 was enhanced by neratinib (Fig. 8k and Supplementary Fig. 9).

Neratinib improves β -cell survival in an ex vivo approach.

While neratinib improved glycemia in db/db mice in vivo, we aimed to confirm whether this effect occurs directly in islets ex vivo. Thus, we isolated mouse islets from severely diabetic db/db mice, where β -cell apoptosis was 3.2-fold increased, compared with islets from nondiabetic db/+ littermates. Adding neratinib to the islet cultures fully restored β -cell survival (Fig. 9a, b). MST1 activation and proapoptotic BIM in islets were reversed by ex vivo neratinib treatment (Fig. 9c, d). Neratinib also enhanced nuclear PDX1 expression (Supplementary Fig. 10).

We then addressed the question whether cytokine-induced β -cell apoptosis can also be normalized by neratinib and designed another therapeutic approach by treating the islets with the cytokine mixture of IL-1 β /IFN γ cytokine mixture for 48 h and then added neratinib to the culture for another 24 h. While the cytokines induced a dramatic increase in β -cell apoptosis, neratinib fully restored β -cell survival (Fig. 9e, f).

Neratinib is enriched and distributed in the pancreas. To provide further evidence that neratinib mediates the antidiabetic effects through a direct impact on the β -cell, we sought to confirm meaningful pharmacokinetic exposure of neratinib in the pancreas by using matrix-assisted laser desorption ionization imaging mass spectrometry (MALDI-IMS)⁴¹. Specificity of the signal was tested on a liver phantom model, where neratinib was spotted on frozen mouse liver sections at concentrations ranging from 0 to 500 pmol/ μ l and peaks analyzed by MALDI imaging MS (Supplementary Fig. 11a). Starting at a concentration of 50 pmol/ μ l, neratinib could clearly be detected on liver sections at *m/z* 557.2, which represents the monoisotopic peak of neratinib (Supplementary Fig. 11a). Linear regression of signal intensity to neratinib concentration could be observed until 400 pmol/ μ l. The mass spectrum of the neratinib standard (Supplementary Fig. 11c) showed the expected isotope distribution as the simulated spectrum for neratinib (Supplementary Fig. 11b). Note the high abundance of the third peak at *m/z* 559.2, which is mostly caused by the stable isotope ³⁷Cl, which occurs in nature with an abundance of 24.2% (sum formula of neratinib C₃₀H₂₉ClN₆O₃).

This characteristic isotope distribution could also be detected in single spectra of high neratinib-intense regions in the pancreas after treatment (Supplementary Fig. 11d). A specific signal was obtained in pancreas tissue sections after a 4-week daily i.p. injection in the db/db mice with no signal evident from vehicle-treated control mice (Supplementary Fig. 11e). Neratinib was also clearly detected in pancreatic tissue 4 h after intraperitoneal (i.p.) injection of WT mice (Supplementary Fig. 11f).

Discussion

In this study, we demonstrate neratinib as the inhibitor of MST1, a previously unappreciated activity alongside the dual inhibition of HER2/EGFR that drives its clinical utility in breast cancer. We show that neratinib protects β -cells from the apoptosis-inducing effects of a complex diabetic milieu in vitro in rat INS-1E β -cells and primary human and mouse islets, and lowers hyperglycemia in vivo in two widely used rodent models of diabetes. Repurposing of FDA-approved drugs has been a topic of great interest amidst the escalating costs of new drug development, particularly in the case of diseases with high-unmet medical need, such as T1D. Our studies suggest that neratinib—shown to be safe and well-tolerated in thousands of subjects in many Phase II and III clinical trials for cancer therapy^{32,42}—could have a therapeutic effect in treating diabetes. Although diarrhea, vomiting, and nausea were most common neratinib-associated adverse events, they showed no increased risk of long-term toxicity or adverse consequences³². The appropriateness of the tolerability profile of neratinib for patients with a non-immediate-life-threatening disease such as diabetes must be considered carefully; as such, side effects may hinder its direct use in treating patients with either T1D or T2D, and thus, have to be reinvestigated in a clinical diabetes setting. Based on our mouse studies, a short therapeutic interval of 30 days could markedly restore β -cell survival and function, and thus, maybe sufficient for therapy in patients. Especially in the obese db/db model, it becomes clear that neratinib treatment prevented the severe increase in blood glucose over time. We started the experiment, when mice were already mildly hyperglycemic (mean random glucose of all mice was 271.5 mg/dl). After 30 days of therapy, the control group showed a 2.4-fold increase in blood glucose (from 231 to 554 mg/dl), while the neratinib group had no significant blood glucose increase (312–384 mg/dl).

Besides their potent action in cancer therapy, multitarget tyrosine inhibitors have been suggested for a long time for the treatment of diabetes, in some cases driven by polypharmacology outside of the tyrosine kinase target class. For example, imatinib, which targets c-Abl, DDR1/2, c-Kit, and PDGFR; sunitinib, which targets FLT1/3/4, c-Kit, PDGFR, and VEGFR2; erlotinib and PD153035, potent and specific inhibitors of EGFR, have all been reported to have potent anti-hyperglycemic effects in preclinical as well as in several clinical case reports^{43,44}. In a related compound class, the tyrosine phosphatase PTP1b inhibitor ertiprotafib was explored as a novel insulin sensitizer for T2D, based on its ability to improve fasting blood glucose and glucose tolerance in the Zucker diabetic fatty rat⁴⁵, with triglyceride and free fatty acid lowering effects mediated through inhibition of I κ B kinase β ⁴⁶. With regard to EGFR inhibitors, two independent studies show profound reduction of fasting glucose levels and normalization of HbA1c in two lung cancer patients with T2D treated with the EGFR inhibitor erlotinib^{47,48}. Although such cases were not reported with neratinib, one wonders whether the well-known polypharmacology of erlotinib may overlap with neratinib and thus exhibit antidiabetic effects.

EGFR signaling is associated with insulin resistance and liver, muscle, and adipose inflammation. EGFR inhibition through

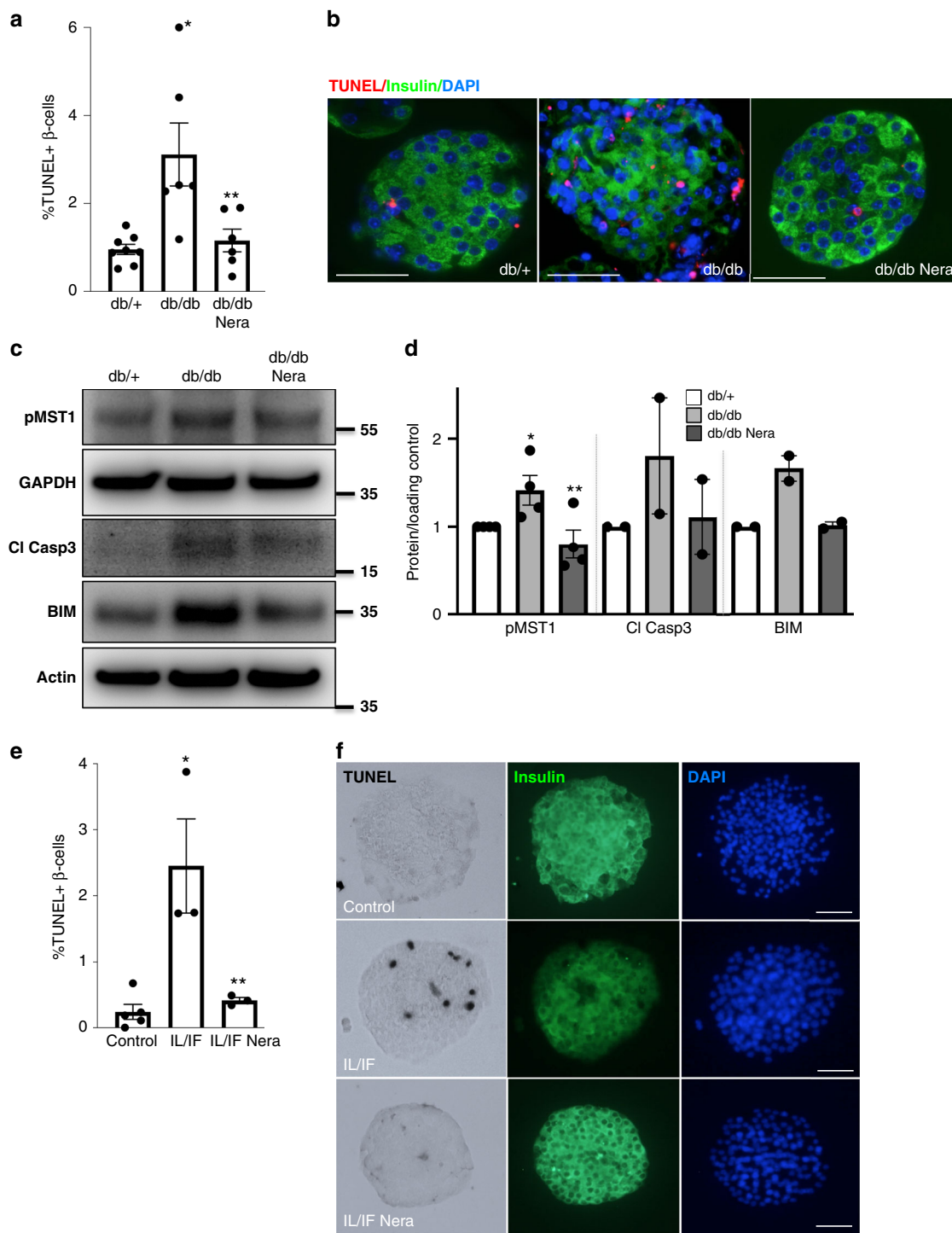


Fig. 9 Neratinib improves β -cell survival in islets in a therapeutic ex vivo approach. **a, b** Isolated islets from 10-week-old obese diabetic $Lepr^{db/db}$ mice or their heterozygous $db/+$ littermates were exposed to 10 μ M neratinib for 24 h, fixed, and 2- μ m sections were prepared. **a** Percentage of TUNEL-positive β -cells is shown as means \pm SEM. **b** β -cell apoptosis was analyzed from islet sections by triple staining of TUNEL (red nuclei), insulin (green), and dapi (blue); scale bar, 100 μ m. **c** Phospho-MST1 (pMST1; pThr183), caspase-3 cleavage, BIM and GAPDH, or actin were analyzed by western blotting shown by a representative blot (**c**) and pooled quantitative densitometry analysis (**d**). **e, f** Isolated islets from 2-month-old WT C57Bl/6 mice were exposed to the IL-1 β /IFN γ cytokine mixture for 72 h (IL/IF); 10 μ M neratinib was added to the culture for the last 24 h. **e** Percentage of TUNEL-positive β -cells is shown as means \pm SEM. **f** β -cell apoptosis was analyzed from attached islet cultures by triple staining of TUNEL (black nuclei), insulin (green), and dapi (blue). Scale bar, 100 μ m. All data are means \pm SEM from multiple mice/condition ($n = 6-8$ for (**a**); $n = 2-4$ for (**c**); $n = 3-5$ for (**e**)). * $p < 0.05$ db/db or IL/IF to heterozygous $db/+$ or untreated control islets, ** $p < 0.05$ neratinib to vehicle-treated islets under the same diabetogenic conditions; all by Student's *t* tests. Source data are provided as a Source Data file

tyrosine kinase inhibition was suggested as therapy of insulin resistance, because its inhibition could restore insulin sensitivity by decreasing inflammation in insulin target tissue⁴³. EGFR inhibition improved tyrosine phosphorylation levels of the insulin receptor and the insulin receptor substrate in obese mice, which are classically associated with improved insulin sensitivity; however, direct analysis of insulin sensitivity was not performed in these studies⁴⁴.

Although FDA was approved for cancer therapy, further medicinal chemistry optimization to improve drug selectivity and remove its covalent linkage would be desirable to limit drug toxicity and to provide better specificity for a chronic indication like diabetes. Neratinib inhibits MST1 very potently; however, it targets many other kinases, as the development of kinase inhibitor has been challenging^{38,49}. A foundation for kinase inhibitor biology and toxicity has been set by an excellent previous study, which also reported potent activity of neratinib (also formerly known as HKI-272) on MST family members³⁸. Studies to improve MST1 specificity and potency are currently under way.

While neratinib is not at all selective for MST1, we believe that the underlying mechanisms of diabetes protection still derive from a direct protective effect on the β -cell mediated by MST1 and not from an effect on insulin sensitivity mediated by EGFR. Improved glucose tolerance and insulin secretion were observed in both models, while insulin sensitivity was unaffected by neratinib in the STZ model and modestly impaired in the obese insulin-resistant db/db model, which was only evident after normalization of the fasting glucose levels. Without such normalization applied, glucose levels during the insulin tolerance test were not significantly affected by neratinib, despite the significant glucose reduction in neratinib-treated mice after 4 h of fasting. Also, neratinib almost fully blocked β -cell apoptosis in human islets induced by MST1 overexpression and also had no additive effect in islets isolated from MST1-KO mice, in which apoptosis was already blocked by the genetic disruption of MST1 itself.

A general concern in targeting the reduction of β -cell apoptosis and the induction of β -cell proliferation in diabetes therapy is the potential for uncontrolled expansion of multiple cell types and oncogenic transformation. Organ-specific double knockout of MST1/2, e.g., in the liver has been shown to lead to tumor growth, because of the lack of constraints on cellular proliferation in these mice driven by the Hippo-YAP pathway⁵⁰. Although neratinib shows some modest selectivity toward MST1 than to MST2, one of our long-term objectives will be to generate an MST1 inhibitor with greater selectivity versus MST2 than neratinib (e.g., more than 50-fold). In our previous work, we carefully explored the phenomenon of β -cell proliferation in both the global as well as β -cell-specific MST1-knockout mice. At basal normoglycemic level, there was no change in β -cell proliferation in the MST1-KO, but there was increased β -cell proliferation under conditions of STZ-induced hyperglycemia both in the global as well as β -cell-specific MST1-KO mice. Also, β -cell-specific MST1 ablation fosters β -cell compensatory hyperplasia in HFD-treated mice^{11,24}. This suggests that there is no proliferative potential of MST1 inhibition under non-stressed conditions, but the capacity to overcome β -cell stress by increased proliferation and reduced β -cell apoptosis is triggered under circumstances of such stress, leading to reestablishment of glucose homeostasis. Similarly, neratinib did not affect apoptosis or proliferation in nondiabetic mice, but increased β -cell proliferation in db/db mice together with profound reduction in β -cell apoptosis, leading to β -cell mass compensation and improved glycemia. However, in the absence of CRISPR-mediated deletion of all other potential neratinib-sensitive kinases, similarly as done previously⁵¹ we cannot formally exclude off-target effects and definitively assign MST1 as the only target of neratinib in this study.

Overall, basal β -cell proliferation is very limited in mouse islets and negligible in human islets⁵². This is probably an evolved property that protects from insulin production during long times of starvation. This proliferative incapacity can be attributed at the molecular level to the loss of YAP, the major downstream component of the Hippo-YAP pathway, which controls organ development and size^{37,53–55}. YAP disappears exactly at the point of islet development, when Ngn3 becomes present in order to drive endocrine cell differentiation^{37,56,57}. Therefore, MST1 inhibition in the absence of YAP expression would not lead to tumor development. The Hippo-YAP pathway acts in coordination with many other cell-size and proliferation-determining factors in development, including insulin-like growth factor (IGF1R⁵⁸) and EGF receptor signaling (EGFR⁵⁹). Such interaction can even be cell-autonomous, as shown in *Drosophila*, where YAP-EGFR crosstalk promotes proliferation in neighboring cells⁶⁰. Thus, we cannot rule out the possibility that simultaneous EGFR inhibition could be important for limiting the oncogenic potential of MST1 and MST2 inhibition and subsequent activation of YAP directed transcription.

Several MST1 inhibitors have been identified recently⁶¹. Compound 9E1, the first small-molecule MST1 inhibitor identified from an organometallic library screen²⁷, showed strong off-target effects on other kinases such as proto-oncogene serine/threonine protein kinase PIM1 (PIM-1) and glycogen synthase kinase 3 (GSK-3 β)²⁷, and thus did not enter any preclinical studies. MST1 inhibition by LP-945706 has anti-inflammatory efficacy in an experimental autoimmune encephalomyelitis (EAE) model²⁹. The reversible and selective MST1/2 inhibitor XMU-MP-1 promotes tissue repair and regeneration by cellular proliferation induction in human liver cells and in a mouse model of liver and intestine injury²⁸. It will be interesting to test the efficiency of the novel MST1 inhibitors LP-945706 or XMU-MP-1 to promote β -cell survival exposed to a complex diabetic milieu or in diabetic mice in comparison with neratinib.

This study shows the beneficial effects of the kinase inhibitor neratinib in ameliorating hyperglycemia as well as improving β -cell survival and function under diabetogenic conditions. The subject of our ongoing work in this regard is the design of neratinib-based MST1 inhibitors that exhibit enhanced potency and selectivity for MST1, with safety profiles commensurate with the chronic treatment of diabetes. The identification of neratinib as an MST1 inhibitor thus amounts to an accelerated path to a preclinical proof of concept, shown herein, as well as a firm basis for a follow-on medicinal chemistry optimization program aimed at retaining the drug-like properties of neratinib but improving upon its selectivity and safety.

Methods

Cell culture, treatment, and islet isolation. Human islets were isolated from eight pancreases of nondiabetic organ donors at PRODO Labs and at Lille University and cultured on extracellular matrix-coated dishes (Novamed, Jerusalem, Israel)⁶² or on Biocoat Collagen I coated dishes (#356400, Corning, ME, USA). Islet purity was greater than 95% as judged by dithizone staining (if this degree of purity was not achieved by routine isolation, islets were handpicked). Islets from MST1-knockout (MST1-KO) mice and their WT littermates⁶³ were isolated by pancreas perfusion with a Liberase TM (#0540119001, Roche, Mannheim, Germany) solution⁶² according to the manufacturer's instructions and digested at 37 °C, followed by washing and handpicking. The clonal rat β -cell line INS-1E was kindly provided by Dr. Claes Wollheim, Geneva & Lund University. Human islets were cultured in complete CMRL-1066 (Invitrogen) medium at 5.5 mM glucose, mouse islets and INS-1E cells at complete RPMI-1640 medium at 11.1 mM glucose¹¹. Mouse macrophage Raw264.7 cell line was purchased from ATCC and cultured in DMEM (Gibco) supplemented with 10% FBS. Islets and INS-1E were exposed to complex diabetogenic conditions: 22.2–33.3 mM glucose, 0.5 mM palmitic acid, the mixture of 2 ng/ml recombinant human IL-1 β (R&D Systems, Minneapolis, MN) + 1000 U/ml recombinant human IFN- γ (PeProTech) for 24–72 h, 100 μ M H₂O₂ for 6 h, or 0.1, 1 mM thapsigargin for 6 or 24 h. Neratinib or vehicle (0.1% DMSO) was added to the cell culture 1–2 h before treatment. Palmitic acid (Sigma) was

dissolved at 10 mmol/l in RPMI-1640 medium containing 11% fatty acid-free bovine serum albumin (BSA) (Sigma) under an N₂-atmosphere and added to the culture at 0.5 mM⁶⁴. In some experiments, human or mouse islets or INS-1E cells were additionally cultured with various concentrations of neratinib (Calibr). Isolated human islets or INS-1E cells were infected with adenovirus carrying LacZ as control or MST1 or LATS2 (all Vector Biolabs), at a multiplicity of infection of 100 (human islets) or 20 (INS-1E) for 4 h¹¹. Adenovirus was subsequently washed off with PBS and replaced by fresh medium with 10% FBS and the respective analysis performed after 48 h post infection.

All human islet experiments were performed in the islet biology laboratory, University of Bremen. Ethical approval for the use of human islets had been granted by the Ethics Committee of the University of Bremen. The study complied with all relevant ethical regulations for work with human cells for research purposes. Organ donors are not identifiable and anonymous; such approved experiments by using human islet cells for research are covered by the NIH Exemption 4 (Regulation PHS 398). Human islets were distributed by the two JDRF and NIH-supported approved coordination programs in Europe (Islet for Basic Research program; European Consortium for Islet Transplantation ECIT) and in the United States (Integrated Islet Distribution Program IIDP)⁶⁵.

High-throughput screening and hits confirmation. High-throughput screening targeting MST1 was conducted in low-binding 1536 microplate (Corning, NY) by using LanthaScreen Eu Kinase Binding assay. In total, 641 annotated compounds in a Kinase inhibitor library (Calibr) were screened at 1, 0.2, 0.04, 0.008, and 0.0016 μ M, with staurosporine as the positive control. Compounds in 1000 \times DMSO stock solution were dispensed by using Echo555 liquid dispensing system (Labcyte, CA) to 1536-well microplate (Corning, NY). Kinase buffer A (ThermoFisher, MA) was prepared and added to each well. MST1 kinase (ThermoFisher) and Eu-anti-GST Antibody (ThermoFisher) was prepared at 15 nM and 6 nM, respectively. Kinase tracer 222 (ThermoFisher) was prepared at 300 nM. Each reagent was added to the microplate in equal volume. Plates were incubated at room temperature for 1.5 h in the dark, scanned on Envision plate reader with excitation at 340 nm, emission at 665 and 615 nm. Data were analyzed based on the emission ratio of 665 nm/615 nm, normalized to DMSO as negative control. The criteria of picking primary hits was $\geq 75\%$ inhibition at 1 μ M and $\geq 50\%$ inhibition at 0.2 μ M, compared with staurosporine (1 μ M), which is considered 100% inhibition at 1 μ M. For hit confirmation, primary hits were assayed in triplicates with 12 points in a dose-dependent manner, starting at a neratinib dose of 5 μ M followed by 1:3 serial dilution.

Nanosyn kinase profiling. Neratinib was tested at Nanosyn (Santa Clara, CA) in a panel of 50 biochemical kinase assays identified in Fig. 1c at 10 μ M, and later on, in a panel of 250 biochemical kinase assays (Supplementary Fig. 1a) at 3 μ M in duplicate wells. A selected set of kinases where more than 90% of inhibition was observed at 3 μ M was retested in dose response for neratinib and IC₅₀ was determined (Supplementary Fig. 1b). The testing was performed by using microfluidics mobility shift assay technology using ATP concentrations at Km level of each kinase. Data presented as average from the two duplicate wells.

Cytotoxicity CellTiter-Glo[®] assay. INS-1E cells were treated with compounds in a dose-dependent manner in 384-well microplates (Corning, NY) at 10⁴ cells/well in 25 μ L of complete growth medium. After 24 h of compound treatment, 5 μ L of CellTiter-Glo[®] reagent (Promega, WI) was added to each well. Assay plates were shaken vigorously for 1 min at RT to achieve completed cell lysis. Luminescence intensity was detected on Envision plate reader (Perkin Elmer, MA).

Caspase-3 activation Nucview assay. INS-1E cells were treated with compounds in a dose-dependent manner in 384-well microplates (Corning, NY) at 10⁴ cells/well. Apoptosis was induced after 24 h of compound treatment by 0.1 μ M Thapsigargin (Torics, Bristol, United Kingdom) with caspase-3 substrate, Nucview 488 (Biotium, CA) in the treatment. Sixteen hours later, cells were fixed in 3% paraformaldehyde (Electron Microscopy Sciences, PA) and stained with Hoechst33342 (ThermoFisher). Data analysis was based on the fluorescence intensity of Nucview488 and Hoechst33342. Similarly, in caspase-3 activation assay induced by the cytokine mixtures in high-glucose conditions, INS-1E cells were exposed up to 6.7 μ M of neratinib for 2 h followed by 16 h of induction in 100 ng/mL of TNF α and 200 ng/mL of IFN γ with 33 mM glucose in assay medium. Caspase-3 activity was evaluated through Nucview488 and Hoechst33342 staining.

RT-PCR assay. Mouse macrophage Raw264.7 cells were treated with vehicle (0.1% DMSO) or neratinib in triplicates at different concentrations for 2 h, followed by 100 ng/mL LPS stimulation for 4 h. Cells were washed and RNA isolated by using RNeasy Mini Kit (Qiagen). One microgram of cDNA of each treatment sample was synthesized by using SuperScript III First-Strand Synthesis (Invitrogen). Taqman mouse primers were purchased from ThermoFisher: TNF α (Catalog No. Mm00443258_m1), IL-6 (Catalog No. Mm00446190_m1), IL-1 β (Catalog No. Mm00434228_m1), and GAPDH as endogenous housekeeping control (Catalog No. Mm99999915_g1). The qPCR reaction was set up for TNF α , IL-6, IL-1 β , and GAPDH individually, with technical triplicates for each gene per treatment sample

and performed by the Applied Biosystems ViiA 7 real-time PCR system. The $\Delta\Delta$ CT method was used to analyze the relative changes in gene expression.

CETSA assay. For the CETSA assay³⁹, INS-1E cells were treated with 5 μ M neratinib or canertinib for 2 h in the CO₂ incubator at 37 °C in a 6-well plate. Thereafter, cells were pelleted at 200 g for 4 min and resuspended in PBS supplemented with phosphatase and protease inhibitor cocktail at the cell density of 3 Mill./100 μ L. Each cell suspension was distributed into five 0.2-ml PCR tubes with 100 μ L of cell suspension per tube. PCR tubes were heated at their designated temperature (43–55 °C) on a thermal cycler for 3 min, incubated at room temperature for 3 min, and snap-frozen in liquid nitrogen. Cell lysates were prepared by freezing–thawing the samples in liquid nitrogen twice, and soluble MST1 was detected by western blot analysis.

Animals. For the MLD–STZ experiment, 8–10-week-old male C57BL/6J mice were i.p. injected with streptozotocin (STZ; 40 mg/kg; Sigma) freshly dissolved in 50 mM sodium citrate buffer (pH 4.5) or citrate buffer as control for 5 consecutive days (referred to as multiple low doses/MLD–STZ). Obese diabetic Lep^{db/db} mice on the C57BLKS/J background (db/db) were obtained from Charles River at the age of 5 weeks and randomized in 2 groups at the age of 6 weeks. Neratinib or vehicle (30% PEG400/0.5% Tween80/5% propylene glycol in NaCl) was daily i.p. injected at a concentration of 5 mg/kg starting 3 h before the first STZ injection or at 6 weeks of age (db/db) throughout the whole experiment. Random blood was obtained from the tail vein of non-fasted mice, and glucose was measured by using a Glucometer (Freestyle; TheraSense Inc., Alameda, CA). Mice were killed at the end of the experiment, and their pancreases were isolated. Throughout the whole study, body weight was measured weekly. All animals were housed in a temperature-controlled room with a 12-h light/dark cycle and were allowed free access to food and water in agreement with NIH animal care guidelines, §8 German animal protection law, German animal welfare legislation, and with the guidelines of the Society of Laboratory Animals and the Federation of Laboratory Animal Science Associations. All protocols were approved by the Bremen Senate (Senator for Science, Health, and consumer protection), and we have complied with all relevant ethical regulations for animal testing and research.

Glucose and insulin tolerance tests, insulin secretion. For intraperitoneal glucose tolerance tests, mice were fasted 12 h overnight and injected i.p. with glucose (40%; B.Braun, Melsungen, Germany) at a dose of 1 g/kg body weight. Blood samples were obtained at time points 0, 15, 30, 60, 90, and 120 min for glucose measurements by using a Glucometer. For i.p. insulin tolerance tests, mice were injected with 0.75 U/kg body weight recombinant human insulin (Novolin, Novo Nordisk) after 4–5 h fasting, and glucose concentration was determined with the Glucometer. Insulin secretion was measured before (0 min) and after (15 and 30 min) i.p. injection of glucose (2 g/kg) and measured by using ultrasensitive mouse Elisa kit (ALPCO Diagnostics, Salem, NH).

Immunohistochemistry. Mouse pancreases were dissected and fixed in 4% formaldehyde at 4 °C for 12 h before embedding in paraffin⁶². Two-four-micrometer sections were deparaffinized, rehydrated, and incubated overnight at 4 °C with anti-PDX-1 (Abcam; #47267), anti-Glut2 (Chemicon; #07-1402), anti-Ki67 (Dako; #M7249), anti-phospho-Histone H3 (Ser10; Merck #06-570), and anti-NKX6.1 (DSHB, University of Iowa #F55A12⁶⁶) in combination with TSA (Invitrogen #T30955), or for 2 h at room temperature with anti-insulin (Dako; A0546) antibodies (all at a dilution of 1:100, except anti-PDX-1, which was diluted 1:400) followed by fluorescein isothiocyanate (FITC)- or Cy3-conjugated secondary antibodies (Jackson ImmunoResearch Laboratories, West Grove, PA). Slides were mounted with Vectashield with 4'-diamidino-2-phenylindole (DAPI) (Vector Labs). β -cell apoptosis was analyzed by the terminal deoxynucleotidyl transferase-mediated dUTP nick-end labeling (TUNEL) technique according to the manufacturer's instructions (In Situ Cell Death Detection Kit, TMR red; Roche) and double stained for insulin. Fluorescence was analyzed by using a Nikon MEA53200 (Nikon GmbH, Dusseldorf, Germany) microscope, and images were acquired by using NIS-Elements software (Nikon).

Morphometric analysis. For morphometric data, ten sections (spanning the width of the pancreas) per mouse were analyzed. Pancreatic tissue area and insulin-positive area were determined by computer-assisted measurements by using a Nikon MEA53200 (Nikon GmbH, Dusseldorf, Germany) microscope, and images were acquired by using NIS-Elements software (Nikon). β -cell mass was obtained by multiplying the β -cell fraction by the weight of the pancreas.

Western Blot analysis. At the end of the incubation periods, islets and INS-1E cells were washed in ice-cold PBS and lysed in RIPA lysis buffer containing 50 mM Tris HCl, pH 8, 150 mM NaCl, 1% NP-40, 0.5% sodium deoxycholate, and 0.1% SDS supplemented with Protease- and phosphatase inhibitors (Pierce, Rockford, IL, USA). Protein concentrations were determined with the BCA protein assay (Pierce). Equivalent amounts of protein from each treatment group were run on a NuPAGE 4–12% Bis-Tris gel (Invitrogen) and electrically transferred onto PVDF

membranes. After blocking by 2.5% milk (Cell Signaling) and 2.5% BSA, membranes were incubated overnight at 4 °C with rabbit anti-cleaved caspase-3 (#9664), rabbit anti-PARP (#9532), rabbit anti-cleaved PARP (rat specific #9545), rabbit anti-phospho YAP(S127) (#4911), rabbit anti-LATS2 (#5888), rabbit anti-tubulin (#2146), rabbit anti-GAPDH (#2118), rabbit anti- β -actin (#4967) (all Cell Signaling Technology), and rabbit anti-PDX1 (#47267) and rabbit anti-p-MST1 (#79199) (both from Abcam) antibodies, all at a dilution of 1:1000, followed by horseradish-peroxidase-linked anti-rabbit IgG (Jackson). Membrane was developed by using a chemiluminescence assay system (Pierce) and analyzed using DocIT[®]LS image acquisition 6.6a (UVP BioImaging Systems, Upland, CA, USA). Uncropped and unprocessed scans of all Western blots are available in the Source Data file.

In vitro luciferase assay. INS1-E cells were transfected with LATS-BS firefly luciferase reporter constructs by using jetPRIME transfection reagent (PolyPlus, Illkirch, France). pCDNA3.1neo-NLucYAP15 and pCDNA3.1neo-14-3-3-CLuc was a gift from Xiaolong Yang (Addgene plasmid # 107610; <http://n2t.net/addgene:107610>; RRID:Addgene_107610)³⁵. As internal transfection control, pRL-Renilla luciferase control reporter vector (Promega) was co-transfected into each sample. Twenty-four hours after transfection, cells were transfected with Ad-h-LacZ, or Ad-h-LATS2 and Ad-h-MST1 (Vector Biolabs) for another 48 h. Neratinib or canertinib (10 μ M) was added for the last 24 h. Thereafter, Western blot analysis (see above) and luciferase assay was performed by using Dual-Luciferase Reporter Assay System (Promega)¹¹ in a parallel set of experiments. Luciferase signal was calculated based on the ratio of luciferase activity of LATS-BS to control reporter vector.

Marix-assisted laser desorption ionization. MALDI imaging mass spectrometry (MALDI imaging MS) was performed on pancreas, liver, colon, stomach, kidney, heart, and brain tissue sections from WT C57BL/6J and db/db mice in triplicates. Neratinib distribution in the pancreas was studied after neratinib treatment for five days with a dosage of 5 mg/kg neratinib in WT control mice or after the 31-day treatment period in db/db mice; animals were killed 4 h after the last treatment. For MALDI imaging MS, 10- μ m cryo sections were cut with a cryo-microtome (CM1860, Leica Biosystems, Nussloch, Germany) and mounted on indium-tin-coated conductive glass slides (Bruker Daltonics, Bremen, Germany). The matrix (HCCA in 50% ACN, 0.5% TFA) was applied with the ImagePrep Device (Bruker Daltonics), and MALDI spectra were recorded by using a Bruker autoflex speed mass spectrometer in positive reflector mode with a mass range of 400–1400 m/z. A large-size laser diameter was used with a lateral resolution of 100 μ m, and 500 laser shots per pixel were accumulated with the random walk option set to 100 shots per position. For data analyses, the unprocessed raw data were imported into the Software SciLS Lab, version 2016b (SciLS GmbH, Bremen, Germany). The dynamic range of the neratinib signal was analyzed by using drug standards (0–500 pmol/ μ l). Standards were spotted on mice liver cryo-sections and the spectral intensity was plotted.

Statistical analysis. Samples in different experiments were evaluated in a randomized manner by six investigators (D.A., A.D., K.A., R.H., B.L. and SG) who were blinded to the treatment conditions (Fig. 3c, d; 4d–g; 6g–i; 7g–j; 8a, b, e, f). Data are presented as means \pm SEM unless otherwise stated with the number of independent individual experiments (biological replicates) or analyzed mice presented in the figure legends. Mean differences were tested by Student's *t* tests. ANOVA for multiple group comparisons with Bonferroni corrections was performed for data in Figs. 6a, b and 7a. *P* values < 0.05 were considered statistically significant.

Reporting summary. Further information on research design is available in the Nature Research Reporting Summary linked to this article.

Data availability

All data generated or analyzed during this study are included in this published article and its supplementary information files. Source data are provided as a Source Data file. All additional data are available from the corresponding authors upon reasonable request.

Received: 19 January 2019; Accepted: 2 October 2019;

Published online: 01 November 2019

References

- Kurrer, M. O., Pakala, S. V., Hanson, H. L. & Katz, J. D. Beta cell apoptosis in T cell-mediated autoimmune diabetes. *Proc. Natl Acad. Sci. USA* **94**, 213–218 (1997).
- Mathis, D., Vence, L. & Benoist, C. beta-Cell death during progression to diabetes. *Nature* **414**, 792–798 (2001).
- Butler, A. E. et al. Beta-cell deficit and increased beta-cell apoptosis in humans with type 2 diabetes. *Diabetes* **52**, 102–110 (2003).
- Rhodes, C. J. Type 2 diabetes—a matter of beta-cell life and death? *Science* **307**, 380–384 (2005).
- Vetere, A., Choudhary, A., Burns, S. M. & Wagner, B. K. Targeting the pancreatic beta-cell to treat diabetes. *Nat. Rev. Drug Discov.* **13**, 278–289 (2014).
- Masini, M. et al. Autophagy in human type 2 diabetes pancreatic beta cells. *Diabetologia* **52**, 1083–1086 (2009).
- Tomita, T. Immunocytochemical localisation of caspase-3 in pancreatic islets from type 2 diabetic subjects. *Pathology* **42**, 432–437 (2010).
- Rahier, J., Guiot, Y., Goebbels, R. M., Sempoux, C. & Henquin, J. C. Pancreatic beta-cell mass in European subjects with type 2 diabetes. *Diabetes Obes. Metab.* **10**, 32–42 (2008).
- Marselli, L. et al. Are we overestimating the loss of beta cells in type 2 diabetes? *Diabetologia* **57**, 362–365 (2014).
- Meier, J. J., Bhushan, A., Butler, A. E., Rizza, R. A. & Butler, P. C. Sustained beta cell apoptosis in patients with long-standing type 1 diabetes: indirect evidence for islet regeneration? *Diabetologia* **48**, 2221–2228 (2005).
- Ardestani, A. et al. MST1 is a key regulator of beta cell apoptosis and dysfunction in diabetes. *Nat. Med.* **20**, 385–397 (2014).
- Cinti, F. et al. Evidence of beta-Cell dedifferentiation in human type 2 diabetes. *J. Clin. Endocrinol. Metab.* **101**, 1044–1054 (2016).
- Jeffery, N. & Harries, L. W. Beta-cell differentiation status in type 2 diabetes. *Diabetes Obes. Metab.* **18**, 1167–1175 (2016).
- Talchai, C., Xuan, S., Lin, H. V., Sussel, L. & Accili, D. Pancreatic beta cell dedifferentiation as a mechanism of diabetic beta cell failure. *Cell* **150**, 1223–1234 (2012).
- Tiwari, S. et al. Definition of a Skp2-c-Myc pathway to expand human beta-cells. *Sci. Rep.* **6**, 28461 (2016).
- Ardestani, A. & Maedler, K. The Hippo signaling pathway in pancreatic beta-cells: functions and regulations. *Endocr. Rev.* **39**, 21–35 (2017).
- Group, T. D. Ca. C. T. R. Effect of intensive therapy on residual beta-cell function in patients with type 1 diabetes in the diabetes control and complications trial. A randomized, controlled trial. The Diabetes Control and Complications Trial Research Group. *Ann. Intern. Med.* **128**, 517–523 (1998).
- Ling, P., Lu, T. J., Yuan, C. J. & Lai, M. D. Biosignaling of mammalian Ste20-related kinases. *Cell. Signal.* **20**, 1237–1247 (2008).
- Avruch, J. et al. Protein kinases of the Hippo pathway: regulation and substrates. *Semin. Cell. Dev. Biol.* **23**, 770–784 (2012).
- Lee, K. K. et al. Proteolytic activation of MST/Krs, STE20-related protein kinase, by caspase during apoptosis. *Oncogene* **16**, 3029–3037 (1998).
- Kakeya, H., Onose, R. & Osada, H. Caspase-mediated activation of a 36-kDa myelin basic protein kinase during anticancer drug-induced apoptosis. *Cancer Res.* **58**, 4888–4894 (1998).
- Bi, W. et al. c-Jun N-terminal kinase enhances MST1-mediated pro-apoptotic signaling through phosphorylation at serine 82. *J. Biol. Chem.* **285**, 6259–6264 (2010).
- Cheung, W. L. et al. Apoptotic phosphorylation of histone H2B is mediated by mammalian sterile twenty kinase. *Cell* **113**, 507–517 (2003).
- Ardestani, A. & Maedler, K. MST1: a promising therapeutic target to restore functional beta cell mass in diabetes. *Diabetologia* **59**, 1843–1849 (2016).
- Gao, T. et al. Pdx1 maintains beta cell identity and function by repressing an alpha cell program. *Cell. Metab.* **19**, 259–271 (2014).
- Augeri, D. J. MST1 kinase inhibitors and methods of their use. US Patent Application Publication US 2012/0225857A1 (2012).
- Anand, R. et al. Toward the development of a potent and selective organoruthenium mammalian sterile 20 kinase inhibitor. *J. Med. Chem.* **52**, 1602–1611 (2009).
- Fan, F. et al. Pharmacological targeting of kinases MST1 and MST2 augments tissue repair and regeneration. *Sci. Transl. Med.* **8**, 352ra108 (2016).
- Salojin, K. V. et al. Genetic deletion of Mst1 alters T cell function and protects against autoimmunity. *PLoS One* **9**, e98151 (2014).
- Normanno, N. et al. Epidermal growth factor receptor (EGFR) signaling in cancer. *Gene* **366**, 2–16 (2006).
- Chan, A. et al. Neratinib after trastuzumab-based adjuvant therapy in patients with HER2-positive breast cancer (ExteNET): a multicentre, randomised, double-blind, placebo-controlled, phase 3 trial. *Lancet Oncol.* **17**, 367–377 (2016).
- Martin, M. et al. Neratinib after trastuzumab-based adjuvant therapy in HER2-positive breast cancer (ExteNET): 5-year analysis of a randomised, double-blind, placebo-controlled, phase 3 trial. *Lancet Oncol.* **18**, 1688–1700 (2017).
- Singh, H. et al. U.S. Food and Drug Administration Approval: neratinib for the extended adjuvant treatment of early stage HER2-positive breast cancer. *Clin. Cancer Res.* **24**, 3486–3491 (2018).
- Bose, P. & Ozer, H. Neratinib: an oral, irreversible dual EGFR/HER2 inhibitor for breast and non-small cell lung cancer. *Expert Opin. Investig. Drugs* **18**, 1735–1751 (2009).
- Azad, T. et al. A LATS biosensor screen identifies VEGFR as a regulator of the Hippo pathway in angiogenesis. *Nat. Commun.* **9**, 1061 (2018).

36. Yuan, T., Kerr-Conte, J. & Ardestani, A. LATS2 controls beta cell apoptosis by regulating the MOB1-Praja2 axis. *Diabetologia* **57**, S181–S182 (2014).
37. George, N. M., Boerner, B. P., Mir, S. U., Guinn, Z. & Sarvetnick, N. E. Exploiting expression of hippo effector, yap, for expansion of functional islet mass. *Mol. Endocrinol.* **29**, 1594–1607 (2015).
38. Davis, M. I. et al. Comprehensive analysis of kinase inhibitor selectivity. *Nat. Biotechnol.* **29**, 1046–1051 (2011).
39. Jafari, R. et al. The cellular thermal shift assay for evaluating drug target interactions in cells. *Nat. Protoc.* **9**, 2100–2122 (2014).
40. Harmon, J. S. et al. beta-Cell-specific overexpression of glutathione peroxidase preserves intranuclear MafA and reverses diabetes in db/db mice. *Endocrinology* **150**, 4855–4862 (2009).
41. Oetjen, J. et al. Benchmark datasets for 3D MALDI- and DESI-imaging mass spectrometry. *Gigascience* **4**, 20 (2015).
42. Tiwari, S. R., Mishra, P. & Abraham, J. Neratinib, a novel HER2-targeted tyrosine kinase inhibitor. *Clin. Breast Cancer* **16**, 344–348 (2016).
43. Fountas, A., Diamantopoulos, L. N. & Tsatsoulis, A. Tyrosine kinase inhibitors and diabetes: a novel treatment paradigm? *Trends Endocrinol. Metab.* **26**, 643–656 (2015).
44. Prada, P. O. & Saad, M. J. Tyrosine kinase inhibitors as novel drugs for the treatment of diabetes. *Expert. Opin. Investig. Drugs* **22**, 751–763 (2013).
45. Erbe, D. V. et al. Ertiprotafib improves glycemic control and lowers lipids via multiple mechanisms. *Mol. Pharmacol.* **67**, 69–77 (2005).
46. Shrestha, S., Bhattarai, B. R., Cho, H., Choi, J. K. & Cho, H. PTP1B inhibitor Ertiprotafib is also a potent inhibitor of IkkappaB kinase beta (IKK-beta). *Bioorg. Med. Chem. Lett.* **17**, 2728–2730 (2007).
47. Costa, D. B. & Huberman, M. S. Improvement of type 2 diabetes in a lung cancer patient treated with Erlotinib. *Diabetes Care* **29**, 1711 (2006).
48. Brooks, M. B. Erlotinib appears to produce prolonged remission of insulin-requiring type 2 diabetes associated with metabolic syndrome and chronic kidney disease. *Br. J. Diabetes Vasc. Dis.* **12**, 87–90 (2012).
49. Cohen, P. The development and therapeutic potential of protein kinase inhibitors. *Curr. Opin. Chem. Biol.* **3**, 459–465 (1999).
50. Song, H. et al. Mammalian Mst1 and Mst2 kinases play essential roles in organ size control and tumor suppression. *Proc. Natl Acad. Sci. USA* **107**, 1431–1436 (2010).
51. Plouffe, S. W. et al. Characterization of hippo pathway components by gene inactivation. *Mol. Cell* **64**, 993–1008 (2016).
52. Rutti, S. et al. In vitro proliferation of adult human beta-cells. *PLoS ONE* **7**, e35801 (2012).
53. George, N. M., Day, C. E., Boerner, B. P., Johnson, R. L. & Sarvetnick, N. E. Hippo signaling regulates pancreas development through inactivation of Yap. *Mol. Cell. Biol.* **32**, 5116–5128 (2012).
54. Gao, T. et al. Hippo signaling regulates differentiation and maintenance in the exocrine pancreas. *Gastroenterology* **144**, 1543–1553 (2013). 1553 e1541.
55. Yuan, T. et al. Proproliferative and antiapoptotic action of exogenously introduced YAP in pancreatic β cells. *JCI Insight* **1**, e86326 (2016).
56. Pullen, T. J. et al. Identification of genes selectively disallowed in the pancreatic islet. *Islets* **2**, 89–95 (2010).
57. Pullen, T. J., Huisling, M. O. & Rutter, G. A. Analysis of purified pancreatic islet beta and alpha cell transcriptomes reveals 11beta-hydroxysteroid dehydrogenase (Hsd11b1) as a novel disallowed gene. *Front. Genet.* **8**, 41 (2017).
58. Xin, M. et al. Regulation of insulin-like growth factor signaling by Yap governs cardiomyocyte proliferation and embryonic heart size. *Sci. Signal.* **4**, ra70 (2011).
59. McNeill, H. & Woodgett, J. R. When pathways collide: collaboration and connivance among signalling proteins in development. *Nat. Rev. Mol. Cell Biol.* **11**, 404–413 (2010).
60. Zhang, J. et al. YAP-dependent induction of amphiregulin identifies a non-cell-autonomous component of the Hippo pathway. *Nat. Cell Biol.* **11**, 1444–1450 (2009).
61. Ardestani, A. & Maedler, K. The hippo signaling pathway in pancreatic beta-cells: functions and regulations. *Endocr. Rev.* **39**, 21–35 (2018).
62. Schulthess, F. T. et al. CXCL10 impairs beta cell function and viability in diabetes through TLR4 signaling. *Cell. Metab.* **9**, 125–139 (2009).
63. Dong, Y. et al. A cell-intrinsic role for Mst1 in regulating thymocyte egress. *J. Immunol.* **183**, 3865–3872 (2009).
64. Maedler, K. et al. Distinct effects of saturated and monounsaturated fatty acids on beta-cell turnover and function. *Diabetes* **50**, 69–76 (2001).
65. Hart, N. J. & Powers, A. C. Use of human islets to understand islet biology and diabetes: progress, challenges and suggestions. *Diabetologia* **62**, 212–222 (2019).
66. Ben-Othman, N. et al. Long-term GABA administration induces alpha cell-mediated beta-like cell neogenesis. *Cell* **168**, 73–85 e11 (2017).

Acknowledgements

Human islets were kindly provided through the ECIT Islet for Basic Research program supported by JDRF (JDRF award 31-2008-413). We thank J. Kerr-Conte and Francois Pattou (European Genomic Institute for Diabetes, Lille) and ProdoLabs for high-quality human islet isolations, Katrischa Hennekens (University of Bremen) for excellent technical assistance and animal care, Jeff Janes, Mitch Hull, Hung Nguyen and Megan Wogan (CALIBR) for technical assistance and Petra Schilling (University of Bremen) for pancreas sectioning, and Jason Roland (CALIBR), Patricia Kilian, Andrew Rakeman, Peter Lomedico, and Frank Martin (all JDRF) for helpful discussions. MST1-KO mice were kindly provided by Wufan Tao (Institute of Developmental Biology and Molecular Medicine, Fudan University, Shanghai, China), INS-1E cells by Claes Wollheim (Lund and Geneva Universities), and the anti-NKX6.1 antibody was kindly provided from Ole Dragsbæk Madsen & Claude Rescan, Novo Nordisk A/S. This work was supported by JDRF through a Translational Academic Research Partnership (TARP).

Author contributions

K.M., A.A. and M.T. conceived the project. K.M. and A.A. supervised and designed the experiments and analyzed the data in Figs. 2–4, 5b, c, 6–9, and Supplementary Figs. 4, 6b, c, and 7–10. M.T., W.S., P.G.S., and A.K.C. supervised and designed the experiments in Figs. 1, 5a, and Supplementary Figs. 1–3, 5, and 6a. S.L., S.Y., T.B. and M.S. performed the screening and medicinal chemistry experiments and analyses. K.A., A.D., B.L., R.H., D.A., S.L., S.Y. and S.G. performed the mouse experiments and analyses as well as immunostaining and analysis. KA performed the bioluminescence assay and analysis. S.Z. performed the CETS assay and analysis. J.O., L.H.L. performed the MALDI analysis. B.L., S.A. and K.A. performed Western blots for the INS-1E as well as mouse and human islet experiments. V.N.T. and S.J. performed PK analyses. K.M., A.A., N.R., W.S. and M.T. wrote the paper. All authors critically reviewed the paper for important intellectual content and approved the final version to be published.

Competing interests

The authors declare no competing interests.

Additional information

Supplementary information is available for this paper at <https://doi.org/10.1038/s41467-019-12880-5>.

Correspondence and requests for materials should be addressed to A.A., M.S.T., W.S. or K.M.

Peer review information *Nature Communications* thanks the anonymous reviewer(s) for their contribution to the peer review of this work.

Reprints and permission information is available at <http://www.nature.com/reprints>

Publisher's note Springer Nature remains neutral with regard to jurisdictional claims in published maps and institutional affiliations.



Open Access This article is licensed under a Creative Commons Attribution 4.0 International License, which permits use, sharing, adaptation, distribution and reproduction in any medium or format, as long as you give appropriate credit to the original author(s) and the source, provide a link to the Creative Commons license, and indicate if changes were made. The images or other third party material in this article are included in the article's Creative Commons license, unless indicated otherwise in a credit line to the material. If material is not included in the article's Creative Commons license and your intended use is not permitted by statutory regulation or exceeds the permitted use, you will need to obtain permission directly from the copyright holder. To view a copy of this license, visit <http://creativecommons.org/licenses/by/4.0/>.

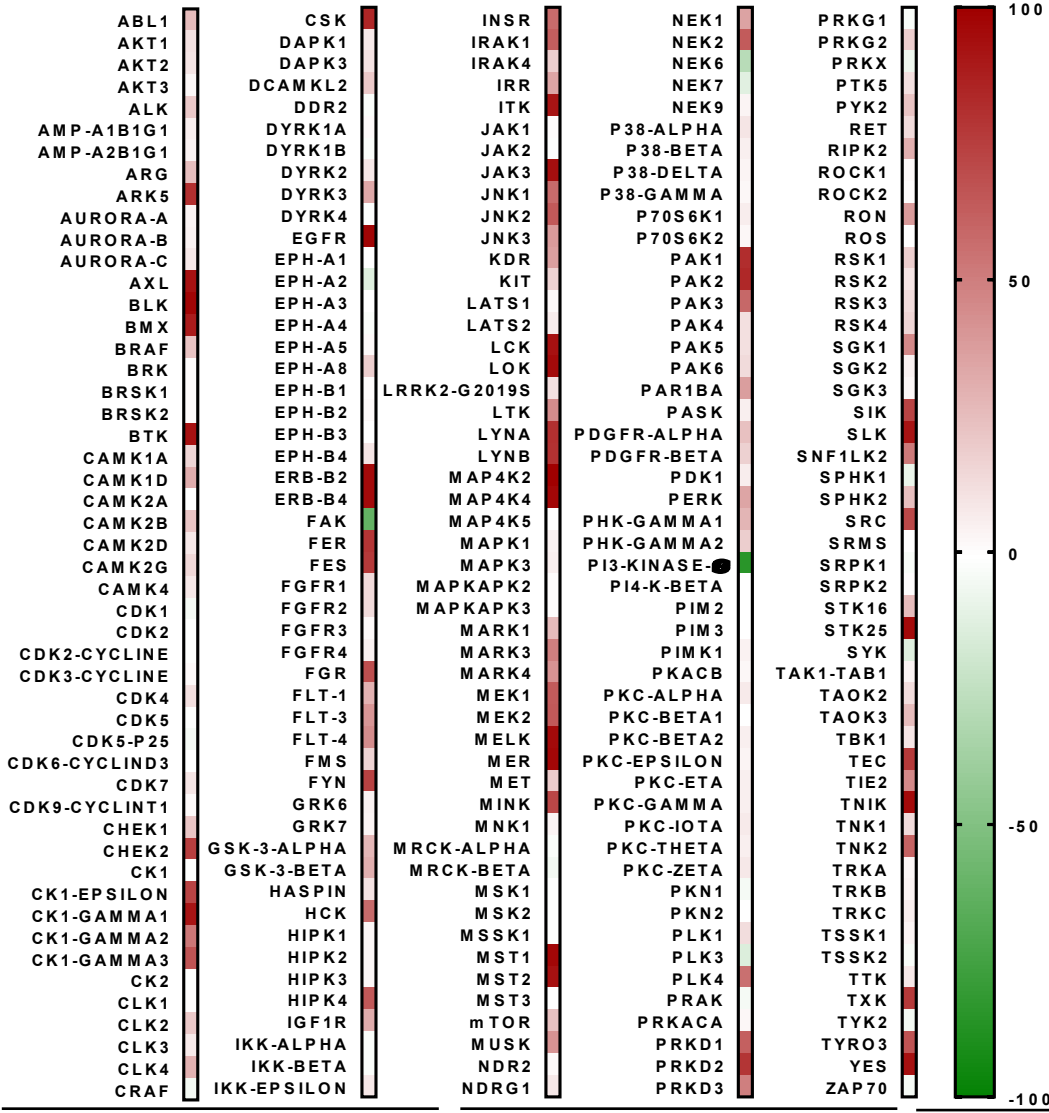
© The Author(s) 2019

Supplementary Figures

Neratinib Protects Pancreatic Beta Cells in Diabetes

Ardestani et al.

a

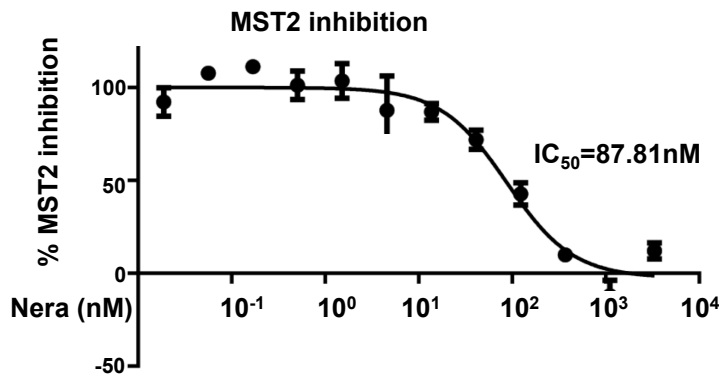
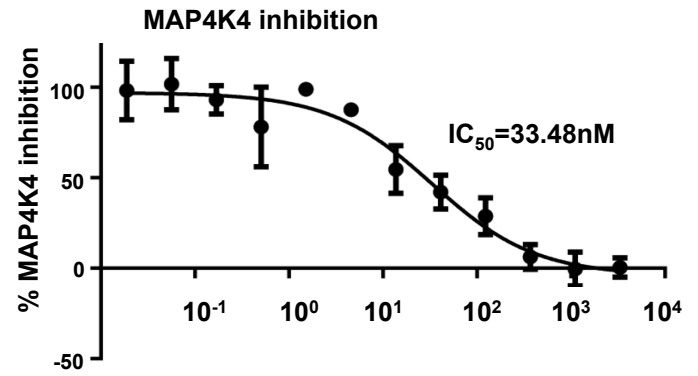
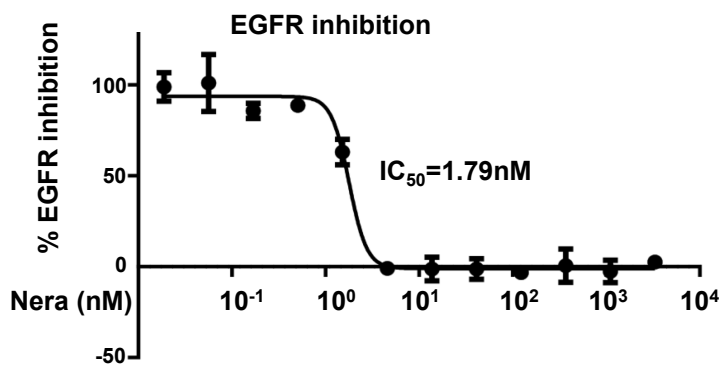


b

Kinases	Neratinib (IC ₅₀ uM)	Kinases	Neratinib (IC ₅₀ uM)	Kinases	Neratinib (IC ₅₀ uM)
LCK	0.066	PAK3	1.5	YES	0.087
LYNA	0.379	PAK5	>20	AXL	0.185
MAP4K2	0.102	PHK1	5.85	EGFR	0.0003
MAP4K5	0.0001	MST2	0.21	HCK	2.75
MEK1	1.49	SIK	1.05	HIPK4	1.66
MER	0.026	SRC	0.727	BLK	0.016

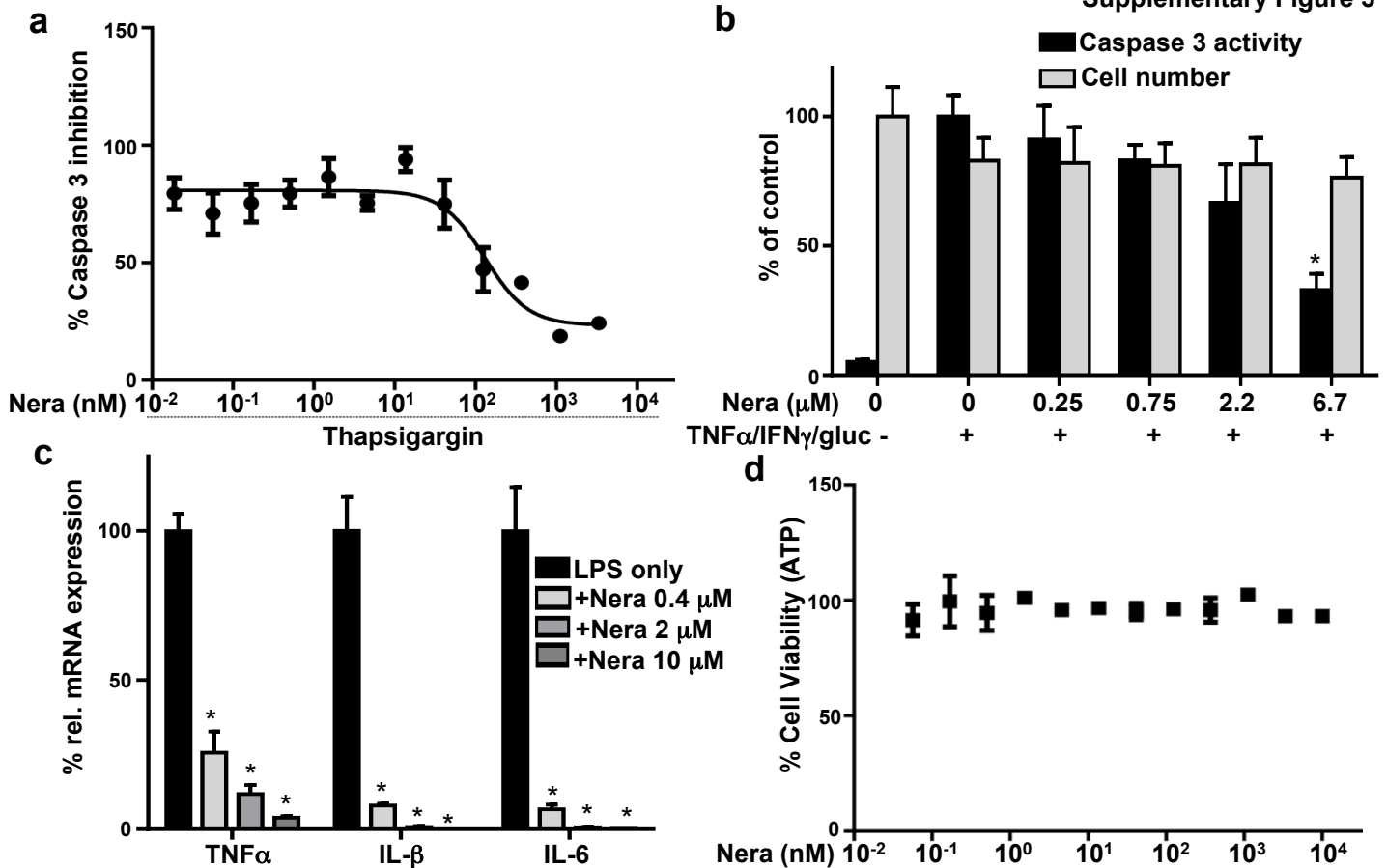
Supplementary Figure 1. Results of kinase profiling for Neratinib by Nanosyn. (A) Neratinib was assayed at 3 μ M in duplicate wells against 250 biochemical kinase assays. % inhibition was determined for each assay. (B) Neratinib was assayed in a 12 points dose-dependent serial concentration and IC_{50} was determined against 38 biochemical kinases. Related to Figure 1.

Supplementary Figure 2

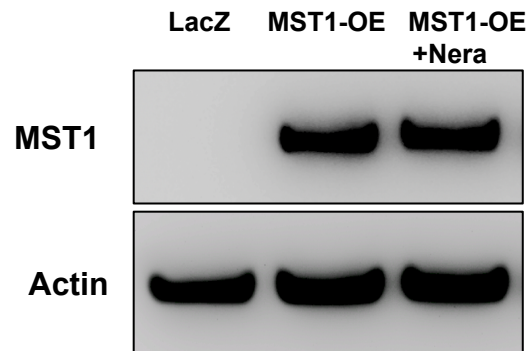


Supplementary Figure 2. Neratinib's effect on EGFR, MAP4K4 and MST2 inhibition. Biochemical dose response of EGFR, MAP4K4 and MST2 inhibition by neratinib. Data show means \pm SEM from 3 independent experiments (n=3). Related to Figure 1.

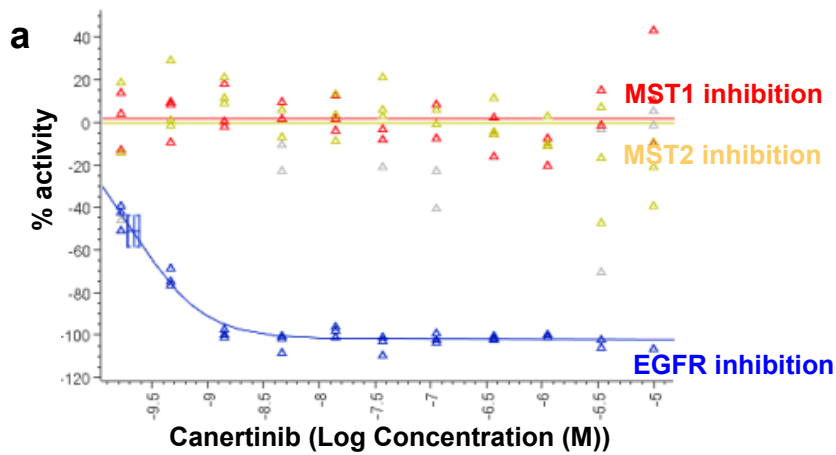
Supplementary Figure 3



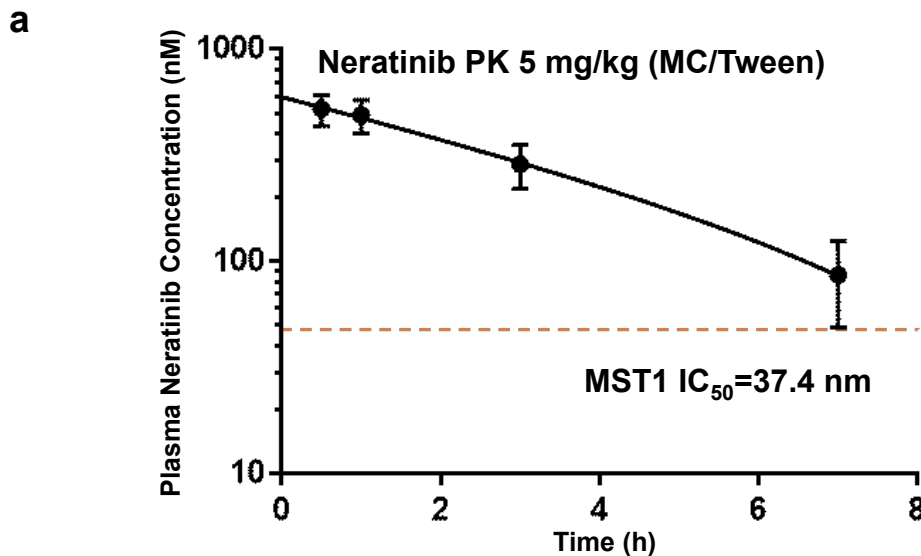
Supplementary Figure 3. Neratinib protects INS-1E β -cells from ER and cytokine induced stresses. (A) Caspase-3 activation induced by thapsigargin mediated ER stress. INS-1E cells were treated with compounds in a dose-dependent manner at 10^4 cells/well. Apoptosis was induced after 24 hours by $0.1 \mu\text{M}$ thapsigargin with caspase-3 substrate Nucview488. 16 hours later, cells were fixed in 3% paraformaldehyde and stained with Hoechst33342. Data analysis is based on the fluorescence intensity of Nucview 488 and Hoechst33342, with normalization to cell cytotoxicity, which was evaluated through Celltiter-Glo. (B) Caspase-3 activation induced by cytokine mixture at high glucose. INS-1E cells were exposed up to $6.7 \mu\text{M}$ of neratinib for 2h followed by 16h of induction in 100 ng/mL of $\text{TNF}\alpha$ and 200 ng/mL of $\text{IFN}\gamma$ with 33 mM glucose in assay medium. Caspase-3 activity was evaluated through Nucview488 and Hoechst33342. (C) Anti-inflammatory effect of neratinib through gene expression assay (RT-PCR). Mouse macrophage Raw264.7 cells were treated with neratinib in different concentrations for 2 hours, and followed by 100 ng/mL LPS stimulation for 4 hours. Cells were harvested and gene expression of $\text{TNF}\alpha$, IL-6 and IL-1 β were analyzed through qRT-PCR. (D) Cytotoxicity of neratinib evaluated by CellTiter-Glo®. INS1E cells were treated with neratinib in a dose-dependent manner at 10^4 cells/well. 24 hours later, Celltiter-Glo® reagent was added to each well and luminescence intensity was detected on plate reader. Data show means \pm SD from 3 independent experiments ($n=3$). * $p<0.01$ neratinib compared to vehicle treated cells. Related to Figure 2.



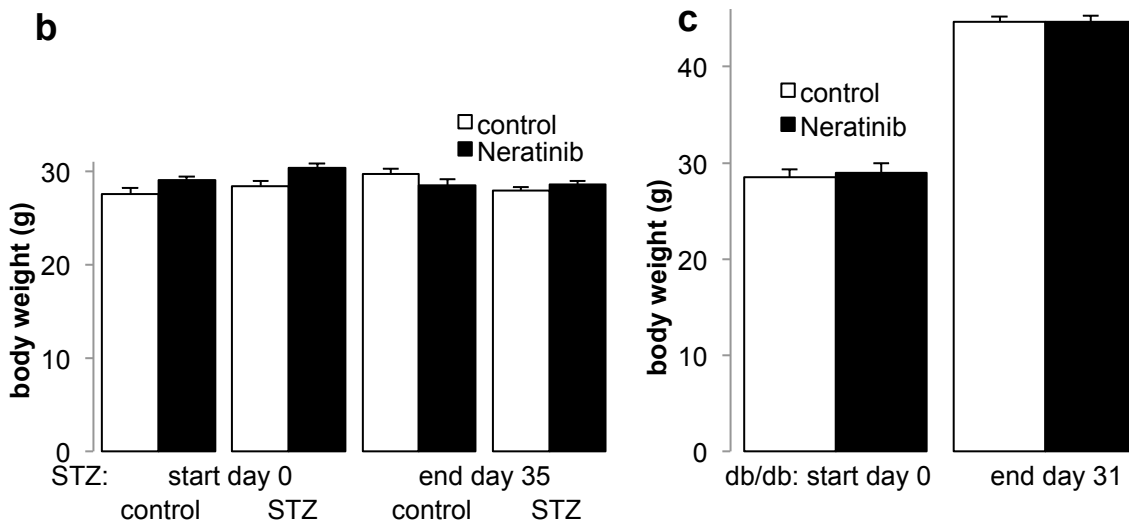
Supplementary Figure 4. MST1 overexpression in human islets. Human islets were infected with Ad-LacZ (control) or Ad-MST1 adenoviruses and exposed to 10 μ M neratinib for 48h; successful MST1 overexpression is shown by western blot analysis. Related to Figure 3.



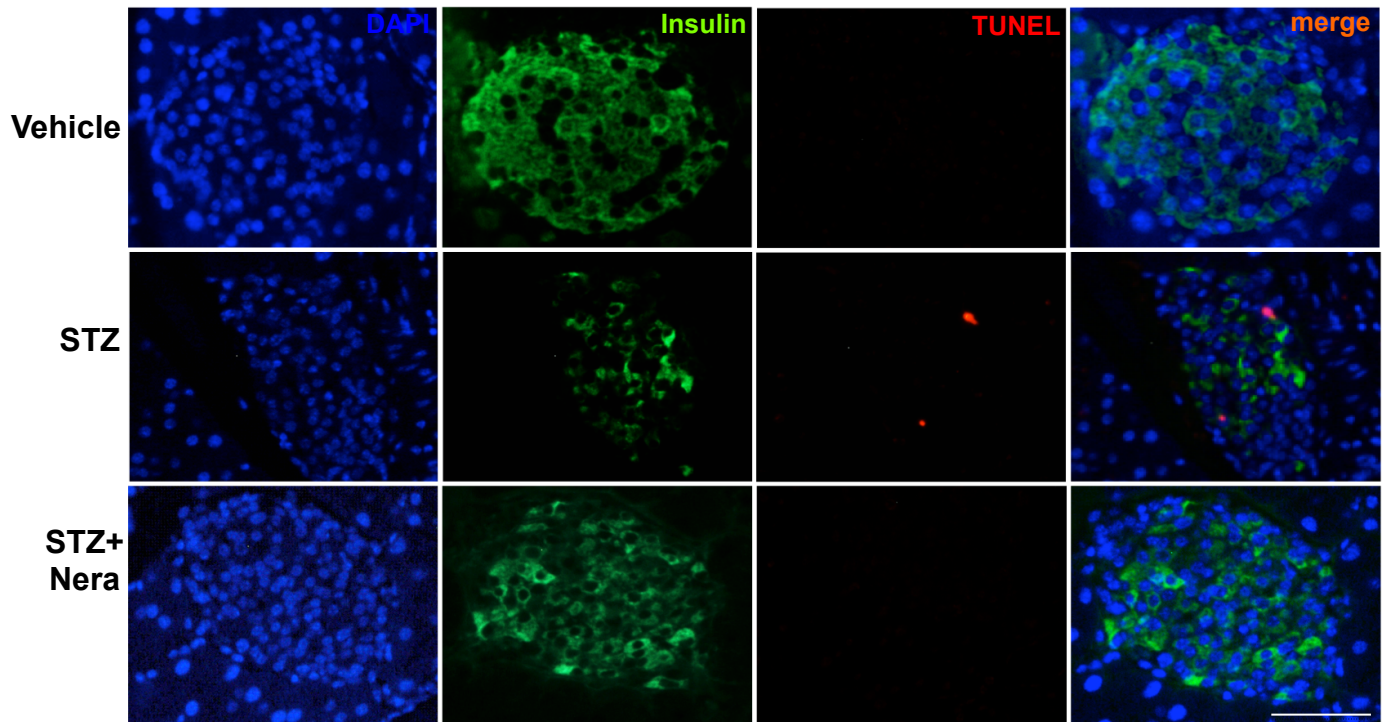
Supplementary Figure 5. Canertinib's effect on EGFR, MST1 and MST2 inhibition. Biochemical kinase assays in dose response to EGFR (blue), MST1 (red) and MST2 (yellow) inhibition by canertinib (**A**) and IC_{50} summary table (**B**). Data show means from 3 independent experiments (n=3). Related to Figure 5.



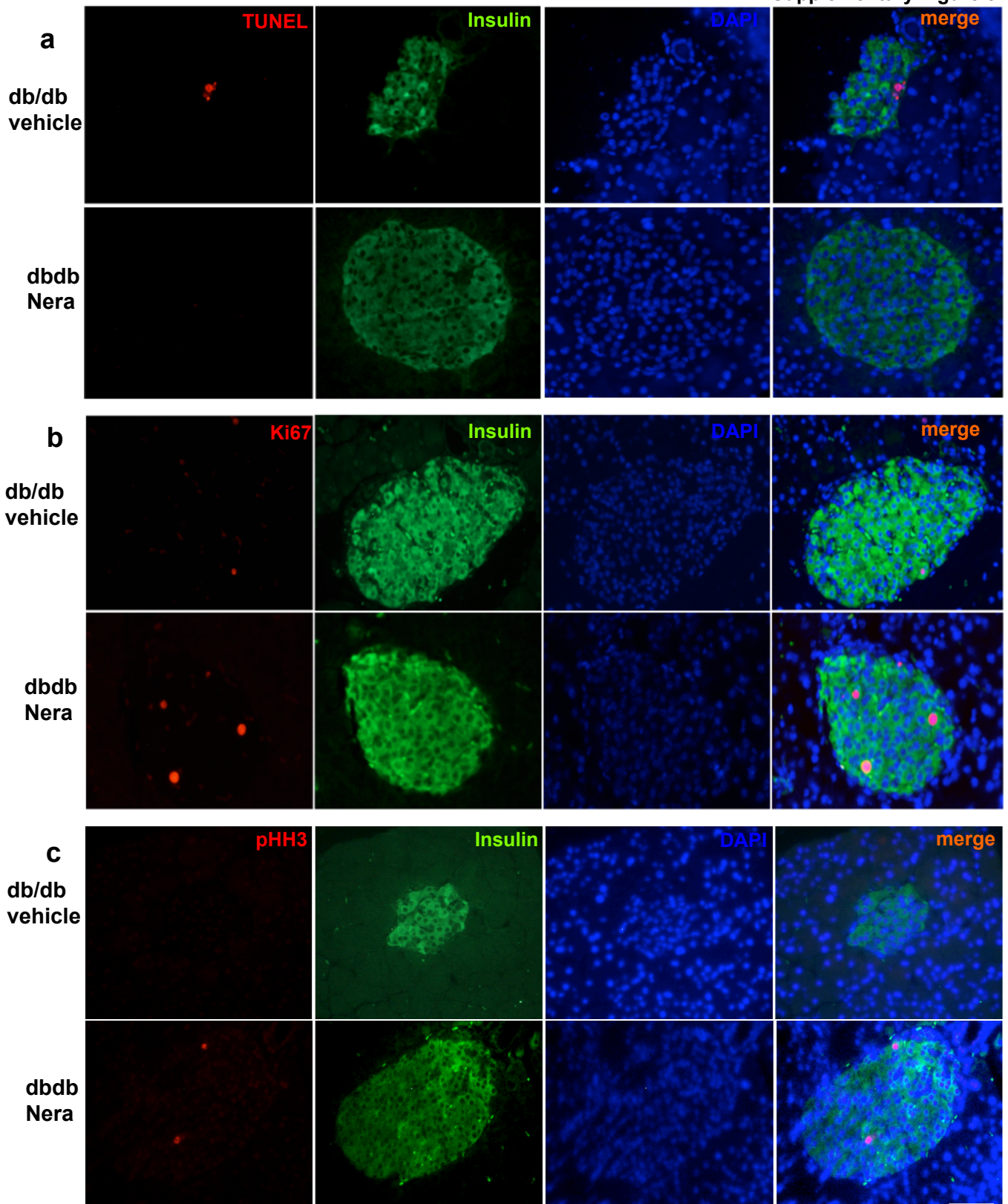
Animal	t _{1/2} (hr)	C _{max} (nM)	T _{max} (hr)	AUC ₀₋₂₄ (hr*nM)	AUC _{LAST} (hr*nM)	AUC _{INF} (hr*nM)	Cl (mL/min/kg)	MRT (hr)	V _D (L/kg)
1	4.0	468.6	0.5	1621.8	1621.8	2364.4	253.1	2.7	86.9
2	1.9	556.6	1.0	1967.1	1967.1	2153.7	277.9	2.3	46.7
3	1.9	623.0	0.5	2125.2	2125.2	2298.5	260.4	2.3	43.1
AVERAGE	2.6	549.4	0.7	1904.7	1904.7	2272.2	263.8	2.4	58.9
ST DEV	1.2	77.4	0.3	257.4	257.4	107.8	12.7	0.2	24.3
CV%	0.5	0.1	0.4	0.1	0.1	0.0	0.0	0.1	0.4



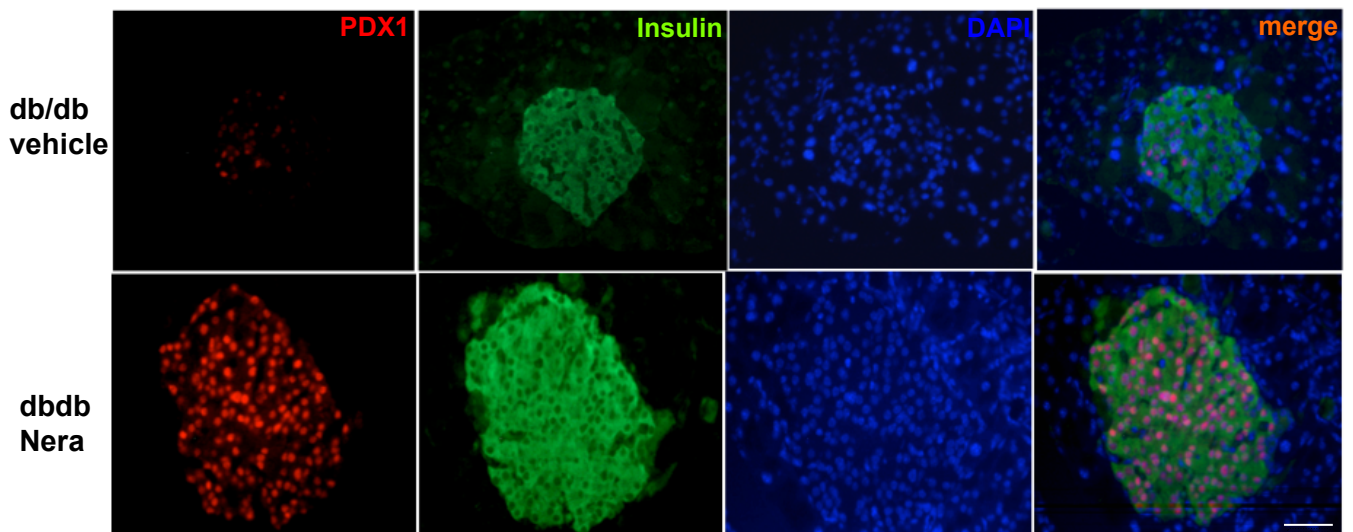
Supplementary Figure 6. (a) Neratinib's IP PK profile in mice and body weights. Neratinib was dosed at 5 mg/kg IP to mice (n=3) which were fasted overnight. The compound was administered in 30% PEG400: 0.5% Tween80: 5% propylene glycol in saline through a single dose. Plasma samples were collected at 30 min., 1, 3 and 7 h post dosing and analyzed by LC-MS to determine the plasma Neratinib concentration. **(b,c)** Mean body weights of all mice in the study from the MLD-STZ mice and db/db mice. Related to Figures 6 and 7.



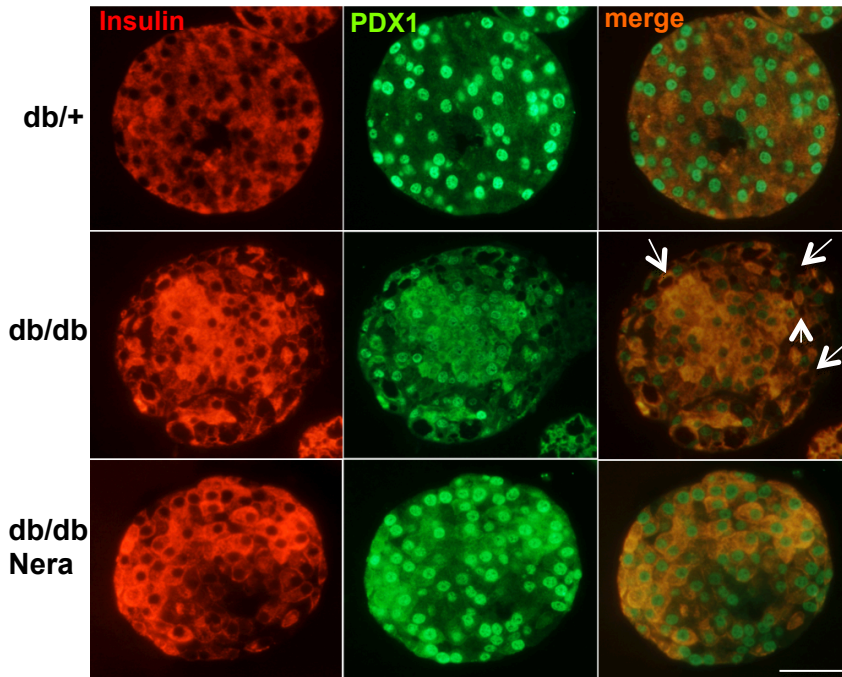
Supplementary Figure 7. Neratinib restores β -cell survival in MLD-STZ-induced diabetes. Representative triple-stainings of pancreatic sections for TUNEL (red), insulin (green) and DAPI (blue) shown from MLD-STZ diabetic mice (STZ) treated with neratinib or vehicle throughout the whole experiment of 35 days and their control (vehicle). Quantification of data are shown in Figure 6h. Related to Figure 6. Scale bar, 100 μ m.



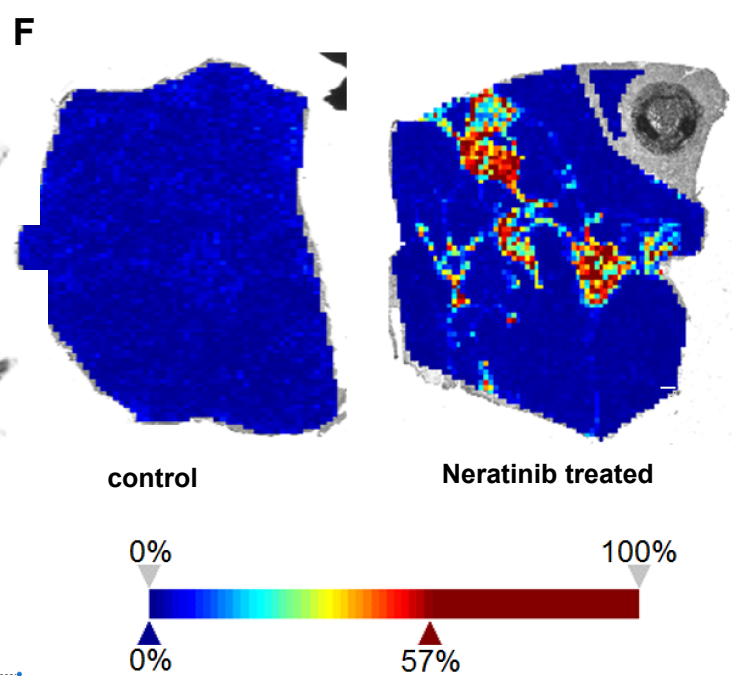
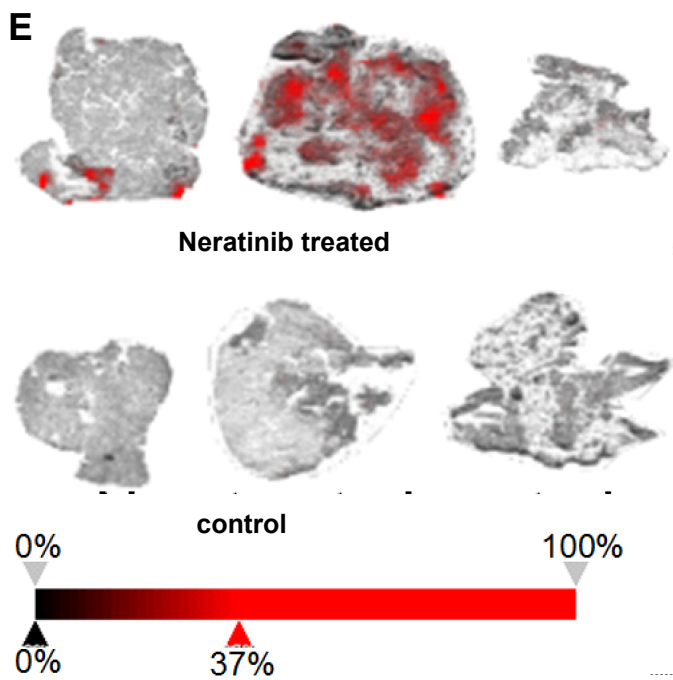
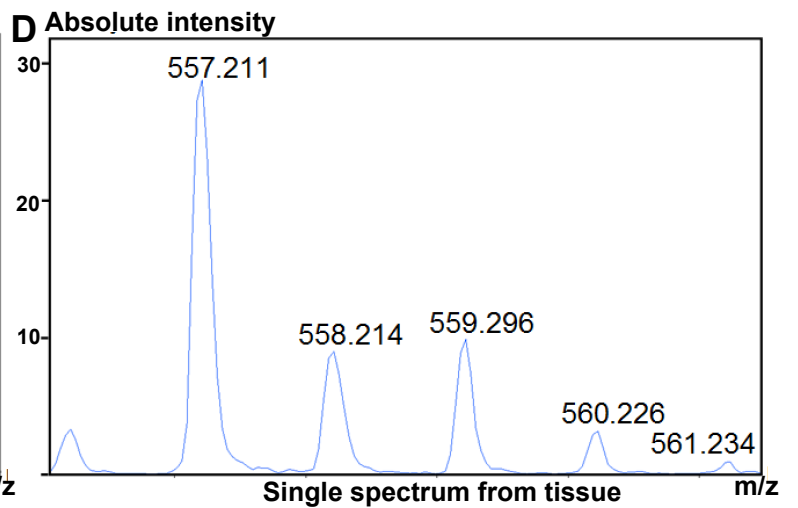
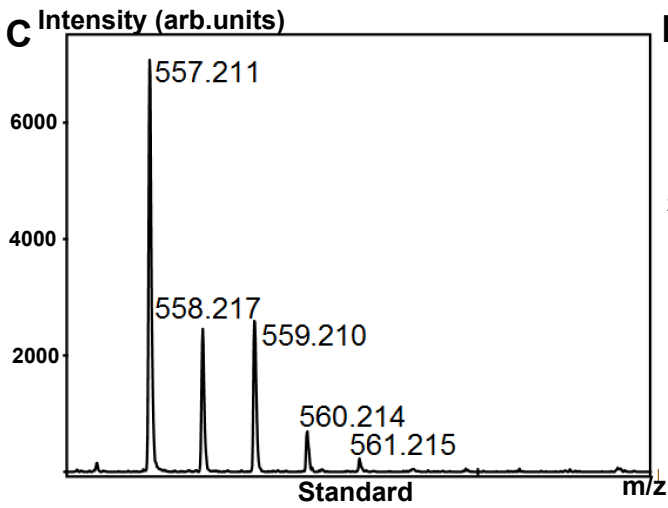
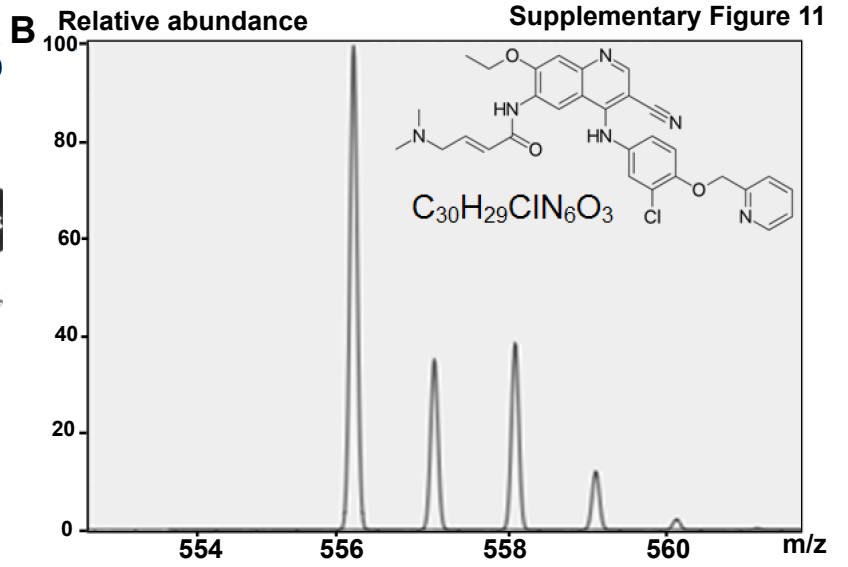
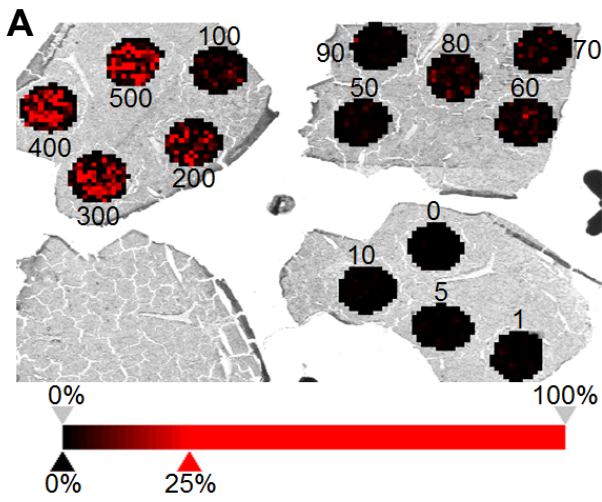
Supplementary Figure 8. Neratinib restores β -cell survival in db/db mice. Representative triple-stainings of pancreatic sections for TUNEL (a), Ki67 (b) and pHH3 (c) (red), insulin (green) and DAPI (blue) shown from db/db diabetic mice (dbdb) treated with neratinib or vehicle throughout the whole experiment of 31 days. Quantification of data are shown in Figure 8h-j. Related to Figure 8. Scale bar, 100 μ m.



Supplementary Figure 9. Neratinib restores PDX1 in db/db mice. Representative triple-stainings of pancreatic sections for PDX1 (red), insulin (green) and DAPI (blue) shown from db/db diabetic mice (dbdb) treated with neratinib or vehicle throughout the whole experiment of 31 days. Quantification of data are shown in Figure 8k. Related to Figure 8. Scale bar, 100 μ m.



Supplementary Figure 10. Neratinib improves PDX1 nuclear localization in db/db mouse islets ex vivo. Representative double-stainings for PDX1 (green) and insulin (red) shown from isolated islets from 10-week old heterozygous db/+ mice or db/db littermates exposed to vehicle or to 10 μ M neratinib for 24h. Representative microscopical images are shown. White arrow point to PDX1 deficient nuclei in db/db mouse islets. Related to Figure 9. Scale bar, 100 μ m



Supplementary Figure 11. Neratinib is enriched and distributed throughout the pancreas. MALDI Imaging MS of Neratinib for localization of drug distribution in mice tissue sections. **(A)** The dynamic range of the Neratinib signal (monoisotopic peak) in mice liver tissue sections after spotting neratinib standard with concentrations ranging from 0 to 500 pmol/ μ l is presented. **(B)** The single spectrum of the Neratinib standard spotted on a MALDI steel target shows the distinct isotopic pattern of the drug **(C)** compared to the simulated isotope pattern of $C_{30}H_{29}ClN_6O_3$ (Patiny and Borel, 2013). **(D)** This pattern could be unambiguously detected in the MALDI imaging MS study of pancreas tissue sections as shown by the representative single spectrum. **(E)** The neratinib signal at m/z 577.2 is clearly located in the treated pancreas sections (top) and absent in the non-treated control sections from obese db/db mice used in the study (bottom). **(F)** Distribution of Neratinib in the pancreas sections of wild-type mice 4h after injection (right) compared to the non-treated control (left). Scale bar, 100 μ m

Manuscript II

2.2 The Hippo kinase LATS2 impairs pancreatic β -cell survival in diabetes through the mTORC1-autophagy axis

Ting Yuan*, Karthika Annamalai* *et al.*

* shared first authors

Published in Nature communications online 2021 Aug 13. doi: [10.1038/s41467-021-25145-x](https://doi.org/10.1038/s41467-021-25145-x)

My contribution:






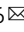


Designed, performed experiments, analysed data and assembled the figures for:

Figures: 1A-G; 3F,G,J,K; 5F, 5I,J (partially contributed), 6A-G; 8D


Supplementary Figures: 1D,E; 3C-E; 4B,C; 5A,B (partially contributed); 6B (partially contributed); 7A,B; 8F (partially contributed).

Contributed in writing the paper.

The Hippo kinase LATS2 impairs pancreatic β -cell survival in diabetes through the mTORC1-autophagy axis

Ting Yuan ^{1,4,5}, Karthika Annamalai^{1,5}, Shruti Naik ¹, Blaz Lupse¹, Shirin Geravandi¹, Anasua Pal¹, Aleksandra Dobrowolski¹, Jaee Ghawali¹, Marina Ruhlandt ¹, Kanaka Durga Devi Gorrepati¹, Zahra Azizi^{1,2}, Dae-Sik Lim ³, Kathrin Maedler ^{1,6}  & Amin Ardestani ^{1,2,6} 

Diabetes results from a decline in functional pancreatic β -cells, but the molecular mechanisms underlying the pathological β -cell failure are poorly understood. Here we report that large-tumor suppressor 2 (LATS2), a core component of the Hippo signaling pathway, is activated under diabetic conditions and induces β -cell apoptosis and impaired function. LATS2 deficiency in β -cells and primary isolated human islets as well as β -cell specific LATS2 ablation in mice improves β -cell viability, insulin secretion and β -cell mass and ameliorates diabetes development. LATS2 activates mechanistic target of rapamycin complex 1 (mTORC1), a physiological suppressor of autophagy, in β -cells and genetic and pharmacological inhibition of mTORC1 counteracts the pro-apoptotic action of activated LATS2. We further show a direct interplay between Hippo and autophagy, in which LATS2 is an autophagy substrate. On the other hand, LATS2 regulates β -cell apoptosis triggered by impaired autophagy suggesting an existence of a stress-sensitive multicomponent cellular loop coordinating β -cell compensation and survival. Our data reveal an important role for LATS2 in pancreatic β -cell turnover and suggest LATS2 as a potential therapeutic target to improve pancreatic β -cell survival and function in diabetes.

¹Centre for Biomolecular Interactions Bremen, University of Bremen, Bremen, Germany. ²Department of Molecular Medicine, School of Advanced Technologies in Medicine, Tehran University of Medical Sciences, Tehran, Iran. ³Department of Biological Sciences, KAIST 291 Daehak-ro, Yuseong-gu, Daejeon, Republic of Korea. ⁴Present address: Institute of Cardiovascular Regeneration, Centre for Molecular Medicine, Goethe University Frankfurt, Frankfurt, Germany. ⁵These authors contributed equally: Ting Yuan, Karthika Annamalai. ⁶These authors jointly supervised this work: Kathrin Maedler, Amin Ardestani. email: kmaedler@uni-bremen.de; ardestani.amin@gmail.com

Both type 1 diabetes (T1D) and type 2 diabetes (T2D) result from an absolute or relative decline in pancreatic β -cell function and/or mass^{1, 2}, and β -cell apoptosis is its hallmark^{3–6}. T1D is an autoimmune disease resulting from selective destruction of pancreatic islet β -cells⁷. T2D is a complex metabolic disorder characterized by insulin resistance as well as decreased insulin secretory function and ultimately reduced β -cell mass, resulting in the development of chronic β -cell dysfunction and relative insulin deficiency⁸. Given these complex causes of β -cell failure, inhibition of apoptosis and/or β -cell dysfunction represents a potential therapeutic intervention to the treatment of diabetes. Understanding the varied β -cell responses to metabolic assaults and how diabetes-related signals impair β -cell function and survival is important for the understanding of pathogenesis as well as target identification towards a β -cell-directed therapy of diabetes.

Hippo signaling—first discovered using genetic screens in *Drosophila*—is an evolutionarily conserved pathway that critically regulates development, growth, and homeostasis of various tissues in response to a wide range of extra- and intracellular signals⁹. The mammalian Hippo pathway constitutes core kinases (MST1/2 and LATS1/2), adaptor proteins (SAV1 for MST1/2 and MOB1 for LATS1/2), downstream terminal effectors (YAP and TAZ), and transcription factors (TEAD1–4). Mammalian Sterile 20-like kinases (MST1/2) and Large-tumor suppressors (LATS1/2) represent core kinases of the Hippo pathway. MST1/2, in complex with a regulatory protein Salvador (Sav1), phosphorylates and activates LATS1/2 kinases, which also form a complex with a regulatory protein Mps-one binder 1 (MOB1). The function of the effector transcriptional coactivator Yes-associated protein (YAP) is therefore mainly regulated by phosphorylation-dependent mechanisms. The kinases LATS1/2 inactivate YAP by direct phosphorylation on multiple serine residues including at S127, enhancing YAP binding to 14-3-3 proteins, its cytoplasmic sequestration and subsequent proteasomal degradation. In association with TEA domain (TEAD) family transcription factors, YAP fosters the expression of target genes, with pro-proliferative and anti-apoptotic outcomes^{9–12}.

Hippo's dysregulation has been implicated in many human disorders such as cancer and metabolic diseases^{9, 13}. Hippo components such as MST1, Merlin/NF2, YAP, and TEAD control various aspects of β -cell life including development, β -cell function, survival, and proliferation^{13–20}. For example, MST1 is an important regulator of pancreatic β -cell death and dysfunction in human and rodent β -cells. MST1 inhibition restores normoglycemia, β -cell function, and survival under diabetic conditions in vitro and in vivo^{14, 21}. LATS2, an MST1 downstream substrate, is a ubiquitously expressed serine/threonine kinase and involved in multiple cellular processes such as morphogenesis, proliferation, stress responses, apoptosis, and differentiation^{22–27}. LATS2 promotes cell death through regulation of multiple downstream targets such as P53, FOXO1, c-Abl, and YAP^{24, 28–31}. In this regard, the MST1-LATS2 axis is an important regulator of apoptosis in the heart: knockdown or genetic deletion of MST1 or LATS2 in cardiomyocytes provides protection against ischemic injury^{26, 30, 32}. As YAP is excluded from mature β -cells during development^{13–19, 33}, MST1 and LATS2 core kinases can also act independently of their classical terminal effector YAP. In this study, we investigated whether LATS2 hyper-activation would trigger β -cell death and impaired insulin secretion, whether its deficiency would promote β -cell survival under diabetic conditions in vitro and in vivo as well as the molecular mechanism of pathogenic action of LATS2 in the β -cells.

Results

LATS2 was activated under diabetogenic conditions and induced β -cell death and dysfunction. In order to identify

whether LATS is activated in response to diabetogenic stimuli, a recently established bioluminescence-based biosensor (LATS-BS) that monitors the activity of LATS kinase in cells in real-time with accurate quantification, high sensitivity, and excellent reproducibility has been used³⁴ (Fig. 1a). LATS1/2 kinases phosphorylate their own established target YAP on S127, which exposes the docking site for binding of 14-3-3 proteins leading to YAP cytoplasmic sequestration. LATS-BS consists of a minimal YAP fragment that interacts with 14-3-3 in a phosphorylation-dependent manner. Therefore, a LATS-BS construct has been generated with fusion of YAP fragment and 14-3-3 with N-terminal and C-terminal Firefly luciferase fragments (N-luc and C-luc), respectively that measures LATS kinase activity by assessing the complementation between pS127-YAP and 14-3-3 in a LATS-phosphorylation-dependent manner³⁴ (Fig. 1a). The β -cell line INS-1E was transfected with LATS-BS and control Renilla constructs and then exposed chronically to increased glucose concentrations (glucotoxicity), or its combination with the free fatty acid palmitate (glucolipotoxicity). Both diabetogenic treatments increased bioluminescence signals indicating enhanced exogenously expressed YAP phosphorylation at S127 (LATS specific site) and thus hyper-activated Hippo kinases LATS1/2 (Fig. 1b, c). LATS1/2 hyper-activation under diabetic conditions was further confirmed by immunoblot analysis of increased exogenously expressed YAP-S127 phosphorylation levels triggered by high glucose as well as high glucose/palmitate (Fig. 1d, e). Since the Hippo pathway adaptor protein MOB1 interacts with and activates LATS1/2 kinase activity^{23, 35}, we analyzed the protein expression of MOB1 in β -cells. Prolonged culture of INS-1E cells under high glucose or high glucose/palmitate up-regulated MOB1 protein levels (Supplementary Fig. 1a). Also, overexpression of LATS2 itself increased MOB1 levels in INS-1E β -cells and human islets (Supplementary Fig. 1b, c). LATS activation (as represented by exogenously expressed pYAP levels) and MOB1 were also increased in islets of hyperglycemic high fat/ high sucrose (HFD) fed mice for 16 weeks (Fig. 1f and Supplementary Fig. 1d). Similarly, exogenously expressed pYAP and MOB1 protein levels were robustly elevated in islets of another model of T2D, the obese diabetic leptin receptor-deficient db/db mice (Fig. 1g and Supplementary Fig. 1e). These data show that LATS activity and its associated protein MOB1 is markedly elevated by pro-diabetic conditions in metabolically stressed β -cells and islets isolated from mouse models of diabetes.

In subsequent experiments we investigated whether LATS2 overexpression is directly detrimental for β -cell survival. LATS2 was overexpressed through adenoviral transduction, which efficiently up-regulated LATS2 (Fig. 2a, b). Overexpression of LATS2 itself was sufficient to induce β -cell apoptosis in both INS-1E cells and human islets, as determined by cleavage of caspase-3 and poly-(ADP-ribose) polymerase (PARP), a downstream substrate of caspase 3 (Fig. 2a, b). In line with these findings, LATS2 overexpression increased the number of TUNEL-positive apoptotic β -cells in human islets confirming β -cell-specific induction of apoptosis by LATS2 hyper-activation (Fig. 2c, d). Furthermore, in isolated human islets, LATS2 overexpression led to impairment of glucose-stimulated insulin secretion (GSIS; Fig. 2e, f). Together, our data show that LATS2 impairs β -cell survival and function.

Loss of the LATS2-MOB1 axis improved β -cell survival in vitro. Further analyses aimed to investigate whether LATS2 inhibition can rescue β -cells from apoptosis under diabetogenic conditions. β -cells were transfected with small interfering RNA (siRNA) against LATS1 and/or LATS2 and then exposed to

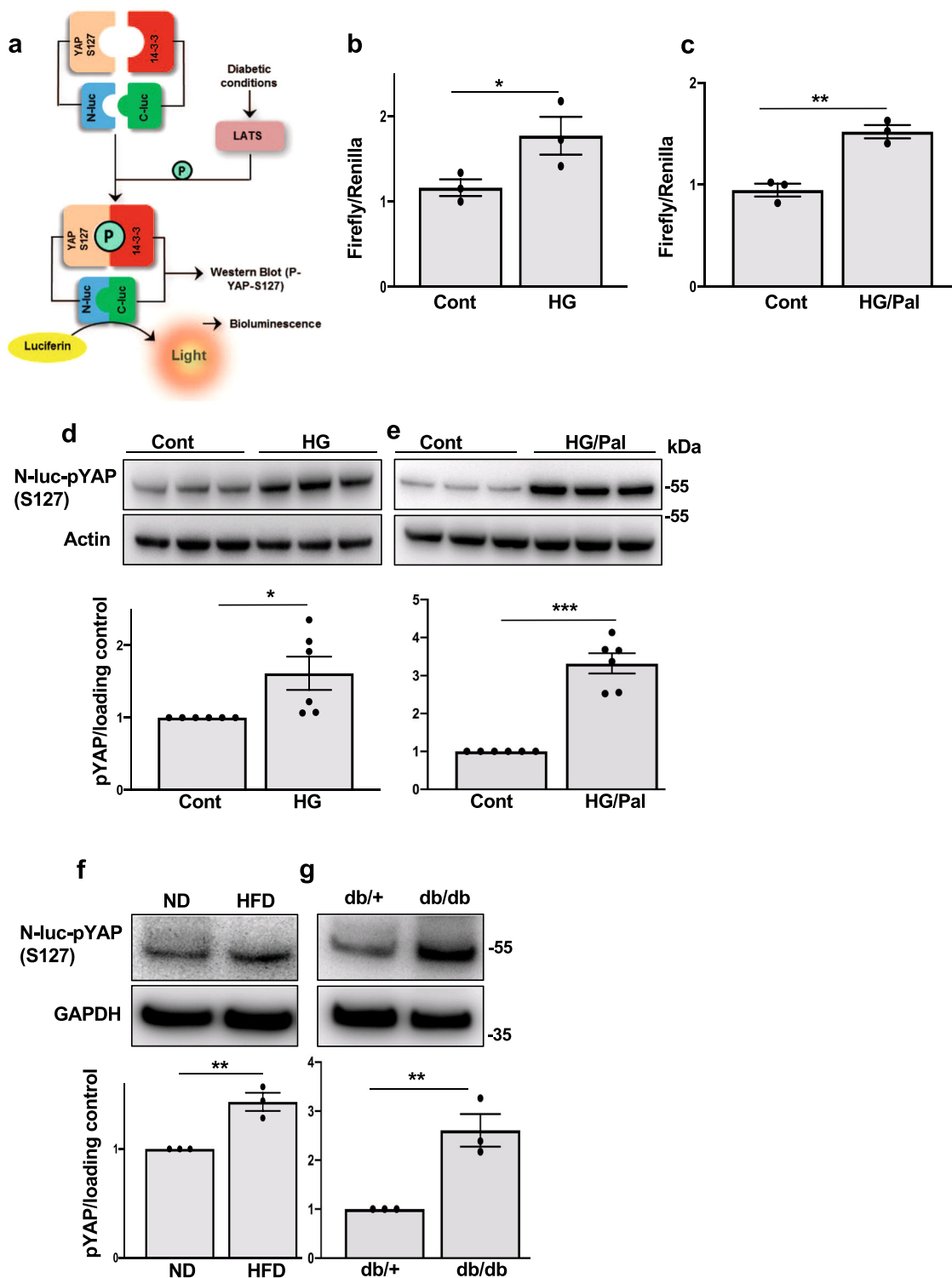


Fig. 1 LATS2 is activated under diabetogenic conditions. **a** Schematic structure and mechanism of action for LATS-BS. **b–e** INS-1E cells transfected with the firefly luciferase reporter plasmids N-luc-YAP15-S127, C-luc-14-3-3, and pRL-Renilla luciferase were treated with 22.2 mM glucose alone or in combination with 0.5 mM palmitate for 24 h. **b, c** Downstream phosphorylation of the exogenously expressed YAP-S127 fragment was determined by firefly luciferase activity and normalized to the Renilla signal ($n = 3$ biologically independent samples). **d, e** Representative western blots and pooled quantitative densitometry analysis for exogenously expressed YAP-127 by a phospho-specific antibody are shown ($n = 6$ biologically independent samples). Isolated islets from **f** HFD-treated C57BL/6 J mice for 16 weeks or **g** the obese diabetic leptin receptor-deficient db/db mice and their corresponding controls cultured overnight and transfected with the N-luc-YAP15-S127 plasmid for 24 h. Representative western blots and pooled quantitative densitometry are shown ($n = 3$ independent experiments) and results were normalized to the respective control conditions and ratios, in which a normal distribution of results cannot be proven, were analyzed. Data are expressed as means \pm SEM. * $p < 0.05$, ** $p < 0.01$, *** $p < 0.001$; all by two-tailed Student's *t*-tests.

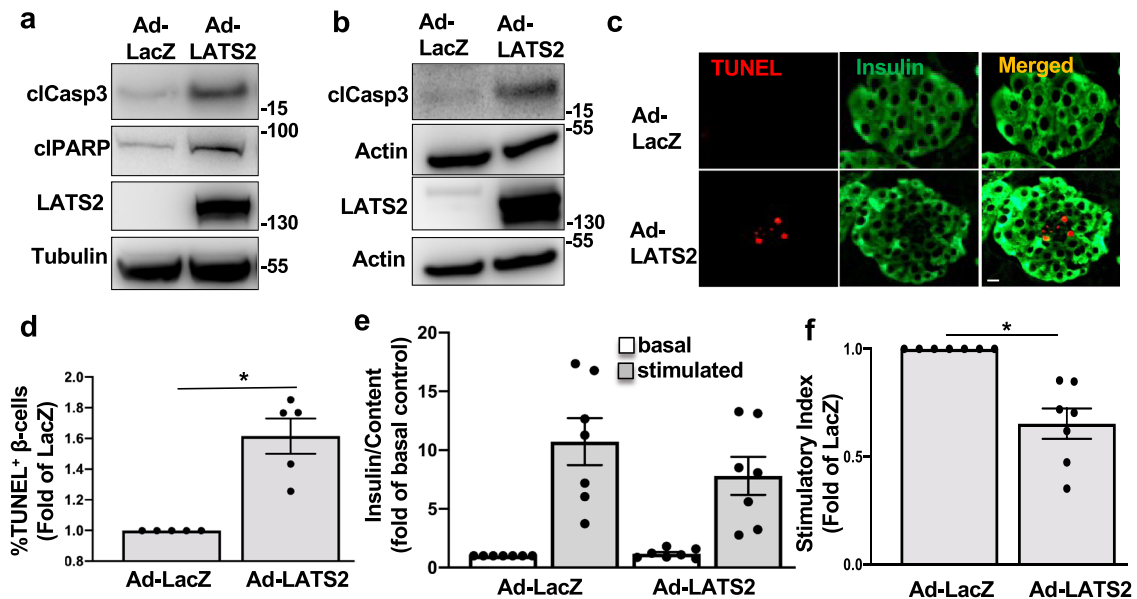


Fig. 2 LATS2 induces β -cell death and dysfunction. INS-1E cells (**a**) and human islets (**b–f**) transduced with LacZ control or LATS2 adenoviruses for 48 h. **a, b** Representative western blots, **c** double staining for TUNEL (red) and insulin (green) and **d** pooled TUNEL analysis (**c, d**: $n = 5$ different human islets isolations). **e** Insulin secretion during 1 h incubation with 2.8 mM (basal) and 16.7 mM (stimulated) glucose, normalized to insulin content. **f** Insulin stimulatory index denotes the ratio of stimulated (16.7 mM glucoses) and basal (2.8 mM glucose) (**e, f**: $n = 7$ different human islets isolations). All western blots show representative results from at least three independent experiments. Data are expressed as means \pm SEM. * $p < 0.001$; all by two-tailed Student's *t*-tests. scale bar depicts 10 μ m.

glucotoxic and glucolipotoxic conditions as well as the mixture of pro-inflammatory cytokines interleukin-1 β (IL-1 β) and interferon-gamma (IFN- γ). Depletion of endogenous LATS2 but not LATS1 activity protected β -cells from glucose-, glucose/palmitate- and cytokine-induced apoptosis as demonstrated by decreased caspase-3- and PARP-cleavage (Fig. 3a–c and Supplementary Fig. 2a, b) showing a potential functional diversity between LATS1 and LATS2 in the regulation of β -cell apoptosis. The pro-survival function of loss of LATS2 in the β -cells was further validated by a second siRNA pool to the LATS2 gene with comparable gene silencing efficiency (Supplementary Fig. 2c). LATS kinases redundantly exert phosphorylation-induced inactivation of the transcription factors YAP/TAZ³⁶. We thus assessed whether LATS2's canonical kinase activity was necessary for its pro-apoptotic function by overexpressing LATS2 kinase dead (KD) mutant (K697R), where the ATP-binding site K697 was mutated to another positively charged amino acid arginine (R)³⁷. LATS2-KD overexpression profoundly reduced the levels of β -cell apoptosis under diabetogenic conditions (Fig. 3d, e). Also, β -cell specific LATS2 deletion in mice markedly suppressed the number of TUNEL-positive β -cells under a pro-diabetic milieu in vitro (Fig. 3f, g). In human islets, LATS2 was silenced by siRNA-mediated transfection as well as adenoviral-mediated infection either with Ad-shLATS2 or control shScr viruses. In line with rodent β -cells, apoptosis triggered by pro-inflammatory cytokines as well as by the mixture of high glucose/palmitate was diminished by LATS2 knockdown in isolated primary human islets (Fig. 3h, i). Consistently, repression of LATS2 by shRNA-mediated depletion of LATS2 expression efficiently prevented human β -cell death induced by diabetogenic conditions in human islets (Fig. 3j, k). Our data show that loss of LATS2 expression markedly protected both rodents and human β -cells from apoptosis under several diabetogenic conditions in vitro.

Mechanistically, silencing of endogenous LATS2 abolished MOB1 levels induced by prolonged treatment with high glucose suggesting a LATS2-dependent regulation of MOB1 by pro-diabetic stimuli (Supplementary Fig. 2d). To further prove such

regulatory LATS2-MOB1 axis, MOB1 was silenced in order to directly assess its pro-apoptotic function. Knockdown of MOB1 antagonized the apoptotic effect of high glucose as well as high glucose/palmitate in INS-1E β -cells (Fig. 4a, b). Consistently, MOB1 knockdown antagonized LATS2-induced caspase-3 cleavage (Fig. 4c) indicating an indispensable role of MOB1 in the mechanism of LATS2-induced β -cell apoptosis. These data suggest the LATS2-MOB1 axis as a determinant for β -cell apoptosis under a diabetic milieu in β -cells.

β -cell specific LATS2 ablation protected from STZ induced diabetes in vivo. As LATS2 depletion protected from β -cell apoptosis under multiple diabetogenic conditions in vitro, we hypothesized that LATS2 deficiency may protect from diabetes development in vivo. To test this hypothesis, we generated β -cell-specific LATS2 knockout mice (β -LATS2^{-/-}) by crossing LATS2 floxed (LATS2^{fl/fl}) mice with the β -cell-specific Cre transgenic line driven by the rat insulin-2 promoter (Rip-Cre). Cre recombinase expression, as well as Rip-Cre-mediated specific deletion of LATS2 gene in pancreatic β -cell, was confirmed in isolated islets from β -LATS2^{-/-} and LATS2^{fl/fl} mice (Supplementary Fig. 3a). As Rip-Cre has been reported to delete genes in β -cells but also in hypothalamic neurons³⁸, the specificity of LATS2 gene deletion was tested in genomic DNA from isolated liver, spleen, kidney, heart, hypothalamus, and pancreatic islets of β -LATS2^{-/-} mice. PCR analysis demonstrated that Cre-mediated LATS2 deletion was islet specific with no leakage in the hypothalamus or any other tested tissues (Supplementary Fig. 3b). β -LATS2^{-/-} mice were viable, fertile and showed no difference in food intake and body weight neither under a normal (ND) nor under a high fat diet (HFD) compared to LATS2^{fl/fl} mice, or to LoxP-negative mice (Supplementary Fig. 3c, d). To assess whether β -LATS2^{-/-} might protect against β -cell injury and diabetes, we induced diabetes by multiple-low dose streptozotocin (MLD-STZ) injection in β -LATS2^{-/-}, LATS2^{fl/fl}, and Rip-Cre mice. While MLD-STZ injection induced progressive hyperglycemia and severely impaired glucose tolerance in LATS2^{fl/fl} and Rip-Cre mice,

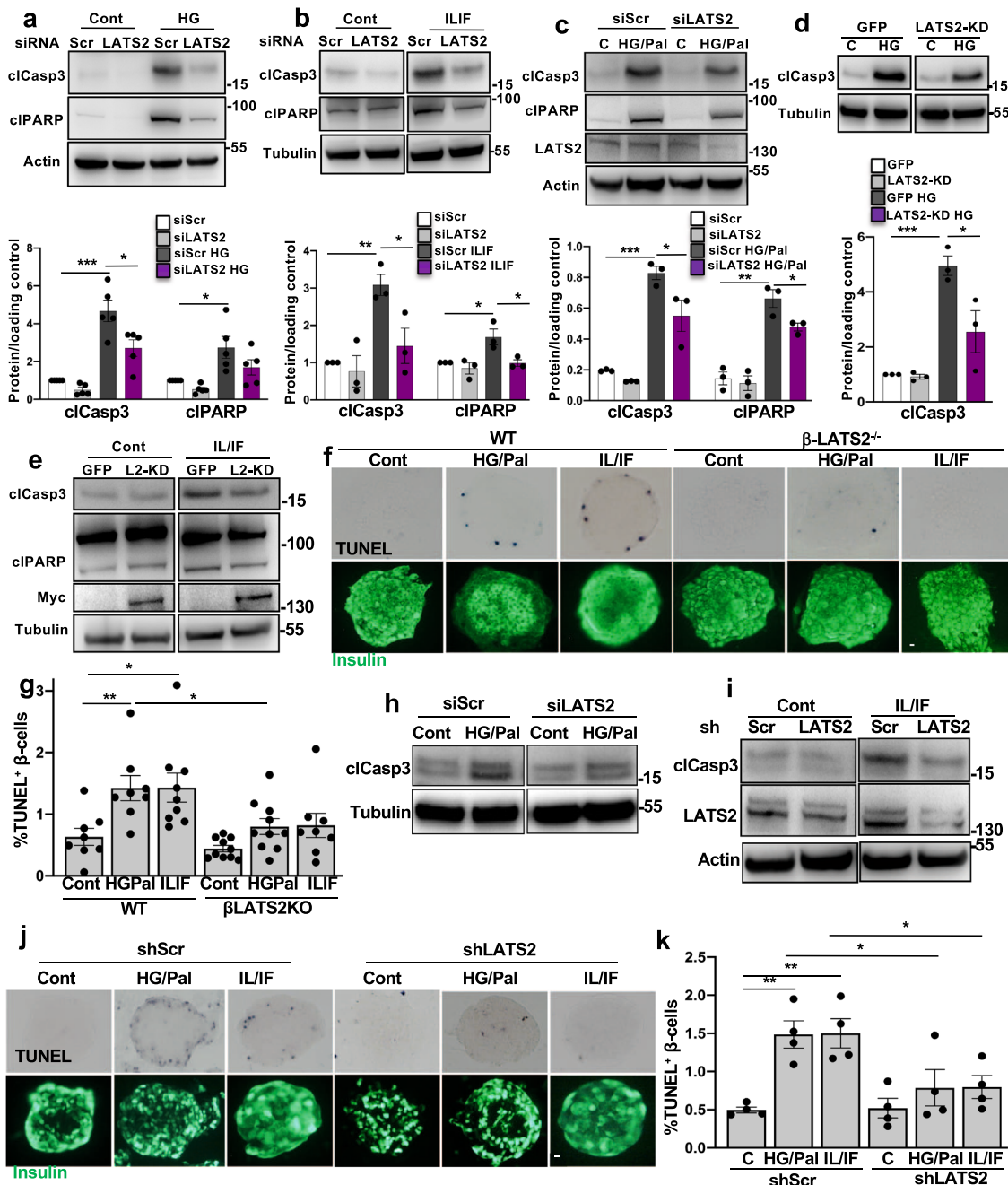


Fig. 3 Loss of the LATS2 improves β -cell survival in vitro. **a–c** Representative western blots and pooled quantitative densitometry analysis (lower panels) of INS-1E cells transfected with LATS2 siRNA or control siScr and treated with **a** 22.2 mM glucose, **b** 2 ng/mL IL1 β (IL) plus 1000 U/mL IFN γ (IF) and **c** 22.2 mM glucose plus 0.5 mM palmitate for 48 h ($n = 5, 3$ and 3 independent experiments, respectively for **a–c**). **d, e** Representative western blots and pooled quantitative densitometry analysis (lower panel) of INS-1E cells transfected with GFP or kinase-dead form of LATS2 (LATS2-KD) and then treated with **d** 22.2 mM glucose or **e** mixture of IL/IF for 48 h ($n = 3$ independent experiments). **f, g** Isolated islets from β -LATS2KO and Rip-Cre control mice were recovered after isolation overnight and exposed to diabetogenic conditions (IL-1 β /IFN γ or the mixture of 22.2 mM glucose and 0.5 mM palmitate (HG/Pal)) for 72 h. β -cell apoptosis was analyzed by double staining of TUNEL (black nuclei), and insulin (green). Representative images (**f**) and quantitative percentage of TUNEL positive β -cells (**g**) are shown ($n = 8, 8, 9, 10, 10, 8$ mice, respectively for WT cont, WT HG/Pal, WT IL/IF, β -LATS2-KO cont, β -LATS2-KO HG/Pal, and β -LATS2-KO IL/IF conditions). **h, i** Representative western blots of human islets transfected with siLATS2 or transduced with Ad-hShLATS2 and treated with **h** 22.2 mM glucose plus 0.5 mM palmitate or **i** mixture of IL/IF for 72 h ($n = 2$ different human islets isolations). **j, k** Human islets transduced with Ad-hShLATS2 or Ad-shScr control were exposed to diabetogenic conditions (IL-1 β /IFN γ or the mixture of 22.2 mM glucose and 0.5 mM palmitate (HG/Pal)) for 72 h. β -cell apoptosis was analyzed by double staining of TUNEL (black nuclei) and insulin (green). Representative images (**j**) and quantitative percentage of TUNEL positive β -cells (**k**) ($n = 4$ different human islets isolations) are shown. All lanes were run on the same gel but were noncontiguous (**b, d, e, h, i**). Data are expressed as means \pm SEM. Pooled quantitative densitometry of western blots were normalized to the respective control conditions and ratios (except **c**), in which a normal distribution of results cannot be proven, were analyzed. * $p < 0.05$, ** $p < 0.01$, *** $p < 0.001$; all by two-tailed Student's t -tests. scale bar depicts 10 μ m.

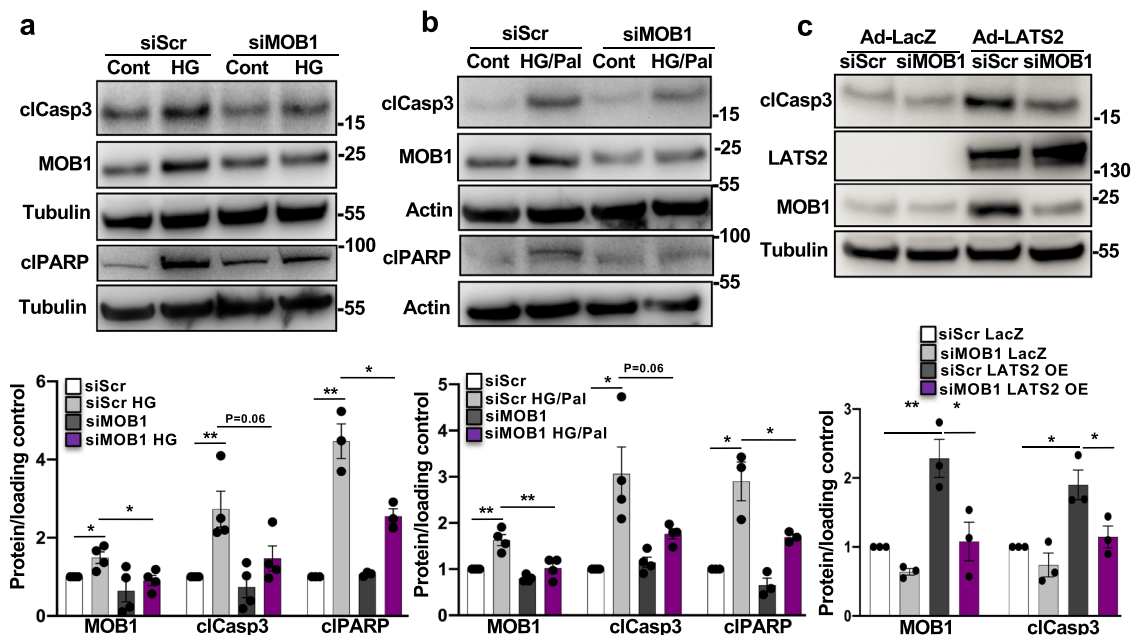


Fig. 4 MOB1 knockdown protects from β -cell apoptosis *in vitro*. **a, b** Representative western blots and pooled quantitative densitometry analysis (lower panels) of INS-1E cells transfected with siMOB1 or control siScr and treated with **a** 22.2 mM glucose or **b** 22.2 mM glucose plus 0.5 mM palmitate for 48 h ($n = 4$ independent experiments; $n = 3$ for cIPARP). **c** Representative western blot and pooled quantitative densitometry analysis (lower panel) of INS-1E cells transfected with siMOB1 or siScr and transduced with Ad-LacZ or Ad-LATS2 for 48 h ($n = 3$ independent experiments). Results were normalized to the respective control conditions and ratios, in which a normal distribution of results cannot be proven, were analyzed. Data are expressed as means \pm SEM. * $p < 0.05$, ** $p < 0.01$; all by two-tailed Student's *t*-tests.

random blood glucose levels were significantly reduced and glucose tolerance improved in β -LATS2^{-/-} mice (Fig. 5a, b). Also, glucose-induced insulin secretion was fully blunted in MLD-STZ-treated LATS2^{fl/fl} and Rip-Cre mice, but significantly restored in β -LATS2^{-/-} mice, together with an increased insulin-to-glucose ratio, compared to both LATS2^{fl/fl} and Rip-Cre controls (Fig. 5c–e). Histological examination of the pancreas and quantification of β -cell mass revealed an increased β -cell mass in STZ-injected β -LATS2^{-/-} mice, compared to control groups (Fig. 5f). To identify whether the restoration in β -cell mass was a result of increased β -cell numbers due to enhanced β -cell proliferation and/or decreased β -cell apoptosis, we next assessed β -cell proliferation and apoptosis in response to MLD-STZ treatment. A significant increase in double-labeled proliferation marker Ki67/insulin-positive β -cells was observed in MLD-STZ-treated β -LATS2^{-/-} relative to control from LATS2^{fl/fl} mice (Fig. 5g, h). Additionally, TUNEL-positive β -cells were markedly reduced in β -LATS2^{-/-} mice compared to the control group (Fig. 5i, j). This suggests a combined additive impact on augmented proliferation as well as reduced apoptosis as mechanism of β -cell mass restoration in β -LATS2^{-/-} mice. Altogether, our data show that β -cell-specific ablation of LATS2 diminished progressive hyperglycemia and improved glucose tolerance, insulin secretion, and β -cell mass in the MLD-STZ mouse model of β -cell destruction and diabetes.

β -cell specific LATS2 ablation protected from HFD induced diabetes *in vivo*. In a second model of diet induced diabetes, we checked whether LATS2 is critical for the long-term β -cell compensatory response by subjecting 8-week-old control Rip-Cre and β -LATS2^{-/-} mice to normal or diabetogenic high-fat/high sucrose diets (ND or HFD) for 17 weeks, which led to chronic hyperglycemia, insulin resistance as well as β -cell failure in wild-type mice^{14, 39}. HFD treatment revealed impaired glucose tolerance in Rip-Cre control mice compared to the ND-treated group.

Conversely, HFD fed β -LATS2^{-/-} mice exhibited marked improvement in glucose tolerance relative to the HFD Rip-Cre control (Fig. 6a). To further examine β -cell function, an *in vivo* GSIS was performed. A significant increase in basal (0 min) and glucose-stimulated insulin levels (15 and 30 min) was found in HFD fed β -LATS2^{-/-} mice compared to Rip-Cre counterparts (Fig. 6b) indicating higher insulin secretion in LATS2 deleted β -cells. Consistent with the improved metabolic phenotype in the HFD model, a marked compensatory β -cell mass expansion in response to high-fat/high sucrose feeding was observed in the β -LATS2^{-/-} mice. In contrast, Rip-Cre control mice failed to compensatively increase β -cell mass in response to HFD feeding (Fig. 6c). We next analyzed β -cell proliferation and death in response to HFD. As expected, an increase in Ki-67 positive proliferating β -cells in the β -LATS2^{-/-} mice vs. their Rip-Cre controls was observed when HFD-treated animals were compared (Fig. 6d, e). While β -cell apoptosis remained unchanged in β -LATS2^{-/-} mice under the ND, HFD-treated β -LATS2^{-/-} mice showed a highly attenuated response; the number of TUNEL-positive β -cells was $\sim 70\%$ reduced, compared to HFD-treated Rip-Cre control mice (Fig. 6f, g). This is consistent with the anti-apoptotic effect of LATS2 depletion observed *in vitro* and in the STZ *in vivo* model. The glucose-lowering effect of LATS2 deletion seems to be fully attributable to the β -cell, as β -LATS2^{-/-} HFD mice exhibited comparable insulin sensitivity to that of age-matched HFD-treated Rip-Cre control mice, irrespective of the diet (Supplementary Fig. 3e).

Taken together, these data suggest that the HFD induced LATS2 hyper-activation has a detrimental impact on β -cell viability, β -cell compensatory response and insulin secretion in the diet induced HFD model of β -cell decompensation and diabetes.

LATS2 induced β -cell apoptosis by activating the mTORC1 pathway. Previous studies revealed β -cell-mTORC1 hyper-

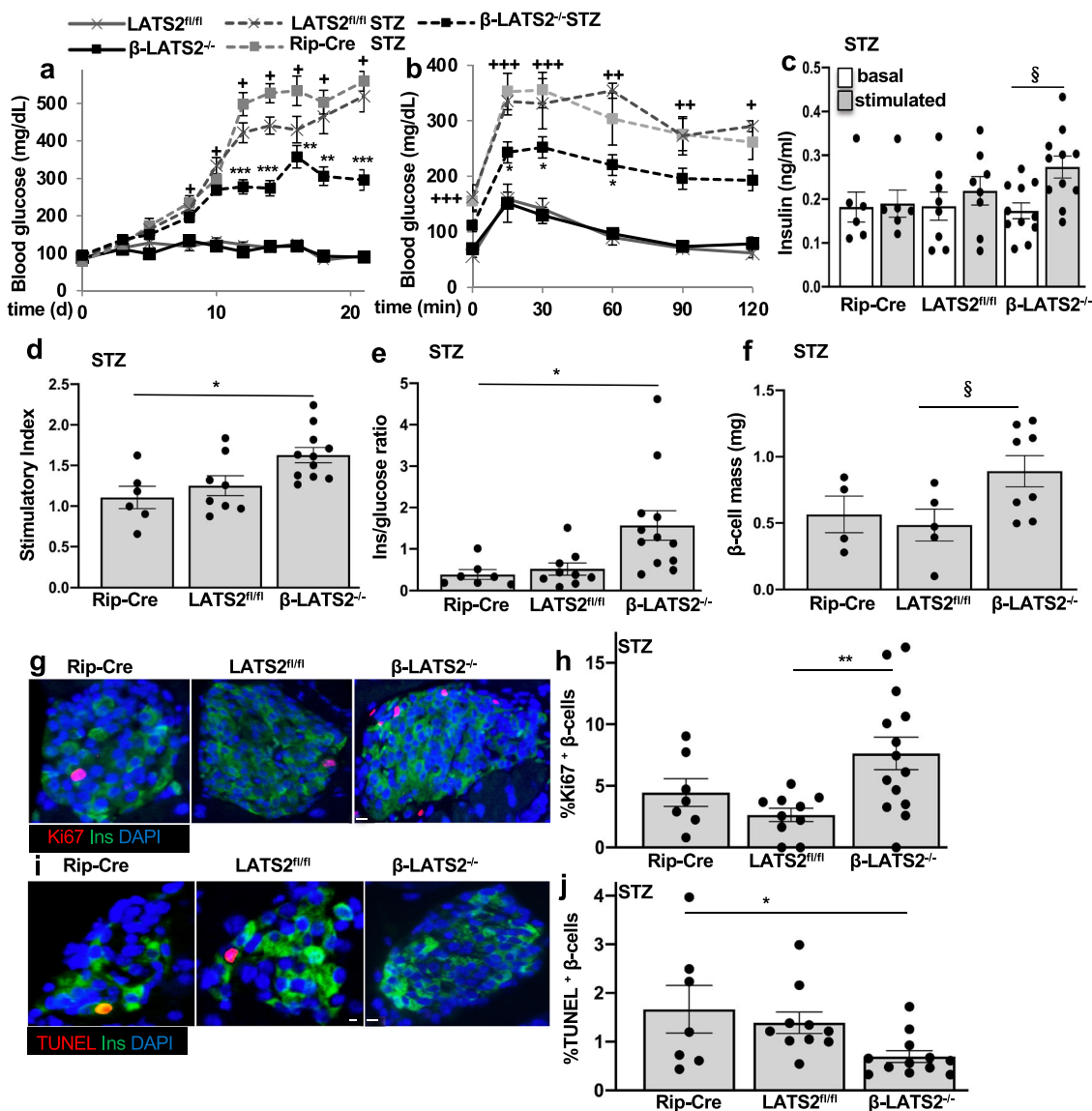


Fig. 5 β-cell specific LATS2 ablation protects from STZ induced diabetes in vivo. **a–j** β -LATS2^{-/-} mice ($n = 14$), RIP-Cre ($n = 7$) and LATS2^{fl/fl} controls ($n = 10$) injected with streptozotocin (STZ) (40 mg per kg body weight for 5 consecutive days) or saline (β -LATS2^{-/-} $n = 4$; LATS2^{fl/fl} $n = 5$) for 5 consecutive days. **a** Random fed blood glucose measurements after first saline or STZ injection (day 0) over 21 days and **b** i.p. glucose tolerance test (GTT) at day 19 in β -LATS2^{-/-}, RIP-Cre and LATS2^{fl/fl} mice. **c** Insulin secretion during an i.p. GTT measured before (0 min) and 15 min after glucose injection and expressed **d** as ratio of secreted insulin at 15 min to that secreted at 0 min (stimulatory index) (RIP-Cre STZ $n = 6$; LATS2^{fl/fl} STZ $n = 8$; β -LATS2^{-/-} STZ $n = 11$). **e** Ratio of secreted insulin and glucose calculated at fed state (RIP-Cre STZ $n = 7$; LATS2^{fl/fl} STZ $n = 9$; β -LATS2^{-/-} STZ $n = 12$). **f–j** Mice were sacrificed at day 22. **f** β -cell mass (given as percentage of the whole pancreatic section from 10 sections spanning the width of the pancreas) (RIP-Cre STZ $n = 4$; LATS2^{fl/fl} STZ $n = 5$; β -LATS2^{-/-} STZ $n = 8$). Representative images and quantitative analyses from triple staining for Ki67 (**g, h**) or TUNEL (**i, j**), insulin and DAPI expressed as percentage of TUNEL- or Ki67-positive β -cells \pm SEM (Ki67: RIP-Cre STZ $n = 7$; LATS2^{fl/fl} STZ $n = 10$; β -LATS2^{-/-} STZ $n = 14$; TUNEL: RIP-Cre STZ $n = 7$; LATS2^{fl/fl} STZ $n = 10$; β -LATS2^{-/-} STZ $n = 12$). Data are expressed as means \pm SEM. $^+p < 0.001$ LATS2^{fl/fl}-STZ or RIP-Cre-STZ to LATS2^{fl/fl} control mice. $^{++}p < 0.01$ LATS2^{fl/fl}-STZ or RIP-Cre-STZ to LATS2^{fl/fl} control mice. $^{+++}p < 0.05$ LATS2^{fl/fl}-STZ or RIP-Cre-STZ to LATS2^{fl/fl} control mice. $^*p < 0.05$ β -LATS2^{-/-}-STZ to LATS2^{fl/fl}-STZ or RIP-Cre-STZ. $^{**}p < 0.01$ β -LATS2^{-/-}-STZ to LATS2^{fl/fl}-STZ or RIP-Cre-STZ. $^{***}p < 0.001$ β -LATS2^{-/-}-STZ to LATS2^{fl/fl}-STZ or RIP-Cre-STZ. $^{\S}p < 0.05$. One-way ANOVA with Tukey's post hoc test for (**a, b, d, e, h, j**); by two-tailed Student's *t*-tests for (**c, f**). scale bar depicts 10 μ m.

activation under chronic diabetogenic conditions; in islets isolated from T2D patients and from animal models of T2D as well as in β -cells cultured under diabetes-associated glucotoxic conditions^{40–43}. It is still not well-understood which signals regulate such mTORC1 hyperactivation and downstream β -cell apoptosis. Both, Hippo and mTORC1 are major growth/viability regulating pathways in our cells and it is not surprising that they mutually control each other^{44–47}. mTORC1 activity was profoundly elevated by LATS2 overexpression in INS-1E β -cells

(Fig. 7a) and isolated human islets (Fig. 7b). Hyper-activation of mTORC1 was demonstrated by increased phosphorylation of its downstream target S6K1 at Thr 389 (pS6K), and the direct S6K substrate ribosomal protein S6 at Ser 235/236 (pS6) (Fig. 7a, b). Also, inhibition of mTORC1 by genetic and pharmacological tools restores insulin secretion in human T2D islets as well as in islets of diabetic mice^{41, 48} and corrects metabolic derangement in metabolically stressed β -cells⁴⁹. Therefore, we further analyzed the LATS2-mTORC1 crosstalk and whether mTORC1 mediates

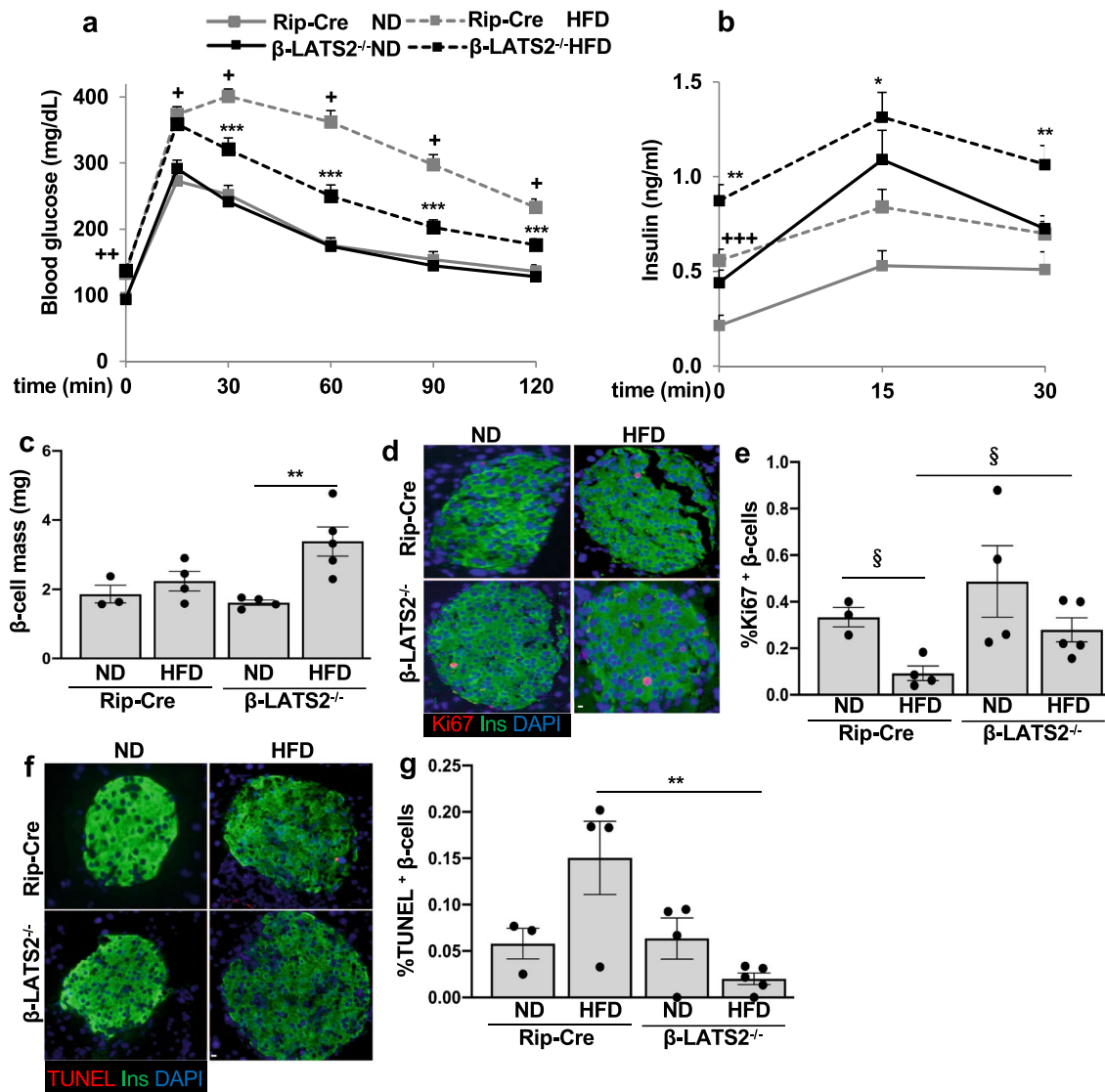


Fig. 6 β -cell specific LATS2 ablation protects from HFD induced diabetes in vivo. **a–g** β -LATS2^{-/-} and Rip-Cre control mice were fed a normal (ND) or high fat/ high sucrose diet (“Survit”; HFD) for 17 weeks. **a** intraperitoneal glucose tolerance test (ipGTT) (Rip-Cre ND $n = 8$; Rip-Cre HFD $n = 21$; β -LATS2^{-/-} ND $n = 10$; β -LATS2^{-/-} HFD $n = 19$). **b** Insulin secretion during an ipGTT measured before (0 min), 15 and 30 min after glucose injection (Rip-Cre ND $n = 7$; Rip-Cre HFD $n = 18$; β -LATS2^{-/-} ND $n = 10$; β -LATS2^{-/-} HFD $n = 15$). **c–g** Mice were sacrificed at week 17. **c** β -cell mass given as percentage of the whole pancreatic section from 10 sections spanning the width of the pancreas (Rip-Cre ND $n = 3$; Rip-Cre HFD $n = 4$; β -LATS2^{-/-} ND $n = 4$; β -LATS2^{-/-} HFD $n = 5$). Representative images and quantitative analyses from triple staining for Ki67 (**d, e**) or TUNEL (**f, g**), insulin and DAPI expressed as percentage of TUNEL- or Ki67-positive β -cells (Rip-Cre ND $n = 3$; Rip-Cre HFD $n = 4$; β -LATS2^{-/-} ND $n = 4$; β -LATS2^{-/-} HFD $n = 5$). Data are expressed as means \pm SEM. + $p < 0.001$ RIP-Cre-HFD to RIP-Cre ND mice. ++ $p < 0.01$ RIP-Cre-HFD to RIP-Cre ND mice. +++ $p < 0.05$ RIP-Cre-HFD to RIP-Cre ND mice. * $p < 0.05$ β -LATS2^{-/-}-HFD compared to RIP-Cre-HFD mice. ** $p < 0.01$ β -LATS2^{-/-}-HFD compared to RIP-Cre-HFD mice. *** $p < 0.001$ β -LATS2^{-/-}-HFD compared to RIP-Cre-HFD mice. § $p < 0.05$. All by one-way ANOVA with Tukey’s post hoc test except “e” by two-tailed Student’s *t*-tests. Scale bar depicts 10 μ m.

the pro-apoptotic function of LATS2 in the context of diabetes. In order to define whether LATS2 regulate mTORC1 activity under diabetic conditions, LATS2 was first silenced and then, islets/ β -cells were exposed to elevated glucose or its combination with palmitate. LATS2 knockdown resulted in decreased levels of pS6K1, pS6, and p4EBP1 (mTORC1 readouts) which were up-regulated upon exposure to a diabetic milieu in INS-1E β -cells and human islets providing a direct evidence for mTORC1 regulation by LATS2 (Fig. 7c, d). To establish whether inhibition of mTORC1-S6K1 signaling is sufficient to block pro-apoptotic function of LATS2 in β -cells, we blocked mTORC1 by the use of selective inhibitors against mTORC1 (rapamycin) and S6K1 (PF-4708671; S6K1i)⁵⁰ (Fig. 7e, f). Rapamycin and S6K1i fully blocked

LATS2-induced mTORC1 (represented by pS6) in INS-1E β -cells and human islets; together with counteracting apoptosis, as observed by reduced caspase-3 or PARP cleavage (Fig. 7e, f). In line with this observation, selective inhibition of endogenous mTORC1 by siRNA-mediated silencing of Raptor, mTORC1’s critical subunit, efficiently reduced mTORC1 signaling and substantially protected INS-1E β -cells from LATS2-induced apoptosis (Fig. 7g), further corroborating hyper-activated mTORC1 as downstream player of LATS2 in the context of β -cell apoptosis.

The growth factor (e.g., insulin or IGF), as well as nutrient (amino acid) branches, are two major distinct inputs that regulate mTORC1 activity/localization through small GTPases of the Ras superfamily: Rheb and Rag GTPases. While growth factors

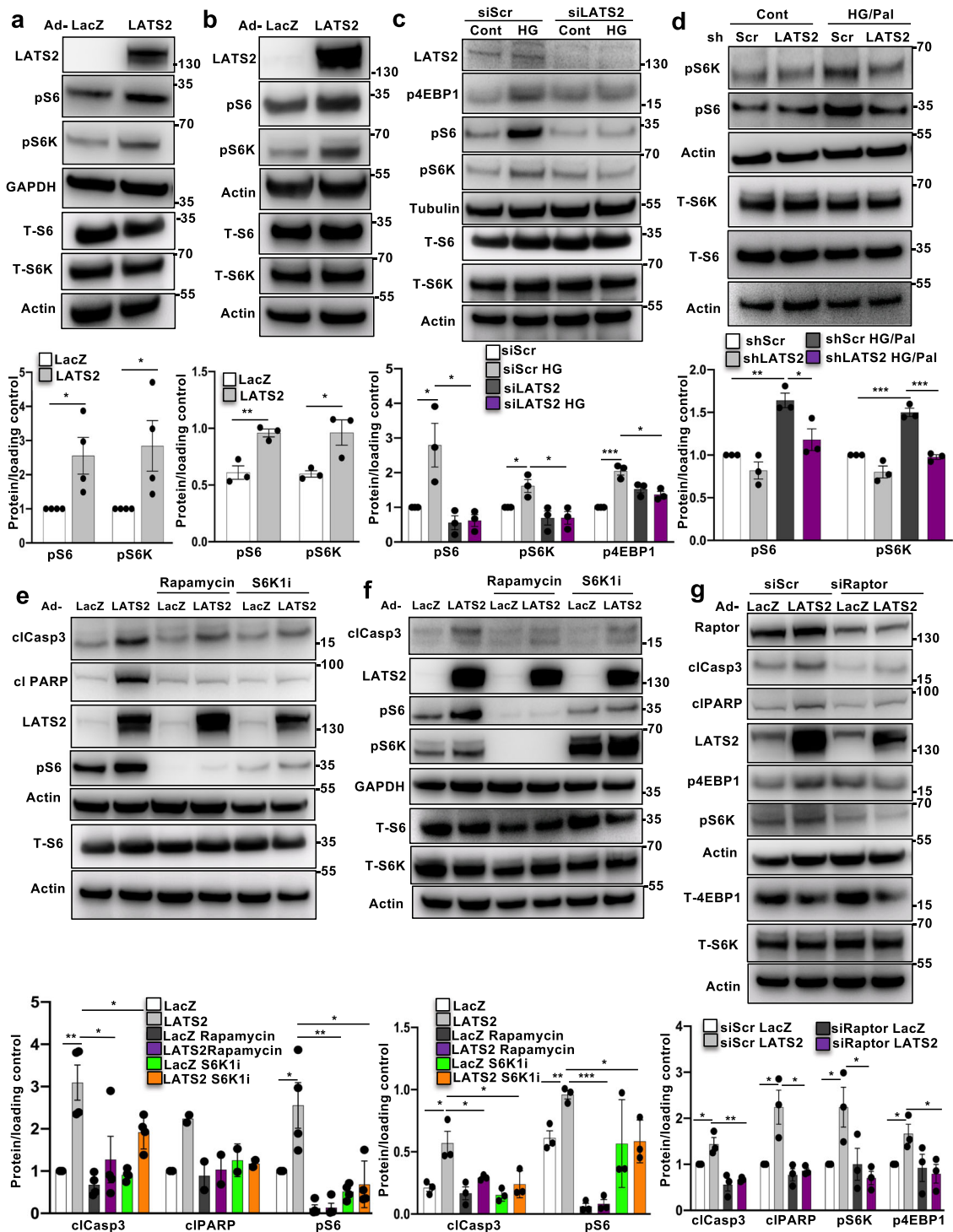


Fig. 7 LATS2 induces β -cell apoptosis by activating mTORC1 pathway. **a, b** Representative western blots and pooled quantitative densitometry analysis (lower panels) of INS-1E cells (**a**) and human islets (**b**) transduced with LacZ control or LATS2 adenoviruses for 48 h ($n = 4$ and 3 independent experiments respectively for **a, b**). **c** Representative western blot and pooled quantitative densitometry analysis (lower panel) of INS-1E cells transfected with LATS2 siRNA or control siScr and treated with the 22.2 mM glucose ($n = 3$ independent experiments). **d** Representative western blot and pooled quantitative densitometry analysis (lower panel) of human islets transduced with Ad-hShLATS2 and treated with 22.2 mM glucose plus 0.5 mM palmitate for 72 h ($n = 3$ different human islets isolations). **e, f** Representative western blots and pooled quantitative densitometry analysis (lower panels) of INS-1E cells (**e**) and human islets (**f**) transduced with LacZ control or LATS2 adenoviruses for 24 h and then exposed to 100 nM Rapamycin or 10 μ M S6K1 inhibitor (S6K1i) for additional 24 h ($n = 4$ and 3 independent experiments respectively for (**e, f**); $n = 2$ for cIPARP). **g** Representative western blot and pooled quantitative densitometry analysis (lower panel) of INS-1E cells transfected with siRaptor or siScr and then transduced with Ad-LacZ or Ad-LATS2 for 48 h ($n = 3$ independent experiments). Data are expressed as means \pm SEM. Pooled quantitative densitometry of western blots were normalized to the respective control conditions and ratios (except b, f), in which a normal distribution of results cannot be proven, were analyzed. * $p < 0.05$, ** $p < 0.01$, *** $p < 0.001$; all by two-tailed Student's *t*-tests.

control mTORC1 through the PI3K-AKT-TSC-Rheb signaling axis, nutrients such as amino acids act through the Rag family of GTPases⁵¹. Insulin-dependent AKT activation via PI3K signaling stimulates the GTPase Rheb by blocking the tuberous sclerosis protein complex (TSC), composed of TSC1, TSC2, and TBC1D7 subunits, which function as inhibitor of Rheb. AKT phosphorylates TSC1/2 displacing the TSC complex from the lysosomes, where Rheb is located and functions to activate mTORC1^{51, 52}. Instead, amino acid-dependent activation of mTORC1 involves the lysosomal Rag GTPases and recruitment of mTORC1 to the lysosomal membrane to stimulate mTORC1⁵¹. Of note, glucose-dependent mTORC1 activation also appears to be partially regulated by Rag GTPases, making Rag a “multi-input nutrient sensor”, which signals nutrients to the downstream mTORC1 activation^{40, 53}. To examine the effect of LATS2 on key components of the growth factor dependent branch, we overexpressed LATS2 in INS-1E β -cells, which activated mTORC1. LATS2 hyperactivation did not change the level of AKT-Ser473 phosphorylation (important event downstream of PI3K-IRS activation triggered by growth factors) as well as TSC2-Thr1462 phosphorylation (AKT specific site; Supplementary Fig. 4a) suggesting that the AKT-TSC1/2 axis is dispensable for LATS2-induced mTORC1 activation. In contrast, loss- and gain-of-functional experiments using exogenously introduced RagA mutants⁵⁴ showed that LATS2-induced mTORC1 activation is controlled by the amino acid branch. In particular, overexpression of dominant negative GDP bound RagA (HA-RagA-GDP; RagA-T21L) diminished LATS2-induced mTORC1 activation (Supplementary Fig. 4b; HA-metap2 was used as negative control⁵⁵). Conversely, constitutively active GTP bound RagA (HA-RagA-GTP; RagA-Q66L) restored mTORC1 activation in LATS2 depleted INS-1E β -cells treated with high glucose (Supplementary Fig. 4c).

Altogether, these data suggest that LATS2-induced β -cell apoptosis is mediated by Rag-mTORC1 activation.

It has recently been shown that LATS1 phosphorylates Raptor at Ser606, leading to mTORC1 inhibition in HEK293 kidney cells⁴⁷. We took advantage of the phospho-null (S606A) Raptor mutant⁴⁷ to investigate the potential regulation of Ser606-phosphorylation in pancreatic β -cells. As presented in Supplementary Fig. 5a, overexpression of WT-Raptor as well as S606A mutant in INS-1E β -cells similarly activated mTORC1 signaling represented by higher pS6, pS6K, and p4EBP1, compared to control transfected cells. Also, neither WT-Raptor nor S606A mutant altered high glucose induced S6-phosphorylation or apoptosis in INS-1E cells, compared to the high glucose treated control (Supplementary Fig. 5b). All this suggests that Raptor-Ser606 phosphorylation is dispensable for basal mTORC1 activation as well as mTORC1's deleterious role under glucotoxic conditions in β -cells.

Bidirectional regulation of LATS2 and autophagy in β -cells.

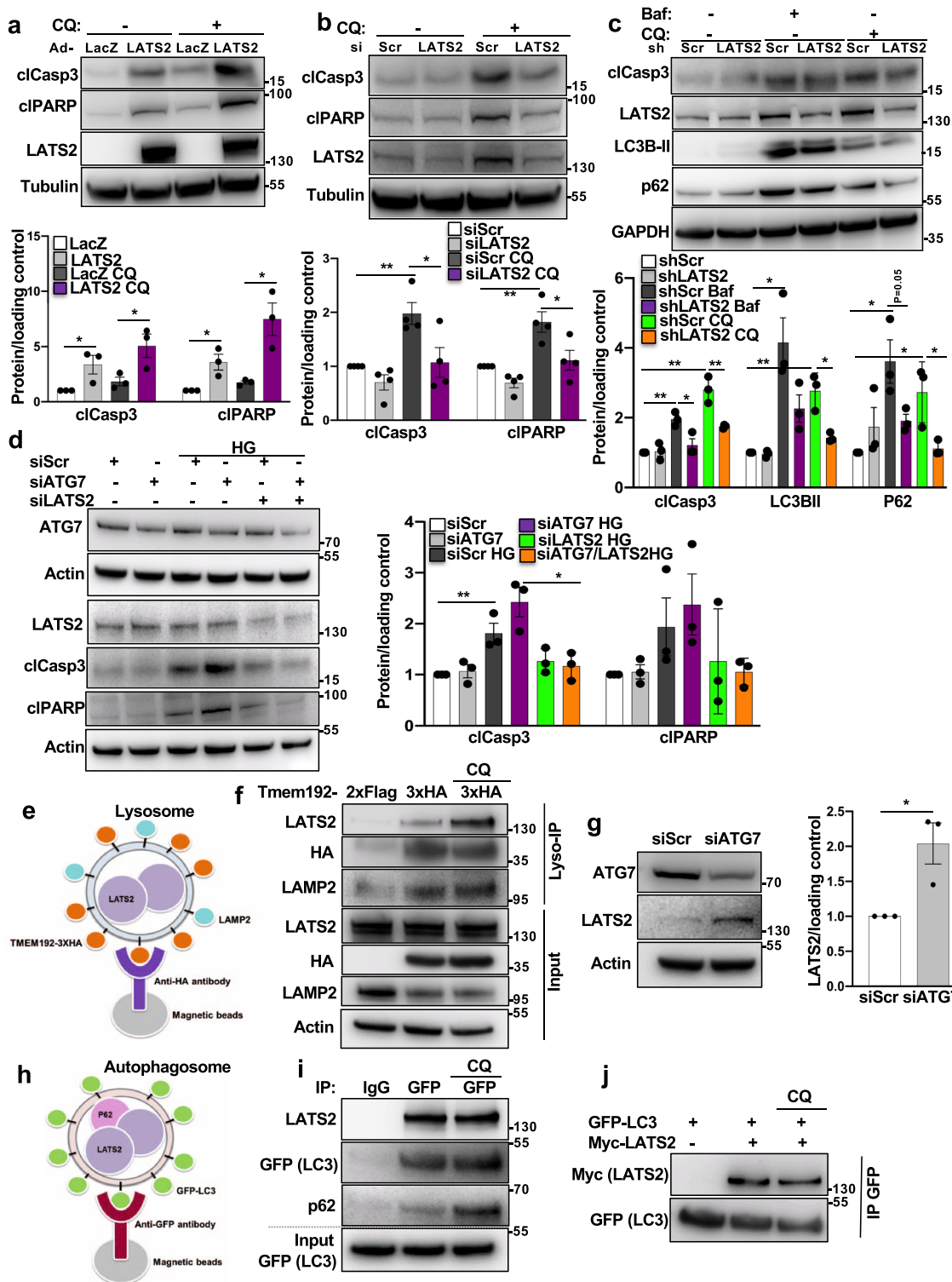
The nutrient-sensing pathway mTORC1 is the most characterized negative regulator of autophagy and its sustained activation compromises autophagic flux and induces apoptosis in pancreatic β -cells^{40, 56}. As LATS2 activates mTORC1 and the latter inhibits a protective-autophagy response in β -cells, we determined the direct impact of blocked autophagy on reduced β -cell viability in the context of LATS2 signaling. We first tested whether gain-/loss-of- LATS2 function could modulate the enhanced cell death under diminished autophagy. INS-1E β -cells and isolated human islets were treated with two different well-established late-stage autophagy inhibitors: BafilomycinA1 (Baf) and Chloroquine (CQ). As expected, suppression of autophagic flux by Baf as well as CQ triggered apoptosis, which was further exacerbated by

LATS2 overexpression in INS-1E β -cells (Fig. 8a and Supplementary Fig. 6a). Consistently, also LATS2-overexpressing human islets exhibited increased caspase-3 cleavage (Supplementary Fig. 6b). Conversely, Baf- or CQ-induced β -cell apoptosis was greatly decreased by LATS2 silencing in INS-1E β -cells as well as in human islets (Fig. 8b, c and Supplementary Fig. 6c). Together with exacerbated apoptosis, LATS2 impaired the autophagic flux. Both, the autophagic flux markers microtubule-associated protein 1A/1B-light chain 3 (LC3-II), a key component of the autophagosome membrane, and p62 (also known as SQSTM1), an adapter protein that recruits the cargo proteins into the autophagosome, showed a strong accumulation upon LATS2 overexpression indicating that the forced expression of LATS2 further impaired autophagic flux in human islets (Supplementary Fig. 6b). In contrast, loss of LATS2 attenuated LC3-BII and p62 accumulation induced by autophagy blockers in human islets (Fig. 8c) suggesting a restrictive function of LATS2 in autophagic flux. In line with chemical inhibition of autophagy, knockdown of autophagy-related gene 7 (ATG7), a key component of macroautophagy, exacerbated high glucose-induced apoptosis as represented by increased cleavage of caspase 3 and PARP which is reversed by LATS2 silencing further confirming that LATS2 mediates defective autophagy-induced β -cell apoptosis (Fig. 8d). These results show LATS2 as mediator of defective autophagy-induced apoptosis and autophagic flux in β -cells.

To further assess the effect of LATS2 deficiency on mTORC1 and autophagy, immunohistochemical analyses for pS6 and p62 were performed on pancreatic sections isolated from the HFD-fed mice. HFD-treated control mice (Rip-Cre) showed a markedly higher pS6 in pancreatic islet β -cells compared to the ND mice. This is consistent with the previously reported mTORC1 hyperactivation in HFD diabetic islets by us⁴¹ and others⁵⁷. In contrast, pS6-expression was normalized in HFD-treated β -LATS2^{-/-} mice (Supplementary Fig. 7a).

In line with our *in vitro* results in β -cells and human islets, where LATS2 depletion correlated with reduced p62 levels, protein expression of p62 was clearly seen in β -cells in diabetic HFD-fed mice, but not in β -LATS2^{-/-} mice (Supplementary Fig. 7b). These findings show that LATS2 deletion inhibits HFD induced mTORC1 activation as well as p62 accumulation and further support the interplay between LATS2 and the mTORC1-autophagy axis.

We also noticed that endogenous LATS2 protein was increased by autophagy inhibition, suggesting LATS2 as potential substrate for autophagy-mediated degradation (Fig. 8b, c and Supplementary Figs. 6c and 8a). The culminating step for both major autophagy pathways macroautophagy and chaperone-mediated autophagy (CMA) is the degradation of substrate proteins in the lysosomes. Therefore, the presence of a non-lysosomal protein in isolated lysosomes corroborates that the protein is an autophagy substrate. To provide direct evidence for LATS2 not only regulating autophagy, but also *vs.* for autophagy as regulator of LATS2 protein levels in β -cells, we demonstrated the lysosomal localization of LATS2. Because of the relatively low sensitivity of available specific LATS2 antibodies, immunoprecipitation of endogenous LATS2 was not feasible and therefore, lysosomes of LATS2-overexpressing INS-1E β -cells were isolated by immunoprecipitation, the “Lyso-IP method”⁵⁸. Lysosomes were labeled with the HA-expressing lysosomal membrane protein TMEM192 (TMEM192-3xHA) and anti-HA magnetic beads used for immunoprecipitation of intact lysosomes (Fig. 8e). As a negative control for precipitation, Flag-expressing TMEM192 (TMEM192-2xFLAG) was used. HA-TMEM192-isolated lysosomes represented a highly pure fraction as determined by the absence of markers for other cellular compartments such as mitochondria, ER, Golgi, and endosomes (Supplementary Fig. 8b); 3xHA tagged



organelles were successfully isolated seen by the enrichment of HA (TMEM192-3xHA), as compared to the FLAG tagged control (Fig. 8f and Supplementary Fig. 8b). The pull-down efficiency was equal for samples treated with or without CQ as similar levels of HA/TMEM192 as well as LAMP2, the other lysosomal membrane marker, were enriched in both test samples, compared to the Flag precipitated negative control (Fig. 8f). Both the lysosome enriched samples displayed an accumulation of LATS2 protein. LATS2 was considerably higher in the presence of CQ which is unequivocally in line with our previous observation of increased LATS2 by

autophagy inhibition. These data suggest LATS2 as substrate for autophagy, as blocking lysosomal degradation by lysosomotropic agents like CQ resulted in the accumulation of LATS2 in the lysosomes. Also, immunofluorescence microscopy of cultured β -cells showed colocalization of LATS2 with LAMP1-containing compartments in CQ-treated cells indicating the lysosomal localization of LATS2 (Supplementary Fig. 8c).

In order to identify the specific type of autophagy pathway that may be involved in the lysosomal degradation of LATS2, we selectively targeted ATG7 and lysosome-associated membrane

Fig. 8 Bidirectional regulation of LATS2 and autophagy in β -cells. **a** Representative western blot and pooled quantitative densitometry analysis (lower panel) of INS-1E cells transduced with Ad-LacZ or Ad-LATS2 and treated with 50 μ M Chloroquine (CQ) for 4 h ($n = 3$ independent experiments). **b** Representative western blot and pooled quantitative densitometry analysis (lower panel) of INS-1E cells transfected with siLATS2 or siScr and treated with CQ for 4 h ($n = 4$ independent experiments). **c** Representative western blot and pooled quantitative densitometry analysis (lower panel) of human islets transduced with Ad-hShLATS2 or Ad-shScr and treated with Bafilomycin (Baf) or CQ for 4 h ($n = 3$ different human islets isolations). **d** Representative western blot and pooled quantitative densitometry analysis (right panel) of INS-1E cells transfected with ATG7 siRNA and/or LATS2 siRNA or control siScr and treated with the 22.2 mM glucose for 24 h ($n = 3$ independent experiments). **e** Schematic representation of LysolIP method for immunoprecipitation of intact lysosomes. **f** INS-1E cells were co-transfected with LATS2-Myc and Tmem192-3xHA or Tmem192-2xFlag plasmids for 48 h. One set of cells were treated with 50 μ M CQ for last 4 h. Representative western blot of input and lysosomes isolated from INS-1E cells is shown ($n = 2$ independent experiments). **g** Representative western blot and pooled quantitative densitometry analysis (right panel) of INS-1E cells transfected with siScr or siAtg7 for 48 h ($n = 3$ independent experiments). **h** Schematic representation of method for immunoprecipitation of autophagosomes. **i** Stable GFP-LC3 expressing INS-1E cells were transfected with LATS2-Myc plasmid for 48 h. One set of cells were treated with 50 μ M CQ for last 4 h. Representative western blot of input and autophagosomes isolated from GFP-LC3 expressing INS-1E cells is shown ($n = 2$ independent experiments). **j** GFP-LC3 expressing INS-1E cells were transfected with or without LATS2-Myc plasmid for 48 h. One set of cells were treated with 50 μ M CQ for last 4 h. Representative western blot of immunoprecipitation using anti-GFP magnetic beads is shown ($n = 2$ independent experiments). Data are expressed as means \pm SEM. Pooled quantitative densitometry of western blots were normalized to the respective control conditions and ratios, in which a normal distribution of results cannot be proven, were analyzed. * $p < 0.05$, ** $p < 0.01$; all by two-tailed Student's t -tests.

protein type 2A (LAMP2A) proteins, which are the major essential components of canonical macroautophagy and CMA, respectively. siRNA mediated genetic downregulation of ATG7 (Fig. 8g) but not of LAMP2A (Supplementary Fig. 8d) induced substantial upregulation of endogenous LATS2 again confirming LATS2 upregulation by autophagy inhibition and supporting macroautophagy as major autophagic mechanism for LATS2 destruction in pancreatic β -cells. In order to corroborate that macroautophagy is involved in the autophagic regulation of LATS2 in β -cells, we isolated autophagosomes from stable GFP-LC3 expressing INS-1E β -cells, which have a GFP tagged to the N-terminus of the autophagosomal membrane protein LC3. The GFP tag on the cytosolic side of the membrane can then be exploited to isolate autophagosomes^{59, 60}. Autophagosomes were immunoprecipitated in LATS2-overexpressing INS-1E β -cells using anti-GFP coated magnetic beads (Fig. 8h) in the presence or absence of CQ. LATS2 was enriched in isolated autophagosomes as represented by successful pull-down of GFP (GFP-LC3), compared to IgG control, where LATS2 was absent, indicating the selective LATS2 accumulation in autophagosomes as a direct evidence for LATS2 regulation by macroautophagy (Fig. 8i). While no significant difference was observed in the autophagosomal accumulation of LATS2 by CQ treatment, the level of autophagosomal p62 was higher than without the inhibitor suggesting a cargo-associated accumulation. In addition, the colocalization of LATS2 and LC3 was confirmed by immunofluorescence microscopy in CQ-treated INS-1E cells (Supplementary Fig. 8e).

Another evidence for the macroautophagy-LATS2 interaction comes from direct protein co-immunoprecipitation experiments. Myc-LATS2 was overexpressed in stable GFP-LC3 expressing INS-1E β -cells and anti-GFP magnetic beads were used to immunoprecipitate GFP-LC3 and its potential interacting partners. Subsequent immunoblot analysis revealed that LATS2 co-immunoprecipitated with GFP-LC3 providing an experimental proof for the direct interaction of LC3 and LATS2 (Fig. 8j). We repeated this experiment with normal INS-1E cells, transiently transfected with GFP-LC3 and/or Myc-LATS2 constructs and included all appropriate negative controls (GFP-LC3 alone vs Myc-LATS2 alone). The specific LATS2-LC3 interaction was confirmed and none of the controls showed any unspecific signals (Supplementary Fig. 8f).

It has been shown in multiple cases that the interaction between target proteins (receptors) and LC3-family proteins is mediated by an LC3-interacting region (LIR) motif^{61–63}. Therefore, the presence of a LIR would be a potential molecular signature for LC3-interacting

proteins. We took advantage of the freely available iLIR database (<https://ilir.warwick.ac.uk>) developed by Jacomin et al.⁶⁴ and searched for putative canonical LIR motifs in the human LATS2 protein. Based on the in silico analysis of experimentally verified functional LIR motifs, Jacomin et al. redefined the previously described LIR motif- WxxL (where x can be any amino acid) to the 6 amino acids consensus sequence-referred to as the xLIR motif: (ADEFGLPRSK)(DEGMSTV)(WFY)(DEILQTV)(ADEFHIKLMPS TV)(ILV), where the residues marked in bold (positions 3 and 6) correspond to the important residues for the interaction with LC3-family proteins⁶⁴. Our in silico analysis identified one complex xLIR motif as well as more than ten LIR motifs- WxxL (Supplementary Fig. 9a, b) supporting our co-IP data which showed interaction between LATS2 and LC3. Further experimental investigation using LIR-inactive LATS2 mutants is required to verify this. Altogether, our data suggest the existence of a mutual regulatory axis between LATS2 and autophagy to fine-tune the β -cell apoptosis program.

Discussion

The pancreatic β -cell's vast metabolic plasticity as well as its stress response to cope with high metabolic demands and subsequent pro-diabetic signals is directed by the structure and spatio-temporal dynamics of complex signal transduction networks. Diabetes-associated perturbations in these orchestrated networks occur at various levels, resulting in the dysregulation of physiological functional β -cell mass adaptation. Our work provides direct evidence that Hippo pathway's central kinase LATS2 is activated under diabetogenic conditions, which induced β -cell failure through increased β -cell apoptosis and impaired β -cell function, while LATS2's inactivation resulted in resistance to β -cell apoptosis, improved glycemia, insulin secretion and β -cell mass in in vitro, ex vivo and in vivo experimental models of diabetes.

We identified LATS2 as a key upstream activator of mTORC1 in stressed β -cells in which mTORC1 inhibition blocked β -cell apoptosis, suggesting that the pro-apoptotic action of LATS2 is mTORC1-dependent. While LATS2 activated mTORC1 in β -cells, LATS2 kinases can also do the contrary in a different cellular context, namely suppress mTORC1 by phosphorylating Raptor at Serine 606 and subsequently impairing the Raptor downstream interaction with Rheb⁴⁷. There are several possible explanations for such distinct effect: (i) LATS1 and LATS2 kinases do not necessarily share redundant functions in all cell types. In the Gan et al. study, the majority of biochemical and functional experiments have been performed in the model HEK293 kidney cell line, and not in primary cells, or other cell types and thus, a

unifying nature for the proposed mechanism was not provided. This is supported by data from the homozygous phosphomimetic (S606D; *Raptor*^{D/D}) knock-in mice, in which the LATS mediated Raptor-S606 phosphorylation site is constitutively active. Diminished mTORC1 signaling shown in the liver, heart and kidneys but not in the spleen and brain indeed suggests a tissue or cell type dependent regulation of mTORC1 by LATS kinases. (ii) Another explanation may arise from a different cellular context in our and Gan's et al. studies. While contact inhibition - as a result of high cell density- is a driving force and critical factor for the LATS1/2 mediated mTORC1 suppression, LATS2 induced mTORC1 hyperactivation under diabetogenic conditions of stress and nutrient overload in β -cells is likely to be independent of cell density. (iii) Additionally, LATS mediated phosphorylation of Raptor reduces growth factor induced mTORC1 stimulation through Rheb⁴⁷, while we show here that LATS2-induced mTORC1 activation is regulated, at least in part, by the other amino acid branch of mTORC1 activation through its key component Rag-GTPase.

Downstream of mTORC1, autophagy is a key process for maintaining β -cell viability and functional homeostasis⁴⁰. Defective autophagy is a hallmark of β -cell failure in T2D^{65–68}. Our current study expands a previously unrecognized mechanistic link between LATS, mTORC1, and autophagy. Firstly, LATS2 controls the autophagic flux and autophagy-induced apoptosis through the regulation of mTORC1. Secondly, autophagy itself regulates LATS2's protein turnover by directly targeting LATS2. This suggests that LATS2, mTORC1 and autophagy may constitute a stress-sensitive survival pathway (Fig. 9). Under acute stress conditions, autophagy promotes β -cell survival by directly degrading LATS2 and consequently reinforcing protective-autophagy mechanism through a positive-feedback loop. However, prolonged stress activated LATS2 leading to mTORC1 hyper-activation, defective autophagy, ultimately further LATS2 accumulation and subsequent β -cell apoptosis. This antagonism between LATS2 and autophagy suggests that the outcome of the mutual regulation of both pathways under conditions of increased β -cell stress and demand in a diabetic microenvironment is probably determined by the extent and duration of activated LATS2. In this context, aberrant LATS2 activity triggered by diabetic stimuli may shift the balance towards chronic mTORC1 activation, resulting in defective autophagic flux and β -cell apoptosis. This highlights the existence of a functional bidirectional cross-communication between LATS2 and autophagy for the regulation of β -cell viability under physiological conditions and uncovers LATS2 to mediate a crosstalk between the Hippo pathway and autophagy.

The Hippo pathway and autophagy share a complex network with bidirectional connections tightly controlling the autophagic flux in response to extracellular cues, nutrients availability, and metabolic adaptations to direct cellular and systemic homeostasis⁶⁹. For instance, LATS1/2 upstream kinases MST1/2 were shown to differentially regulate autophagic outcomes. While MST1 directly phosphorylates LC3 to foster autophagosomes-lysosomes fusion and autophagic flux for intracellular cargo clearance (such as bacteria) in mouse-embryonic fibroblasts (MEFs)⁷⁰, it phosphorylates the autophagy regulator Beclin1, subsequently inhibiting the Beclin1-Vps34 complex, which leads to autophagy inhibition in cardiomyocytes⁷¹ suggesting contextual and perhaps cell-type dependent regulation of autophagy.

Downstream target of LATS1/2 kinases is the Hippo effector, the transcriptional co-activator YAP, which itself is also strongly linked to autophagy⁶⁹. Like LATS2 (but with opposite functional outcomes), YAP not only functions as upstream regulator of autophagy by regulating the degradation of autophagosomes as well as the maturation of autophagosomes^{72, 73}, but also acts as an

autophagic substrate in a way that the autophagic flux triggers protein turnover of YAP and its targets^{74, 75}. During embryonic development, YAP is highly expressed throughout the pancreas in a multipotent progenitor stage^{13, 16–18, 33}. However, after differentiation, YAP remains expressed in ductal and acinar cells¹⁸, but is excluded from β -cells and other endocrine islet cells at the time when the key endocrine progenitor transcription factor and marker Ngn3 emerges¹⁹ coinciding with their very low proliferative capacity. Re-expression of the “disallowed” YAP in human islets specifically fosters β -cell proliferation^{19, 76}. Single cell RNA-seq data (for example, ref. ⁷⁷), as well as gene and protein functional expression analyses^{17–19, 76}, confirm that YAP is not expressed in terminally differentiated mature primary human and mouse islets and β -cell lines. While YAP signals are excluded as Hippo targets in mature islets and β -cells, functional MST1/2 and LATS1/2 kinases operate Hippo signaling in the absence of YAP directing alternative Hippo downstream effector (s). Thus, in our experimental setting, LATS2 maneuvers its downstream events, i.e., apoptosis, impaired insulin secretion by a crosstalk with autophagy signals through non-canonical YAP independent mechanisms in β -cells. Such YAP-independent actions of LATS have also been reported in other cellular contexts; e.g., the mitotic spindle orientation in mammals⁴⁷ in which YAP knockdown has insignificant effects on mTORC1 activity, indicating that the Hippo/LATS pathway primarily regulates mTORC1 independent of YAP. While we could show by multiple experimental settings that LATS-induced effects on β -cell apoptosis and autophagy is mediated by mTORC1 activation, it is equally possible that LATS2 activation and mTORC1 hyperactivation act in parallel under stress- and diabetogenic conditions to dysregulate the β -cell compensatory machinery and induce β -cell death, dysfunction and thus metabolic failure and diabetes.

The role of the Hippo pathway in human disease, especially in cancer has been substantiated by a robust line of research over the past 10 years^{9, 10, 79}. Using a multi-model approach, we have identified LATS2 as pro-apoptotic kinase whose abnormal activation led to impaired β -cell survival and function, while its depletion restored functional β -cell mass and protected against diabetes progression. Blocking LATS2 could be a promising strategy to improve β -cell survival in diabetes.

Methods

Cell culture, treatment, and islet isolation. Human islets were isolated from pancreases of non-diabetic organ donors at the Universities of Illinois at Chicago, Wisconsin, Lille or ProdoLabs and cultured on extra cellular matrix (ECM)-coated dishes (Novamed, Jerusalem, Israel)⁸⁰ or on Biocoat Collagen I coated dishes (#356400, Corning, ME, USA). Human islets were cultured in complete CMRL-1066 (Invitrogen) medium at 5.5 mM glucose and mouse islets, the clonal rat β -cell line INS-1E, and the human insulinoma CM cell line in complete RPMI-1640 medium at 11.1 mM glucose^{14, 81}. Islets from β -cell specific LATS2 knockout (β -LATS2^{-/-}) and control mice were isolated by pancreas perfusion with a Liberase TM (#05401119001, Roche, Mannheim, Germany) solution⁸⁰ according to the manufacturer's instructions and digested at 37 °C, followed by washing and handpicking. Human and mouse islets and INS-1E cells were exposed to complex diabetogenic conditions: 22.2 mM glucose, 0.5 mM palmitic acid⁸², the mixture of 2 ng/mL recombinant human IL-1 β (R&D Systems, Minneapolis, MN) plus 1,000 U/ml recombinant human IFN- γ (PeProTech) for 24–72 h. In some experiments, cells and islets were additionally cultured with 100 nM Rapamycin or 10 μ M S6K1 selective inhibitor PF-4708671 (Calbiochem) for 24 h, 50 μ M chloroquine (Sigma), 20 nM Bafilomycin (Sigma) or a cocktail of Leupeptin (Sigma) and NH₄Cl for 12 h.

Human islets were distributed by the two JDRF and NIH supported approved coordination programs in Europe (Islet for Basic Research program; European Consortium for Islet Transplantation ECIT) in agreement with the French Regulations and the Institutional Ethical Committee (“Comité d’Ethique du Centre Hospitalier Régional et Universitaire de Lille”) and in the US (Integrated Islet Distribution Program IIDP)⁸³, which is, in collaboration with the islet isolation centers, responsible for obtaining consent from donors. The IIDP requires

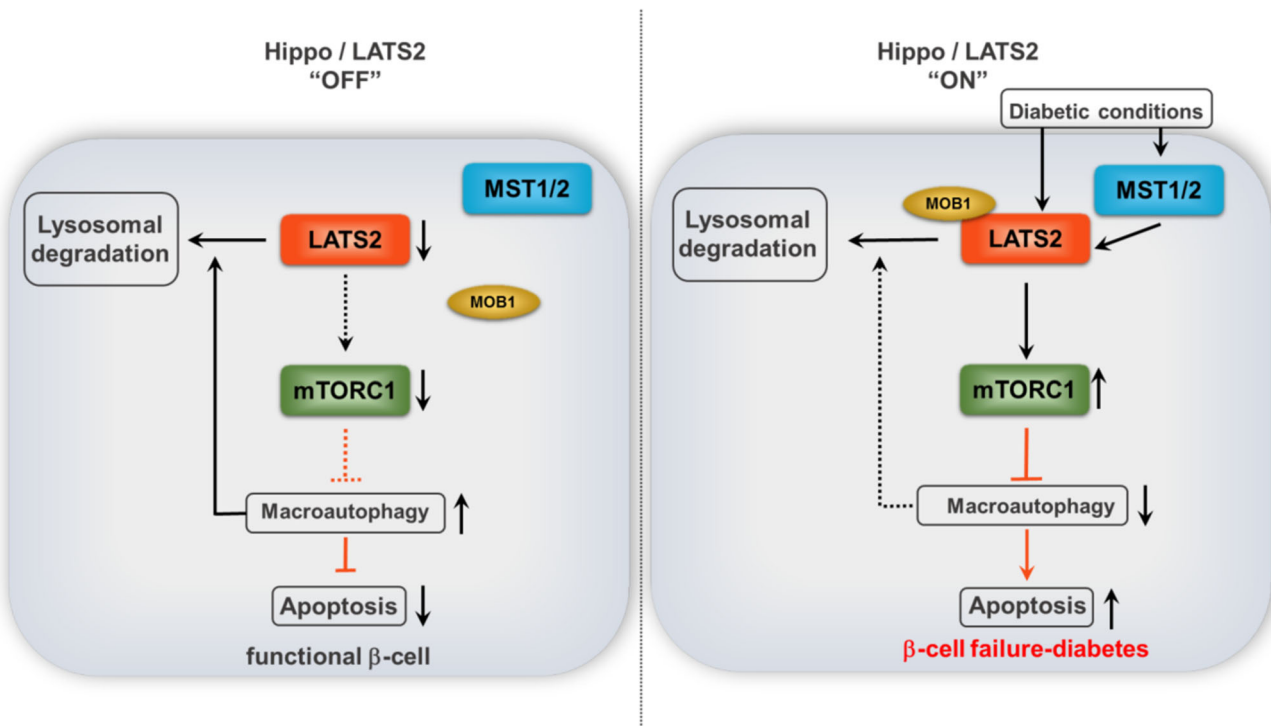


Fig. 9 Proposed model of LATS2 action in β -cells. LATS2, mTORC1, and autophagy may constitute a stress-sensitive survival pathway. Under physiological (Hippo “OFF”) or acute stress conditions, autophagy promotes β -cell survival by directly degrading LATS2 and consequently reinforcing protective-autophagy mechanism through a positive-feedback loop. However, prolonged diabetogenic stress activated LATS2 (Hippo “ON”) leading to mTORC1 hyper-activation, defective autophagy, ultimately further LATS2 accumulation and subsequent β -cell apoptosis. LATS2 (Large tumor suppressor 2; in orange), MST1/2 (Mammalian Sterile 20-like kinases 1/2; in blue), MOB1 (Mps-one binder 1; in beige), mTORC1 (Mammalian target of rapamycin complex 1; in green).

informed consent for research use by the donor or the donor’s legal representative. Every islet isolation offered through the IIDP is designated by the isolation centers as having received sufficient documentation of consent of research use of the pancreas.

Organ donors are not identifiable and anonymous. This work includes islet cells from adult brain-deceased donors insufficient in number for clinical transplantation with informed consent (USA) or when there has been no written refusal for organ transplantation after verification there has been no written refusal (national refusal registry) for research; verbal consent for research donation given is requested from next of kin (Europe; France). France has presumed consent legislation in place for deceased donors. All human islet experiments were performed in the islet biology laboratory, University of Bremen. Ethical approval for the use of human islets in this project had been granted by the Ethics Committee of the University of Bremen. The study complied with all relevant ethical regulations for work with human cells for research purposes.

Mice. β -cell-specific LATS2 knockout (β -LATS2^{-/-}) mice were generated by crossing mice harboring exon 4 of the LATS2 gene flanked by *loxP* sites (LATS2^{fl/fl}), provided by Dr. Dae-Sik Lim, Korea Advanced Institute of Science and Technology, South Korea⁸⁴) with C57BL/6J strain mice expressing Cre under the rat insulin-2 promoter (B6;D2-Tg(Ins-cre)23Herr:RIP-Cre⁸⁵, kindly provided by Susanne Ullrich (Medizinische Klinik, Universitätsklinikum, Tübingen). RIP-Cre-LATS2^{fl/fl} mice on the C57BL/6J background were intercrossed to generate RIP-Cre-LATS2^{fl/fl} (β -LATS2^{-/-}). For multiple low dose streptozotocin (MLD-STZ) experiments, 8- to 10-week old β -LATS2^{-/-}, flox control (LATS2^{fl/fl}) and flox-negative littermates (RIP-Cre) were injected with STZ for 5 consecutive days (40 mg/kg STZ or citrate buffer vehicle control). For the high fat diet (HFD) experiments, 8-week old β -LATS2^{-/-} mice and Rip-Cre controls were fed a normal diet (ND, Harlan Teklad Rodent Diet 8604, containing 12.2, 57.6, and 30.2% calories from fat, carbohydrate, and protein, respectively) or a high fat/ high sucrose diet (HFD, “Surwit” Research Diets, New Brunswick, NJ, containing 58, 26, and 16% calories from fat, carbohydrate and protein, respectively⁸⁶) for 17 weeks. For both models, random blood was obtained from the tail vein of non-fasted mice and glucose was measured using a Glucometer (Freestyle; TheraSense Inc., Alameda, CA). Heterozygous leptin receptor-deficient mice on the C57BLKs/J background (Lep^{db/+}, db^{+/+}) were purchased from Jackson Laboratory. By breeding of these mice, we obtained diabetic Lep^{db/db} (db/db) as well as non-diabetic heterozygous Lep^{db/+} (db^{+/+}) mice. For data presented in Fig. 1 and Supplementary Fig. 1, islets were isolated after 16 weeks of HFD or at the age of 12 weeks (db/db). Mice were

killed and pancreases isolated at the end of experiment. All mice used in this experiment were male and housed in a temperature-controlled room with a 12-h light–dark cycle and were allowed free access to food and water in agreement with NIH animal care guidelines, §8 German animal protection law, German animal welfare legislation and with the guidelines of the Society of Laboratory Animals (GV-SOLAS) and the Federation of Laboratory Animal Science Associations (FELASA). All protocols were approved by the Bremen Senate (Senator for Science, Health and consumer protection) and we have complied with all relevant ethical regulations for animal testing and research.

Glucose and insulin tolerance tests and measurement of insulin release. For ipGTTs of control and hyperglycemic HFD/STZ-treated mice, mice were fasted 12 h overnight and injected with glucose (40%; B. Braun, Melsungen, Germany) at a dose of 1 g/kg body weight according to an established protocol⁸⁷. Blood samples were obtained at time points 0, 15, 30, 60, 90, and 120 min for glucose measurements using a glucometer. For i.p. insulin tolerance tests, mice were injected with 0.75 U/kg body weight recombinant human insulin (Novolin, Novo Nordisk) after 4–5 h fasting, and glucose concentration was determined with the Glucometer. Insulin secretion was measured before (0 min) and after (15 and 30 min) i.p. injection of glucose (2 g/kg body weight) and measured using ultrasensitive mouse Elisa kit (ALPCO Diagnostics, Salem, NH).

Plasmids and siRNAs. Myc-LATS2 and kinase dead Myc-LATS2 (LATS2-KD) were provided by Dr. Jixin Dong (Nebraska Medical Center, Omaha, NE)³⁷. Raptor-WT and Raptor-S606A mutant were kindly provided by Wenjian Gan (Medical University of South Carolina, SC, USA) and Wenyi Wei (Harvard Medical School, Boston, MA, USA)⁴⁷. pRK5-HA GST Raga 66L was a gift from David Sabatini (Addgene plasmid # 19300; RRID:Addgene_19300)⁵⁴. pRK5-HA GST Raga 21L was a gift from David Sabatini (Addgene plasmid # 19299; RRID:Addgene_19299)⁵⁴. pBABE-puro GFP-LC3 was a gift from Jayanta Debnath (Addgene plasmid # 22405; <http://n2t.net/addgene:22405>; RRID:Addgene_22405)⁸⁸. pCDNA3.1neo-NLucYAP15 and pCDNA3.1neo-14-3-3-CLuc (LATS-BS) were gift from Xiaolong Yang (Addgene plasmid # 107610; RRID:Addgene_107610)³⁴. pLJC5-Tmem192-3xHA and pLJC5-Tmem192-2xFlag were gifts from David Sabatini (Addgene plasmid # 102930; RRID:Addgene_102930). pRK5-HA-metap2 was a gift from David Sabatini (Addgene plasmid # 100512; RRID: Addgene_100512)⁸⁹. GFP or metap2 was used as a control. All siRNAs were purchased from Dharmacon. A mix of ON-TARGETplus siRNAs directed against human LATS2 (26524) sequences GAAGUGAACCGGAAAUGC, AAUCAGAAU

UUCUUGUUG, ACACUCACCUCGCCAAUA, GCACGCAUUUACGAA UUC, rat LATS2 (305922) sequences GGAAUAGCCGCGACGAC, UCAUAU AUGACUUGUACGA, GCAGGUUCUUCGACGACAA, ACCAGAAGGAGUC GAACUA, rat LATS1 (308265) sequences CCGAAAACCGGCACGAUU, AUCC AAAGCCCAUCGAAUA, CAAGAAAAGUCGAUACGAA, GAGCGAUGGUAA CGAGGAA, rat MOB1a (297387) sequences GGAUAGCGGUUAGGUAA, CAU ACUAAAUAUAGCGUCU, AGUCAGUACUUGAUUU, CCGAUUGACUGU GAAUUC, rat Raptor (287871) sequences GAGCUUGACUCCAGUUCGA, GC UAGGAAACCUGAACAAU, GCACACAGCAUGGGUGUA, GAAUCAUGAGG UGGUUAUA, and rat Atg7 (312647), sequences CAAAGUUAACAGUCGGUGU, AGUGAAUUGCCAGCGGUUC, CUGGAGGAACUCAUCAUA, CCCAGAGA AGUUGAACGA. Four different custom siRNAs were designed against Lamp2A, sequences siLAMP2A#1- GCGCCAUAUCUGGAUUAUU, siLAMP2A#2- GUG CAGAUGAAGACAACUUUU, siLAMP2A#3- GGGAGGAGUACUUUAUUUAU U, and siLAMP2A#4- AGAGUAUUCUACAGCUCUAAUU. A second mix of siRNAs directed against rat LATS2 (siGENOME; 305922) sequences GGAACAGCCUCA UAAUGA, GGAACAGCCUGCACCCUA, GAAGUUUGGACCUUAUCA, AA GUGGCCUUGCCUGUUA. An ON-TARGETplus non-targeting siRNA pool from Dharmacon served as a control.

Transfections. LATS2, LATS2-KD, LATS-BS, LC3, pLJC5-Tmem192-3xHA, pLJC5-Tmem192-2xFlag, Raptor-WT, Raptor-S606A, HA-RagA-T21L, HA-RagA-Q66L, HA-metap2, and GFP plasmids were used to overexpress these proteins in INS-1E cell. 100 nM siRNAs were used for the transfection in human islets and INS-1E cells¹⁴. To deliver desired siRNA/DNA into dispersed isolated islets as well as INS-1E cells two different transfection methods were used. (1) In brief, isolated islets or INS-1E cells were pre-incubated in transfection Ca²⁺-KRH medium for 1 h; and then lipoplexes (Lipofectamine 2000, Invitrogen)/siRNA ratio 1:20 pmol or lipoplexes/DNA ratio 2.5:1 were added to islets or INS-1E cells; after an additional 4–6 h incubation, CMRL-1066 or RPMI-1640 medium containing 20% FCS was added to the transfected islets or INS-1E cells. (2) jetPRIME[®] transfection reagent (#114-75; Polyplus transfection, France) was mixed with jetPRIME buffer and siRNA/DNA according to the manufacturer's instructions. The jetPRIME-siRNA/DNA complexes were then added to complete CMRL-1066 or RPMI-1640 to transfect dispersed human islets or INS-1E cells. Efficient transfection was evaluated based on western blot, qPCR, and fluorescent microscopy.

Adenovirus transduction. The adenoviruses Ad-h-LATS2 expressing human LATS2 and Ad-GFP-U6-hLATS2-shRNA expressing GFP and human LATS2 shRNA were obtained from Vector Biolabs. The sequence for the shRNA of LATS2 was:

CCGG-CTACTCGCCATACGCTTTAACTCGAGTTAAAGGCGTATGGCG AGTAG-TTTTTG. Ad-LacZ or Ad-GFP-U6-shRNA were used as respective controls. For transduction, human islets or INS-1E cells were plated for 24 h; then infected at a multiplicity of infection (MOI) of 20 (for INS-1E) or 100 (for human islets) for 4 h in CMRL/RPMI medium without FCS. After 4 h incubation, human islets or INS-1E cells were washed with medium and incubated for an additional 48 h or treated with 2.2 mM glucose alone/ plus palmitate, or 2 ng/mL IL1- β plus 1000 U/mL IFN- γ .

Glucose-stimulated insulin secretion (GSIS). Glucose-stimulated insulin secretion was performed by pre-incubating primary human islets in Krebs-Ringer bicarbonate buffer (KRB) containing 2.8 mM glucose for 30 min, followed by KRB buffer containing 2.8 mM glucose for 1 h (basal) and then an additional 1 h in KRB containing 16.7 mM glucose (stimulated). Islets were washed with PBS and lysed with RIPA buffer to extract protein. Insulin was determined using human insulin ELISA (ALPCO Diagnostics, Salem, NH). Secreted insulin was normalized to insulin content.

Immunohistochemistry. Mouse pancreases were dissected and fixed in 4% formaldehyde at 4 °C for 12 h before embedding in paraffin⁸⁰. 4- μ m sections were deparaffinized, rehydrated, and incubated overnight at 4 °C with anti-Ki67 (Dako; #M7249) or guinea pig anti-P62 (GP62-C) from PROGEN or anti-pS6 (CST; 4858) in combination with TSA (Invitrogen #T30955) and for 2 h at room temperature with anti-insulin (Dako; A0546) antibodies (all at a dilution of 1:100) followed by Cy3-conjugated donkey anti-rat (712-165-150), or anti-guinea pig (706-165-148), or anti-rabbit (711-165-152) and fluorescein isothiocyanate (FITC)- conjugated donkey anti-guinea pig (706-096-148) (all from Jackson ImmunoResearch Laboratories, West Grove, PA; 1:200 dilution) for 1 h at RT. Slides were mounted with Vectashield with 4'-diamidino-2-phenylindole (DAPI) (Vector Labs). β -cell apoptosis in Bouin's fixed isolated human islets or mouse pancreatic sections was analyzed by the terminal deoxynucleotidyl transferase-mediated dUTP nick-end labeling (TUNEL) technique according to the manufacturer's instructions (In Situ Cell Death Detection Kit, TMR red; Roche) and double stained for insulin. Fluorescence was analyzed using a Nikon MEA53200 (Nikon GmbH, Dusseldorf, Germany) microscope and images were acquired using NIS-Elements software (Nikon).

For autophagy analyses, INS-1E β -cells and the human β -cell line CM were seeded on gelatin coated glass coverslips in 24-well plates and then transfected with

GFP-LC3 and Myc-LATS2 plasmids or with the Myc-LATS2 plasmid alone using jetPRIME[®] transfection reagent. After 24 h, cells were treated with 100 μ M Chloroquine for 6 h to inhibit autophagosomal degradation. Slides were rinsed with PBS once and fixed for 30 min with 4% paraformaldehyde in PBS at RT followed by 4 min permeabilization with 0.5 % TritonX-100 in PBS. After rinsing twice with PBS, cells were blocked with blocking buffer containing 3% BSA and then incubated overnight at 4 °C with GFP (CST; #2956, 1:100) and Myc (CST; #2276, 1:700) primary antibodies followed by the secondary antibodies: Cy3-conjugated donkey anti-mouse (715-165-150) or fluorescein isothiocyanate (FITC)-conjugated donkey anti-rabbit (711-096-152); (all from Jackson ImmunoResearch Laboratories, West Grove, PA; 1:200 dilution) for 1 h at RT. Co-staining of LATS2 and lysosomal marker LAMP1 was performed using Myc (CST; #2276, 1:700) and Alexa Fluor[®]488-conjugated LAMP1 (CST; #58996, 1:50) antibodies and anti-mouse Cy3-conjugated secondary antibody (for Myc). Coverslips were mounted on glass slides using Vectashield with 4'-diamidino-2-phenylindole (DAPI; Vector Labs). Confocal analyses were performed with an LSM880 ZEISS confocal laser scanning microscope (Zeiss, Jena, Germany).

Morphometric analysis. For morphometric data, ten sections (spanning the width of the pancreas) per mouse were analyzed. Pancreatic tissue area and insulin-positive area were determined by computer-assisted measurements using a Nikon MEA53200 (Nikon GmbH, Dusseldorf, Germany) microscope and images were acquired using NIS-Elements software (Nikon). β -cell mass was obtained by multiplying the β -cell fraction by the weight of the pancreas¹⁴.

Western blot analysis. Human or mouse islets and INS-1E cells were washed twice with ice-cold PBS and lysed with RIPA lysis buffer containing Protease and Phosphatase Inhibitors (Pierce, Rockford, IL, USA). Protein concentrations were measured by the BCA protein assay (Pierce). Lysates were fractionated by NuPAGE 4–12% Bis-Tris gel (Invitrogen) and electrically transferred into PVDF membranes. Membranes were blocked in 2.5% non-fat dry milk (CST) and 2.5% BSA (Sigma) for 1 h at room temperature and incubated overnight at 4 °C with the following antibodies: rabbit anti-LATS2 (5888), rabbit anti-LATS1 (9153), mouse anti-Myc (2276), rabbit anti-cleaved caspase-3 (9664), rabbit anti-PARP (9542), rabbit anti-cleaved PARP (9545), rabbit anti-Raptor (2280), rabbit anti-phospho-p70 S6 Kinase (9234), rabbit anti-phospho-S6 ribosomal protein (4858), rabbit anti-phospho-4EBP1 (2855), rabbit anti-LC3B (2775), rabbit anti-Atg7 (8558), rabbit anti-GFP (2956), rabbit anti-HA (2367), rabbit anti-phospho-Tubulin/TSC2 (3611), rabbit anti-Tubulin/TSC2 (4308), rabbit anti-pAKT (4058), rabbit anti-AKT (9272), mouse anti-S6 ribosomal protein (2317), rabbit anti-p70 S6 Kinase (2708), rabbit anti-4EBP1 (9644), rabbit anti-tubulin (2146), rabbit anti-glyceraldehyde 3-phosphate dehydrogenase (2118) and rabbit anti- β -actin (4967) all from Cell signaling technology (CST) and guinea pig anti-P62 (GP62-C) from PROGEN and rabbit anti-LAMP2A (AB10971511) from Abcam. Organelle identification markers data presented in Supplementary Fig. 8b were detected using antibodies from the Organelle Localization IF Antibody Sampler Kit (CST; 8653). Primary antibodies were followed by horseradish-peroxidase-linked anti-rabbit (111-035-003), anti-mouse (115-035-003) or anti-guinea pig (106-035-003) secondary antibodies (all from Jackson; 1:3000 dilution). All primary antibodies were used at 1:1000 dilution in Tris-buffered saline plus Tween-20 (TBS-T) containing 5% BSA. Membrane was developed using a chemiluminescence assay system (Pierce) and analyzed using DocITLS image acquisition 6.6a (UVP BioImaging Systems, Upland, CA, USA). Uncropped and unprocessed scans of all blots are provided in the Source data file.

LATS-BS luciferase assay. INS-1E cells or isolated mouse islets were transfected with LATS-BS firefly luciferase reporter constructs using jetPRIME transfection reagent (PolyPlus, Illkirch, France). As internal transfection control, pRL-Renilla luciferase control reporter vector (Promega) was co-transfected into each sample. 24 h after transfection, INS-1E cells were treated with 2.2 mM glucose alone or plus palmitate for another 24 h. Thereafter, Western blot analysis (see above) and luciferase assay was performed using Dual-Luciferase Reporter Assay System (Promega)⁸⁹ in a parallel set of experiments. Luciferase signal was calculated based on the ratio of luciferase activity of LATS-BS to control reporter vector.

Lyso-IP. Approx. 30 million INS-1E cells were used for each condition. Each dish was transfected with Tmem192-2XFlag/Tmem192-3XHA and LATS2-Myc plasmids after an adapted previously well-established protocol for the isolation of lysosomes⁵⁸. INS-1E cells were washed with ice-cold PBS and collected in 1 ml KPBS (136 mM KCl, 10 mM KH₂PO₄, [pH 7.25 adjusted with KOH]) supplemented with Protease and Phosphatase Inhibitors and centrifuged at 1000 \times g for 2 min at 4 °C. Pellet was resuspended in 950 μ l of KPBS and 25 μ l suspension was saved for the input. The remaining cell suspension was homogenized with 60 strokes of a dounce homogenizer (125 rpm, setting 1). Lysate was centrifuged at 1000 \times g for 2 min at 4 °C. The supernatant was incubated with 25 μ l of KPBS prewashed anti-HA magnetic beads (ThermoFischer) on rotation at 4 °C for 15 min. Beads were separated using a magnet and immuno-captured lysosomes were gently washed 4 times with 1 ml KPBS on rotation at 4 °C for 4 min each. Proteins were extracted from bound lysosomes directly by adding 2 \times loading buffer followed by heating at 95 °C for 10 min. Beads were separated, sample was spun

shortly and collected for immunoblot analysis, for which half of the eluted sample was loaded on the gel (approximately 50–60× enrichment of the loaded input).

Isolation of autophagosomes. An adapted protocol from ref. 59 has been used for the isolation of autophagosomes. Approximately 20 million stable GFP-LC3 expressing INS-1E β -cells were used per condition. Cells were washed twice with PBS, scrapped in 2 ml ice-cold PBS and centrifuged at 1000 \times g for 3 min at 4 °C. Pellet was resuspend in 1 ml cold PBS and 50 μ l was removed for input. The remaining suspension was centrifuged at 1000 \times g for 3 min at 4 °C and pellet was resuspend in 1 ml ice-cold resuspension buffer (0.25 M sucrose, 1 mM EDTA, and 10 mM HEPES-NaOH [pH 7.4]). Cell were lysed by a Dounce homogenizer (60 strokes, 125 rpm, 1st setting) followed by centrifugation at 1000 \times g for 10 min at 4 °C to remove cell debris and nucleus. The supernatant was then centrifuged at 20,000 \times g for 20 min at 4 °C to enrich autophagosomes. Pellet containing autophagosomes were resuspended in resuspension buffer and incubated with equilibrated anti-GFP-Trap[®] Magnetic beads (Chromotek, Planegg, Germany) or rabbit IgG (CST) conjugated magnetic beads (25 μ l) for 2 h at 4 °C on rotation. The beads were separated using a magnet and washed four times 4 min each with wash buffer (resuspension buffer supplemented with 0.15 M NaCl) at 4 °C. The beads were separated and boiled in 2 \times SDS sample buffer at 95 °C for 10 min and spun down. Beads were separated and the sample was centrifuged at high speed for 5 min and collected for immunoblot analysis.

Co-immunoprecipitation. Protocol adapted from GFP-Trap Magnetic Agarose Kit (Chromotek, Planegg, Germany). For one immunoprecipitation reaction, approximately 10 million GFP-LC3 expressing INS-1E cells or normal INS-1E cells were used. INS-1E cells were washed twice with PBS, scrapped in 2 ml ice-cold PBS and centrifuged at 1000 \times g for 3 min at 4 °C. Pellet was resuspended in 200 μ l ice-cold lysis buffer (10 mM Tris/Cl pH 7.5, 150 mM NaCl, 0.5 mM EDTA, 0.5 % Nonidet[™] P40 Substitute, 0.09% sodium azide) supplemented with Protease and Phosphatase Inhibitors. The tube was placed on ice for 30 min with extensively pipetting every 10 min. Cell lysate was centrifuged at 15,000 \times g for 15 min at 4 °C and 300 μ l dilution buffer (10 mM Tris/Cl pH 7.5, 150 mM NaCl, 0.5 mM EDTA, 0.018% sodium azide) supplemented with Protease and Phosphatase Inhibitors was added to the supernatant. 50 μ l of the suspension was saved for input. The remaining suspension was incubated with equilibrated anti-GFP conjugated magnetic beads (25 μ l) for 1 h at 4 °C on rotation. The beads were separated using a magnet and washed four times 4 min each with dilution buffer at 4 °C. The beads were separated and boiled in 2 \times SDS sample buffer at 95 °C for 10 min and spun down. Beads were separated and the sample was collected for immunoblot analysis.

Generation of INS-1E cell with stable GFP-LC3 expression. To overexpress GFP-LC3 in INS-1E cells, cultured cells were transfected with pBABEpuro GFP-LC3 and selected with 1.5–3 μ g/mL puromycin. Resistant colonies were identified by GFP under fluorescent microscopy and used for further experiments. After selection, INS-1E cells were maintained in culture medium containing 2 μ g/ml puromycin.

Genomic PCR. Genomic DNA was extracted from liver, heart, spleen, kidney, hypothalamus, and isolated pancreatic islets according to the manufacturer's instruction (DNeasy[®] Blood&Tissue Kit, QIAGEN). Genotyping was performed using the following primers: flox-F 5' CCG GAG TCA TTG CTT GTT TT 3', flox-R 5' GGA GAT CCT GGG TAC TGC AC 3', flox-F del 5' ACA TGA CAC TAC GGG GCC TAG C 3'⁸⁴. A 300 bp band was amplified from floxed mice and 400 bp band was amplified if the LATS2 gene was deleted.

Statistical analyses. To perform statistical analysis, at least 3 independent experiments were performed for the human islets (3 different donors) and INS-1E cells, as reported in all figure legends. Data are presented as means \pm SEM. Mean differences were determined by two-tailed Student's *t*-tests or one-way ANOVA for multiple group comparisons with Tukey's post hoc test. Densitometry analyses of western blot bands were examined by two-tailed Student's *t*-tests. Results were normalized to the respective control conditions and ratios analyzed, in which a normal distribution of results cannot be proven. *P* value < 0.05 was considered statistically significant.

Reporting summary. Further information on research design is available in the Nature Research Reporting Summary linked to this article.

Data availability

All data generated or analyzed during this study are included in this article and its Supplementary information files. All original source data are provided as a Source Data file. Source data are provided with this paper.

Received: 11 May 2020; Accepted: 20 July 2021;

Published online: 13 August 2021

References

- Vetere, A., Choudhary, A., Burns, S. M. & Wagner, B. K. Targeting the pancreatic beta-cell to treat diabetes. *Nat. Rev. Drug Disco.* **13**, 278–289 (2014).
- Aguayo-Mazzucato, C. & Bonner-Weir, S. Pancreatic beta cell regeneration as a possible therapy for diabetes. *Cell Metab.* **27**, 57–67 (2018).
- Kurrer, M. O., Pakala, S. V., Hanson, H. L. & Katz, J. D. Beta cell apoptosis in T cell-mediated autoimmune diabetes. *Proc. Natl Acad. Sci. USA* **94**, 213–218 (1997).
- Mathis, D., Vence, L. & Benoist, C. β -Cell death during progression to diabetes. *Nature* **414**, 792–798 (2001).
- Butler, A. E. et al. Beta-cell deficit and increased beta-cell apoptosis in humans with type 2 diabetes. *Diabetes* **52**, 102–110 (2003).
- Rhodes, C. J. Type 2 diabetes—a matter of beta-cell life and death? *Science* **307**, 380–384 (2005).
- Katsarou, A. et al. Type 1 diabetes mellitus. *Nat. Rev. Dis. Prim.* **3**, 17016 (2017).
- Alejandro, E. U., Gregg, B., Blandino-Rosano, M., Cras-Meneur, C. & Bernal-Mizrachi, E. Natural history of beta-cell adaptation and failure in type 2 diabetes. *Mol. Asp. Med.* **42**, 19–41 (2015).
- Yu, F. X., Zhao, B. & Guan, K. L. Hippo pathway in organ size control, tissue homeostasis, and cancer. *Cell* **163**, 811–828 (2015).
- Harvey, K. F., Zhang, X. & Thomas, D. M. The Hippo pathway and human cancer. *Nat. Rev. Cancer* **13**, 246–257 (2013).
- Halder, G. & Johnson, R. L. Hippo signaling: growth control and beyond. *Development* **138**, 9–22 (2011).
- Harvey, K. & Tapon, N. The Salvador-Warts-Hippo pathway—an emerging tumour-suppressor network. *Nat. Rev. Cancer* **7**, 182–191 (2007).
- Ardestani, A., Lupse, B. & Maedler, K. Hippo signaling: key emerging pathway in cellular and whole-body metabolism. *Trends Endocrinol. Metab.* **29**, 492–509 (2018).
- Ardestani, A. et al. MST1 is a key regulator of beta cell apoptosis and dysfunction in diabetes. *Nat. Med.* **20**, 385–397 (2014).
- Yuan, T., Gorrepati, K. D., Maedler, K. & Ardestani, A. Loss of Merlin/NF2 protects pancreatic beta-cells from apoptosis by inhibiting LATS2. *Cell Death Dis.* **7**, e2107 (2016).
- Cebola, I. et al. TEAD and YAP regulate the enhancer network of human embryonic pancreatic progenitors. *Nat. Cell Biol.* **17**, 615–626 (2015).
- George, N. M., Day, C. E., Boerner, B. P., Johnson, R. L. & Sarvetnick, N. E. Hippo signaling regulates pancreas development through inactivation of Yap. *Mol. Cell Biol.* **32**, 5116–5128 (2012).
- Gao, T. et al. Hippo signaling regulates differentiation and maintenance in the exocrine pancreas. *Gastroenterology* **144**, 1543–1553.e1541 (2013).
- George, N. M., Boerner, B. P., Mir, S. U., Guinn, Z. & Sarvetnick, N. E. Exploiting expression of Hippo effector, Yap, for expansion of functional islet mass. *Mol. Endocrinol.* **29**, 1594–1607 (2015).
- Ardestani, A. & Maedler, K. The Hippo signaling pathway in pancreatic beta-cells: functions and regulations. *Endocr. Rev.* **39**, 21–35 (2018).
- Ardestani, A. et al. Neratinib protects pancreatic beta cells in diabetes. *Nat. Commun.* **10**, 5015 (2019).
- Aylon, Y. et al. Silencing of the Lats2 tumor suppressor overrides a p53-dependent oncogenic stress checkpoint and enables mutant H-Ras-driven cell transformation. *Oncogene* **28**, 4469–4479 (2009).
- Yabuta, N. et al. Lats2 is an essential mitotic regulator required for the coordination of cell division. *J. Biol. Chem.* **282**, 19259–19271 (2007).
- Ke, H. et al. Putative tumor suppressor Lats2 induces apoptosis through downregulation of Bcl-2 and Bcl-x(L). *Exp. Cell Res.* **298**, 329–338 (2004).
- Aylon, Y., Sarver, A., Tovy, A., Ainbinder, E. & Oren, M. Lats2 is critical for the pluripotency and proper differentiation of stem cells. *Cell Death Differ.* **21**, 624–633 (2014).
- Matsui, Y. et al. Lats2 is a negative regulator of myocyte size in the heart. *Circ. Res.* **103**, 1309–1318 (2008).
- Moroishi, T. et al. The Hippo pathway kinases LATS1/2 suppress cancer immunity. *Cell* **167**, 1525–1539.e1517 (2016).
- Aylon, Y. et al. A positive feedback loop between the p53 and Lats2 tumor suppressors prevents tetraploidization. *Genes Dev.* **20**, 2687–2700 (2006).
- Aylon, Y. et al. The Lats2 tumor suppressor augments p53-mediated apoptosis by promoting the nuclear proapoptotic function of ASPP1. *Genes Dev.* **24**, 2420–2429 (2010).
- Shao, D. et al. A functional interaction between Hippo-YAP signalling and FoxO1 mediates the oxidative stress response. *Nat. Commun.* **5**, 3315 (2014).
- Reuven, N., Adler, J., Meltser, V. & Shaul, Y. The Hippo pathway kinase Lats2 prevents DNA damage-induced apoptosis through inhibition of the tyrosine kinase c-Abl. *Cell Death Differ.* **20**, 1330–1340 (2013).
- Odashima, M. et al. Inhibition of endogenous Mst1 prevents apoptosis and cardiac dysfunction without affecting cardiac hypertrophy after myocardial infarction. *Circ. Res.* **100**, 1344–1352 (2007).

33. Zhang, Z. W. et al. miR-375 inhibits proliferation of mouse pancreatic progenitor cells by targeting YAP1. *Cell Physiol. Biochem* **32**, 1808–1817 (2013).
34. Azad, T. et al. A LATS biosensor screen identifies VEGFR as a regulator of the Hippo pathway in angiogenesis. *Nat. Commun.* **9**, 1061 (2018).
35. Avruch, J. et al. Protein kinases of the Hippo pathway: regulation and substrates. *Semin Cell Dev. Biol.* **23**, 770–784 (2012).
36. Furth, N. & Aylon, Y. The LATS1 and LATS2 tumor suppressors: beyond the Hippo pathway. *Cell Death Differ.* **24**, 1488–1501 (2017).
37. Xiao, L., Chen, Y., Ji, M. & Dong, J. KIBRA regulates Hippo signaling activity via interactions with large tumor suppressor kinases. *J. Biol. Chem.* **286**, 7788–7796 (2011).
38. Choudhury, A. I. et al. The role of insulin receptor substrate 2 in hypothalamic and beta cell function. *J. Clin. Invest* **115**, 940–950 (2005).
39. Collins, S. C. et al. Progression of diet-induced diabetes in C57BL6J mice involves functional dissociation of Ca2(+) channels from secretory vesicles. *Diabetes* **59**, 1192–1201 (2010).
40. Ardestani, A., Lupse, B., Kido, Y., Leibowitz, G. & Maedler, K. mTORC1 signaling: a double-edged sword in diabetic beta cells. *Cell Metab.* **27**, 314–331 (2018).
41. Yuan, T. et al. Reciprocal regulation of mTOR complexes in pancreatic islets from humans with type 2 diabetes. *Diabetologia* **60**, 668–678 (2017).
42. Bachar, E. et al. Glucose amplifies fatty acid-induced endoplasmic reticulum stress in pancreatic beta-cells via activation of mTORC1. *PLoS ONE* **4**, e4954 (2009).
43. Mir, S. U. et al. Inhibition of autophagic turnover in beta-cells by fatty acids and glucose leads to apoptotic cell death. *J. Biol. Chem.* **290**, 6071–6085 (2015).
44. Nelson, N. & Clark, G. J. Rheb may complex with RASSF1A to coordinate Hippo and TOR signaling. *Oncotarget* **7**, 33821–33831 (2016).
45. Tumaneng, K. et al. YAP mediates crosstalk between the Hippo and PI(3)K-TOR pathways by suppressing PTEN via miR-29. *Nat. Cell Biol.* **14**, 1322–1329 (2012).
46. Liang, N. et al. Regulation of YAP by mTOR and autophagy reveals a therapeutic target of tuberous sclerosis complex. *J. Exp. Med.* **211**, 2249–2263 (2014).
47. Gan, W. et al. LATS suppresses mTORC1 activity to directly coordinate Hippo and mTORC1 pathways in growth control. *Nat. Cell Biol.* **22**, 246–256 (2020).
48. Bachar-Wikstrom, E. et al. Stimulation of autophagy improves endoplasmic reticulum stress-induced diabetes. *Diabetes* **62**, 1227–1237 (2013).
49. Rumala, C. Z. et al. Exposure of pancreatic beta-cells to excess glucose results in bimodal activation of mTORC1 and mTOR-dependent metabolic acceleration. *iScience* **23**, 100858 (2020).
50. Pearce, L. R. et al. Characterization of PF-4708671, a novel and highly specific inhibitor of p70 ribosomal S6 kinase (S6K1). *Biochem J.* **431**, 245–255 (2010).
51. Saxton, R. A. & Sabatini, D. M. mTOR signaling in growth, metabolism, and disease. *Cell* **168**, 960–976 (2017).
52. Dibble, C. C. & Cantley, L. C. Regulation of mTORC1 by PI3K signaling. *Trends Cell Biol.* **25**, 545–555 (2015).
53. Efeyan, A. et al. Regulation of mTORC1 by the Rag GTPases is necessary for neonatal autophagy and survival. *Nature* **493**, 679–683 (2013).
54. Sancak, Y. et al. The Rag GTPases bind raptor and mediate amino acid signaling to mTORC1. *Science* **320**, 1496–1501 (2008).
55. Zoncu, R. et al. mTORC1 senses lysosomal amino acids through an inside-out mechanism that requires the vacuolar H(+)-ATPase. *Science* **334**, 678–683 (2011).
56. Bartolome, A. et al. Pancreatic beta-cell failure mediated by mTORC1 hyperactivity and autophagic impairment. *Diabetes* **63**, 2996–3008 (2014).
57. Shigeyama, Y. et al. Biphasic response of pancreatic beta-cell mass to ablation of tuberous sclerosis complex 2 in mice. *Mol. Cell Biol.* **28**, 2971–2979 (2008).
58. Abu-Remaileh, M. et al. Lysosomal metabolomics reveals V-ATPase- and mTOR-dependent regulation of amino acid efflux from lysosomes. *Science* **358**, 807–813 (2017).
59. Yamamoto, S. et al. Autophagy differentially regulates insulin production and insulin sensitivity. *Cell Rep.* **23**, 3286–3299 (2018).
60. Gao, W. et al. Biochemical isolation and characterization of the tubulovesicular LC3-positive autophagosomal compartment. *J. Biol. Chem.* **285**, 1371–1383 (2010).
61. Noda, N. N., Ohsumi, Y. & Inagaki, F. Atg8-family interacting motif crucial for selective autophagy. *FEBS Lett.* **584**, 1379–1385 (2010).
62. Kirkin, V. et al. A role for NBR1 in autophagosomal degradation of ubiquitinated substrates. *Mol. Cell* **33**, 505–516 (2009).
63. Novak, I. et al. Nix is a selective autophagy receptor for mitochondrial clearance. *EMBO Rep.* **11**, 45–51 (2010).
64. Jacomin, A. C., Samavedam, S., Promponas, V. & Nezis, I. P. iLIR database: a web resource for LIR motif-containing proteins in eukaryotes. *Autophagy* **12**, 1945–1953 (2016).
65. Jung, H. S. et al. Loss of autophagy diminishes pancreatic beta cell mass and function with resultant hyperglycemia. *Cell Metab.* **8**, 318–324 (2008).
66. Ebato, C. et al. Autophagy is important in islet homeostasis and compensatory increase of beta cell mass in response to high-fat diet. *Cell Metab.* **8**, 325–332 (2008).
67. Bachar-Wikstrom, E., Wikstrom, J. D., Kaiser, N., Cerasi, E. & Leibowitz, G. Improvement of ER stress-induced diabetes by stimulating autophagy. *Autophagy* **9**, 626–628 (2013).
68. Rivera, J. F., Costes, S., Gurlo, T., Glabe, C. G. & Butler, P. C. Autophagy defends pancreatic beta cells from human islet amyloid polypeptide-induced toxicity. *J. Clin. Invest.* **124**, 3489–3500 (2014).
69. Wang, D. et al. Emerging role of the Hippo pathway in autophagy. *Cell Death Dis.* **11**, 880 (2020).
70. Wilkinson, D. S. et al. Phosphorylation of LC3 by the Hippo kinases STK3/STK4 is essential for autophagy. *Mol. Cell* **57**, 55–68 (2015).
71. Maejima, Y. et al. Mst1 inhibits autophagy by promoting the interaction between Beclin1 and Bcl-2. *Nat. Med.* **19**, 1478–1488 (2013).
72. Tataro, A. et al. Cell phenotypic plasticity requires autophagic flux driven by YAP/TAZ mechanotransduction. *Proc. Natl Acad. Sci. USA* **116**, 17848–17857 (2019).
73. Pavel, M. et al. Contact inhibition controls cell survival and proliferation via YAP/TAZ-autophagy axis. *Nat. Commun.* **9**, 2961 (2018).
74. Lee, Y. A. et al. Autophagy is a gatekeeper of hepatic differentiation and carcinogenesis by controlling the degradation of Yap. *Nat. Commun.* **9**, 4962 (2018).
75. Wang, P. et al. Activation of Aurora A kinase increases YAP stability via blockage of autophagy. *Cell Death Dis.* **10**, 432 (2019).
76. Yuan, T. et al. Proproliferative and antiapoptotic action of exogenously introduced YAP in pancreatic β cells. *JCI Insight* **1**, e86326 (2016).
77. Fang, Z. et al. Single-cell heterogeneity analysis and CRISPR screen identify key beta-cell-specific disease genes. *Cell Rep.* **26**, 3132–3144 e3137 (2019).
78. Dewey, E. B., Sanchez, D. & Johnston, C. A. Warts phosphorylates mud to promote pins-mediated mitotic spindle orientation in *Drosophila*, independent of Yorkie. *Curr. Biol.* **25**, 2751–2762 (2015).
79. Plouffe, S. W., Hong, A. W. & Guan, K. L. Disease implications of the Hippo/YAP pathway. *Trends Mol. Med.* **21**, 212–222 (2015).
80. Schulthess, F. T. et al. CXCL10 impairs beta cell function and viability in diabetes through TLR4 signaling. *Cell Metab.* **9**, 125–139 (2009).
81. Burkart, V. et al. Natural resistance of human beta cells toward nitric oxide is mediated by heat shock protein 70. *J. Biol. Chem.* **275**, 19521–19528 (2000).
82. Maedler, K. et al. Distinct effects of saturated and monounsaturated fatty acids on beta-cell turnover and function. *Diabetes* **50**, 69–76 (2001).
83. Hart, N. J. & Powers, A. C. Use of human islets to understand islet biology and diabetes: progress, challenges and suggestions. *Diabetologia* **62**, 212–222 (2019).
84. Kim, M. et al. cAMP/PKA signalling reinforces the LATS-YAP pathway to fully suppress YAP in response to actin cytoskeletal changes. *EMBO J.* **32**, 1543–1555 (2013).
85. Herrera, P. L. Adult insulin- and glucagon-producing cells differentiate from two independent cell lineages. *Development* **127**, 2317–2322 (2000).
86. Sauter, N. S., Schulthess, F. T., Galasso, R., Castellani, L. W. & Maedler, K. The antiinflammatory cytokine interleukin-1 receptor antagonist protects from high-fat diet-induced hyperglycemia. *Endocrinology* **149**, 2208–2218 (2008).
87. Smith, N., Ferdaoussi, M., Lin, H. & MacDonald, P. E. IP glucose tolerance test in mouse. *protocols.io* <https://doi.org/10.17504/protocols.io.wxhffj6> (2020).
88. Fung, C., Lock, R., Gao, S., Salas, E. & Debnath, J. Induction of autophagy during extracellular matrix detachment promotes cell survival. *Mol. Biol. Cell* **19**, 797–806 (2008).
89. Gu, X. et al. SAMTOR is an S-adenosylmethionine sensor for the mTORC1 pathway. *Science* **358**, 813–818 (2017).

Acknowledgements

This work was supported by JDRF advanced postdoctoral fellowship (JDRF-APF), the German Research Foundation (DFG) and the European Foundation for the Study of Diabetes (EFSD). Human pancreatic islets were kindly provided by the NIDDK-funded Integrated Islet Distribution Program (IIDP) at City of Hope, NIH Grant # 2UC4DK098085, the JDRF-funded IIDP Islet Award Initiative and through the ECIT Islet for Basic Research program supported by JDRF (JDRF award 31-2008-413). We thank J. Kerr-Conte and Francois Pattou (European Genomic Institute for Diabetes, Lille) and ProdoLabs for high quality human islet isolations, Katrischa Hennekens (University of Bremen) for excellent technical assistance and animal care, Petra Schilling (University of Bremen) for pancreas sectioning. We are very grateful to Dario Furlani (Zeiss, Jena) for the continuous help and excellent support of the confocal analyses. INS-1E cells were kindly provided by Claes Wollheim (Lund and Geneva Universities), the human insulinoma CM cell line by Paolo Pozzilli (Barts and the London School of Medicine, Queen Mary, University of London, UK), Rip-Cre mice by Susanne Ullrich (Medizinische Klinik, Universitätsklinikum, Tübingen, Germany) and plasmids from

Jixin Dong (Nebraska Medical Center, Omaha, NE), Jayanta Debnath (UCSF, San Francisco, CA, USA), Xiaolong Yang (Queen's University, Kingston, Ontario, Canada), Wenjian Gan (Medical University of South Carolina, SC, USA), Wenyi Wei (Harvard Medical School, Boston, MA, USA) and David Sabatini (MIT, Boston, MA, USA).

Author contributions

Conceptualization: A.A.; methodology: T.Y., K.A., K.M., and A.A.; formal analysis: T.Y., K.A., K.M., and A.A.; investigation: T.Y., K.A., S.N., S.G., A.P., J.G., M.R., B.L., K.D.D.G., Z.A., K.M., and A.A.; writing—original draft: T.Y., K.A., K.M., and A.A.; writing—review & editing: T.Y., K.A., K.M., and A.A.; resources: D.S.L., K.M., and A.A.; funding acquisition: K.M. and A.A.; supervision: K.M. and A.A.

Funding

Open Access funding enabled and organized by Projekt DEAL.

Competing interests

The authors declare no competing interests.

Additional information

Supplementary information The online version contains supplementary material available at <https://doi.org/10.1038/s41467-021-25145-x>.

Correspondence and requests for materials should be addressed to K.M. or A.A.

Peer review information *Nature Communications* thanks Mark Magnuson and the other, anonymous, reviewer(s) for their contribution to the peer review of this work.

Reprints and permission information is available at <http://www.nature.com/reprints>

Publisher's note Springer Nature remains neutral with regard to jurisdictional claims in published maps and institutional affiliations.



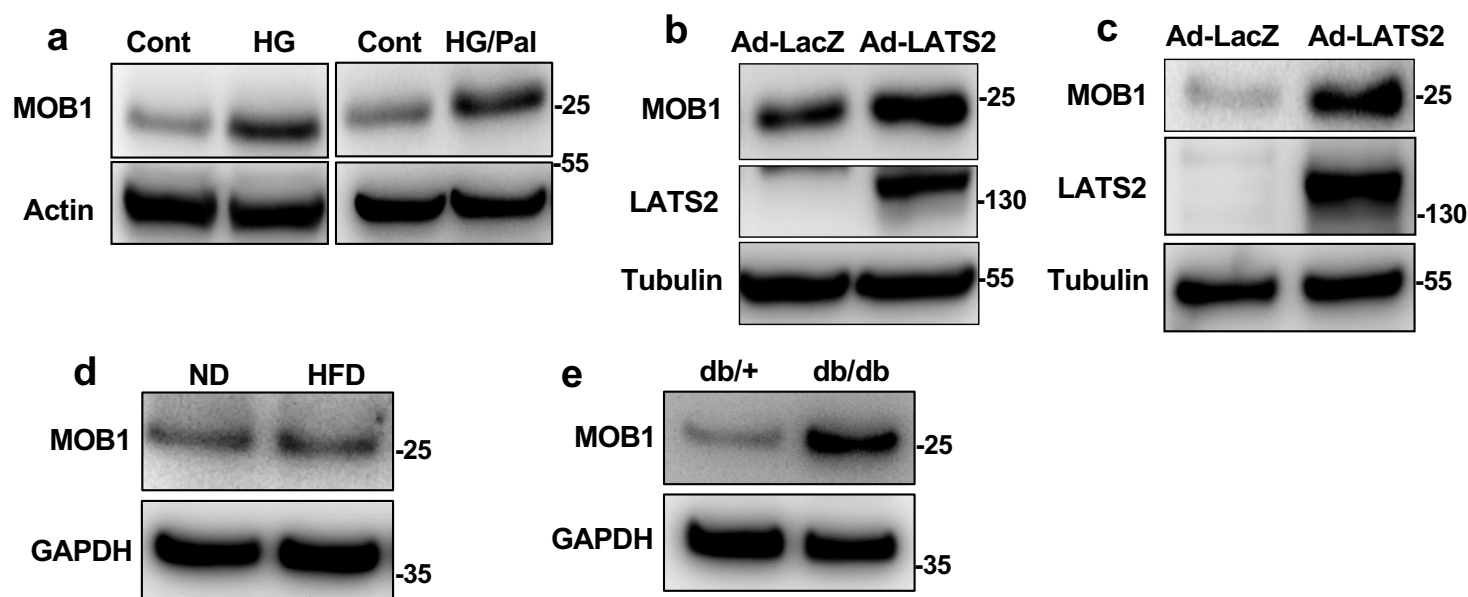
Open Access This article is licensed under a Creative Commons Attribution 4.0 International License, which permits use, sharing, adaptation, distribution and reproduction in any medium or format, as long as you give appropriate credit to the original author(s) and the source, provide a link to the Creative Commons license, and indicate if changes were made. The images or other third party material in this article are included in the article's Creative Commons license, unless indicated otherwise in a credit line to the material. If material is not included in the article's Creative Commons license and your intended use is not permitted by statutory regulation or exceeds the permitted use, you will need to obtain permission directly from the copyright holder. To view a copy of this license, visit <http://creativecommons.org/licenses/by/4.0/>.

© The Author(s) 2021

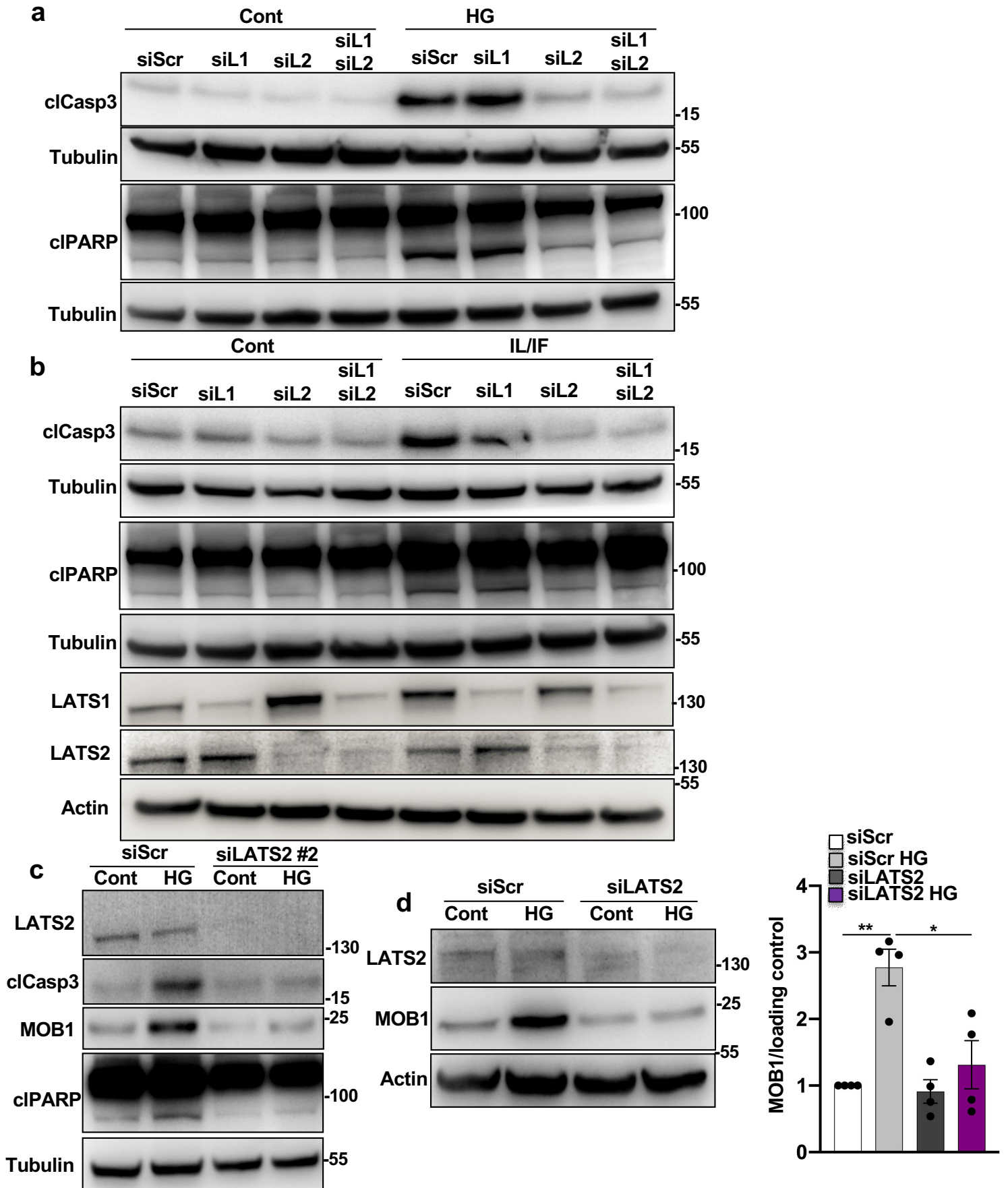
Supplementary Information

**The Hippo kinase LATS2 impairs pancreatic β -cell survival in diabetes
through the mTORC1-autophagy axis**

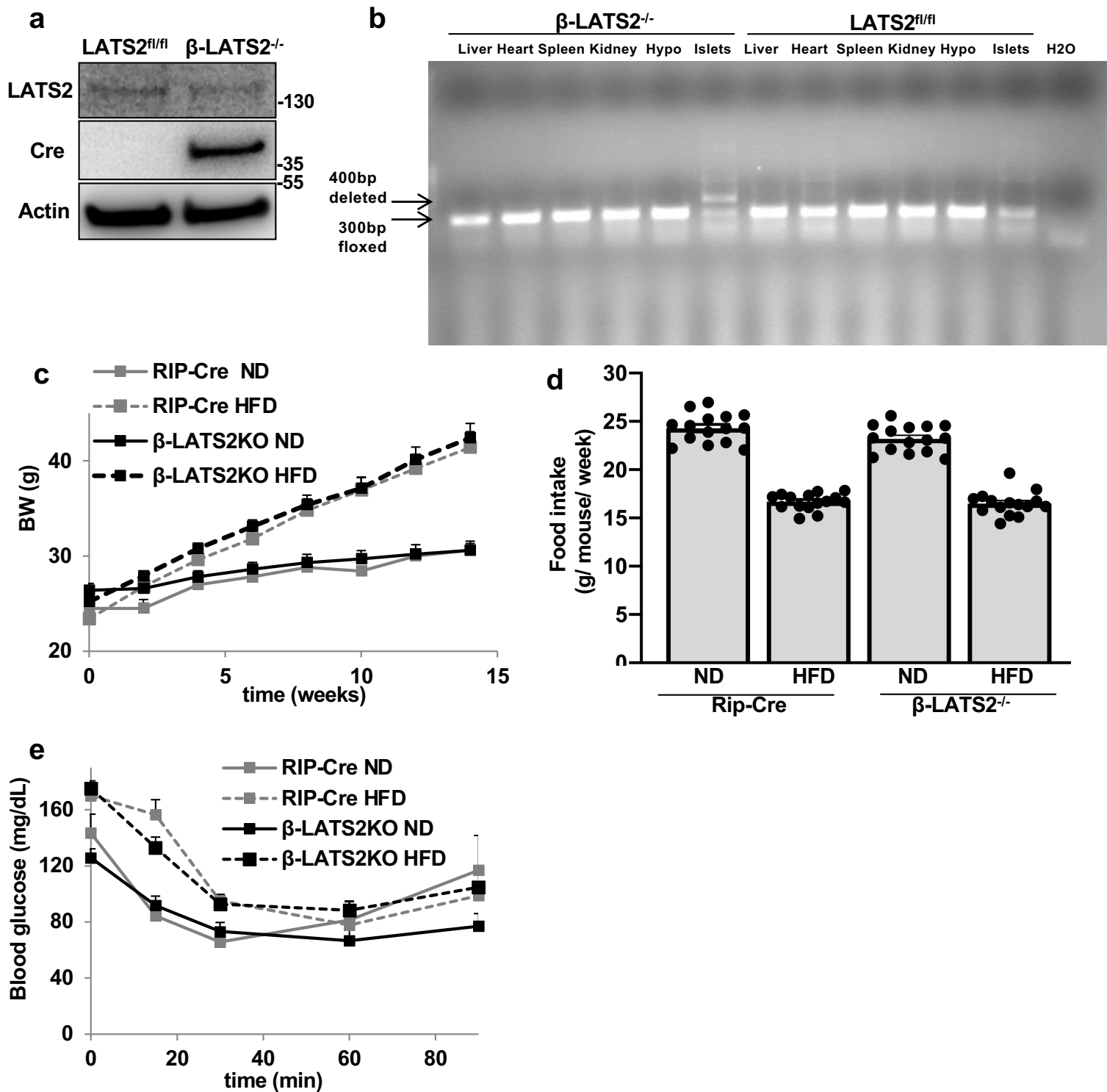
Ting Yuan, Karthika Annamalai, *et al.*



Supplementary Figure 1. MOB1 is upregulated by diabetogenic conditions and LATS2. Representative Western blots **(a)** of INS-1E cells treated with 22.2 mM glucose (HG) alone or with 0.5 mM palmitate (HG/Pal) for 48h, **(b,c)** of INS-1E cells **(b)** and human islets **(c)** transduced with LacZ control or LATS2 adenoviruses for 48 h, **(d,e)** of isolated islets from **(d)** HFD-treated C57BL/6J mice for 16 weeks or **(e)** from obese diabetic leptin receptor-deficient db/db mice and their corresponding controls cultured overnight and transfected with the N-luc-YAP15-S127 plasmid for 24 hours. GAPDH blots in d,e are from same experiment of Figure 1f,g, respectively. a,c-e: n=3 independent experiments; b: n=3 different human islets isolations.

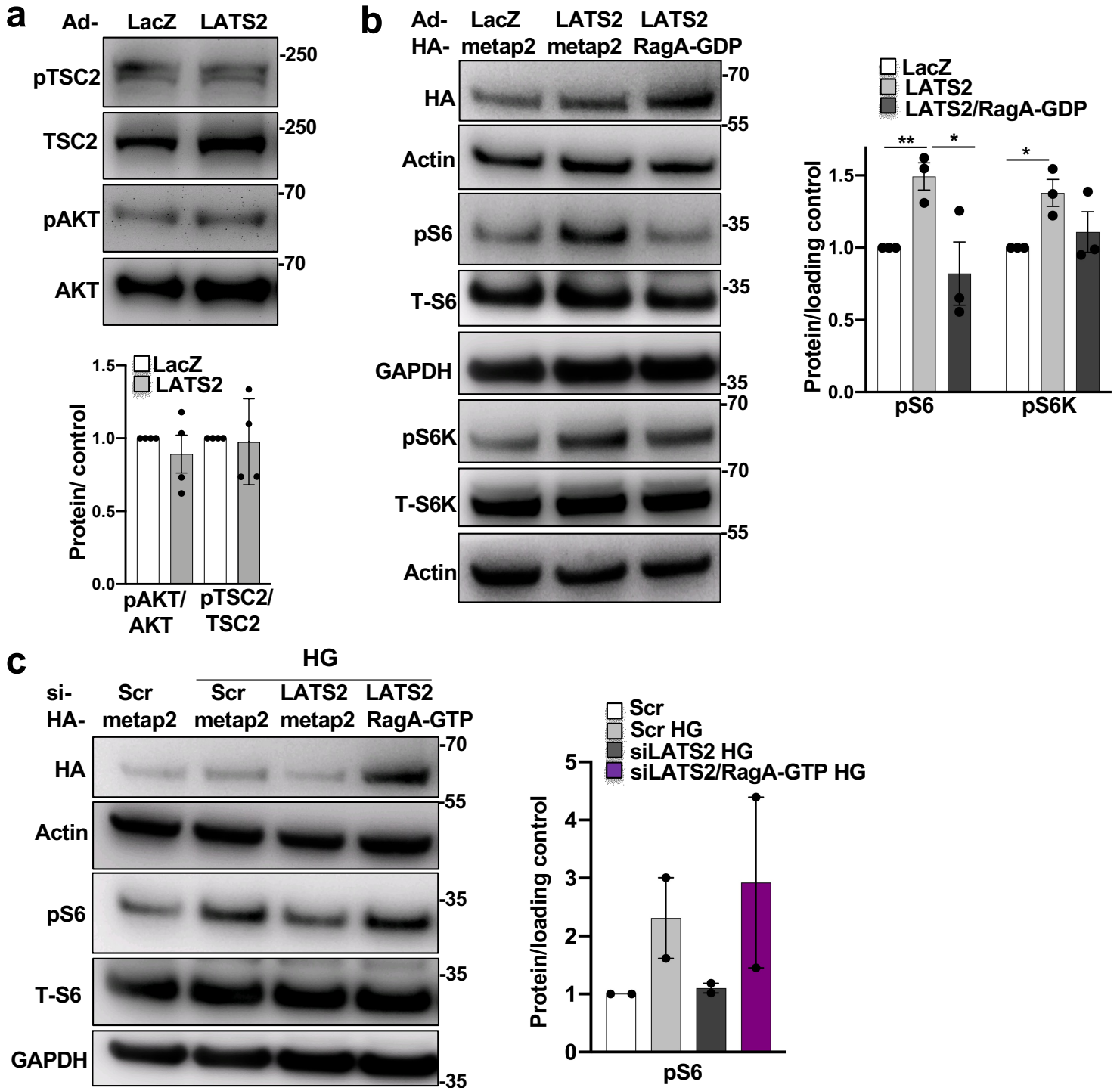


Supplementary Figure 2. LATS2 but not LATS1 knockdown protects from β -cell apoptosis. (a,b) Representative Western blots of INS-1E cells transfected with LATS1 and/or LATS2 siRNA or control siScr and treated with (a) 22.2 mM glucose (HG) or (b) 2 ng/mL IL1 β plus 1000U/mL IFN γ (IL/IF) for 48 h, (c) of INS-1E cells transfected with LATS2 siRNA (second pool #2) or control siScr and treated with the 22.2 mM glucose (HG) for 48 h (a-c: n=1 experiment), (d) of INS-1E cells transfected with LATS2 siRNA or control siScr and treated with 22.2 mM glucose (HG) for 48 h with the respective pooled quantitative densitometry analysis (right panel; n=4 independent experiments). Data are expressed as means \pm SEM. * p <0.05, ** p <0.001; by two-tailed Student's t -test.

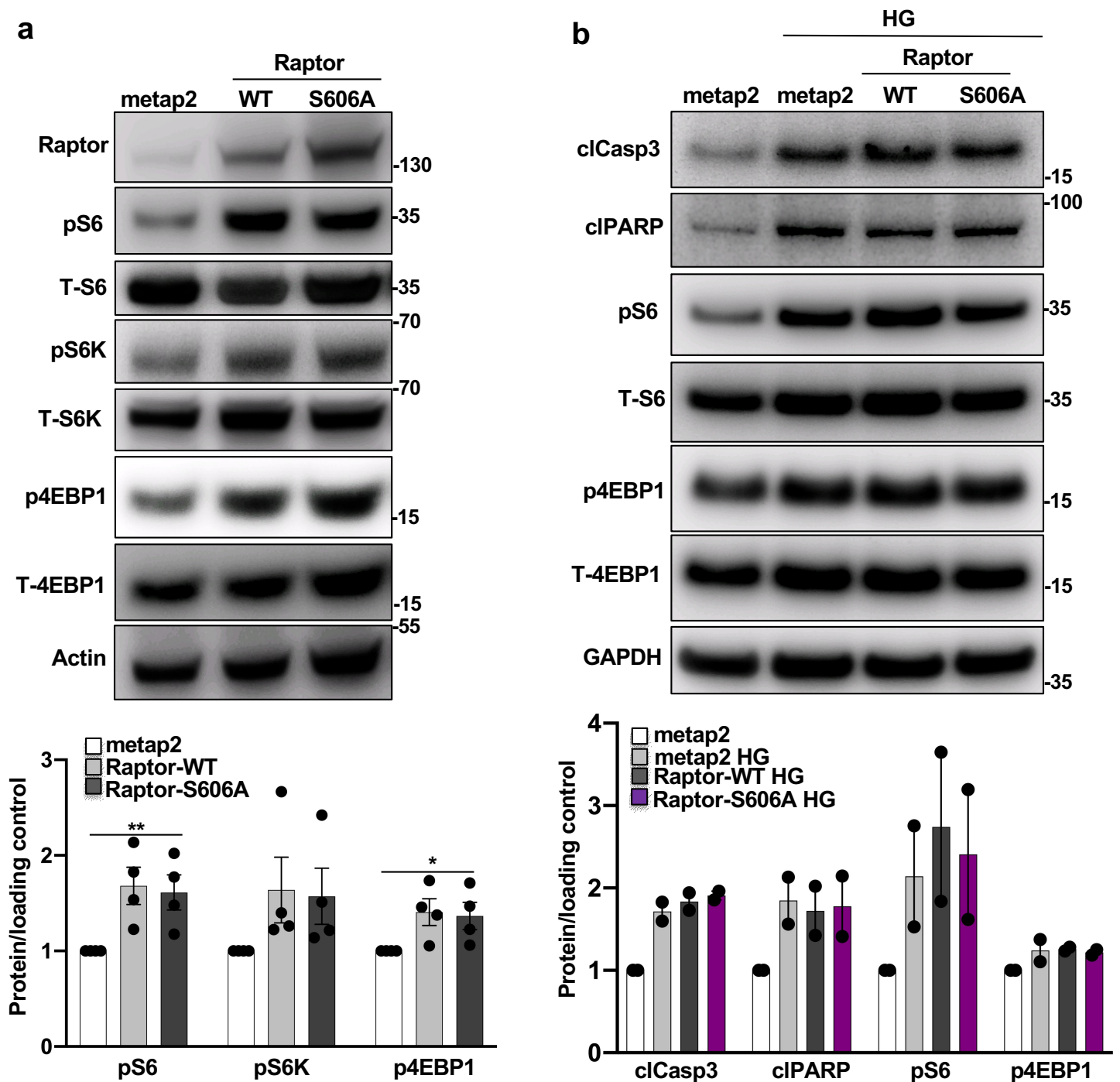


Supplementary Figure 3. Characterization of β -cell specific LATS2 knockout mice (β -LATS2^{-/-}).

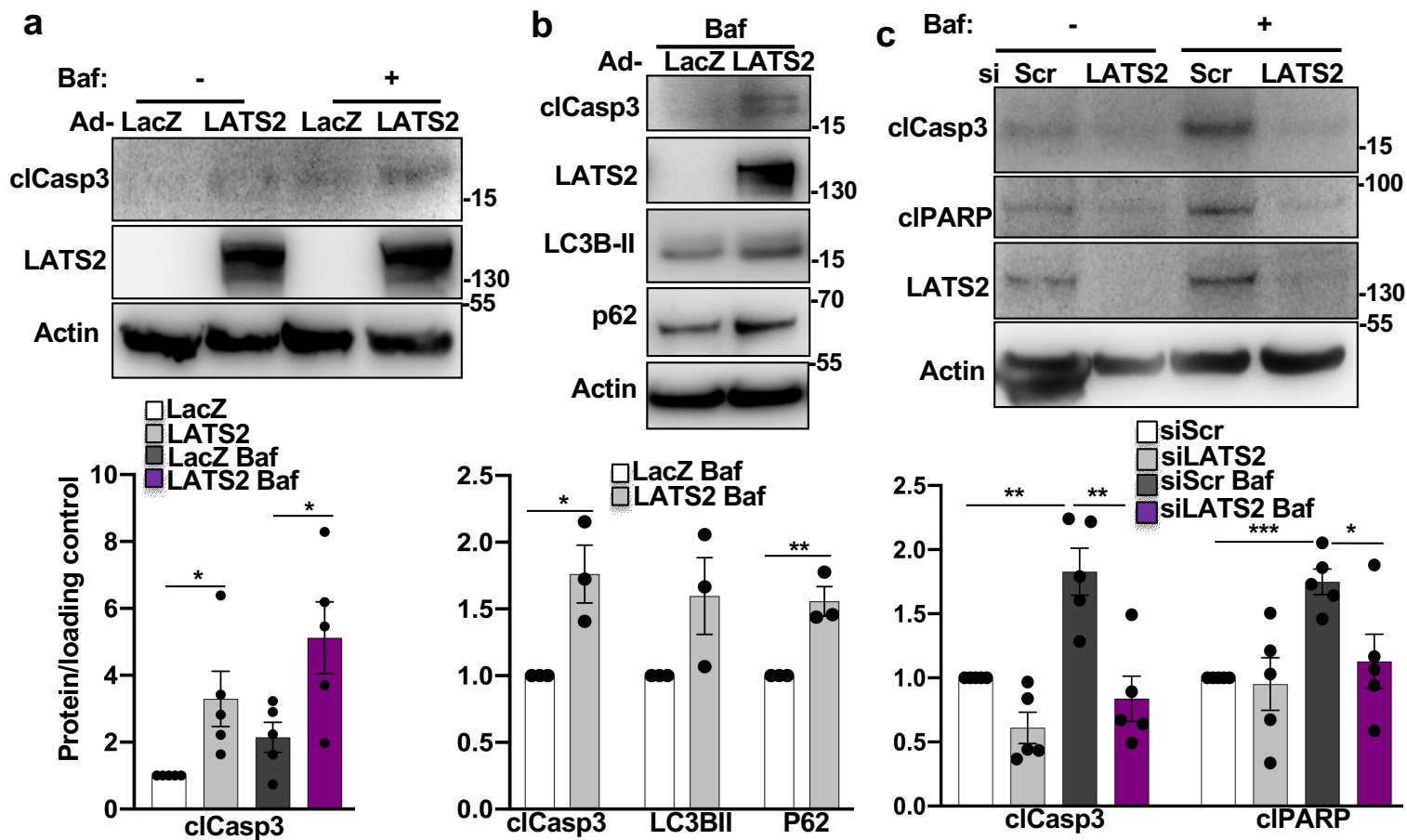
(a) Representative Western blot analysis of protein lysates from islets of β -LATS2^{-/-} and LATS2^{fl/fl} control mice (n=3 independent experiments). (b) PCR analysis of Cre-mediated LATS2 gene deletion in genomic DNA isolated from liver, heart, spleen, kidney, hypothalamus and pancreatic islets of β -LATS2^{-/-} and LATS2^{fl/fl} control mice (n=3 mice/group). (c-e) β -LATS2^{-/-} and Rip-Cre control mice were fed a normal (ND) or high fat/ high sucrose diet ("Surwit"; HFD) for 17 weeks. (c) Body weight is expressed as means \pm SEM from Rip-Cre ND n=8; Rip-Cre HFD n=19; β -LATS2^{-/-} ND n=10; β -LATS2^{-/-} HFD n=16 mice. (d) Average weekly food intake/mouse (average of n=15 weeks). (e) Intraperitoneal insulin tolerance test (ipITT) with 0.75IU/kg BW insulin. Data are expressed as means \pm SEM from Rip-Cre ND n=7; Rip-Cre HFD n=17; β -LATS2^{-/-} ND n=10; β -LATS2^{-/-} HFD n=13 mice.



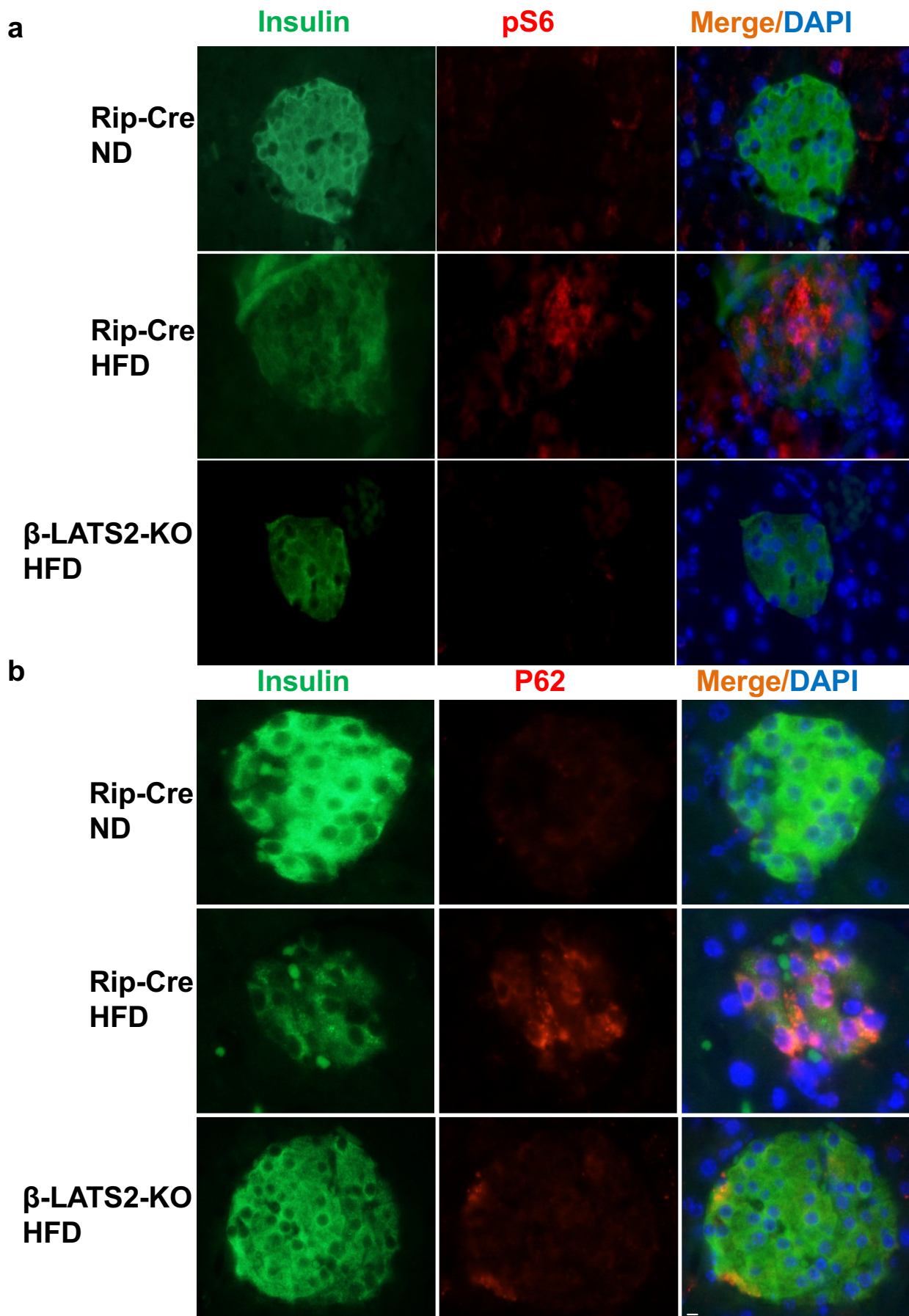
Supplementary Figure 4. LATS2-mTORC1 signaling axis. Representative Western blots and respective pooled quantitative densitometry analysis of (a) INS-1E cells transduced with LacZ control or LATS2 adenoviruses for 48 h (n=4 independent experiments), (b) of INS-1E cells transfected with dominant negative GDP bound RagA (HA-RagA-GDP; RagA-T21L) or metap2 (control) and then transduced with Ad-LacZ or Ad-LATS2 for 48 h (n=3 independent experiments), (c) of INS-1E cells transfected with siLATS2 or control siScr and constitutively active GTP bound RagA (HA-RagA-GTP; RagA-Q66L) or control metap2 and then treated with 22.2 mM glucose (HG) for 24 h (n=2 independent experiments). Data are expressed as means \pm SEM. *p<0.05, **p<0.01; by two-tailed Student's *t*-tests.



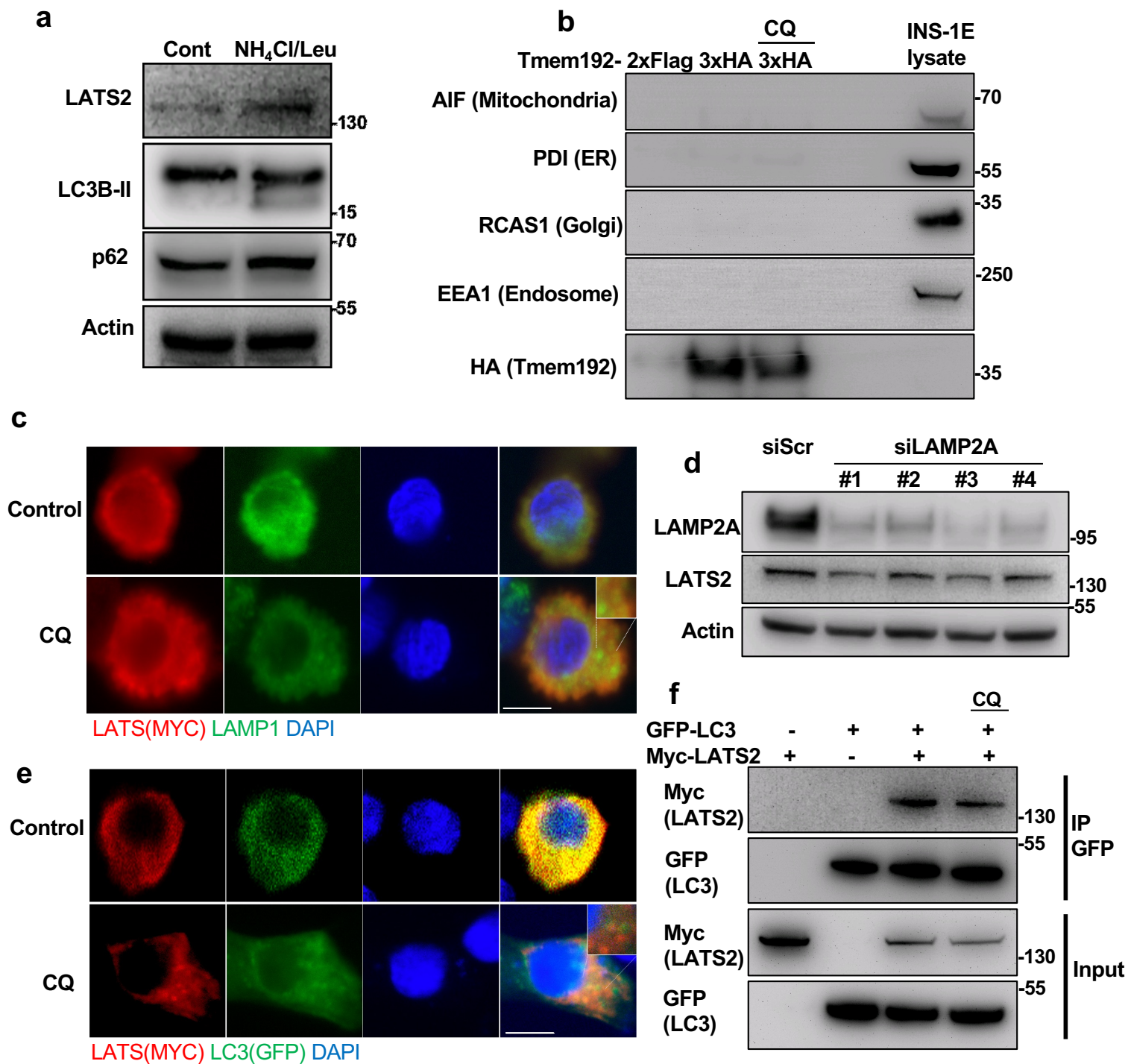
Supplementary Figure 5. Raptor-S606A mutant does not regulate mTORC1 and apoptosis in the β -cells. Representative Western blots (upper panels) and pooled quantitative densitometry analysis (lower panels) of **(a)** INS-1E cells transfected with Raptor-WT or Raptor-S606A mutant or control metap2 for 48 h ($n=4$ independent experiments), **(b)** of INS-1E cells transfected with Raptor-WT, Raptor-S606A mutant or control metap2 and then treated with 22.2 mM glucose (HG) for 24 h ($n=2$ independent experiments). Data are expressed as means \pm SEM. * $p<0.05$, ** $p<0.01$; by two-tailed Student's t -test.



Supplementary Figure 6. LATS2-autophagy crosstalk. Representative Western blots and pooled quantitative densitometry analysis (lower panels) of INS-1E cells **(a)** and human islets **(b)** transduced with LacZ control or LATS2 adenoviruses and then treated with 20 nM Bafilomycin A1 (Baf) for 4h (n=5,3 independent experiments respectively for INS-1E and human islets), **(c)** of INS-1E cells transfected with siLATS2 or siScr and then treated with Bafilomycin A1 (n=5 independent experiments). Data are expressed as means \pm SEM. * $p < 0.05$, ** $p < 0.01$, *** $p < 0.001$; by two-tailed Student's *t*-test.



Supplementary Figure 7. LATS2 regulates mTORC1 and autophagy in HFD induced diabetic mice. Representative triple-stainings for phospho-S6 (pS6; red, a), or p62 (red, b), insulin (green) and DAPI (blue) are shown from pancreatic sections obtained from β -LATS2^{-/-} and Rip-Cre control mice fed a normal (ND) or high fat/ high sucrose diet (“Surwit”; HFD) for 17 weeks. Scale bar depicts 10 μ m.



Supplementary Figure 8. LATS2-autophagy crosstalk. (a) Representative Western blot of INS-1E cells treated with a cocktail of 100 μ M Leupeptin and 10 mM NH_4Cl for 12h. (b) INS-1E cells were co-transfected with LATS2-Myc and Tmem192-3xHA or Tmem192-2xFlag plasmids for 48h. One set of cells were treated with 50 μ M CQ for last 4h. Representative Western blot of lysosomes isolated from INS-1E cells together with INS-1E total lysate is shown. (c) Representative confocal microscopy-acquired triple-stainings for Myc-LATS2 (Myc; red) or LAMP1 (green) and DAPI (blue) are shown from human insulinoma CM β -cells left untreated or treated with CQ (100 μ M CQ for the last 6h). (d) Representative Western blot of INS-1E cells transfected with with siScr or LAMP2A for 72h. (e) Representative confocal microscopy-acquired triple-stainings for Myc-LATS2 (Myc; red) or LC3-GFP (GFP; green) and DAPI (blue) are shown from INS-1E cells left untreated or treated with CQ (100 μ M CQ for the last 6h). (f) INS-1E cells were transfected GFP-LC3 and /or LATS2-Myc plasmids for 48h. One set of cells were treated with 50 μ M CQ for last 4h. Representative Western blot of immunoprecipitation using anti-GFP magnetic beads is shown. Scale bar depicts 10 μ m.

a

Motif	Start	End	Pattern	PSSM Score
xLIR	666	671	SMFVKI	12
WxxL	80	85	IRYSLL	4
WxxL	181	186	ASYHQL	7
WxxL	214	219	YLFPGV	-3
WxxL	284	289	GGYASL	8
WxxL	653	658	SNYNRL	7
WxxL	677	682	GAFGEV	3
WxxL	840	845	DLWDDV	16
WxxL	888	893	KGYTQL	10
WxxL	894	899	CDWWSV	13
WxxL	902	907	ILFEML	7
WxxL	971	976	PFFSAI	3
WxxL	1000	1005	SNFDPV	10
WxxL	1020	1025	KAWDTL	16

b

```

>NP_055387.2 serine/threonine-protein kinase LATS2 [Homo sapiens]
MRPKTFPATTYSGNSRQLQEIREGLKQPSKSSVQGLPAGPNSDTSLDKVLGSKDATRQQQMRATPKF
GPYQKALREIRYSLLPFANESGTSAAAENVNRQMLQELVNAGCDQEMAGRALKQTGSRSEIAALEYISKMG
YLDPRNEQIVRVIKQTS PGKGLMPTPVTRRPSFEGTGDSFASYHQLSGTPYEGPSFGADGPTALEEMPRP
YVDYLFPGV GPHGPGHQHQHPPKGYGASVEAAGAHFPLQGAHYGRPHLLVPGEPLGYGVQRSPSFQSKTP
PETGGYASL PTKGQGPPGAGLAFPPPAAGLYVPHPHHKQAGPAAHQHLVLSRSQVFASDSPQSLLTP
SRNSLNVLDLYELGSTSVQQWPAATLARRDSLQKPGLEAPPRAHVAFRPDCPVPSRTNSFNHQPRPGPPG
KAEPSPAPNTVTAVTAAHILHPVKSVRVL RPEPQTAVGSPHPAWVPAPAPAPAPAPAAEGLDAKEEH
ALALGGAGAFPLDVEYGGPDRRCPPPPYPKHL LRSKSEQYDLDSL CAGMEQSLRAGPNEPEGGDKSRKS
AKGDKGGKDKKQIQ TSPVPVRKNSRDEEKRESRIKSYSPYAFKFFMEQHVENVIKTYQQQVNRRLQLEQE
MAKAGLCEAEQE QMRKI LYQKE SNYNRL KRAKMDK SMFVKI KTLGI GAFGEV CLACKVDTHALYAMKTLR
KKDVLNRNQVAHVKAERDILAEADNEWVKLYYSFQDKDSL YFVMDY I PGGDMMSLLIRMEVFPEHLARF
YIAELTLAIESVHKMGFIHRDIKPDN ILIDL DGHIKLTD FGLCTGFRWTHNSKYYQKGS HVRQDSMEPSD
LWDDVSNCR CGDRLK TLEQRARKQHQRCLAHSLVGT PNYIAPEVLLR KGYTQLCDWWSVGV ILFEMLVGQ
PPFLAPTPTETQLKVINWENTLH I PAQVKLSPEARDLITK LCCSADHRLGRNGADDLKAHPFFSAIDFSS
DIRKQPAPYVPTISHPMDT SNFDPV DEESPWN DASEGST KAWDTL TSPNNKHPEHAFYEFTFRFFDDNG
YFRCPKPSGAEASQAESSDLESSDLVDQTEGCQPVYV

```

Supplementary Figure 9. Identification of LIR motifs in human LATS2 protein sequence. (a) Screenshot of sequences, position and PSSM scores of the several putative LIR and xLIR motifs for human LATS2 protein obtained from the iLIR database (<https://ilir.warwick.ac.uk>). (b) xLIR (green) and LIR (yellow) motifs are highlighted in FASTA sequence of human LATS2 protein.

3 DISCUSSION

1. Neratinib protects pancreatic β -cells in diabetes

Why neratinib as a MST1 kinase inhibitor ?

The key finding that the upregulation and hyperactivation of the Hippo central component MST1 kinase in the stressed β -cells cause increased β -cell apoptosis led us to work on the identification and elaboration of potent small molecule MST1 inhibitors, as MST1 inhibition is shown to be a promising approach for β -cell protective therapy in diabetes [1, 2]. Our collaboration team at CALIBR developed a high-throughput LanthaScreen Eu kinase binding assay platform to test for 641 drug-like kinase inhibitors and as a result, we identified neratinib as a potent MST1 kinase inhibitor. Although neratinib is a well-known irreversible pan-HER/EGFR tyrosine kinase inhibitor which has been approved by the FDA as an effective drug for HER2-positive breast cancer, our data showed its steadfast potency on MST1 inhibition along with additional kinases other than HER2/EGFR family such as LOK, MAP4K4, MAP4K5 and YES, indicating the non-selective nature of neratinib, as the development of a selective kinase inhibitor is highly challenging. Also, it was reported that the administration of tyrosine kinase inhibitors (TKI) such as imatinib (against c-Abl and PDGFR), erlotinib (against EGFR family) and sunitinib (against PDGFR and VEGFR2) exhibited antihyperglycemic effects reversing both T1D and T2D in several preclinical as well as clinical cases [3, 4]. Moreover, neratinib is tolerable and safe as it could enter the phase 2 and 3 clinical trials of cancer therapy without any hesitation, and at this time my lab has started the investigation of its effect on β -cell death and dysfunction in diabetes with a hope that this drug could be recapitulated in the clinical diabetes setting.

Neratinib blocks MST1 signaling and MST1 induced β -cell apoptosis in vitro and in vivo

I put my efforts to analyze whether the protective effect of neratinib on β -cell apoptosis is MST1 dependent in both INS1-E cells and isolated primary human islets. Neratinib strongly abolished MST1 phosphorylation and β -cell apoptosis under diabetogenic conditions. Specifically, I observed very significant reduction in the number of apoptotic human β -cells triggered by both glucolipotoxicity and pro-inflammatory cytokines in the neratinib treated human islets. The LATS biosensor (LATS-BS) was developed by Azad *et al* [5], with the purpose of identifying the novel regulators of Hippo pathway, which further enlightened us to use the unique LATS-BS for the purpose of measuring the MST1-LATS2 signaling activation in INS-1E cells under diabetic conditions. As a result, I observed strong induction in the phosphorylation of transfected YAP fragment at serine 127 under MST1 and LATS2 overexpression, this robust induction was significantly reduced by neratinib but not canertinib, an EGFR inhibitor similar to neratinib without

the MST1 family inhibitory activity. These results indicate that the inhibitory action of neratinib against the MST1-LATS2 axis is independent of HER/EGFR inhibition. In line with our finding, Dent *et al.* predicted that neratinib reduced MST auto-phosphorylation and activation in F1199 pancreatic cancer cells [6], which corroborates our data of neratinib based MST1 inhibition. Moreover, I observed restoration of β -cell survival by neratinib from β -cell apoptosis induced by forced MST1 overexpression in human islets. Altogether, neratinib rescues β -cells from apoptosis possibly through direct inhibition of MST1 and its subsequent downstream signaling.

At a preclinical level *in vivo*, neratinib attenuated hyperglycemia, improved glucose tolerance and increased insulin secretion in both the T1D (MLD-STZ) and the T2D mouse model (obese diabetic LepR-deficient db/db mice). Notably, from the *ex vivo* analysis, I observed significant increase in β -cell mass as a consequence of increased β -cell proliferation and decreased β -cell apoptosis in the pancreatic sections of db/db mice, however, this effect was partially fulfilled in the pancreatic sections of STZ mice as there was no change in β -cell proliferation but we could notice reduced β -cell apoptosis which reflected in increased β -cell mass. Moreover, neratinib remarkably restored β -cell function in the diabetic mouse models as we observed significant increase in insulin secretion as well as the nuclear expression of β -cell functional markers namely PDX1 and NKX6.1. As MST1 directly targets PDX1 for degradation [2], these data suggest that neratinib blocks MST1 induced PDX1 nuclear export and degradation under diabetic conditions, resulting in the controlled maintenance of β -cell identity and function.

Could neratinib be a promising therapeutic target for β -cell protection and diabetes treatment?

Beyond breast cancer, neratinib is one of the most widely studied drug in other types of cancer such as non-small cell lung, colorectal, pancreatic and biliary cancer as a single agent or in combination with other drugs by mainly targeting the EGFR/HER2 pathway. Importantly, neratinib exhibited therapeutic potency against liver fibrosis by blocking FGFR expression in hepatic stellate cells that resulted in reduced inflammatory response and hepatic stellate cell (HSC) activation indicating the broad role of neratinib in other pathological diseases [7]. Also, MST1 was shown to phosphorylate autophagy regulator Beclin1 and increase its affinity for mitochondrial protein BCL-2, resulting in suppression of autophagy induction [8]. This insight provides evidence for speculation that MST1 inhibition by neratinib could be critical for enhanced pro-survival autophagy response and reduced β -cell apoptosis, which is in line with our data showing that the protective effect of β -cells by neratinib comes from MST1 inhibition and not from other targets. However, the direct impact of neratinib on autophagy in this context needs to be experimentally investigated.

Another inevitable fact is that EGFR signaling is associated with insulin resistance and inflammation in the insulin target tissues such as liver, muscle and adipose tissue. As a consequence, EGFR inhibition could improve insulin sensitivity and reduce inflammation i.e. reduction in proinflammatory cytokines IL-1 β , TNF α , IL6 and M1 macrophagic infiltration suggesting EGFR inhibition as a therapy for insulin resistance [3, 4]. However, in case of β -cells, we cannot rule out that EGFR signaling is essential for β -cell mass regulation at the postnatal stage and attenuation in EGFR signaling lead to impairment in β -cell growth and eventually diabetes [9, 10]. As several other complex pathways interfere during the utility of neratinib due to its non-selective nature, we are currently developing neratinib-structurally based specific small inhibitors that selectively target MST1 kinase with no significant inhibition of EGFR for the effective MST1 inhibition in diabetes treatment, also with the goal to prevent the perturbing gastrointestinal effects of many EGFR inhibitors. Although an enantiopure organoruthenium inhibitor 9E1 was one of the first developed MST1 inhibitors, it was precluded as it consistently showed off-target effects for unrelated protein kinases such as proto-oncogene serine/threonine protein kinase PIM1 and glycogen synthase kinase 3, GSK-3 β [11]. Recently, Faizah *et al* disclosed in their study on XMU-MP-1, another recently identified MST1/2 inhibitor, that XMU increased β -cell survival in INS1-E cells in vitro and significantly improved glucose tolerance and enhanced β -cell area and number in the STZ induced diabetic mouse model [12], which evidently strengthens the idea of MST1 inhibition as a therapeutic intervention for the treatment of diabetes.

2. The Hippo kinase LATS2 impairs pancreatic β -cell survival in diabetes through mTOR-autophagy axis.

2.1. Endogenous LATS is activated in β -cells under diabetogenic conditions.

We moved further with the investigation of downstream targets of MST1 kinase that regulate β -cell apoptotic signals. Here, I used LATS biosensor LATS-BS as mentioned above, for the purpose of measuring LATS activity in INS1-E cells under different diabetic conditions. LATS-BS based dual luciferase assay showed significant increase in the firefly luciferase signal in INS1-E cells cultured under glucotoxicity and glucolipotoxicity, as a result of exogenously transfected N-luc-YAP(15) and C-luc-14-3-3 complementation. This was further corroborated by the immunoblot data, which showed increased p-YAP(S127) signal in the INS1-E cells cultured under diabetogenic conditions. The increased p-YAP(S127) signal that is detectable in the INS1-E cells under diabetic conditions is from the exogenously transfected LATS-BS luciferase reporter constructs which contains 15 aa residue of YAP(S127), as YAP is not expressed and it is

undetectable at the protein level in adult human and mouse primary islet cells as well as commonly preferred β -cell lines, namely MIN6, INS1 and RIN β -cell lines [13].

However, there are few limitations regarding the use of LATS-BS for LATS activity detection. There is a probability of existence of additional signaling pathways that influence and regulate p-YAP(15) and 14-3-3 interaction, which influence LATS-BS based LATS activity measurement. It was reported that nemo-like kinase (NLK) phosphorylates YAP at the Ser128 region interrupting the p-YAP-14-3-3 interaction and enhances its nuclear localization [14, 15]. However, the significant increase in LATS-BS signal in INS1 β -cells under diabetic conditions documented by both luciferase assay and immunoblot analysis of p-YAP-S127 is mainly from increased LATS activity despite the potential existence of signaling interruptions.

Additionally, I proved that LATS activity is also upregulated in islets isolated from HFD-fed mice as well as from extreme diabetic db/db mice. This is in line with the recent study published by Guo *et al.*, where LATS2 mRNA and protein levels were markedly upregulated in both steric acid treated β -TC6 cells and islets from mice fed with steric acid diet [16]. Hence, altogether our data suggests that LATS is highly upregulated in β -cells under diabetic conditions.

Another indirect proof of LATS signaling activation is the upregulation of MOB1 in the INS1-E cells treated with either glucotoxicity or with glucolipotoxicity. MOB1 functions as a scaffolding protein binding to both Hippo LATS1/2 and MST1/2 kinases, and importantly facilitates the activation of LATS1/2 kinases by the MST1/2 kinases via transphosphorylation event [17]. We also showed that MOB1 is regulated by loss- and gain-of functional modulation of LATS2 activity in β -cells confirming (i) the increased activation of MOB1-LATS axis in the Hippo pathway in diabetic β -cells and (ii) LATS2's control of MOB1 levels.

2.2. Why LATS2 hyperactivation is detrimental for β -cell survival?

Our data showed that LATS2 overexpression increased β -cell apoptosis and impaired glucose stimulated insulin secretion in human islets suggesting that LATS2 impairs both β -cell function and survival. This is consistent with Guo *et al.*'s work [16], where they noticed LATS2-dependent impairment in glucose stimulated insulin secretion and apoptosis in steric acid treated β -TC6 cells and in primary pancreatic islets. In line with LATS2's function as a pro-apoptotic kinase in β -cells, its role in cell death and especially mitochondria-dependent pathway of apoptosis is well established in several other cell types. Tian *et al.* showed that LATS2 overexpression triggers apoptosis in cardiomyocyte H9C2 cells by repressing protective mitophagy via inactivation of Prx3-Mfn2 pathway [18]. Moreover, LATS2 overexpression in A549 lung cancer cells promoted mitochondria dysfunction by Mff (mitochondria fission factor) mediated mitochondria fission via

MAPK-JNK signaling pathway subsequently resulting in cell apoptosis [19]. Likewise LATS2 overexpression in SW480 human colon cancer cells determined enhanced mitochondria elongation factor-1 (MIEF-1) mediated mitochondria division via the JNK pathway resulting in amplified mitochondrial damage and apoptosis [20]. Furthermore, LATS2 overexpression in two different hepatocellular carcinoma cell lines increased Drp1 mediated mitochondrial division in a wnt/ β -catenin dependent manner causing mitochondria dysfunction, energy depletion and subsequently apoptosis [21]. However, in relation to pancreatic β -cells, one study has shown the significance of Drp1 (dynamin related protein 1) phosphorylation at S616 in instigating mitochondrial fission and cell apoptosis under hypoxia conditions [22]. Thus, under diabetic conditions, the upregulated LATS2 might play a crucial role in modulating key factors such as Drp1 either directly or indirectly to facilitate increased mitochondrial fragmentation, energy depletion, impaired insulin secretion and eventually β -cell apoptosis. Further mechanistic investigations are required to disclose such possibility.

The Hippo kinases LATS2 and LATS1 have both divergent and redundant functions in different cell types [23-35]. Accordingly, we observed that genetic inhibition of LATS2 but not LATS1 played a crucial role in protecting INS-E cells and human islets from apoptosis indicating the distinct role of LATS2 in pancreatic β -cells as a pro-apoptotic kinase under diabetic state. Moreover, I observed significant reduction in the number of TUNEL positive apoptotic β -cells in both isolated islets from β -LATS2-KO mice as well as LATS2 depleted human islets treated with glucolipotoxicity and pro-inflammatory cytokines compared to the control. Consistently, Guo *et al* [16] reported that LATS2 knockdown in β -TC6 cells as well as in isolated mouse primary islets attenuated impairment in insulin secretion and β -cell apoptosis under lipotoxic condition. Altogether, under diabetic state, LATS2 deficiency in a pure β -cell line as well as in human and mouse islets/ β -cells strongly improved β -cell survival.

2.3. LATS2 knockout protects from HFD-induced β -cell failure and diabetes development.

The distinct role of LATS2 as a pro-apoptotic kinase for β -cell turnover under pathological conditions inspired my lab to execute *in vivo* studies using β -cell specific LATS2 knockout mice (β -LATS2-KO). I used mice with a pure C57B/6J background for a diet induced obesity and diabetes study with the aim to identify whether β -LATS2-KO may have a β -cell protective phenotype during β -cell decompensation and failure. As a result, metabolic studies in the long-term HFD fed β -LATS2-KO mice showed highly improved glucose tolerance, increased basal and glucose stimulated insulin secretion with no impact on insulin sensitivity, compared to the HFD-

Rip-Cre control group. The analysis of β -cell mass showed significant increase in compensatory β -cell expansion in pancreatic sections from HFD β -LATS2-KO mice, compared to the control. This enhanced β -cell compensation in response to HFD induced insulin resistance in β -LATS2-KO mice was apparent from the proliferation and apoptosis analyses, as I detected significant increase in the number of Ki67 positive β -cells and a marked decline in TUNEL positive β -cells. This was consistent with our data from STZ model corroborating that β -cell specific LATS2 ablation is beneficiary in subsiding the diabetes development in both STZ and HFD mouse models.

The pancreatic β -cell proliferation and expansion is an integrated signaling process; there are several growth factors and hormones reported to induce β -cell proliferation [36]. In that line, it was shown that epigenetic modulator EZH2, one of the PRC2 complex subunit, is ultimately involved in the adult β -cell expansion via the stimulation and activation of PDGFR- α and ERK1/2 [37, 38]. However, the mRNA levels of EZH2 declines upon ageing in human pancreatic β -cells which might be one of the reasons for a restricted β -cell proliferation and expansion. On the other hand, the work of Torigata *et al* showed that the kinase LATS2 plays a substantial role in coordinating epigenome by directly phosphorylating PRC2 subunits EZH2 and SUZ12 at multiple sites, thereby positively regulating histone methyltransferase activity of PRC2 complex [33]. However, the role of LATS2 in the adult β -cells at the physiological conditions is not clearly known. There could be a probability that LATS2 association with EZH2 tightly restrict its involvement in β -cell proliferation and expansion, which might be for the stemness maintenance, and hence the loss of LATS2 in the adult β -cells may influence the increased β -cell compensation via EZH2 mediated β -cell expansion. As I observed significant increase in proliferation and β -cell mass in HFD-treated β -LATS2-KO mice, an EZH2-directed epigenetic modulation in the LATS2 KO β -cells might play a significant role in the increased β -cell compensation, but this needs to be investigated.

2.4. LATS2 hyperactivation triggers β -cell apoptosis via mTORC1 signaling pathway

As mentioned in the introductory chapter, previous data from my lab and other groups showed that the master metabolic pathway mTORC1 is chronically hyperactivated in pancreatic islets/ β -cells from human T2D patients, T2D animal models and also in INS1-E cells and human islets cultured under glucotoxicity [39-44]. Consistent with my lab's previous findings [44] and data presented in this thesis, Jaafar *et al* recently showed that islets isolated from diabetic mice demonstrate a higher expression of mTORC1 activators and effector genes [45], correlated with islet immunostaining of pS6 (at Ser240/244 activity), and inversely correlated with downregulation

of β -cell maturation genes (Ins2, Ucn3, G6pc2, Erol1b, and Pcsk1). This suggests that, as hyperglycemia progresses, mTORC1 activity is increased by generating a shift from the AMPK catabolic pathway to mTORC1 signaling, as there is a reduction in AMPK activity and increase in the expression of disallowed genes. This phenocopies an immature phenotype of neonatal pancreatic β -cells with increased basal insulin secretion and impairment in glucose response [45]. Hence, a T2D state is characterized by reversion of β -cells from a mature to an immature phenotype with increased mTORC1 activity [45].

Usually, the short-term transient hyperactivation of mTORC1 plays a positive role in β -cell metabolic adaptation and mediates β -cell compensatory mechanisms such as β -cell hypertrophy or hyperplasia, and subsequent hyperinsulinemia. However, chronic hyperinsulinemia for a prolonged period may stimulate constitutive increase in proinsulin biosynthesis causing increased ER stress, increase in accumulation of damaged mitochondria and mitochondrial dysfunction [41]. Moreover, prolonged mTORC1 hyperactivation showed reduced mitophagy as a result of impairment in autophagic machinery [41]. Correspondingly, the prolonged mTORC1 hyperactivation causes increase in insulin resistance in β -cells by several proposed ways of negative feedback loops [43], firstly, by mTORC1 and S6K1 mediated direct phosphorylation and degradation of IRS1/2, secondly, by mTORC1 mediated direct phosphorylation and activation of Growth factor bound receptor 10 (Grb10), which negatively regulates RTK-PI3K signaling, thirdly, the hyperactivated S6K1 directly phosphorylates mTORC2 component, Rictor at T1135 and diminishes the activity of mTORC2-AKT signaling, and lastly, the chronically activated S6K1 phosphorylates sin1, a key component of mTORC2, and triggers the dissociation of sin1 from mTORC2. Hence, the sustained nutrient overload in the diabetic environment further potentiates the over-activated mTORC1 mediated negative feedback loops, subsequently leading to disruption in insulin and mTORC2 signaling as a contribution towards increased insulin resistance in β -cells [43]. All the above-mentioned factors associated with prolonged hyperactivation of mTORC1 for a longer period, namely, increased ER stress, increased dysfunctional mitochondrial aggregates, reduced mitophagy and increased insulin resistance in β -cells act together to cause T2D.

2.4.1. Does LATS2 control mTORC1 mediated β -cell failure?

Although chronic mTORC1 hyperactivation is deleterious for β -cell function and survival, the signaling pathways regulating mTORC1 hyperactivation are poorly understood. In this context, our data showed that LATS2 knockdown reduced the hyperactivity of mTORC1 and restored β -

cell survival in response to glucotoxicity and glucolipotoxicity in β -cells. Additionally, LATS2 overexpression alone was sufficient to activate mTORC1 activity and induce β -cell apoptosis. In line with this, pharmacological and genetic inhibition of endogenous mTORC1 activity in LATS2 overexpressing β -cells reversed LATS2-induced β -cell apoptosis. Furthermore, I assessed the effect of LATS2 deficiency on mTORC1 by immunohistochemical analysis of pancreatic sections isolated from HFD fed mice. Rip-Cre HFD mice showed higher activity of pS6 (at Ser240/244 activity) which is in line with our previously reported mTORC1 hyperactivity in islets of HFD fed diabetic mice. However, the hyperactivity of mTORC1 is subsided in HFD β -LATS2-KO mice as the pS6 activity is not detected in the pancreatic sections isolated from HFD treated β -LATS2-KO mice, suggesting that LATS2 deletion in β -cells plays a crucial role in the inhibition of HFD induced mTORC1 hyperactivation. All above scenarios clearly show that LATS2 works upstream of mTORC1 in mediating β -cell apoptosis under diabetic conditions.

Contrary to our finding that LATS2 activates mTORC1 in β -cells, Gan *et al.* recently showed that LATS kinases suppress mTORC1 by phosphorylating Raptor, a core component of mTORC1, at Serine 606 which subsequently impairs the Raptor interaction with Rheb in kidney cells [46]. There are several possible explanations for such a discrepancy:

- 1) While our work exclusively focused on LATS2, Gan *et al.* [46] mostly used the other LATS isoform, LATS1 in their experimental analysis, in which they showed that LATS1 phosphorylates Raptor at S606 and the S606A specific mutation largely reduced LATS1 mediated phosphorylation of Raptor. This may suggest that the LATS isoforms have distinct effects on mTORC1.

- 2) LATS1 and LATS2 do not necessarily share redundant functions in all cell types. In the Gan *et al.* study, the majority of biochemical and functional experiments have been performed in HEK293 kidney cells without experimental data from primary or other cell types, and a unifying nature for the proposed mechanism was not provided. In support of this, homozygous phosphomimetic (S606D; *Raptor*^{D/D}) knock-in mice, in which LATS phosphorylation site is constitutively active, displayed diminished mTORC1 signaling in the liver, heart and kidneys but not in the spleen and brain suggesting a tissue or cell type dependent regulation of mTORC1 by LATS kinases.

In relation to the above two suggestive points, our further investigation on the Raptor S606 phosphorylation site especially under glucotoxicity (diabetic condition) in INS1-E cells disclosed several supportive data. I used a phospho-null (S606A) Raptor mutant to determine the potential regulation of Ser606 phosphorylation in the pancreatic β -cells, and observed a similar functional

activity in mTORC1 signaling as represented by increased phosphorylation of its substrates S6, S6K and 4EBP1, compared to WT-Raptor. Moreover, no significant change was noted by Raptor itself as well as its S606 phosphorylation site under glucotoxicity, as neither WT-Raptor nor S606A-Raptor transfected INS1-E cells differentially altered high glucose induced S6-phosphorylation and apoptosis compared to the high glucose treated INS1-E cells transfected with control plasmids. Altogether, this suggests that the Raptor-Ser606 phosphorylation is not the principal regulator of mTORC1 under both basal and glucotoxic condition in pancreatic β -cells.

3) Another explanation may arise from a different cellular context between our study compared to the Gan *et al.* work. While Gan *et al.* showed contact inhibition -as a result of high cell density- is a driving force and a critical factor for the LATS1/2 mediated mTORC1 suppression, we showed LATS2 induced mTORC1 hyperactivation under multi-model diabetogenic conditions independent of cell density.

4) Additionally, Gan *et al.* showed that LATS mediated phosphorylation of Raptor reduces growth factor induced activation of mTORC1 through Rheb but not of the other mTORC1 regulatory branch: amino acid induced activation of mTORC1 [46]. Although the mechanism behind LATS2 mediated mTORC1 activation in β -cells under diabetic conditions is not known yet, LATS2 might be a signaling component of the amino-acid branch which regulates mTORC1 independent of growth factor signaling which is discussed in detail below.

There are multiple signaling mechanisms that regulate mTORC1 activation [47]. One well-described pathway that mediates mTORC1 activation is the growth factor and mitogen-dependent signaling pathway. This will eventually inhibit the well-established negative regulator of mTORC1, known as Tuberous Sclerosis Complex (TSC Complex) [47]. The TSC complex is a heterotrimer composed of TSC1, TSC2 and TBC1D7 subunits [48], which acts as GTPase activating protein (GAP) for the small GTPase Rheb [49]. The growth factor such as Insulin /Insulin like growth factor (IGF) triggers activation of PI3K-AKT signaling, converges on TSC complex, where AKT phosphorylates TSC1/2 at multiple sites and inhibits its activity, resulting in subsequent dislocation of TSC complex from the lysosomal membrane, which relieves Rheb for consequent activation and stimulation of mTORC1 activity (Figure 1 below) [47, 50, 51].

On the other hand, mTORC1 activation is notably regulated by the amino acid mediated signaling branch. The key finding of heterodimeric Rag GTPases as the potential components of amino acid based mTORC1 activation were proposed by Kim *et al.* and Sancak *et al.* [52, 53]. It has been shown that amino acid stimulation transforms the Rags (obligate heterodimers of RagA, RagB, RagC and RagD) into their active nucleotide bound state (RagA/B-GTP bound and RagC/D-GDP bound) which subsequently bind to Raptor and recruit mTORC1 towards the

lysosome membrane where Rheb is located, finally resulting in mTORC1 activation [54] [47, 55]. These mechanistical pathways reflect the significant role of both growth factors and amino acids for mTORC1 activation (Figure 1). Remarkably, glucose mediated mTORC1 activation is also regulated by Rag GTPases, suggesting the heterodimeric Rag GTPases as the 'multi-input nutrient sensor' which eventually mediates the activation of mTORC1 [43, 55].

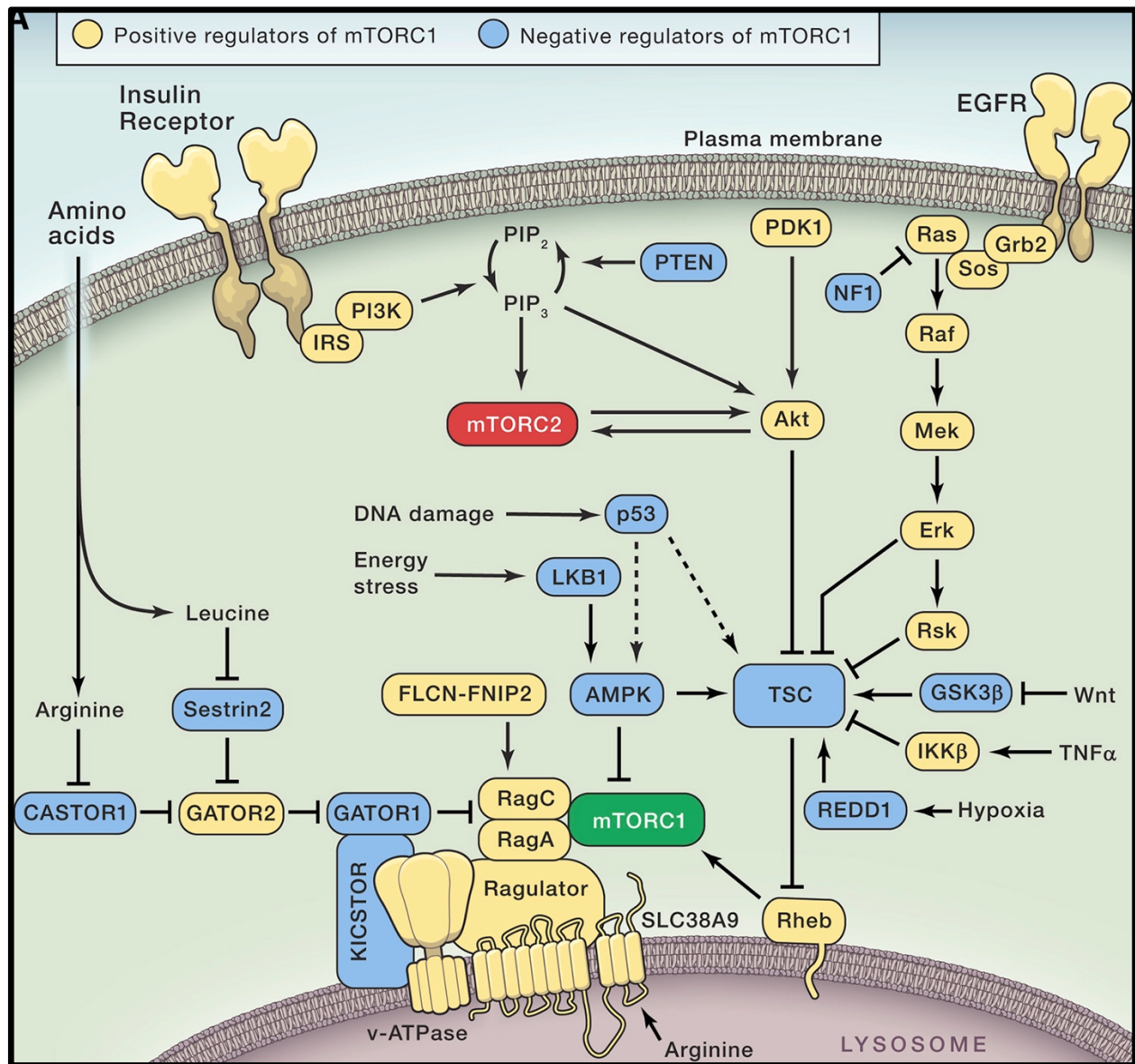


Fig.1. Upstream signaling pathways of mTORC1 at a glance: Growth factor and amino acid branches for mTORC1 activation are illustrated. Yellow represent positive regulators of mTORC1, while blue represent negative regulators of mTORC1. From Saxton R.A. *et al.* [47]

Based on the above insight, we investigated the effect of LATS2 on the proteins involved in both growth factor and amino acid dependent branches of mTORC1 activation. Our data showed that LATS2 hyperactivation neither changed the activity of activated AKT (pAKT; Ser473) nor changed AKT's down-stream phosphorylation on TSC2 (pTSC2; Thr 1462) in INS1-E cells. This suggests that LATS2 dependent mTORC1 activation is not regulated by the growth factor mediated AKT/TSC2 axis.

To then determine the possible influence of amino acid based signaling branch for LATS2 mediated mTORC1 activation, I tested the effects of dominant negative RagA (inactive RagA-GDP bound) upon LATS2 hyperactivation. As a result, overexpressed dominant negative RagA diminished the activity of mTORC1 in the context of LATS2 overexpression suggesting that LATS2 mediated mTORC1 activation is RagA dependent. This was further corroborated by the effect of mTORC1 activation under glucotoxic conditions in LATS2 depleted β -cells transfected with constitutively active RagA (active RagA-GTP bound), where I observed a significant upregulation of mTORC1 activation. This suggests that constitutively active RagA restored mTORC1 activation in LATS2 depleted diabetic pancreatic β -cells. These findings clearly show the engagement of Rag GTPases for the LATS2 mediated activation of mTORC1 in pancreatic β -cells. Hence, contrary to Gan *et al.*, our data suggest that LATS2 might be a signaling component of the Rag based amino acid branch, which regulates mTORC1 independent of growth factor signaling in pancreatic β -cells.

2.4.2. LATS2 regulates mTORC1 independent of YAP

As described in the introductory chapter, the transcriptional activator YAP is repressed during endocrine specification [56-58] and thus is one of the 'disallowed gene' in all developing islet cells [13, 59, 60]. Also, the re-expressing YAP in human islets tremendously fosters β -cell proliferation [13, 61]. Hence, it is evident that the low proliferative rate in mature β -cells might be driven by the terminal repression of the transcriptional activator YAP. However, the activity of core kinases of the Hippo pathway such as MST1/2 and LATS1/2 are functional yet minimal at physiological levels in pancreatic β -cells. In addition to the established bidirectional regulation of Hippo-YAP and mTORC1 [62-65], the Hippo core kinases also function beyond the canonical Hippo pathway independent of YAP. Also, previous work of my lab showed that the core Hippo kinase MST1 impairs β -cell survival and insulin secretion through non-canonical mechanistical actions which is independent of YAP [2]. Also, Gan *et al* [46], showed that the regulatory role of Hippo LATS on

mTORC1 is independent of YAP. This gives us an insight on LATS2 mediated mTORC1 activation in pancreatic β -cells, namely as non-canonical Hippo signaling event independent of YAP.

2.5. The Hippo pathway as autophagy regulator

Several studies provide a mechanistic insight into the direct interplay between the Hippo pathway and autophagy for the regulation of cellular homeostasis, metabolic adaptation and tumorigenesis. Altered autophagy has diverse impacts on Hippo pathway triggered tissue overgrowth in drosophila models, depending on the genotype and cell type [66, 67]. Also, the autophagy inducing kinase Atg1/ULK1 phosphorylates Yorkie (YAP in mammals) at the region Ser74 and Ser97 and inhibits the transcriptional activation of Yorkie, which is independent of Hippo-Warts (LATS) pathway [68]. The kinases LATS1/2 regulate steroidogenesis via an autophagy dependent pathway, lipophagy [69]. This gives us an understanding that autophagy-Hippo pathway crosstalk is conserved in Drosophila. Importantly, the core Hippo kinases MST1/2 play a crucial role in regulating autophagy in mammals. MST1/2 specifically phosphorylate LC3II at Thr50 and mediate the late autophagy phase by the fusion of autophagosome and lysosome, for the clearance of intracellular bacteria cargos, indicating the potential role of MST1/2 kinases in immunity [70]. In contrary and as discussed above, MST1 is also involved in the inhibition of autophagy induction by phosphorylating Beclin 1 at Thr108, which forms a complex with BCL2 proteins (Beclin-BCL-2) leading to apoptosis [8].

Recently, Zhou *et al.* showed that MST1 upregulation in NAFLD suppresses parkin related mitophagy via the AMPK pathway and triggers apoptosis [71]. Hence, loss of MST1 is considered to be one of the therapeutic interventions for the treatment of fatty liver disease. Conversely, MST1 indirectly enhances autophagy maturation in hepatocellular carcinoma (HCC) by interacting via RASSF1A [72]. Although MST1 regulates autophagy in different cell types, it is also a prey of autophagy in breast cancer cells. The oncoprotein hepatitis B X-interacting protein (HBXIP)-HDAC6 axis is shown to trigger MST1 deacetylation resulting in degradation of MST1 via chaperone mediated autophagy (CMA) [73]. These findings reflect the bidirectional links of Hippo pathway and autophagy in homeostasis and tumorigenesis [67].

2.5.1. Bidirectional regulation of LATS2 and autophagy in β -cells

Tang *et al.* [23] showed that LATS1 suppresses the lethal autophagy induced by sorafenib in hepatocellular carcinoma (HCC) cells. Also, LATS1 coordination with autophagy initiating factor Beclin 1 is independent of its kinase activity. Specifically, the PPxY motif located between the amino acids 167 and 524 in the protein domain of LATS1, which is not present in LATS2 is

involved in its autophagy suppression activity [23] [74]. This finding again gives us a clear insight that LATS2 and LATS1 regulatory roles are distinct in different cell types at different pathological conditions. However, we investigated whether LATS2 has an effect on the pro-survival autophagic machinery under diabetic conditions in pancreatic β -cells.

Using late-stage autophagy inhibitors to block autophagy, our data show that LATS2 overexpression further increased the accumulation of autophagic flux markers P62 and LC3II as well as pro-apoptotic markers exacerbating the defective autophagic flux and apoptosis in β -cells. Conversely, LATS2 depletion restored autophagic flux and β -cell survival. Furthermore, the role of LATS2 in exacerbating defective autophagic flux induced apoptosis is corroborated by genetic inhibition of Atg7, a vital component of autophagy regulation [75-78]. As Atg7 (homologous to E1 ubiquitin activating enzyme) plays an essential role in the cleavage of LC3I to LC3 II and for the subsequent incorporation of LC3 II into the autophagosome membrane [79-81], I investigated its effect on apoptosis in the context of glucotoxicity. In line with the chemical inhibition of autophagy, Atg7 knockdown exacerbated apoptosis which was reversed by LATS2 deletion under diabetic conditions. Additionally, the data obtained from the immunohistochemical analysis of pancreatic sections from HFD mice showed that P62 accumulation was tremendously increased in diabetic mice indicating the impairment of autophagy. This was obviously reduced by LATS2 depletion in the HFD β -LATS2-KO mice. This suggests that LATS2-induced mTORC1 activation mediates autophagic impairment and exacerbates β -cell apoptosis, eventually leading to β -cell failure.

By serendipity, we observed that the endogenous LATS2 levels were highly upregulated when autophagy was blocked at normal conditions. This prompted us to investigate if the endogenous LATS2 is itself a specific target of autophagy under physiological conditions. As there are three well-known pathways of autophagy, namely macroautophagy, chaperone mediated autophagy (CMA) and microautophagy, the specific pathway responsible for LATS2 degradation needs to be determined. We initially tested for CMA and macroautophagy by silencing CMA specific gene LAMP2A and macroautophagy specific gene ATG7 respectively, in INS1-E cells. Our data showed that LATS2 levels were upregulated upon ATG7 but not LAMP2A silencing, indicating LATS2 as a target for macroautophagy at the basal level. We further corroborated the involvement of macroautophagic machinery in LATS2 degradation, as our data showed that LATS2 localized in the purified intact autophagosomes and lysosomes by immunoprecipitation and also colocalization confirmed by immunofluorescence. We also observed that LATS2 directly bound to LC3 in the pulldown assays, further confirming the role of macroautophagy in the regulation of LATS2 turnover. Although LATS2 is regulated by ubiquitination by the ubiquitin ligases such as CRL4-DCAF1, NEDD4 and SIAH2 which promote subsequent proteasome mediated degradation

in other cell types [82], our data showed a novel layer of regulation for LATS2 protein destruction in β -cells by lysosomal mediated degradation pathway. This indicates that LATS2 degradation is regulated by several regulatory pathways. Altogether, from our investigation, our data reveals that the macroautophagy machinery regulates LATS2 turnover in β -cells at the basal level, however, such relation is compromised under diabetogenic conditions, where the hyperactive LATS2 impairs autophagic flux via mTORC1 hyperactivation.

This highlights the bidirectional link between autophagy and Hippo kinase LATS2 in β -cells.

2.5.2. Considering the Hippo pathway-autophagy regulatory axis for T2D treatment.

Autophagy flux impairment is considered as a key hallmark for reduced β -cell mass and defective insulin secretion in both T1D and T2D [83-86]. It is important to note that autophagy is a critical adaptive mechanism in the prevention of β -cell failure as it mitigates the detrimental effects of oxidative stress, mitochondrial dysfunction and ER stress [87]. There are several known autophagy stimulators such as vitamin D, free-fatty acids, omega-3-fatty acids and also antidiabetic drugs like metformin (that inhibits mTORC1 with or without implication of AMPK), GLP-1 receptor agonists (exendin-4 and liraglutide) and DPP-4 inhibitors (MK-626) that have all been suggested for β -cell protective therapy [87-92]. However, the key factors or signaling pathways that impairs autophagy in the diabetically stressed β -cells are not clearly known and unraveling new targets would enlarge the pharmacological scope for clinical development. Our study on the Hippo signaling pathway revealed that the kinase components such as MST1 and LATS2 that are upregulated in the β -cells under diabetogenic conditions, are the potential major contributors of autophagy impairment and β -cell apoptosis.

Such may constitute a vicious cycle as through impaired autophagy in T2D, Hippo kinases accumulate and potentiate severe β -cell destruction. We believe that the regulatory role of Hippo pathway and autophagy is essential for β -cell homeostasis and hence, targeting Hippo components (inhibition of MST1 and LATS2) specifically in β -cells might be a potent therapeutic strategy for T2D by restoring the protective autophagy response.

OUTLOOK

Although this thesis could further explore the role of Hippo pathway in the pathophysiology of diabetes, there are still several areas to be addressed in order to deeply understand the mechanism of action of Hippo signaling in the physiology and pathology of pancreatic β -cells.

1. MST1 kinase inhibition by neratinib is sufficient for the restoration of β -cell function and survival. Nevertheless, it would be necessary to develop a selective and potent MST1 kinase inhibitor with minimum off-target and side effects in order to have a safe drug to be translated towards clinical studies for diabetes therapy. Such efforts are in progress.
2. As LATS2, the downstream target of MST1 is also hyperactivated under diabetogenic conditions and triggers β -cell apoptosis and dysfunction via the mTORC1-autophagy axis, it is still not clear how LATS2 controls mTORC1 activation and related downstream signaling at the molecular level. In order to comprehensively unravel a detailed molecular mechanism, it is necessary to determine the direct interacting partners of LATS2 that result in the regulation of multiple signaling such as mTORC1 and autophagy with clear outcome on β -cell survival, metabolic as well as growth adaptations and insulin secretion.
3. At the upstream signaling level, the question remains whether MST1 alone is the driving force for LATS2 hyperactivation or are there other upstream kinases such as MAP4K4 that translate diabetogenic signals towards pathological conditions, β -cell apoptosis and failure?
4. As triggering pro-survival protective autophagy could destroy detrimental hyper-activated LATS2 in the β -cells, would fostering the autophagy response pharmaceutically, for example by AMPK activators and specifically metformin (that triggers autophagy and inhibits mTORC1), suppress LATS2 and rescue β -cells?
5. It was reported that the epigenetic modulator EZH2 plays a key role in the β -cell compensation and regeneration. As LATS2 coordinates the epigenome by directly phosphorylating PRC2 subunits EZH2 and SUZ12, we can further investigate the significance of LATS2 in the EZH2-dependent epigenetic regulation of β -cell compensation during the development of diabetes.
6. Although LATS2 as tumor suppressor is crucial for the tight regulation of cell growth, proliferation and homeostasis at cellular and whole-body levels, development of a safe and potent small LATS2 kinase inhibitor highly specific for β -cells may be a future tool for the restoration of β -cell mass and survival.

CONCLUSIONS

This research aimed to answer the questions how the Hippo pathway acts in mature pancreatic β -cells under both physiological and pathological conditions. I could show that

1. the irreversible tyrosine kinase inhibitor neratinib could potently inhibit the core Hippo component MST1 kinase and its downstream signaling in β -cells under diabetogenic conditions and could rescue β -cells from apoptosis. Neratinib restored functional β -cell mass in models of both T1D and T2D.
2. the downstream target of MST1 kinase, LATS2 was hyperactivated under diabetogenic conditions in pancreatic β -cells and conversely, genetic inhibition of LATS2 in both isolated rodent and human islets could improve β -cell survival. Moreover, specific LATS2 deletion in β -cells protected from obesity induced β -cell failure and diabetes development.
3. Mechanistically, under diabetogenic conditions, LATS2 induced β -cell apoptosis through activating mTORC1 signaling.
4. LATS2 hyperactivation impaired macroautophagy under acute stress conditions, and LATS2 turnover itself was regulated by macroautophagy. This establishes a bidirectional link between the Hippo kinase LATS2 and the autophagic machinery in regulating β -cell survival.

REFERENCES

1. Ardestani, A. and K. Maedler, *MST1: a promising therapeutic target to restore functional beta cell mass in diabetes*. *Diabetologia*, 2016. **59**(9): p. 1843-9.
2. Ardestani, A., et al., *MST1 is a key regulator of beta cell apoptosis and dysfunction in diabetes*. *Nat Med*, 2014. **20**(4): p. 385-397.
3. Fountas, A., L.N. Diamantopoulos, and A. Tsatsoulis, *Tyrosine Kinase Inhibitors and Diabetes: A Novel Treatment Paradigm?* *Trends Endocrinol Metab*, 2015. **26**(11): p. 643-656.
4. Prada, P.O. and M.J. Saad, *Tyrosine kinase inhibitors as novel drugs for the treatment of diabetes*. *Expert Opin Investig Drugs*, 2013. **22**(6): p. 751-63.
5. Azad, T., et al., *A LATS biosensor screen identifies VEGFR as a regulator of the Hippo pathway in angiogenesis*. *Nat Commun*, 2018. **9**(1): p. 1061.
6. Dent, P., et al., *Neratinib inhibits Hippo/YAP signaling, reduces mutant K-RAS expression, and kills pancreatic and blood cancer cells*. *Oncogene*, 2019. **38**(30): p. 5890-5904.
7. Park, Y.J., et al., *Tyrosine kinase inhibitor neratinib attenuates liver fibrosis by targeting activated hepatic stellate cells*. *Sci Rep*, 2020. **10**(1): p. 14756.
8. Maejima, Y., et al., *Mst1 inhibits autophagy by promoting the interaction between Beclin1 and Bcl-2*. *Nat Med*, 2013. **19**(11): p. 1478-88.
9. Guo, L., F. Yin, and J. Lin, *[Epidermal growth factor receptor and ligands in pancreatic beta-cell]*. *Sheng Wu Yi Xue Gong Cheng Xue Za Zhi*, 2011. **28**(1): p. 203-7.
10. Miettinen, P., et al., *EGF receptor in pancreatic beta-cell mass regulation*. *Biochem Soc Trans*, 2008. **36**(Pt 3): p. 280-5.

11. Anand, R., et al., *Toward the development of a potent and selective organoruthenium mammalian sterile 20 kinase inhibitor*. J Med Chem, 2009. **52**(6): p. 1602-11.
12. Faizah, Z., et al., *Treatment with Mammalian Ste-20-like Kinase 1/2 (MST1/2) Inhibitor XMU-MP-1 Improves Glucose Tolerance in Streptozotocin-Induced Diabetes Mice*. Molecules, 2020. **25**(19).
13. George, N.M., et al., *Exploiting Expression of Hippo Effector, Yap, for Expansion of Functional Islet Mass*. Mol Endocrinol, 2015. **29**(11): p. 1594-607.
14. Hong, A.W., et al., *Osmotic stress-induced phosphorylation by NLK at Ser128 activates YAP*. EMBO Rep, 2017. **18**(1): p. 72-86.
15. Moon, S., et al., *Phosphorylation by NLK inhibits YAP-14-3-3-interactions and induces its nuclear localization*. EMBO Rep, 2017. **18**(1): p. 61-71.
16. Guo, R., et al., *Overexpression of miR-297b-5p protects against stearic acid-induced pancreatic beta-cell apoptosis by targeting LATS2*. Am J Physiol Endocrinol Metab, 2020. **318**(3): p. E430-E439.
17. Xiong, S., et al., *Regulation of Protein Interactions by Mps One Binder (MOB1) Phosphorylation*. Mol Cell Proteomics, 2017. **16**(6): p. 1111-1125.
18. Tian, Y., et al., *LATS2 promotes cardiomyocyte H9C2 cells apoptosis via the Prx3-Mfn2-mitophagy pathways*. J Recept Signal Transduct Res, 2019. **39**(5-6): p. 470-478.
19. Xie, Y., et al., *LATS2 promotes apoptosis in non-small cell lung cancer A549 cells via triggering Mff-dependent mitochondrial fission and activating the JNK signaling pathway*. Biomed Pharmacother, 2019. **109**: p. 679-689.
20. Yao, W., et al., *Large tumor suppressor kinase 2 overexpression attenuates 5-FU-resistance in colorectal cancer via activating the JNK-MIEF1-mitochondrial division pathway*. Cancer Cell Int, 2019. **19**: p. 97.
21. Zhang, L., et al., *Anti-tumor effect of LATS2 on liver cancer death: Role of DRP1-mediated mitochondrial division and the Wnt/beta-catenin pathway*. Biomed Pharmacother, 2019. **114**: p. 108825.
22. Zhang, D., et al., *Increased mitochondrial fission is critical for hypoxia-induced pancreatic beta cell death*. PLoS One, 2018. **13**(5): p. e0197266.
23. Tang, F., et al., *LATS1 but not LATS2 represses autophagy by a kinase-independent scaffold function*. Nat Commun, 2019. **10**(1): p. 5755.
24. Aylon, Y., et al., *The LATS2 tumor suppressor inhibits SREBP and suppresses hepatic cholesterol accumulation*. Genes Dev, 2016. **30**(7): p. 786-97.
25. Aylon, Y., et al., *A positive feedback loop between the p53 and Lats2 tumor suppressors prevents tetraploidization*. Genes Dev, 2006. **20**(19): p. 2687-700.
26. Aylon, Y., et al., *The Lats2 tumor suppressor augments p53-mediated apoptosis by promoting the nuclear proapoptotic function of ASPP1*. Genes Dev, 2010. **24**(21): p. 2420-9.
27. Cho, W.J., et al., *miR-372 regulates cell cycle and apoptosis of ags human gastric cancer cell line through direct regulation of LATS2*. Mol Cells, 2009. **28**(6): p. 521-7.
28. Furth, N. and Y. Aylon, *The LATS1 and LATS2 tumor suppressors: beyond the Hippo pathway*. Cell Death Differ, 2017. **24**(9): p. 1488-1501.

29. Hergovich, A. and B.A. Hemmings, *Hippo signalling in the G2/M cell cycle phase: lessons learned from the yeast MEN and SIN pathways*. *Semin Cell Dev Biol*, 2012. **23**(7): p. 794-802.
30. Ke, H., et al., *Putative tumor suppressor Lats2 induces apoptosis through downregulation of Bcl-2 and Bcl-x(L)*. *Exp Cell Res*, 2004. **298**(2): p. 329-38.
31. Li, J., et al., *LATS2 suppresses oncogenic Wnt signaling by disrupting beta-catenin/BCL9 interaction*. *Cell Rep*, 2013. **5**(6): p. 1650-63.
32. McPherson, J.P., et al., *Lats2/Kpm is required for embryonic development, proliferation control and genomic integrity*. *EMBO J*, 2004. **23**(18): p. 3677-88.
33. Torigata, K., et al., *LATS2 Positively Regulates Polycomb Repressive Complex 2*. *PLoS One*, 2016. **11**(7): p. e0158562.
34. Visser, S. and X. Yang, *LATS tumor suppressor: a new governor of cellular homeostasis*. *Cell Cycle*, 2010. **9**(19): p. 3892-903.
35. Yang, X., et al., *Human homologue of Drosophila lats, LATS1, negatively regulate growth by inducing G(2)/M arrest or apoptosis*. *Oncogene*, 2001. **20**(45): p. 6516-23.
36. Jiang, W.J., Y.C. Peng, and K.M. Yang, *Cellular signaling pathways regulating beta-cell proliferation as a promising therapeutic target in the treatment of diabetes*. *Exp Ther Med*, 2018. **16**(4): p. 3275-3285.
37. Chen, H., et al., *PDGF signalling controls age-dependent proliferation in pancreatic beta-cells*. *Nature*, 2011. **478**(7369): p. 349-55.
38. Chen, H., et al., *Polycomb protein Ezh2 regulates pancreatic beta-cell Ink4a/Arf expression and regeneration in diabetes mellitus*. *Genes Dev*, 2009. **23**(8): p. 975-85.
39. Ali, M., et al., *Upstream signalling of mTORC1 and its hyperactivation in type 2 diabetes (T2D)*. *BMB Rep*, 2017. **50**(12): p. 601-609.
40. Bachar, E., et al., *Glucose amplifies fatty acid-induced endoplasmic reticulum stress in pancreatic beta-cells via activation of mTORC1*. *PLoS One*, 2009. **4**(3): p. e4954.
41. Bartolome, A., et al., *Pancreatic beta-cell failure mediated by mTORC1 hyperactivity and autophagic impairment*. *Diabetes*, 2014. **63**(9): p. 2996-3008.
42. Guillen, C. and M. Benito, *mTORC1 Overactivation as a Key Aging Factor in the Progression to Type 2 Diabetes Mellitus*. *Front Endocrinol (Lausanne)*, 2018. **9**: p. 621.
43. Ardestani, A., et al., *mTORC1 Signaling: A Double-Edged Sword in Diabetic beta Cells*. *Cell Metab*, 2018. **27**(2): p. 314-331.
44. Yuan, T., et al., *Reciprocal regulation of mTOR complexes in pancreatic islets from humans with type 2 diabetes*. *Diabetologia*, 2017. **60**(4): p. 668-678.
45. Jaafar, R., et al., *mTORC1 to AMPK switching underlies beta-cell metabolic plasticity during maturation and diabetes*. *J Clin Invest*, 2019. **129**(10): p. 4124-4137.
46. Gan, W., et al., *LATS suppresses mTORC1 activity to directly coordinate Hippo and mTORC1 pathways in growth control*. *Nat Cell Biol*, 2020. **22**(2): p. 246-256.
47. Saxton, R.A. and D.M. Sabatini, *mTOR Signaling in Growth, Metabolism, and Disease*. *Cell*, 2017. **168**(6): p. 960-976.
48. Dibble, C.C., et al., *TBC1D7 is a third subunit of the TSC1-TSC2 complex upstream of mTORC1*. *Mol Cell*, 2012. **47**(4): p. 535-46.
49. Inoki, K., et al., *Rheb GTPase is a direct target of TSC2 GAP activity and regulates mTOR signaling*. *Genes Dev*, 2003. **17**(15): p. 1829-34.

50. Long, X., et al., *Rheb binds and regulates the mTOR kinase*. *Curr Biol*, 2005. **15**(8): p. 702-13.
51. Menon, S., et al., *Spatial control of the TSC complex integrates insulin and nutrient regulation of mTORC1 at the lysosome*. *Cell*, 2014. **156**(4): p. 771-85.
52. Kim, E., et al., *Regulation of TORC1 by Rag GTPases in nutrient response*. *Nat Cell Biol*, 2008. **10**(8): p. 935-45.
53. Sancak, Y., et al., *The Rag GTPases bind raptor and mediate amino acid signaling to mTORC1*. *Science*, 2008. **320**(5882): p. 1496-501.
54. Sancak, Y., et al., *Ragulator-Rag complex targets mTORC1 to the lysosomal surface and is necessary for its activation by amino acids*. *Cell*, 2010. **141**(2): p. 290-303.
55. Efeyan, A., et al., *Regulation of mTORC1 by the Rag GTPases is necessary for neonatal autophagy and survival*. *Nature*, 2013. **493**(7434): p. 679-83.
56. Mamidi, A., et al., *Mechanosignalling via integrins directs fate decisions of pancreatic progenitors*. *Nature*, 2018. **564**(7734): p. 114-118.
57. Rosado-Olivieri, E.A., et al., *YAP inhibition enhances the differentiation of functional stem cell-derived insulin-producing beta cells*. *Nat Commun*, 2019. **10**(1): p. 1464.
58. George, N.M., et al., *Hippo signaling regulates pancreas development through inactivation of Yap*. *Mol Cell Biol*, 2012. **32**(24): p. 5116-28.
59. Pullen, T.J., M.O. Huising, and G.A. Rutter, *Analysis of Purified Pancreatic Islet Beta and Alpha Cell Transcriptomes Reveals 11beta-Hydroxysteroid Dehydrogenase (Hsd11b1) as a Novel Disallowed Gene*. *Front Genet*, 2017. **8**: p. 41.
60. Pullen, T.J., et al., *Identification of genes selectively disallowed in the pancreatic islet*. *Islets*, 2010. **2**(2): p. 89-95.
61. Yuan, T., et al., *Pro proliferative and antiapoptotic action of exogenously introduced YAP in pancreatic beta cells*. *JCI Insight*, 2016. **1**(18): p. e86326.
62. Hansen, C.G., et al., *The Hippo pathway effectors YAP and TAZ promote cell growth by modulating amino acid signaling to mTORC1*. *Cell Res*, 2015. **25**(12): p. 1299-313.
63. Liang, N., et al., *Regulation of YAP by mTOR and autophagy reveals a therapeutic target of tuberous sclerosis complex*. *J Exp Med*, 2014. **211**(11): p. 2249-63.
64. Park, Y.Y., et al., *Yes-associated protein 1 and transcriptional coactivator with PDZ-binding motif activate the mammalian target of rapamycin complex 1 pathway by regulating amino acid transporters in hepatocellular carcinoma*. *Hepatology*, 2016. **63**(1): p. 159-72.
65. Tumaneng, K., et al., *YAP mediates crosstalk between the Hippo and PI(3)K-TOR pathways by suppressing PTEN via miR-29*. *Nat Cell Biol*, 2012. **14**(12): p. 1322-9.
66. Perez, E., et al., *Autophagy regulates tissue overgrowth in a context-dependent manner*. *Oncogene*, 2015. **34**(26): p. 3369-76.
67. Wang, D., et al., *Emerging role of the Hippo pathway in autophagy*. *Cell Death Dis*, 2020. **11**(10): p. 880.
68. Tyra, L.K., et al., *Yorkie Growth-Promoting Activity Is Limited by Atg1-Mediated Phosphorylation*. *Dev Cell*, 2020. **52**(5): p. 605-616 e7.
69. Texada, M.J., et al., *Autophagy-Mediated Cholesterol Trafficking Controls Steroid Production*. *Dev Cell*, 2019. **48**(5): p. 659-671 e4.

70. Wilkinson, D.S., et al., *Phosphorylation of LC3 by the Hippo kinases STK3/STK4 is essential for autophagy*. Mol Cell, 2015. **57**(1): p. 55-68.
71. Zhou, T., et al., *Mst1 inhibition attenuates non-alcoholic fatty liver disease via reversing Parkin-related mitophagy*. Redox Biol, 2019. **21**: p. 101120.
72. Li, W., et al., *Suppressor of hepatocellular carcinoma RASSF1A activates autophagy initiation and maturation*. Cell Death Differ, 2019. **26**(8): p. 1379-1395.
73. Li, L., et al., *Deacetylation of tumor-suppressor MST1 in Hippo pathway induces its degradation through HBXIP-elevated HDAC6 in promotion of breast cancer growth*. Oncogene, 2016. **35**(31): p. 4048-57.
74. Tang, F. and G. Christofori, *LATS1-Beclin1 mediates a non-canonical connection between the Hippo pathway and autophagy*. Mol Cell Oncol, 2020. **7**(4): p. 1757378.
75. Kim, H.J., et al., *Deficient autophagy in microglia impairs synaptic pruning and causes social behavioral defects*. Mol Psychiatry, 2017. **22**(11): p. 1576-1584.
76. Lee, Y.A., et al., *Autophagy is a gatekeeper of hepatic differentiation and carcinogenesis by controlling the degradation of Yap*. Nat Commun, 2018. **9**(1): p. 4962.
77. Poillet-Perez, L., et al., *Autophagy maintains tumour growth through circulating arginine*. Nature, 2018. **563**(7732): p. 569-573.
78. Tong, M., et al., *Mitophagy Is Essential for Maintaining Cardiac Function During High Fat Diet-Induced Diabetic Cardiomyopathy*. Circ Res, 2019. **124**(9): p. 1360-1371.
79. Ichimura, Y., et al., *A ubiquitin-like system mediates protein lipidation*. Nature, 2000. **408**(6811): p. 488-92.
80. Shadab, M., et al., *Autophagy protein ATG7 is a critical regulator of endothelial cell inflammation and permeability*. Sci Rep, 2020. **10**(1): p. 13708.
81. Xie, Z. and D.J. Klionsky, *Autophagosome formation: core machinery and adaptations*. Nat Cell Biol, 2007. **9**(10): p. 1102-9.
82. Kim, Y. and E.H. Jho, *Regulation of the Hippo signaling pathway by ubiquitin modification*. BMB Rep, 2018. **51**(3): p. 143-150.
83. Bachar-Wikstrom, E., et al., *Improvement of ER stress-induced diabetes by stimulating autophagy*. Autophagy, 2013. **9**(4): p. 626-8.
84. Ebato, C., et al., *Autophagy is important in islet homeostasis and compensatory increase of beta cell mass in response to high-fat diet*. Cell Metab, 2008. **8**(4): p. 325-32.
85. Jung, H.S., et al., *Loss of autophagy diminishes pancreatic beta cell mass and function with resultant hyperglycemia*. Cell Metab, 2008. **8**(4): p. 318-24.
86. Rivera, J.F., et al., *Autophagy defends pancreatic beta cells from human islet amyloid polypeptide-induced toxicity*. J Clin Invest, 2014. **124**(8): p. 3489-500.
87. Rocha, M., et al., *Mitochondria and T2D: Role of Autophagy, ER Stress, and Inflammasome*. Trends Endocrinol Metab, 2020. **31**(10): p. 725-741.
88. Hwang, W.M., et al., *Omega-3 Polyunsaturated Fatty Acids May Attenuate Streptozotocin-Induced Pancreatic beta-Cell Death via Autophagy Activation in Fat1 Transgenic Mice*. Endocrinol Metab (Seoul), 2015. **30**(4): p. 569-75.
89. Martino, L., et al., *Palmitate activates autophagy in INS-1E beta-cells and in isolated rat and human pancreatic islets*. PLoS One, 2012. **7**(5): p. e36188.
90. Wang, Y., et al., *Vitamin D induces autophagy of pancreatic beta-cells and enhances insulin secretion*. Mol Med Rep, 2016. **14**(3): p. 2644-50.

91. Wu, J., et al., *Autophagy protects against cholesterol-induced apoptosis in pancreatic beta-cells*. *Biochem Biophys Res Commun*, 2017. **482**(4): p. 678-685.
92. Zummo, F.P., et al., *Glucagon-Like Peptide 1 Protects Pancreatic beta-Cells From Death by Increasing Autophagic Flux and Restoring Lysosomal Function*. *Diabetes*, 2017. **66**(5): p. 1272-1285.

Declaration on the contribution of the candidate to a multi-author article/manuscript which is included as a chapter in the submitted doctoral thesis

Chapter 1: Neratinib protects pancreatic β -cells in diabetes.

Contribution of the candidate in % of the total work load (up to 100% for each of the following categories):

Experimental concept and design:	ca. 25%
Experimental work and/or acquisition of (experimental) data:	ca. 25%
Data analysis and interpretation:	ca. 25%
Preparation of Figures and Tables:	ca. 25%
Drafting of the manuscript:	ca. 10%

Chapter 2: The Hippo kinase LATS2 impairs pancreatic β -cell survival in diabetes through mTORC1-autophagy axis.

Contribution of the candidate in % of the total work load (up to 100% for each of the following categories):

Experimental concept and design:	ca. 40%
Experimental work and/or acquisition of (experimental) data:	ca. 40%
Data analysis and interpretation:	ca. 40%
Preparation of Figures and Tables:	ca. 40%
Drafting of the manuscript:	ca. 25%

Appendix: Chapter 1: Ageing potentiates diet-induced glucose intolerance, β -cell failure and tissue inflammation through TLR4.

Contribution of the candidate in % of the total work load (up to 100% for each of the following categories):

Experimental concept and design:	ca. 8%
Experimental work and/or acquisition of (experimental) data:	ca. 8%
Data analysis and interpretation:	ca. 8%
Preparation of Figures and Tables:	ca. 8%

Appendix: Chapter 2: Loss of deubiquitinase USP1 blocks pancreatic β -cell apoptosis by inhibiting DNA damage response.

Contribution of the candidate in % of the total work load (up to 100% for each of the following categories):

Experimental concept and design:	ca. 17%
Experimental work and/or acquisition of (experimental) data:	ca. 17%
Data analysis and interpretation:	ca. 17%
Preparation of Figures and Tables:	ca. 17%

Date: 25.02.2021

Signatures:

4 Appendix

4.1 Ageing potentiates diet-induced glucose intolerance, β -cell failure and tissue inflammation through TLR4


Wei He, Ting Yuan, Dolma Choezom, Hannah Hunkler, Karthika Annamalai, Blaz Lupse and Kathrin Maedler.

Published in Scientific Reports 2018 Feb 9;8(1):2767. doi: 10.1038/s41598-018-20909-w.

My contribution:

Performed experiments and analysed data for Figures 2G,H

SCIENTIFIC REPORTS



OPEN

Ageing potentiates diet-induced glucose intolerance, β -cell failure and tissue inflammation through TLR4

Wei He, Ting Yuan, Dolma Choezom, Hannah Hunkler, Karthika Annamalai, Blaz Lupse & Kathrin Maedler

Ageing and obesity are two major risk factors for the development of type 2 diabetes (T2D). A chronic, low-grade, sterile inflammation contributes to insulin resistance and β -cell failure. Toll-like receptor-4 (TLR4) is a major pro-inflammatory pathway; its ligands as well as downstream signals are increased systemically in patients with T2D and at-risk individuals. In the present study we investigated the combined effects of high fat/high sucrose diet (HFD) feeding, ageing and TLR4-deficiency on tissue inflammation, insulin resistance and β -cell failure. In young mice, a short-term HFD resulted in a mildly impaired glucose tolerance and reduced insulin secretion, together with a β -cell mass compensation. In older mice, HFD further deteriorated insulin secretion and induced a significantly impaired glucose tolerance and augmented tissue inflammation in adipose, liver and pancreatic islets, all of which was attenuated by TLR4 deficiency. Our results show that ageing exacerbates HFD-induced impairment of glucose homeostasis and pancreatic β -cell function and survival, and deteriorates HFD-induced induction of mRNA expression of inflammatory cytokines and pro-inflammatory macrophage markers. TLR4-deficiency protects against these combined deleterious effects of a high fat diet and ageing through a reduced expression of inflammatory products in both insulin sensitive tissues and pancreatic islets.

Type 2 Diabetes mellitus (T2D) is a chronic metabolic disorder characterized by insulin resistance, a progressive decline in pancreatic β -cell function and mass and subsequent hyperglycaemia; all of which is strongly associated with obesity. A chronic, low-grade, “sterile” inflammation is present in obesity, and pro-inflammatory mediators including cytokines and ROS/RNS cause insulin resistance in peripheral insulin sensitive tissues and lead to dysfunction and apoptosis of insulin-producing β -cells in pancreatic islets^{1,2}.

The innate immunity and especially tissue macrophages contribute to such obesity-associated inflammation^{2,3}. Pro-inflammatory macrophages (termed as M1 or classically activated macrophages) infiltrate insulin responsive tissues; the adipose tissue, liver as well as pancreatic islets, and outnumber homeostasis-maintaining and anti-inflammatory tissue-resident macrophages (termed as M2 or alternatively activated macrophages)^{4–6}. This, over time, leads to a chronic low-grade tissue inflammation, subsequent insulin resistance and loss in compensatory adaptation of the pancreatic β -cells with progression to hyperglycemia and diabetes^{2,3}.

Clinical as well as preclinical experimental studies show that Toll-like receptor 4 (TLR4) expression and activation is directly associated with obesity-induced tissue inflammation; abrogation of TLR4 is able to reverse insulin resistance and pancreatic β -cell dysfunction in experimental models^{7–14}. Hyperlipidemia alone or in concert with hyperglycemia, termed as “lipoglucotoxicity” can induce a pro-inflammatory state, shown in fat, where elevated free fatty acids lead to impaired insulin sensitivity. In pancreatic islets, prolonged lipoglucotoxicity initiates a vicious cycle in β -cell destruction^{2,3}. Both of them are shown to be mediated by TLR4 signaling^{4,6}.

TLR4 is a member of the TLR family of pattern recognition receptors, and its signaling is one of the major pro-inflammatory pathways. Two tightly connected pathways in obesity activate TLR4 through specific ligands and result in the exacerbation of inflammation; elevated free fatty acids (FFA) as well as lipopolysaccharide (LPS)-linked to changes in gut microbiota. Three major ligands of TLR4; LPS, CXCL10 and FFA are systemically

Centre for Biomolecular Interactions, University of Bremen, Bremen, Germany. Correspondence and requests for materials should be addressed to W.H. (email: hewei@uni-bremen.de) or K.M. (email: kmaedler@uni-bremen.de)

increased in patients with T2D as well as in at-risk individuals^{15–18}. While LPS is the known classical ligand of TLR4, FFA stimulates TLR4 signalling^{19–21}, but rather than directly bound to TLR4, it acts through the hepatokine fetuin-A^{22,23}, which is also increased in obesity²⁴ and independently associated with T2D²⁵. Plasma LPS levels are increased in rodent models of obesity as well as in obese individuals, this metabolic endotoxemia could be due to increased intestinal permeability and enhanced LPS absorption by HFD^{26,27}. Other described TLR4 ligands increased in T2D patients include HMGB1, hyaluronan, Hsp60/70 as well as S100A8^{16,28}.

Ageing is a major risk factor for the development of T2D, and is paralleled with developing glucose dys-homeostasis in both human and animal studies^{29,30}. During ageing, a low-grade pro-inflammatory state has been observed with an elevation in pro-inflammatory cytokines, macrophages and superoxide products in fat, liver and pancreas, as well as in the circulation^{30–35}. This may again be related to TLR4, as TLR4 mutant mice live longer, have stronger bones and muscles throughout their life³⁶. In addition to diabetes, several other ageing-related diseases are mediated by increased inflammation through the pathological activation of TLR4, such as cardiovascular diseases, atherosclerosis, Alzheimer's disease, arthritis and therefore, the term “inflamm-ageing” has been created to address such disease state with increased inflammation at an older age³⁷.

Given this intersection of ageing, inflammation, TLR4 and diabetes, we hypothesized that ageing may have a potentiating effect upon obesity-induced tissue inflammation through TLR4, which would lead to an acceleration of the diabetes phenotype. Such possibility was addressed in the present study by short-term 8-week high fat/high sucrose diet-feeding of WT and TLR-4 knockout mice. We found that ageing could enhance diet-induced inflammatory cytokines in fat, liver and pancreatic islets, and aggravate impairment of glucose homeostasis and pancreatic β -cell dysfunction, which was prevented by TLR4-deficiency.

Results

Ageing further impairs high fat diet induced glucose intolerance and insulin resistance in old WT but not in TLR4^{-/-} mice. To evaluate whether ageing potentiates hyperglycemia in obesity, we fed WT C57BL/6J mice a normal (ND) or a high fat/high sucrose diet (HFD, “Surwit”). After 8 weeks of HFD feeding, WT mice at an age of 14 weeks, when they are usually investigated, developed obesity and a slightly impaired glucose tolerance, which were severely potentiated in HFD fed older mice of 14 months (Fig. 1A,C). In contrast, glucose tolerance was almost uncompromised in *Tlr4*^{-/-} mice of both ages (Fig. 1B,C).

These data are in line with the impaired insulin tolerance in HFD fed aged mice. While young mice developed only slightly impaired insulin tolerance under the HFD feeding, compared to ND, insulin resistance worsened in the aged mice (Fig. 1D,F). In *Tlr4*^{-/-} mice, insulin tolerance was unchanged -neither HFD nor ageing impaired insulin sensitivity during the 8-week feeding period (Fig. 1E,G). Body weight gain was significantly increased by the HFD, which was similar in both young and old WT and *Tlr4*^{-/-} mice (Suppl. Fig. 1A,B). Also food intake was not affected by age or by genotype (Suppl. Fig. 1C,D).

HFD led to β -cell failure in aged mice, whereas TLR4-depletion could restore β -cell function and survival.

Since HFD and ageing led to an impairment of both glucose and insulin tolerance, we tested whether this may also be a result of impaired β -cell function and survival. Fasted mice were injected with 2 g/kg glucose, and insulin secretion was measured before (0 min) and 30 min after glucose injection. In parallel to the HFD induced hyperglycemia (Fig. 1A), WT HFD fed young as well as old mice (but not *Tlr4*^{-/-} mice) were hyperinsulinemic at the basal state (Fig. 2A), compared to ND mice.

The glucose stimulatory insulin secretion index was reduced in the young HFD mice and was fully abolished in the old HFD group, while it was fully maintained in *Tlr4*^{-/-} mice (Fig. 2B). Similar data were obtained from an *in vitro* GSIS assay, in which islets from all 8 groups were isolated and plated on extracellular matrix coated dishes for one day of recovery. While basal insulin secretion was unaffected in all groups, glucose stimulatory index was reduced by the HFD in islets from young mice and completely deprived in islets from old HFD fed mice (Fig. 2C,E). Again, *Tlr4*^{-/-} islets showed no impairment during the *in vitro* GSIS, and rescued high glucose induced insulin secretion in old mice fed a HFD compared to the wildtype littermates (Fig. 2C,E). Insulin content measured after the *in vitro* GSIS showed no significant changes among the 8 groups; except a significant increase in insulin content in the young *Tlr4*^{-/-} mice in adaptation to the HFD (Fig. 2D).

Previously, we reported a compensatory increase in β -cell mass in mice during the first 8 weeks of HFD feeding³⁸. This was again confirmed in this study; HFD feeding induced a compensatory increase in β -cell mass in young mice, while old mice were unable to increase β -cell mass in response to the HFD (Fig. 2F). In contrast, both young and old *Tlr4*^{-/-} mice showed β -cell mass compensation (Fig. 2F). In line with the reduced β -cell mass, the number of apoptotic β -cells was increased in the old HFD fed mice (Fig. 2G), while apoptosis was significantly reduced in the old *Tlr4*^{-/-} mice fed a HFD, compared to the WT mice of the same group (Fig. 2G,H).

HFD-induced inflammatory cytokine expression was enhanced in old mice and attenuated by TLR4-deficiency.

Multiple studies have revealed that HFD feeding and obesity can induce chronic low-grade tissue inflammation in fat, liver and pancreatic islets. In this study, we attempted to investigate, whether ageing augments cytokine expression induced by HFD feeding. In young mice, 8 weeks of HFD feeding induced *Il1b* expression in adipose tissue (Fig. 3A) and *Tnf* expression in pancreatic islets (Fig. 3C). In old mice, HFD feeding induced expression of *Il1b*, *Il6* and *Ccl2* in fat (Fig. 3A), *Il6*, *Tnf* and *Ccl2* in liver (Fig. 3B), *Il1b* in islets (Fig. 3C). While *Il1b* expression was already induced by HFD in fat of young mice, it was only induced in islets of older mice. Cytokine expression was also further accelerated in older mice on the HFD, especially in fat (e.g. *Il6* and *Ccl2*), but also in the liver, which expressed more *Tnf*, compared to HFD fed young mice. In general in all investigated tissues, the expression of multiple inflammatory cytokines was elevated by a combination of HFD and ageing when compared with young mice fed the control normal chow diet (Fig. 3A–C). Ageing itself induced a

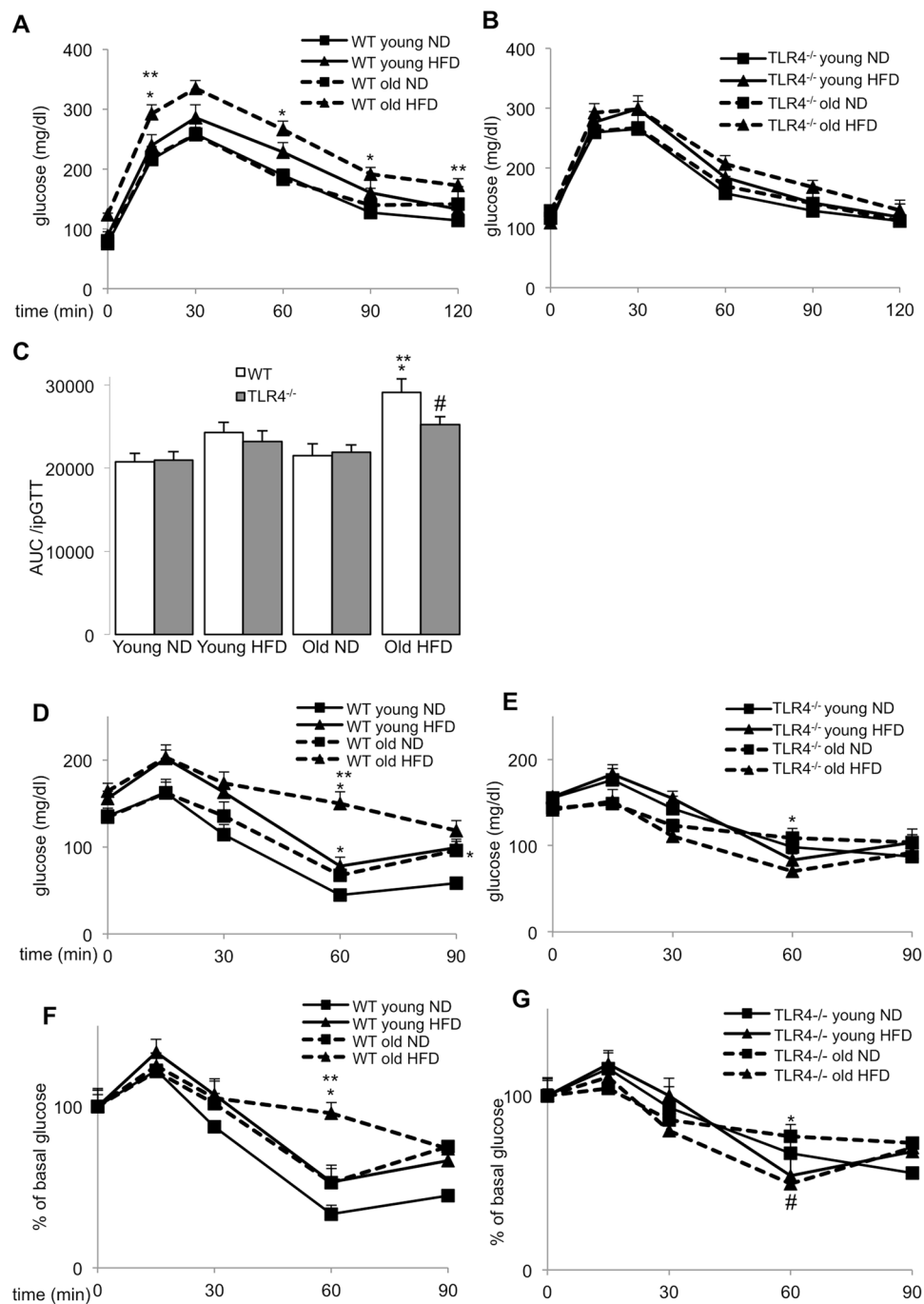


Figure 1. Ageing further impairs high fat diet induced glucose intolerance and insulin resistance in old WT but not in *Tlr4*^{-/-} mice (A–G). Young (6 weeks) and old (12 months) WT and *Tlr4*^{-/-} mice were fed a normal (ND) or high fat/high sucrose diet (“Surwit”; HFD) for 8 weeks. (A–C) Intraperitoneal glucose tolerance test (ipGTT) with 1 g/kg body weight glucose of WT (A) and *Tlr4*^{-/-} mice (B) and area-under-the-curve analysis by definite integrals of the same ipGTT results from the ND and HFD fed WT and *Tlr4*^{-/-} mice after 8 weeks of diet (C). (D–G) Intraperitoneal insulin tolerance test (ipITT) of WT (D,F) and *Tlr4*^{-/-} mice (E,G) with 0.75 IU/kg body weight insulin. Glucose levels were normalized to 100% before glucose injection (F,G). Data are means ± SE. **p* < 0.05 ND vs. HFD; ***p* < 0.05 young vs. old mice; #*p* < 0.05 WT (F) vs. *Tlr4*^{-/-} (G) mice. Due to the congested figure, we split the data from WT and *Tlr4*^{-/-} mice used in the same experiments into two separate graphs (A/B, D/E, F/G). *N* = 12–15 mice per group; three independent experiments were performed.

pro-inflammatory phenotype under the ND; seen by the significantly increased *Il6* expression in adipose tissue, but this was not observed in liver and islets (Fig. 3A–C).

Analysis of the anti-inflammatory cytokines *Il10*, *Tgfb* and *Il4* revealed that ageing together with HFD reduced *Il10* expression in liver and islets (Fig. 3A–C, Suppl. Fig. 2), while *Tgfb* levels remained unchanged under

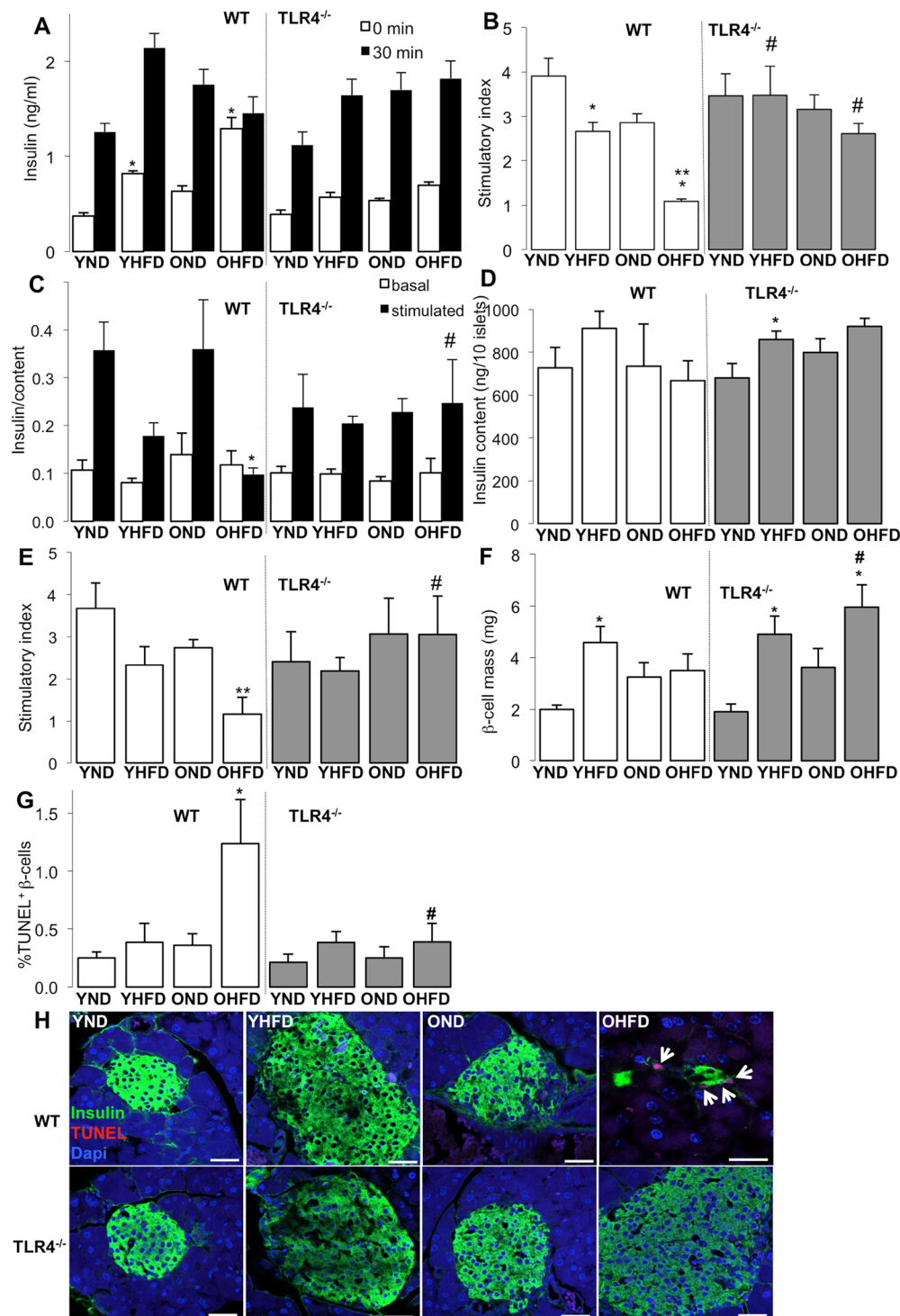


Figure 2. HFD led to β -cell failure in aged mice, whereas TLR4-depletion could restore β -cell function and survival. (A–H) Young (6 weeks) and old (12 months) WT and *Tlr4*^{-/-} mice were fed a normal (ND) or high fat/high sucrose diet (“Surwit”; HFD) for 8 weeks. (A,B) Insulin secretion during an ipGTT with 2 g/kg body weight glucose in week 8 measured before (0 min) and 30 min after glucose injection (A) and calculated as stimulatory index (B). (C–E) Mice were sacrificed at week 8 and islets isolated from all 8 treatment groups, cultured overnight and subjected to an *in vitro* GSIS assay. (C) Insulin secretion during 1h-incubation with 2.8 mM (basal) and 16.7 mM glucose (stimulated), normalized to (D) insulin content. (E) The insulin stimulatory index denotes the ratio of secreted/basal insulin during 1h-incubation with 16.7 mM and 2.8 mM glucose, respectively. (F) β -cell mass analysed from 10 sections/mouse spanning the whole pancreas. (G,H) Results and representative microscopic images from triple staining for TUNEL, insulin and DAPI expressed as percentage of TUNEL-positive β -cells \pm SE. The mean number of β -cells scored was 10,252 for each treatment condition. (H) Arrows point to four TUNEL⁺ β -cells with remaining insulin from an old HFD fed WT mouse. Scale bar, 50 μ m. **p* < 0.05 ND vs. HFD; ***p* < 0.05 young vs. old mice; #*p* < 0.05 WT vs. *Tlr4*^{-/-} mice. N = 5–9 mice per group; three independent experiments were performed.

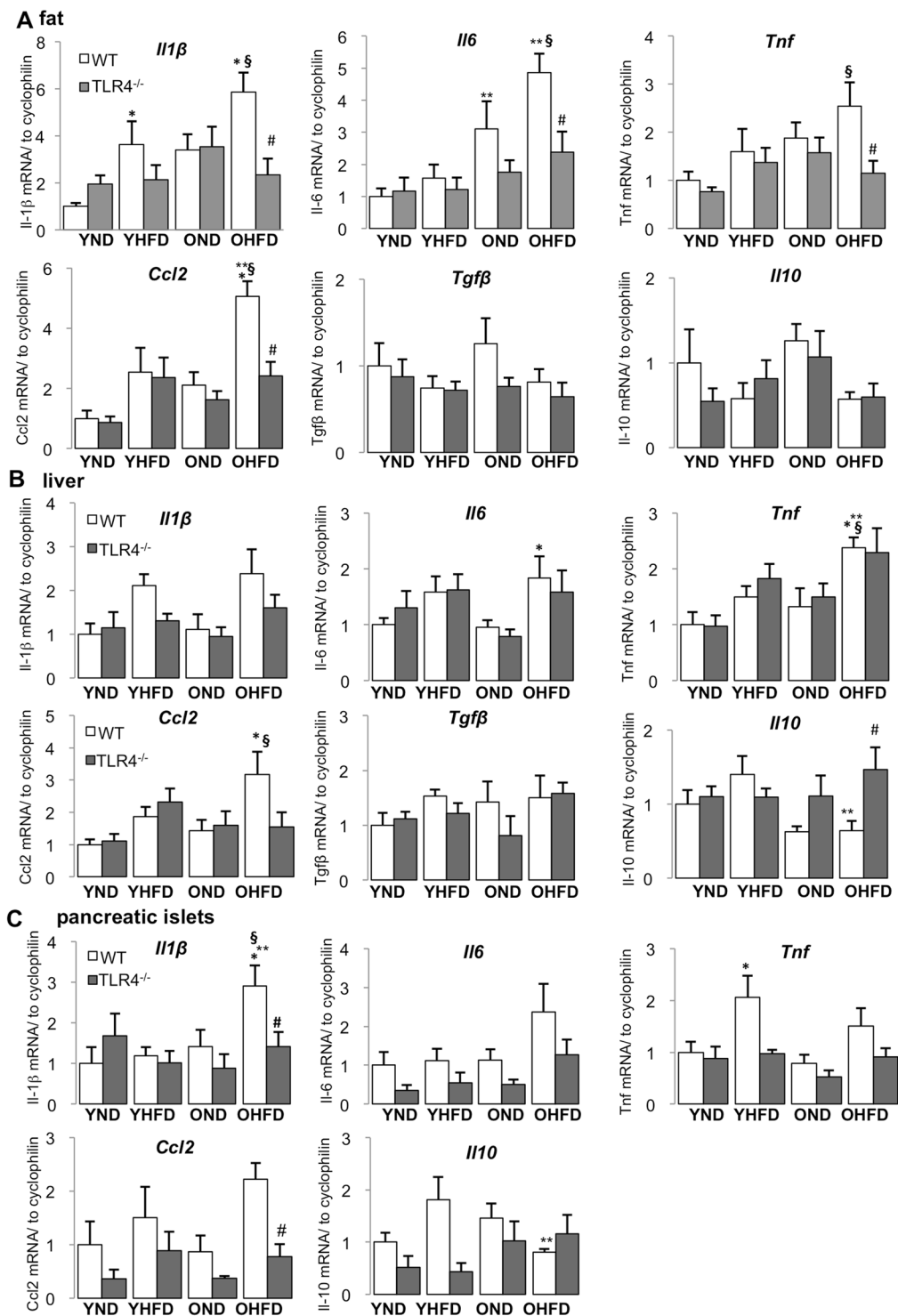


Figure 3. HFD-induced inflammatory cytokine expression was enhanced in old mice and attenuated by TLR4-deficiency. (A–C) Young (6 weeks) and old (12 months) WT and *Tlr4*^{-/-} mice were fed a normal (ND) or high fat/high sucrose diet (“Surwit”; HFD) for 8 weeks. RT-PCR analysis for inflammatory and anti-inflammatory genes with RNA extracted from fat (A), liver (B) and pancreatic islets (C) of mice treated under the indicated conditions. Y, young mice, O, old mice, ND, normal chow diet, HFD, high fat/high sucrose diet, WT, wildtype mice, *Tlr4*^{-/-}, TLR4-knockout mice. All results are normalized to control young-ND, which is arbitrarily set as 1. Data are presented as means ± SE from n = 5–8 mice. *p < 0.05 ND vs. HFD; **p < 0.05 young vs. old mice; #p < 0.05 WT vs. *Tlr4*^{-/-} mice, §p < 0.05 young ND vs. old HFD mice.

all conditions in fat and liver (Fig. 3A,B) and *Il4* was only detectable in liver but was unchanged by HFD and ageing (though TLR4 knockout showed a profound *Il4* induction in old HFD fed mice compared to their WT counterparts (Suppl. Fig. 2)).

Next, we checked if TLR4-deficiency affected such ageing/HFD induced cytokine expression and thus may explain the protective effect of TLR4 inhibition on glycemia, β -cell function and survival. Overall, TLR4-depletion had a tendency to reduce ageing/HFD induced pro-inflammatory cytokine expression (Fig. 3A–C). One exception is *Il6* and *Tnf* expression in liver, where was no change between *Tlr4*^{-/-} mice and WT mice, neither at ageing nor at HFD condition or both (Fig. 3B). Similarly, *Il10* expression was unchanged in fat and islets by TLR4-depletion, while it was increased together with *Il4* by TLR4-deficiency in the liver of old HFD mice (Fig. 3A,B and Suppl. Fig. 2).

These results indicate a very complex regulation of different cytokines in the insulin responsive and insulin-producing tissues, and that TLR4 is an important but unlikely the only pathway to initiate such cytokine expression pattern.

Combined HFD-feeding and ageing shifted tissue macrophage polarization to a more pro-inflammatory phenotype.

Since accumulation and classical activation of macrophages contributes to a pro-inflammatory phenotype observed in insulin sensitive and insulin-producing tissues under HFD feeding, we then analyzed macrophage markers in aged mice fed either ND or HFD. As general macrophage markers, we measured *Cd68*, *Emr1* (F4/80) and the pan-myeloid marker *Cd11b* (*Itgam*). We measured *Cd11c* (*Itgax*) as M1 macrophage marker^{12,33,39,40} and *Cd206* (mannose receptor, *Mrc1*) and *Arg1* (arginase 1) as M2 macrophage markers^{9,12,40–42}. Comparison of young and old mice fed a ND revealed that ageing alone did not significantly change macrophage accumulation and polarization (Fig. 4A–C). Paralleled with the induction of inflammatory cytokines, the expression of general macrophage markers significantly increased by the combination of HFD and ageing in all tested tissues (Fig. 4A–C). In contrast, M2 markers showed the opposite; reduced *Mrc1* and *Arg1* expression, coinciding with the anti-inflammatory cytokine *Il10* (Fig. 3A–C), though detailed analysis revealed differences among tissues (Fig. 4A–C). Unlike in aged mice, the general macrophage markers were not uniformly induced by the 8-week HFD in young mice, only *Cd68* was increased in the liver (Fig. 4A–C).

Again, while an 8-week HFD regime triggers a minimal inflammatory profile in insulin responsive tissues and insulin-producing islets, ageing could potentiate HFD's effect and augment tissue inflammation, macrophage accumulation and inflammatory activation.

Unlike the reduction in pro-inflammatory cytokine expression, TLR4 deficiency didn't influence gene expression of macrophage accumulation and polarization in a universal manner. HFD induced *Itgax* expression was completely blocked in the liver and fat (Fig. 4A–C), and anti-inflammatory macrophage marker *Arg1* expression in liver of HFD fed old mice was enhanced by TLR4-deficiency (Fig. 4A–C), which is in line with the increased *Il4* and *Il10* expression in the same setting (Fig. 3B and Suppl. Fig. 2). The results above demonstrate that TLR4-deficiency could attenuate inflammatory macrophages in fat and liver, in addition to restoring M2-like macrophage polarization in the liver of old mice, both of which could contribute to prevent HFD-induced inflammation in old mice.

Experimental Procedures

Animals. C57BL/6J (wild type; WT) and C57BL/10ScCr (TLR4 knockout; *Tlr4*^{-/-})⁴³ male mice comprising of young (6 weeks) and old (12 months) mice were obtained from Jackson Laboratories (Bar Harbor, ME) and separated into 4 groups. Half of the groups were fed a normal diet (ND) (Harlan Teklad Rodent Diet 8604 containing 12.2, 57.6, and 30.2% calories from fat, carbohydrate, and protein, respectively; Harlan Teklad, Madison, WI) or a high fat/high sucrose diet (HFD) (“Surwit,” containing 58, 26, and 16% calories from fat, carbohydrate, and protein, respectively⁴⁴; Research Diets, Inc., New Brunswick, NJ) for 8 weeks. Body weight and food intake were measured weekly during the study. All mice were housed in a temperature-controlled room with a 12 hours light, 12 hours dark cycle, and were allowed free access to food and water according to the protocol approved by the “Bremen Senate of Health” (the Institutional Animal Care and Use Committee) in agreement with the §8 of the German animal protection law. All methods were carried out in accordance with the guidelines and regulations of the Institutional Animal Care and Use Committee.

Metabolic tests. For intraperitoneal glucose tolerance tests (ipGTT), mice were fasted 12 h overnight and injected i.p. with glucose (40%; B. Braun, Melsungen, Germany) at a dose of 1 g/kg body weight. Blood samples were obtained from the tail vein at time points 0, 15, 30, 60, 90 and 120 min for glucose measurements using a glucometer. Insulin secretion was measured before (0 min) and after (30 min) i.p. injection of glucose (2 g/kg body weight) with plasma taken from retro-orbital blood puncture using ultrasensitive mouse Elisa kit (ALPCO Diagnostics, Salem, NH) as described before⁴⁵. For intraperitoneal insulin tolerance tests (ipITT), mice were fasted for 4 h and intraperitoneally injected with 0.75 IU/kg body weight of recombinant human insulin (InsHuman Rapid, Aventis, Germany) and blood glucose was measured 0, 15, 30, 60 and 90 minutes post injection.

Mouse tissue isolation. After 8 weeks of diet, mice were sacrificed and islets were isolated by pancreas perfusion with LiberaseTM (Roche, Mannheim, Germany) according to the manufacturer's instructions and digested for 10 minutes at 37 °C as previously described⁴⁵. Islets were purified by a density gradient of Histopaque (1:1; 1077 and 1119, Sigma-Aldrich, Steinheim, Germany) and subsequent hand-picking. High purity islets were cultured overnight in RPMI 1640 medium containing 11.1 mM glucose (Lonza, Basel, Switzerland), followed by pelleting islets and adding Trizol (PEQLAB GmbH, Erlangen, Germany) for RNA extraction. Liver and epididymal white adipose tissue (WAT) were cut into small pieces in *RNAlater* solution (Sigma-Aldrich, Steinheim, Germany) and then shaken at 4 °C overnight, followed by homogenization and addition of Trizol for RNA extraction.

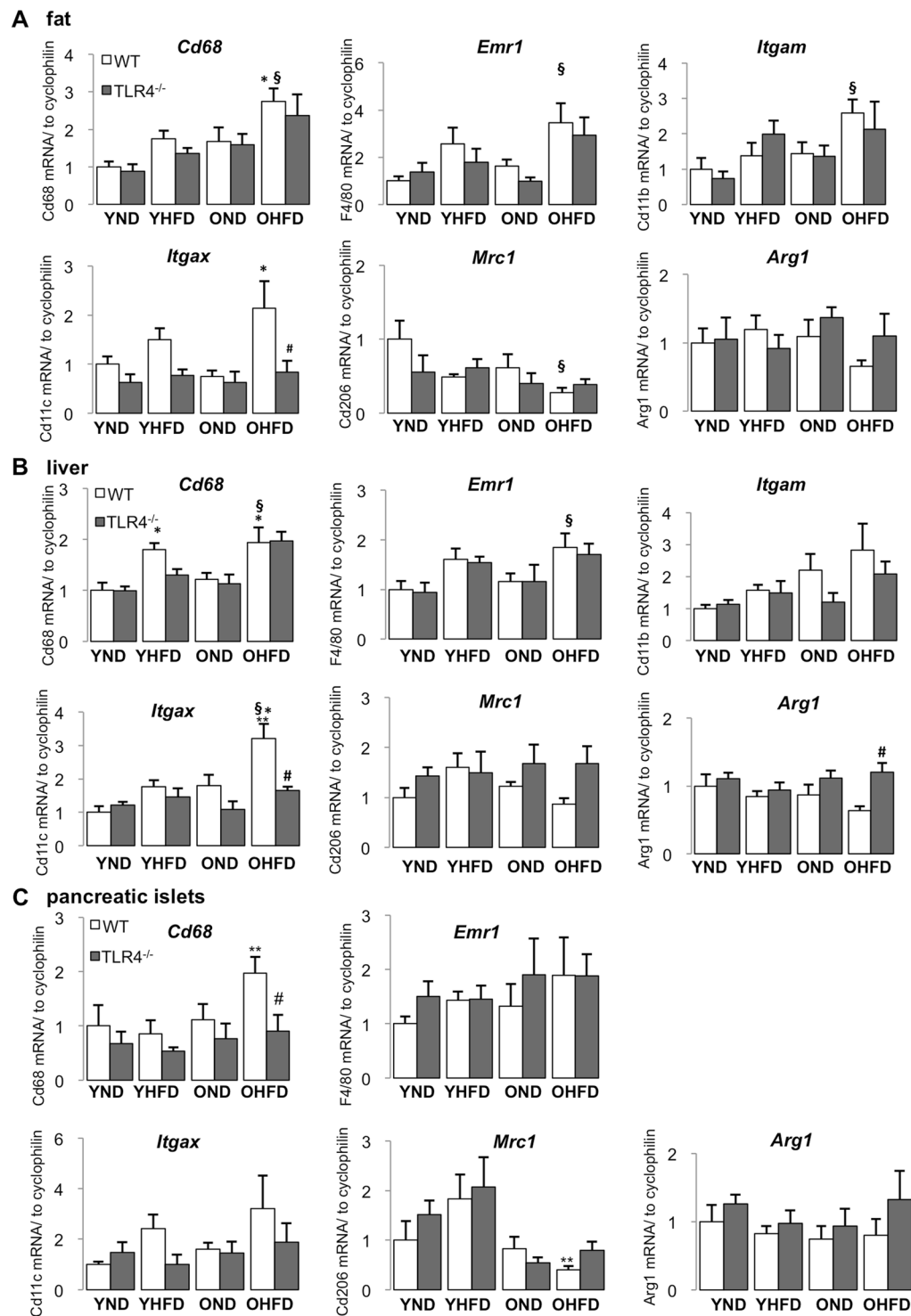


Figure 4. Combined HFD-feeding and ageing shifted tissue macrophage polarization to a more pro-inflammatory phenotype. (A–C) Young (6 weeks) and old (12 months) mice WT and *Tlr4*^{-/-} mice were fed a normal (ND) or high fat/high sucrose diet (“Surwit”; HFD) for 8 weeks. RT-PCR analysis for general macrophage and macrophage polarization markers with RNA extracted from fat (A), liver (B) and pancreatic islets (C) of mice treated under the indicated conditions. Y, young mice, O, old mice, ND, normal chow diet, HFD, high fat/high sucrose diet, WT, wildtype mice, *Tlr4*^{-/-}, TLR4-knockout mice. All results are normalized to control young-ND, which is arbitrarily set as 1. Data are presented as mean \pm SE from $n = 5$ –8 mice. * $p < 0.05$ ND vs. HFD; ** $p < 0.05$ young vs. old mice; # $p < 0.05$ WT vs. *Tlr4*^{-/-} mice, § $p < 0.05$ young ND vs. old HFD mice.

Immunohistochemical analysis. Mouse pancreata were isolated and fixed with 4% PFA for 8 h at 4 °C and then paraffin embedded and cut into 4 µm sections. The slides were deparaffinized and immunostaining was carried out after heat antigen-retrieval⁴⁵. Sections were incubated with anti-insulin (DAKO, Glostrup, Denmark; A0546, 1:100) for 12 h at 4 °C, and secondary antibody (biotin anti-guinea pig, 1:100; Jackson ImmunoResearch, PA) for 1 h at RT and thereafter with Vectastain ABC solution for 1 h at RT and DAB (HRP substrate kit, brown; both from Vector Laboratories, Burlingame, CA, USA) for 10 min. For morphometric analysis, ten sections (spanning the width of the pancreas) per mouse were analyzed as described before⁴⁵. Pancreatic tissue area and insulin-positive area were determined by computer-assisted measurements using a Nikon MEA53200 (Nikon GmbH, Dusseldorf, Germany) microscope and images were acquired using NIS-Elements software (Nikon GmbH, Dusseldorf, Germany). Mean percent β-cell fraction per pancreas was calculated as the ratio of insulin-positive and whole pancreatic tissue area. β-cell mass was obtained by multiplying the β cell fraction by the weight of the pancreas. β-cell apoptosis was analyzed by the TUNEL technique according to the manufacturer's instructions (*In situ* Cell Death Detection Kit, TMR red; Roche/now distributed by Sigma-Aldrich, Steinheim, Germany) and double stained for insulin, followed by FITC anti-guinea pig secondary antibody (Jackson).

Glucose-stimulated insulin secretion (GSIS) *in vitro*. For acute insulin release in response to glucose, primary mouse islets were washed and pre-incubated (30 min) in Krebs-Ringer bicarbonate buffer (KRB) containing 2.8 mM glucose and 0.5% BSA. KRB was then replaced by KRB 2.8 mM glucose for 1 h (basal), followed by an additional 1 h in KRB 16.7 mM glucose (stimulated). Thereafter, islets were washed with PBS and extracted with HCl (0.18 N) in 70% ethanol overnight at 4 °C. The acid-ethanol extracts were collected for determination of insulin content. Insulin was determined using mouse insulin ELISA (ALPCO Diagnostics, Salem, NH). Secreted insulin was normalized to total insulin content.

RNA extraction and quantitative RT-PCR analysis. Total RNA was isolated from mouse islets, liver and WAT with a Trizol extraction system (TriFast, PEQLAB GmbH, Erlangen, Germany). cDNA synthesis and quantitative RT-PCR was performed as previously described⁴⁵. The Applied Biosystems StepOne Real-Time PCR system (Applied Biosystems, CA) with TaqMan[®] Fast Universal PCR Master Mix for TaqMan assays (Applied Biosystems, CA) was used for analysis. Cyclophilin (PPIA) and β-Actin (ACTB) were used as internal house-keeping controls and the quantitative analysis was performed with the $\Delta\Delta$ CT method. The following TaqMan[®] Gene Expression Assays were used: *Ppia* (Mm03024003_g1), *Actb* (Mm00607939_s1), *Illb* (Mm00434228), *Il6* (Mm00446190), *Tnf* (Mm00443258_m1), *Ccl2* (Mm00441242_m1), *Il4* (Mm00445259_m1), *Il10* (Mm00439614_m1), *Tgfb* (Mm01178820_m1), *Cd68* (Mm03047343_m1), *Emr1* (F4/80) (Mm00802529_m1), *Itgam* (CD11b) (Mm00434455_m1), *Itgax* (CD11c) (Mm00498698_m1), *Mrc1* (CD206) (Mm00485148_m1), *Arg1* (Mm00475988_m1).

Statistical analysis. All values were expressed as means \pm SE with the number of independent individual experiments (*in vitro*; biological replicates) or the number of mice (*in vivo*) presented in the figure legends. The different groups were compared by two-way ANOVA with Bonferroni post-tests. P value < 0.05 was considered statistically significant.

Discussion

The present study identifies a deleterious potentiation of impaired glucose homeostasis, β-cell dysfunction and chronic tissue inflammation by the combination of obesity and ageing. Data from our HFD/ageing mouse model support the concept that obesity with ageing leads to further deterioration in blood glucose regulation, which is likely due to a reduced capacity to balance inflammatory genes at an older age.

While our previous studies investigated the effect of chronic HFD feeding on glucose homeostasis and stages of β-cell adaptation, compensation and failure⁴⁶, in this study we exposed the mice with the HFD for a relatively short term of 8 weeks, which only slightly impaired glucose and insulin tolerance in young mice of around 14 weeks, an age when they are usually investigated, but this was apparently exacerbated in older mice of 14 months of age.

Results from the *in vivo* GSIS displayed that β-cell function was impaired by the HFD regardless of age, but the definite amount of secreted insulin was only reduced in aged mice, while young mice could compensate for the increased insulin demand at a mildly insulin resistant stage. This suggests that β-cells from young mice keep a sufficient plasticity to maintain its insulin secretion function. This is also reflected by the changes in β-cell mass and in line with previous data showing that the ability of β-cells to proliferate is lost during ageing^{47,48}. Young but not old mice respond to a HFD with β-cell mass expansion to meet the increased insulin demand. Such differences in the β-cell expansion capacity are not only observed with ageing but also with duration of diet. While high fat diet feeding for up to 8 weeks results in β-cell mass expansion, such adaptive increase in β-cell mass is not observed any more after 12 weeks³⁸. This also correlates with β-cell apoptosis, which is only seen after longer periods of HFD feeding⁴⁵, while after 8 weeks, HFD feeding does not result in changes of β-cell survival in young mice, but induces β-cell apoptosis in old mice. Such effects are certainly also dependent on the diet composition, as an even higher carbohydrate content in the diet (35% of calorie intake) can already severely impair glucose homeostasis in young mice⁴⁹. While the diabetogenic "Surwit diet" of 58, 16 and 26% calories from fat, protein and carbohydrate, respectively⁴⁴, disrupts insulin secretion later in life, β-cells can compensate for this in young mice. Their survival is not significantly affected yet, and there is only minor deterioration in glucose and insulin tolerance. This is reminiscent of our earlier study in human islets *ex vivo*, which shows that β-cell survival *per se* is not impaired in older individuals, but in response to diabetogenic stimulation, such as HFD or hyperglycemia, apoptosis is accelerated⁴⁷. In aged HFD mice, there is a significantly elevated basal insulin secretion, and subsequently insulin secretion cannot be further induced in response to glucose during *in vivo* GSIS, which was just

recently confirmed⁵⁰. Such elevated basal insulin level is mainly due to insulin resistance and elevated FFA levels during an obese insulin resistant stage. The improvement in the β -cell stimulatory index by TLR4 deficiency is mainly attributed to the normalization in basal secretion. Interestingly, despite no obvious impairment in insulin sensitivity by the HFD in TLR4-KO mice, there is a compensatory increase in β -cell mass and insulin content, which suggests that such adaptation may be independent of insulin sensitivity.

In an *in vitro* GSIS assay, in which the effect of insulin resistance can be ruled out, basal insulin levels were similar and glucose stimulated insulin secretion reduced in young HFD mice, and fully abolished in old HFD mice, suggesting the secretory function is also compromised, while TLR4 deficiency protected the islets from such functional depletion. Such obvious loss in the secretory function was also observed in islets from senescent (21–22-month old) Fisher rats, compared to young rats (4–5-month old)⁵¹. Also in 7–8-month old Wistar rats, insulin production as well as secretion is impaired⁴⁷, which is attributed at least in part to the reduction in PDX1^{47,52}, the factor for glucose mediated insulin production in mature β -cells. Other factors, which lead to an almost complete decline in β -cell regeneration in ageing are the increased expression of the cell cycle inhibitor P16⁴⁸, which is initiated by decreased Bmi-1 binding to the Ink4a/Arf locus⁵³ and by decreased Ezh2⁵⁴; both increase P16, and thus disable β -cell proliferation. As cell cycle and senescence markers have been identified in islets during ageing, we specifically focused here on markers of the inflammatory response; not only in islets but also in insulin responsive tissues. Overall, our study indicates that a mild ageing itself doesn't induce β -cell functional impairment and survival, whereas it can potentiate the adverse effects of a short-term HFD.

“Sterile” chronic, low-grade inflammation without any obvious infection is a common feature of ageing, and people over the age of 65 have increased serum levels of IL-6, TNF, and IL-18^{55,56}. Similarly, in rodent models of ageing, IL-1 β , IL-6, MCP-1 (CCL2), TNF and IL-12b increase in fat and liver^{31,33,34}. With respect to the pancreas, oxidative stress increases in aged mouse pancreases *per se* at the age of 14–16 months³² and TNF expression is elevated in pancreatic acinar cells in female mice aged 18–19 months³⁵. In the present study, however, a pro-inflammatory cytokine expression by ageing alone was only seen in fat, but not in liver and islets, though differences in age, species and strains exist among this and other studies. We show that ageing alone neither induced metabolic deterioration nor an overall activated inflammatory state in metabolically active tissues.

Along with inflammatory cytokines, lipotoxicity contributes to insulin resistance and β -cell dysfunction through oxidative stress⁵⁷. Free fatty acids activate TLR4, which further downstream leads to ROS/RNS production⁵⁸. This is likely another mechanism, besides the inhibition of inflammation, by which TLR4 depletion ameliorated glucose homeostasis, β -cell function and survival in aged HFD fed mice in this study, even though we have not addressed such possible mechanism.

To the question whether the number of macrophages increase in tissues during ageing, several studies reported macrophage accumulation in fat, liver and/or pancreas of aged mice or rats^{30,31,34}, although this was not confirmed by others^{32,33}. In our current study, based on gene expression of accepted markers, neither macrophage accumulation nor their polarization status was changed in older mice in any of the three tissues, which is in line with the unchanged tissue inflammation. Mutually contradictory results were obtained from various studies, where down-regulation in both M1 and M2 polarization markers⁵⁹, increased M2 macrophages⁶⁰, or an overall macrophage polarization towards the M1 type during aging were observed³³. The problem is that different age groups were used in these studies, with young animals ranging from 1–6 months and old animals ranging from 12–24 months age, thereby no corresponding correlation between an older age and worsening of the inflammatory phenotype could be drawn.

HFD feeding in the young mice for a short period of 8 weeks did not induce a full cytokine response at the mRNA level. The first elevated cytokines in response to the HFD were *Il1b* in fat and *Tnf* in islets. Since we didn't observe compromised glucose tolerance, the very low-grade inflammation in young mice is consistent with the consensus that inflammation precedes hyperglycemia. In contrast, insulin secretion in young mice, tested by GSIS *in vivo* as well as *in vitro*, was already affected at this stage, together with the β -cell mass compensation response. *Tnf* was the only cytokine, which was induced in pancreatic islets by the short HFD feeding in the young mice, and this could act as mediator of β -cell dysfunction. This is in line with a previous study; while TNF does not affect β -cell apoptosis, it blunts GSIS from sorted β -cells⁶¹. Such results point to the possibility of early detrimental effects on β -cell function mediated by TNF. Especially, TNF is known to trigger insulin resistance and was also highly elevated at an insulin resistant stage in liver and fat in the old HFD mice. Thus, the results of this study also support the strategy to target TNF for the treatment of insulin resistance and β -cell failure⁶².

Neither ageing nor short term HFD itself induced severe hyperglycemia or massive changes in the cytokine pattern. But the combination of both synergistically induced inflammation in all insulin responsive and insulin secreting tissues- fat, liver and pancreatic islets. Along with hyperglycemia, insulin resistance, fully abolished insulin secretion and β -cell apoptosis, tissues were more inflamed in old HFD mice than in young, including a more and stronger pro-inflammatory and reduced anti-inflammatory cytokine expression. One limitation of this study is, that we only assessed mRNA levels of inflammatory products, which allowed quantitative analysis of cytokines at a very low expression levels. Moreover, cytokines are unstable and degrade rapidly, and thus often lay under the assay detection range, which makes their assessment on a protein level in tissues difficult.

Consistent with cytokine profiles, we found that only the combination of ageing and HFD feeding could increase the overall macrophage accumulation, again in line with the finding that ageing could potentiate HFD-induced gene expression of inflammatory cytokines, of markers of pro-inflammatory macrophages, along with a reduction in anti-inflammatory macrophage markers in fat and islets, metabolic dysfunction and β -cell failure.

A scenario emerges, how the HFD-ageing duo affects glucose metabolism: young mice are responsive to HFD with mildly increased macrophages in metabolism active tissues. This contributes to a mild inflammatory cytokine production and, in turn, results in an impairment of β -cell function. However, β -cells are still resilient to maintain compensation and glucose homeostasis. When mice get older, the same short-term diet stress not

only increases M1-like macrophages but also attenuates M2-like macrophage activation, which further imbalances the macrophage phenotype and brings deterioration in the inflammatory status with more pro- and less anti-inflammatory cytokines. This then may lead to insulin resistance and compromised β -cell function, and in combination with reduced β -cell proliferation and increased β -cell apoptosis during ageing, it will finally result in definite insulin deficiency and concomitant hyperglycemia.

Being a crucial pattern recognition receptor and key player in inflammation, TLR4 is involved in many aspects of the pathogenesis of T2D, at the level of both β -cells and insulin responsive tissues^{7,8,10,13}. As we aimed to identify the contribution of TLR4 on whole body glucose metabolism, we used whole-body TLR4-KO mice. This strategy, however, restrained the identification of the primary tissues affected by TLR4 signals. The generation of mouse models with tissue specific TLR4 re-expression in adipocytes/hepatocytes/ β -cells/macrophages, respectively, on a TLR4-KO C57BL/10ScCr background would allow characterization of tissue specific effects, as well as a proof of a TLR4 specific effect upon its re-expression.

Tissue specific TLR4 effects have been studied in the past and confirmed observation from global deletions, e.g. myeloid-specific (as well as global) TLR4-deficiency improves insulin sensitivity and inhibits obesity-induced tissue inflammation in HFD and lipid infusion models^{7,11,22,63,64}. However, in TLR4-deficient mice, both reduced^{7,11,65} and unchanged ATM accumulation has been reported^{9,64}. Notably, Orr *et al.* found that TLR4-depletion promoted M2 polarization in fat⁹. Similarly, Jia *et al.* observed that myeloid-specific *Tlr4*^{-/-} had a trend to promote macrophage alternative activation in fat together with induced IL-10 production¹².

Featuring the combinational effect of a mild HFD and ageing, our results in insulin-responsive and insulin-producing tissues from old HFD mice indicate an overall trend that TLR4-deficiency reduces mRNA expression of inflammatory cytokines and M1 macrophage markers, and additionally promotes alternative macrophage activation specifically in the liver. This *in vivo* study is also in line with previous *ex vivo* studies^{13,66}; TLR4 activation in isolated islets induces cytokine expression, impairs glucose-stimulated insulin secretion and increases β -cell apoptosis. This is again supportive for the role of TLR4 activation in diabetes progression.

In summary, we found that ageing aggravated diet-induced impairment on glucose homeostasis, pancreatic β -cell function and survival and enhanced gene expression of inflammatory products in fat, liver and pancreatic islets in a HFD-fed mouse model. TLR4-deficiency exhibited protection against such deleterious effects through inhibiting pro-inflammatory cytokine expression and modulating tissue macrophage activation to a more anti-inflammatory phenotype. Ageing and obesity synergistically induce diabetes through TLR4, supporting the therapeutic potential of TLR4 inhibition to treat T2D.

References

- Wellen, K. E. & Hotamisligil, G. S. Inflammation, stress, and diabetes. *The Journal of clinical investigation* **115**, 1111–1119 (2005).
- Donath, M. Y. & Shoelson, S. E. Type 2 diabetes as an inflammatory disease. *Nature reviews. Immunology* **11**, 98–107 (2011).
- Osborn, O. & Olefsky, J. M. The cellular and signaling networks linking the immune system and metabolism in disease. *Nature medicine* **18**, 363–374 (2012).
- Hill, A. A., Reid Bolus, W. & Hasty, A. H. A decade of progress in adipose tissue macrophage biology. *Immunological reviews* **262**, 134–152 (2014).
- Kraakman, M. J., Murphy, A. J., Jandeleit-Dahm, K. & Kammoun, H. L. Macrophage polarization in obesity and type 2 diabetes: weighing down our understanding of macrophage function. *Frontiers in immunology* **5**, 470 (2014).
- Morris, D. L. Minireview: Emerging Concepts in Islet Macrophage Biology in Type 2 Diabetes. *Molecular endocrinology* **29**, 946–962 (2015).
- Shi, H. *et al.* TLR4 links innate immunity and fatty acid-induced insulin resistance. *The Journal of clinical investigation* **116**, 3015–3025 (2006).
- Mehta, N. N. *et al.* Experimental endotoxemia induces adipose inflammation and insulin resistance in humans. *Diabetes* **59**, 172–181 (2010).
- Orr, J. S. *et al.* Toll-like receptor 4 deficiency promotes the alternative activation of adipose tissue macrophages. *Diabetes* **61**, 2718–2727 (2012).
- Amyot, J., Semache, M., Ferdaoussi, M., Fontes, G. & Poirout, V. Lipopolysaccharides impair insulin gene expression in isolated islets of Langerhans via Toll-Like Receptor-4 and NF- κ B signalling. *PLoS One* **7**, e36200 (2012).
- Saberi, M. *et al.* Hematopoietic cell-specific deletion of toll-like receptor 4 ameliorates hepatic and adipose tissue insulin resistance in high-fat-fed mice. *Cell metabolism* **10**, 419–429 (2009).
- Jia, L. *et al.* Hepatocyte Toll-like receptor 4 regulates obesity-induced inflammation and insulin resistance. *Nature communications* **5**, 3878 (2014).
- Nackiewicz, D. *et al.* TLR2/6 and TLR4-activated macrophages contribute to islet inflammation and impair beta cell insulin gene expression via IL-1 and IL-6. *Diabetologia* **57**, 1645–1654 (2014).
- Li, J. *et al.* TLR4 is required for the obesity-induced pancreatic beta cell dysfunction. *Acta biochimica et biophysica Sinica* **45**, 1030–1038 (2013).
- Creely, S. J. *et al.* Lipopolysaccharide activates an innate immune system response in human adipose tissue in obesity and type 2 diabetes. *American journal of physiology. Endocrinology and metabolism* **292**, E740–747 (2007).
- Dasu, M. R., Devaraj, S., Park, S. & Jialal, I. Increased toll-like receptor (TLR) activation and TLR ligands in recently diagnosed type 2 diabetic subjects. *Diabetes care* **33**, 861–868 (2010).
- Herder, C. *et al.* Chemokines as risk factors for type 2 diabetes: results from the MONICA/KORA Augsburg study, 1984–2002. *Diabetologia* **49**, 921–929 (2006).
- Schulthess, F. T. *et al.* CXCL10 impairs beta cell function and viability in diabetes through TLR4 signaling. *Cell metabolism* **9**, 125–139 (2009).
- Hwang, D. Modulation of the expression of cyclooxygenase-2 by fatty acids mediated through toll-like receptor 4-derived signaling pathways. *FASEB journal: official publication of the Federation of American Societies for Experimental Biology* **15**, 2556–2564 (2001).
- Lee, J. Y., Sohn, K. H., Rhee, S. H. & Hwang, D. Saturated fatty acids, but not unsaturated fatty acids, induce the expression of cyclooxygenase-2 mediated through Toll-like receptor 4. *The Journal of biological chemistry* **276**, 16683–16689 (2001).
- Nguyen, M. T. *et al.* A subpopulation of macrophages infiltrates hypertrophic adipose tissue and is activated by free fatty acids via Toll-like receptors 2 and 4 and JNK-dependent pathways. *The Journal of biological chemistry* **282**, 35279–35292 (2007).
- Pal, D. *et al.* Fetuin-A acts as an endogenous ligand of TLR4 to promote lipid-induced insulin resistance. *Nature medicine* **18**, 1279–1285 (2012).

23. Gerst, F. *et al.* Metabolic crosstalk between fatty pancreas and fatty liver: effects on local inflammation and insulin secretion. *Diabetologia* (2017).
24. Brix, J. M. *et al.* Elevated Fetuin-A concentrations in morbid obesity decrease after dramatic weight loss. *The Journal of clinical endocrinology and metabolism* **95**, 4877–4881 (2010).
25. Stefan, N. *et al.* Impact of the adipokine adiponectin and the hepatokine fetuin-A on the development of type 2 diabetes: prospective cohort- and cross-sectional phenotyping studies. *PLoS one* **9**, e92238 (2014).
26. Cani, P. D. *et al.* Changes in gut microbiota control metabolic endotoxemia-induced inflammation in high-fat diet-induced obesity and diabetes in mice. *Diabetes* **57**, 1470–1481 (2008).
27. Cani, P. D., Delzenne, N. M., Amar, J. & Burcelin, R. Role of gut microflora in the development of obesity and insulin resistance following high-fat diet feeding. *Pathologie-biologie* **56**, 305–309 (2008).
28. Kuwabara, T. *et al.* Macrophage-mediated glucolipotoxicity via myeloid-related protein 8/toll-like receptor 4 signaling in diabetic nephropathy. *Clinical and experimental nephrology* **18**, 584–592 (2014).
29. Meneilly, G. S. & Tessier, D. Diabetes in elderly adults. *The journals of gerontology. Series A, Biological sciences and medical sciences* **56**, M5–13 (2001).
30. Almaca, J. *et al.* Young capillary vessels rejuvenate aged pancreatic islets. *Proceedings of the National Academy of Sciences of the United States of America* **111**, 17612–17617 (2014).
31. Horrillo, D. *et al.* Age-associated development of inflammation in Wistar rats: Effects of caloric restriction. *Archives of physiology and biochemistry* **117**, 140–150 (2011).
32. Yang, T. *et al.* Abrogation of adenosine A1 receptor signalling improves metabolic regulation in mice by modulating oxidative stress and inflammatory responses. *Diabetologia* **58**, 1610–1620 (2015).
33. Lumeng, C. N. *et al.* Aging is associated with an increase in T cells and inflammatory macrophages in visceral adipose tissue. *Journal of immunology* **187**, 6208–6216 (2011).
34. Lin, L. *et al.* Ghrelin receptor regulates adipose tissue inflammation in aging. *Aging* **8**, 178–191 (2016).
35. Xiong, Y. *et al.* Arginase-II Promotes Tumor Necrosis Factor-alpha Release from Pancreatic Acinar Cells Causing beta-Cell Apoptosis In Aging. *Diabetes* (2017).
36. Johnson, G. B., Riggs, B. L. & Platt, J. L. A genetic basis for the “Adonis” phenotype of low adiposity and strong bones. *FASEB journal: official publication of the Federation of American Societies for Experimental Biology* **18**, 1282–1284 (2004).
37. Salvioli, S. *et al.* Inflamm-aging, cytokines and aging: state of the art, new hypotheses on the role of mitochondria and new perspectives from systems biology. *Current pharmaceutical design* **12**, 3161–3171 (2006).
38. Meyer, A. *et al.* Manganese-mediated MRI signals correlate with functional beta-cell mass during diabetes progression. *Diabetes* **64**, 2138–2147 (2015).
39. Fink, L. N. *et al.* Pro-inflammatory macrophages increase in skeletal muscle of high fat-fed mice and correlate with metabolic risk markers in humans. *Obesity* **22**, 747–757 (2014).
40. Han, M. S. *et al.* JNK expression by macrophages promotes obesity-induced insulin resistance and inflammation. *Science* **339**, 218–222 (2013).
41. Odegaard, J. I. *et al.* Macrophage-specific PPARgamma controls alternative activation and improves insulin resistance. *Nature* **447**, 1116–1120 (2007).
42. Odegaard, J. I. *et al.* Alternative M2 activation of Kupffer cells by PPARdelta ameliorates obesity-induced insulin resistance. *Cell metabolism* **7**, 496–507 (2008).
43. Coutinho, A., Furni, L., Melchers, F. & Watanabe, T. Genetic defect in responsiveness to the B cell mitogen lipopolysaccharide. *European journal of immunology* **7**, 325–328 (1977).
44. Surwit, R. S. *et al.* Differential effects of fat and sucrose on the development of obesity and diabetes in C57BL/6J and A/J mice. *Metabolism: clinical and experimental* **44**, 645–651 (1995).
45. Ardestani, A. *et al.* MST1 is a key regulator of beta cell apoptosis and dysfunction in diabetes. *Nature medicine* **20**, 385–397 (2014).
46. Sauter, N. S., Schulthess, F. T., Galasso, R., Castellani, L. W. & Maedler, K. The antiinflammatory cytokine interleukin-1 receptor antagonist protects from high-fat diet-induced hyperglycemia. *Endocrinology* **149**, 2208–2218 (2008).
47. Maedler, K. *et al.* Aging correlates with decreased beta-cell proliferative capacity and enhanced sensitivity to apoptosis: a potential role for Fas and pancreatic duodenal homeobox-1. *Diabetes* **55**, 2455–2462 (2006).
48. Tschen, S. I., Dhawan, S., Gurlo, T. & Bhushan, A. Age-dependent decline in beta-cell proliferation restricts the capacity of beta-cell regeneration in mice. *Diabetes* **58**, 1312–1320 (2009).
49. Montgomery, M. K. *et al.* Mouse strain-dependent variation in obesity and glucose homeostasis in response to high-fat feeding. *Diabetologia* **56**, 1129–1139 (2013).
50. Aguayo-Mazzucato, C. *et al.* beta Cell Aging Markers Have Heterogeneous Distribution and Are Induced by Insulin Resistance. *Cell metabolism* **25**, 898–910 e895 (2017).
51. Wang, S. Y., Halban, P. A. & Rowe, J. W. Effects of aging on insulin synthesis and secretion. Differential effects on preproinsulin messenger RNA levels, proinsulin biosynthesis, and secretion of newly made and preformed insulin in the rat. *The Journal of clinical investigation* **81**, 176–184 (1988).
52. Reers, C. *et al.* Impaired islet turnover in human donor pancreata with aging. *European journal of endocrinology* **160**, 185–191 (2009).
53. Dhawan, S., Tschen, S. I. & Bhushan, A. Bmi-1 regulates the Ink4a/Arf locus to control pancreatic beta-cell proliferation. *Genes & development* **23**, 906–911 (2009).
54. Chen, H. *et al.* Polycomb protein Ezh2 regulates pancreatic beta-cell Ink4a/Arf expression and regeneration in diabetes mellitus. *Genes & development* **23**, 975–985 (2009).
55. Ferrucci, L. *et al.* The origins of age-related proinflammatory state. *Blood* **105**, 2294–2299 (2005).
56. Pedersen, M. *et al.* Circulating levels of TNF-alpha and IL-6-relation to truncal fat mass and muscle mass in healthy elderly individuals and in patients with type-2 diabetes. *Mechanisms of ageing and development* **124**, 495–502 (2003).
57. Keane, K. N., Cruzat, V. F., Carlessi, R., de Bittencourt, P. I. Jr. & Newsholme, P. Molecular Events Linking Oxidative Stress and Inflammation to Insulin Resistance and beta-Cell Dysfunction. *Oxidative medicine and cellular longevity* **2015**, 181643 (2015).
58. Davis, J. E., Gabler, N. K., Walker-Daniels, J. & Spurlock, M. E. The c-Jun N-terminal kinase mediates the induction of oxidative stress and insulin resistance by palmitate and toll-like receptor 2 and 4 ligands in 3T3-L1 adipocytes. *Hormone and metabolic research = Hormon- und Stoffwechselforschung = Hormones et metabolisme* **41**, 523–530 (2009).
59. Mahbub, S., Deburghraeve, C. R. & Kovacs, E. J. Advanced age impairs macrophage polarization. *Journal of interferon & cytokine research: the official journal of the International Society for Interferon and Cytokine Research* **32**, 18–26 (2012).
60. Jackaman, C. *et al.* Targeting macrophages rescues age-related immune deficiencies in C57BL/6J geriatric mice. *Aging cell* **12**, 345–357 (2013).
61. Bouzakri, K., Ribaux, P. & Halban, P. A. Silencing mitogen-activated protein kinase 4 (MAP4K4) protects beta cells from tumor necrosis factor-alpha-induced decrease of IRS-2 and inhibition of glucose-stimulated insulin secretion. *The Journal of biological chemistry* **284**, 27892–27898 (2009).
62. Donath, M. Y. Targeting inflammation in the treatment of type 2 diabetes: time to start. *Nature reviews. Drug discovery* **13**, 465–476 (2014).

63. Poggi, M. *et al.* C3H/HeJ mice carrying a toll-like receptor 4 mutation are protected against the development of insulin resistance in white adipose tissue in response to a high-fat diet. *Diabetologia* **50**, 1267–1276 (2007).
64. Suganami, T. *et al.* Attenuation of obesity-induced adipose tissue inflammation in C3H/HeJ mice carrying a Toll-like receptor 4 mutation. *Biochemical and biophysical research communications* **354**, 45–49 (2007).
65. Davis, J. E., Gabler, N. K., Walker-Daniels, J. & Spurlock, M. E. Tlr-4 deficiency selectively protects against obesity induced by diets high in saturated fat. *Obesity* **16**, 1248–1255 (2008).
66. Cucak, H. *et al.* Macrophage contact dependent and independent TLR4 mechanisms induce beta-cell dysfunction and apoptosis in a mouse model of type 2 diabetes. *PLoS one* **9**, e90685 (2014).

Acknowledgements

This work was supported by the German Research Foundation (DFG) and the European Research Council (ERC). We thank Katrischa Hennekens (University of Bremen) for excellent technical assistance.

Author Contributions

Conceived this project: K.M. Designed, performed and analyzed research: W.H. and K.M. Performed and analyzed this research: T.Y., D.C., H.H., K.A., B.L. Wrote the paper: W.H., K.M.

Additional Information

Supplementary information accompanies this paper at <https://doi.org/10.1038/s41598-018-20909-w>.

Competing Interests: The authors declare no competing interests.

Publisher's note: Springer Nature remains neutral with regard to jurisdictional claims in published maps and institutional affiliations.



Open Access This article is licensed under a Creative Commons Attribution 4.0 International License, which permits use, sharing, adaptation, distribution and reproduction in any medium or format, as long as you give appropriate credit to the original author(s) and the source, provide a link to the Creative Commons license, and indicate if changes were made. The images or other third party material in this article are included in the article's Creative Commons license, unless indicated otherwise in a credit line to the material. If material is not included in the article's Creative Commons license and your intended use is not permitted by statutory regulation or exceeds the permitted use, you will need to obtain permission directly from the copyright holder. To view a copy of this license, visit <http://creativecommons.org/licenses/by/4.0/>.

© The Author(s) 2018

4.2 Loss of Deubiquitinase USP1 blocks pancreatic β -cell apoptosis by inhibiting DNA damage response

Kanaka Durga Devi Gorrepati , Blaz Lypse , Karthika Annamalaj , Ting Yuan , Kathrin Maedler , Amin Ardestani

Published in iScience. 2018 Mar 23;1:72-86. doi: 10.1016/j.isci.2018.02.003.

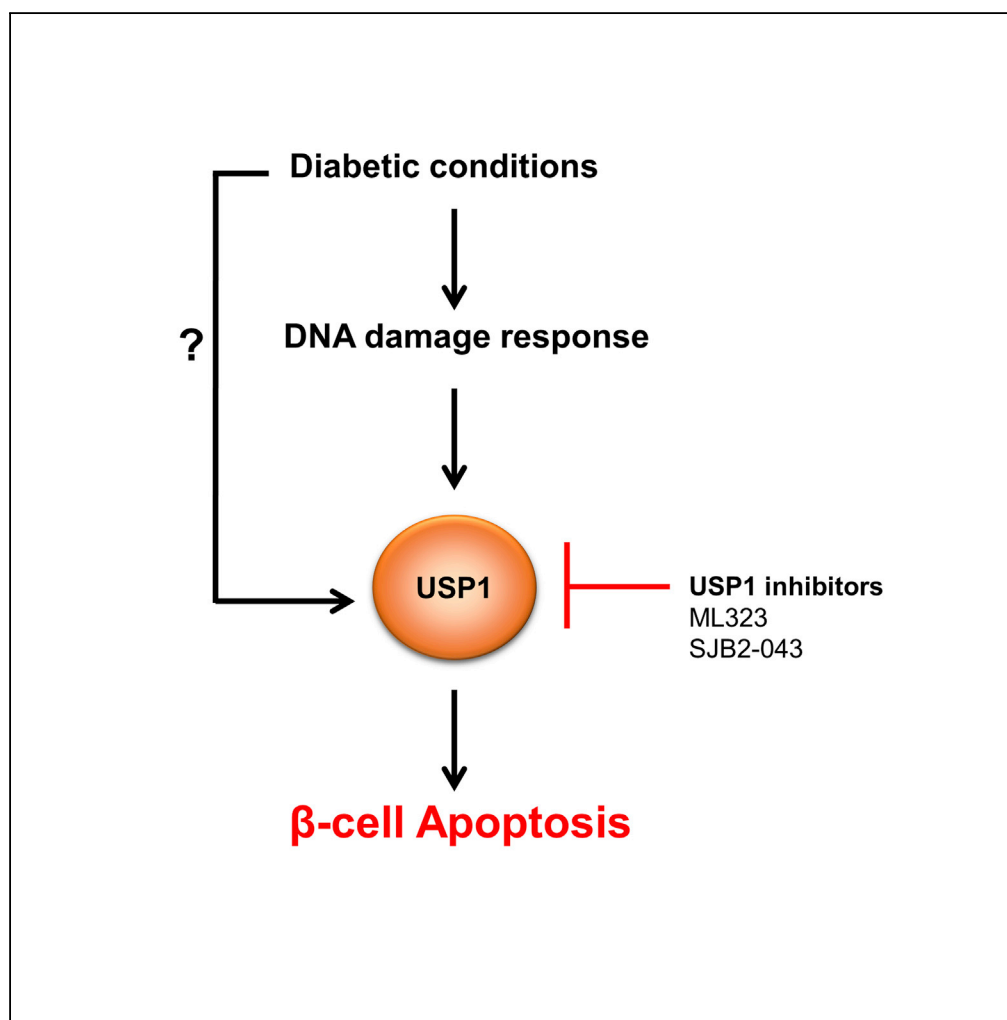
My contribution:

Performed experiments and analysed data for:

Figures: 4I,J ; 6G-J

Article

Loss of Deubiquitinase USP1 Blocks Pancreatic β -Cell Apoptosis by Inhibiting DNA Damage Response



Kanaka Durga Devi
Gorrepati, Blaz
Lupse, Karthika
Annamalai, Ting
Yuan, Kathrin
Maedler, Amin
Ardestani

kmaedler@uni-bremen.de
(K.M.)
ardestani.amin@gmail.com
(A.A.)

HIGHLIGHTS

Genetic and chemical
inhibition of USP1
promoted β -cell survival

USP1 inhibitors blocked
 β -cell death in human
islets without affecting
 β -cell function

USP1 inhibition reduced
DDR signals in stressed
 β -cells

Gorrepati et al., iScience 1,
72–86
March 23, 2018 © 2018 The
Author(s).
[https://doi.org/10.1016/
j.isci.2018.02.003](https://doi.org/10.1016/j.isci.2018.02.003)

Article

Loss of Deubiquitinase USP1 Blocks Pancreatic β -Cell Apoptosis by Inhibiting DNA Damage Response

Kanaka Durga Devi Gorrepati,¹ Blaz Lupse,¹ Karthika Annamalai,¹ Ting Yuan,¹ Kathrin Maedler,^{1,2,*} and Amin Ardestani^{1,2,3,*}

SUMMARY

Impaired pancreatic β -cell survival contributes to the reduced β -cell mass in diabetes, but underlying regulatory mechanisms and key players in this process remain incompletely understood. Here, we identified the deubiquitinase ubiquitin-specific protease 1 (USP1) as an important player in the regulation of β -cell apoptosis under diabetic conditions. Genetic silencing and pharmacological suppression of USP1 blocked β -cell death in several experimental models of diabetes in vitro and ex vivo without compromising insulin content and secretion and without impairing β -cell maturation/identity genes in human islets. Our further analyses showed that USP1 inhibition attenuated DNA damage response (DDR) signals, which were highly elevated in diabetic β -cells, suggesting a USP1-dependent regulation of DDR in stressed β -cells. Our findings highlight a novel function of USP1 in the control of β -cell survival, and its inhibition may have a potential therapeutic relevance for the suppression of β -cell death in diabetes.

INTRODUCTION

Loss of function and/or mass of insulin-producing pancreatic β -cells is a hallmark of both type 1 and 2 diabetes (T1D/T2D) (Butler et al., 2003; Kurrer et al., 1997; Mathis et al., 2001; Rhodes, 2005; Vetere et al., 2014). Pancreatic β -cell death is a critical pathogenic factor contributing to the declined β -cell mass in both T1D and T2D (Ardestani et al., 2014; Butler et al., 2003; Kurrer et al., 1997; Marselli et al., 2014; Masini et al., 2009; Mathis et al., 2001; Meier et al., 2005; Rahier et al., 2008; Rhodes, 2005; Tomita, 2010). Also, β -cell dedifferentiation (Cinti et al., 2016; Jeffery and Harries, 2016; Talchai et al., 2012) and impaired adaptive proliferation (Ardestani and Maedler, 2018; Tiwari et al., 2016) have been proposed as potential additional causes for this diminished β -cell mass in diabetes. Although immune-cell-mediated events predominate in T1D (Chatenoud, 2010), metabolic factors such as elevated levels of glucose, fatty acids, and islet amyloid polypeptide (IAPP), alongside with pro-inflammatory cytokines, drive β -cell loss and dysfunction in T2D (Alejandro et al., 2015; Ardestani et al., 2018; Donath et al., 2013; Haataja et al., 2008; Huang et al., 2007; Maedler et al., 2002; Poyntout and Robertson, 2008; Robertson et al., 2004; Yuan et al., 2017). Excessive β -cell death is commonly seen in the islets of both patients with T1D and lean and obese patients with T2D as determined by multiple complementary approaches (Butler et al., 2003; Masini et al., 2009; Meier et al., 2005; Tomita, 2010). Counter-intuitively, higher levels of β -cell apoptosis in autopsy pancreases from patients with established diabetes inversely correlate with the insulin-positive β -cell area. But even at a pre-diabetic stage, i.e., in at-risk individuals who progressed to T1D, β -cell death is evident and accompanied with diminished insulin secretion (Herold et al., 2015). Correspondingly, in patients with impaired glucose tolerance before T2D diagnosis, loss of β -cells is apparent and correlates with elevated fasting glucose levels (Ritzel et al., 2006); this gradually progresses when hyperglycemia is established and β -cells are unable to sustain insulin production under a higher metabolic demand. Indeed, pancreatic β -cells show a relatively higher susceptibility to apoptosis together with lower stress-induced protective responses compared with many other cell types, including the neighboring pancreatic α -cells. For instance, a recent proteomic analysis shows a very weak induction of β -cell's reactive oxygen species (ROS)-detoxifying enzymes in response to inflammatory assault (Gorasia et al., 2015). This confirms previous observations showing very low levels of protective anti-oxidative enzymes in β -cells (Grankvist et al., 1981; Lenzen, 2008; Lenzen et al., 1996; Tiedge et al., 1997). Consistently, human β -cells are much more sensitive to apoptosis than α -cells in response to T2D-related metabolic stressors (Marroqui et al., 2015). All these seem to represent an "Achilles heel" through which

¹Islet Biology Laboratory, University of Bremen, Centre for Biomolecular Interactions Bremen, Leobener Straße NW2, Room B2080, 28359 Bremen, Germany

²Senior author

³Lead Contact

*Correspondence: kmaedler@uni-bremen.de (K.M.), ardestani.amin@gmail.com (A.A.)

<https://doi.org/10.1016/j.isci.2018.02.003>



diabetogenic stimuli trigger rapid β -cell death and accelerate the collapse in response to environmental stress and demand.

The ubiquitin-proteasome system (UPS) is a highly regulated key intracellular protein degradation pathway, which consists of an enzymatic cascade controlling protein ubiquitination and has important functions in several essential biological processes, such as cell survival, proliferation, development, and DNA damage response (DDR) (Schmidt and Finley, 2014). The UPS is a process of post-translational modification of targeted protein by covalent attachment of one or more ubiquitins to lysine residues by an E3 ubiquitin ligase. This is antagonized by enzyme deubiquitinases (DUBs), such as ubiquitin-specific proteases (USPs). The UPS is primarily responsible for the degradation and clearance of misfolded or damaged proteins as well as of dysfunctional organelles, which compromise cellular homeostasis. Abnormalities in the UPS machinery have been linked to the pathogenesis of many diseases, including cancer, immunological and neurological disorders (Frescas and Pagano, 2008; Schmidt and Finley, 2014; Zheng et al., 2016), as well as β -cell failure in diabetes (Broca et al., 2014; Bugliani et al., 2013; Costes et al., 2011, 2014; Hartley et al., 2009; Hofmeister-Brix et al., 2013; Kaniuk et al., 2007; Litwak et al., 2015). A member of the USP family, ubiquitin-specific protease 1 (USP1), is one of the best known DUBs responsible for removing ubiquitin from target proteins and thus influences several cellular processes such as survival, differentiation, immunity and DDR (Garcia-Santisteban et al., 2013; Liang et al., 2014; Yu et al., 2017). Although USP1 was initially identified as a novel component of the Fanconi anemia DNA repair pathway (Nijman et al., 2005), extensive subsequent studies revealed a pleiotropic function of USP1 and identified novel interacting partners and signaling for USP1 action and regulation in normal physiological conditions and in disease states such as tumorigenesis (Garcia-Santisteban et al., 2013; Liang et al., 2014; Yu et al., 2017). An array-based assay identified reduced USP1 mRNA expression in islets from patients with T2D (Bugliani et al., 2013). As the consequent effects of USP1 in diabetes and especially in the pancreatic β -cell were completely unknown so far, we investigated the role and the mechanism of action of USP1 on β -cell survival under diabetic conditions using clonal β -cells and isolated primary human islets. Although USP1 protein expression was unchanged in a diabetic milieu, we identified a robust protective effect on β -cell survival by USP1 inhibition.

RESULTS

USP1 Knockdown Protects β -cells from Apoptosis Under Diabetic Conditions

Transcriptome analysis of islets isolated from healthy individuals as well as from patients with T2D showed consistent alteration of genes of UPS components, including members of the USP family such as USP1 (Bugliani et al., 2013). Because USP1 is involved in signaling pathways associated with DDR and survival (Liang et al., 2014), we aimed here to identify whether USP1 regulates apoptosis in β -cells under diabetogenic conditions. USP1 was expressed in protein lysates extracted from both human and mouse islets (data not shown) and INS-1E cells (Figure 1). The total protein level was not significantly changed in response to a pro-diabetic milieu in INS-1E cells (Figure 1). To evaluate the function of USP1 in the regulation of β -cell survival, USP1 was depleted in rat INS-1E β -cells by transfection with siUSP1 (Figure S1) and thereafter cultured long term with high glucose concentrations (glucotoxicity; Figures 1A and 1B), a combination of high glucose with saturated free fatty acid palmitate (glucolipotoxicity; Figures 1C and 1D), and a cocktail of pro-inflammatory cytokines (interleukin-1 beta [IL-1 β], interferon gamma [IFN- γ], and tumor necrosis factor alpha [TNF- α]; Figures 1E and 1F). Consistent with our previous observations, long-term culture with elevated glucose, glucose/palmitate, and cytokines robustly induced β -cell apoptosis (Ardestani et al., 2014; Yuan et al., 2016a, 2016b). Knockdown of USP1 markedly reduced the levels of glucose-, glucose/palmitate-, and cytokine-induced apoptosis as indicated by decreased levels of hallmarks of apoptosis, namely, caspase-3 and its downstream target poly(ADP-ribose) polymerase (PARP) cleavage (Figures 1A–1F). These data indicate that loss of USP1 confers apoptosis resistance to β -cells against stress-induced cell death.

Small Molecule USP1 Inhibitors Block β -Cell Apoptosis Under Diabetic Conditions

Several USP1 small molecule inhibitors have been developed recently. Quantitative high-throughput screen and subsequent medicinal chemistry identified compound ML323 (Figure 2A) as a highly potent selective inhibitor of USP1 with excellent specificity, when compared with other DUBs, deSUMOylase, deneddylase, and unrelated proteases (Dexheimer et al., 2010; Liang et al., 2014). ML323 was able to potently inhibit USP1 activity in a dose-dependent manner in several complementary *in vitro* assays as well as in cellular models as represented by increased monoubiquitination of USP1 known substrates proliferating cell nuclear antigen (PCNA) and Fanconi anemia group D2 protein (FANCD2) (Dexheimer et al., 2010; Liang

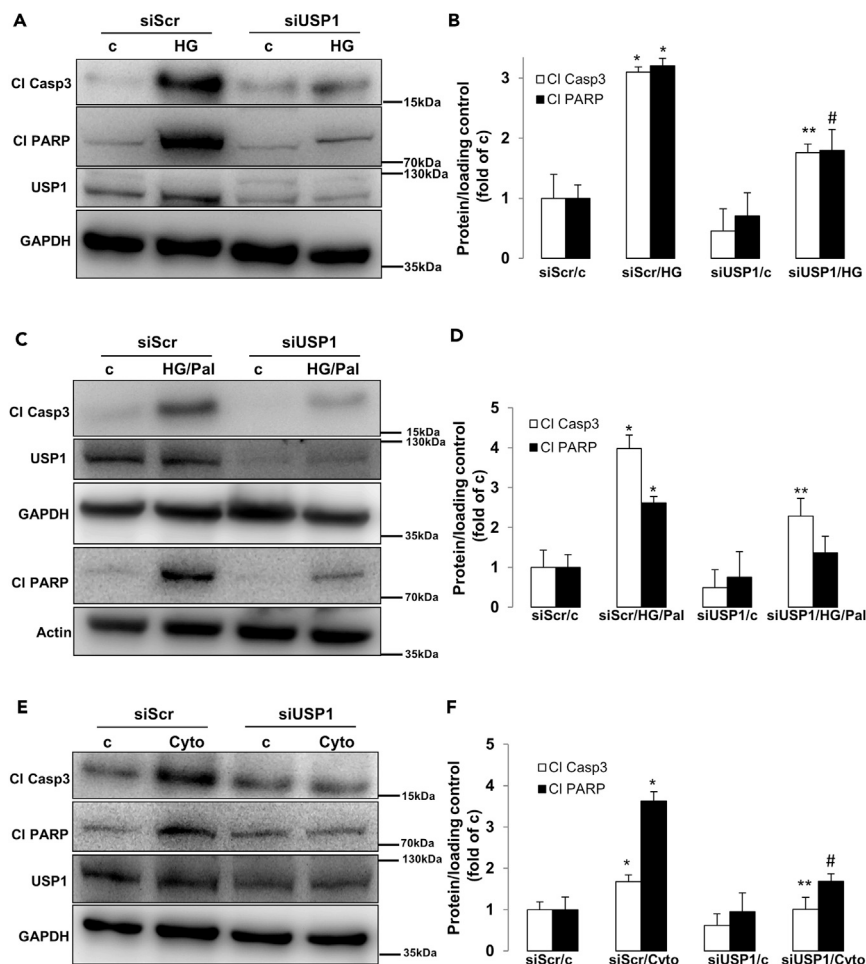


Figure 1. USP1 Knockdown Protects β -Cell from Apoptosis Under Diabetic Conditions

(A–F) INS-1E cells were seeded at 300,000 cells/well and transfected with either control scrambled siRNA (siScr) or siRNA specific to USP1 (siUSP1) and treated with (A and B) 22.2 mM glucose (HG), (C and D) a mixture of 22.2 mM glucose and 0.5 mM palmitate (HG/Pal), or (E and F) pro-inflammatory cytokines (2 ng/mL recombinant human IL-1 β , 1000 U/mL TNF- α , and 1000 U/mL IFN- γ ; Cyto) for 2 days. Representative Western blots (A, C, and E) and quantitative densitometry analysis (B, D, and F) of cleaved caspase 3 (CI Casp3) and cleaved PARP (CI PARP) protein levels are shown. Data are pooled from at least three independent cell line experiments. Data show means \pm SEM. * $p < 0.05$ siScr treated compared with siScr control conditions. ** $p < 0.05$ siUSP1-treated compared with siScr-treated conditions. # $p = 0.05$ compared with HG (B) or Cyto (F). See also Figure S1 for USP1 quantification.

et al., 2014). Inhibition of USP1 was also confirmed in INS-1E cells treated with ML323 as indicated by the accumulation of ubiquitinated PCNA, a USP1 downstream substrate (Figures S2A and S2B). To confirm the anti-apoptotic action of USP1 loss obtained by the genetic approach, we used ML323 to block USP1 activity in INS-1E cells exposed to diabetic conditions. USP1 inhibition by ML323 at two concentrations (5 and 10 μ M), which proved to be non-toxic at basal levels (data not shown), potently inhibited the induction of caspase-3 and PARP cleavage triggered by elevated glucose (Figures 2B and 2C), glucose/palmitate (Figures 2D and 2E), and cytokines (Figures 2F and 2G), further demonstrating the pro-apoptotic activity of USP1 in the presence of the diabetic milieu. Also, by using an ubiquitin-rhodamine-based high-throughput screening, Mistry et al. identified SJB2-043 (Figure 3A) as another potent selective small-molecule inhibitor of USP1. SJB2-043 blocked the deubiquitinating enzyme activity of USP1 *in vitro* with an IC₅₀ in the nanomolar range (Mistry et al., 2013). To further confirm the utility of USP1 blockade in protecting β -cells from apoptosis, we tested the effect of SJB2-043 on β -cell survival in the presence of diabetogenic conditions. Consistent with our genetic and pharmacological approaches using siRNA against USP1 and the USP1 inhibitor ML323, USP1 inhibition by SJB2-043 at two concentrations (20 and 50 nM) attenuated

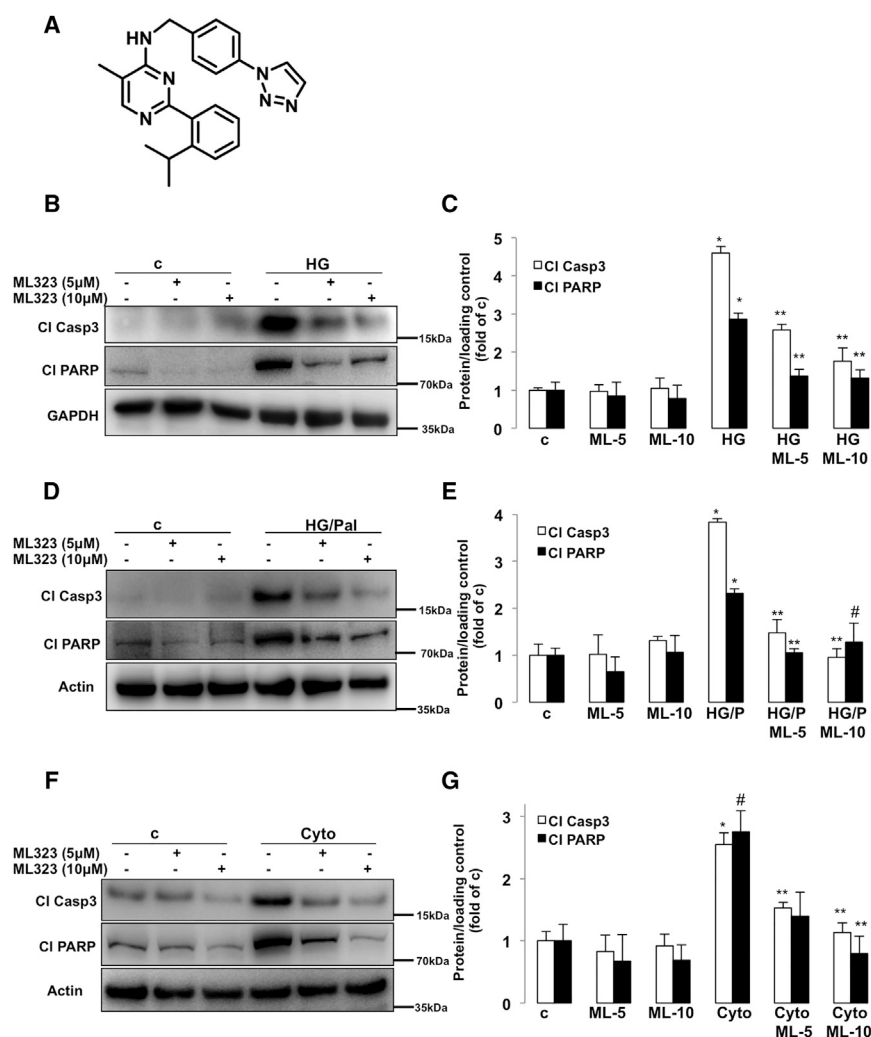


Figure 2. USP1 Inhibitor ML323 Blocks β -Cell Apoptosis Under Diabetic Conditions

(A) Chemical structure of ML323.

(B–G) About 500,000 INS-1E cells/well treated with or without USP1 inhibitor ML323 were exposed to 22.2 mM glucose (HG; B and C), a mixture of 22.2 mM glucose and 0.5 mM palmitate (HG/Pal; D and E), or pro-inflammatory cytokines (2 ng/mL recombinant human IL-1 β , 1000 U/mL TNF- α , and 1000 U/mL IFN- γ ; Cyto; F and G) for 2 days. Representative Western blots and quantitative densitometry analysis of cleaved caspase 3 (CI Casp3) and cleaved PARP (CI PARP) protein levels are shown. Data are pooled from at least three independent cell line experiments. Data show means \pm SEM.

* $p < 0.05$ treated compared with control conditions. ** $p < 0.05$ inhibitor-treated compared with treated conditions.

$p = 0.05$ compared with HG/P (E) or untreated control (G) alone. See also Figure S2 for PCNA ubiquitination.

β -cell apoptosis as represented by the robust reduction of cleaved caspase-3 and PARP induced by glucotoxicity (Figures 3B and 3C), glucolipotoxicity (Figures 3D and 3E), and pro-inflammatory cytokines (Figures 3F and 3G). Altogether, small molecule inhibitors of USP1 improved β -cell survival under diabetic conditions and recapitulated the β -cell protective effect of USP1 silencing.

USP1 Inhibition Protects Human Islets from Apoptosis without Compromising Their Insulin Secretory Function

To test the efficacy of USP1 inhibitors in blocking β -cell apoptosis in human islets with physiologically more relevant properties for human disease, human islets isolated from nondiabetic organ donors were treated with USP1 inhibitors ML323 and SJB2-043 and then exposed to the diabetogenic milieu of glucolipotoxicity and pro-inflammatory cytokines IL-1 β and IFN- γ . Caspase-3 cleavage triggered by high glucose/palmitate as well as by the mixture of cytokines was counteracted by ML323 in isolated human islets, confirmed

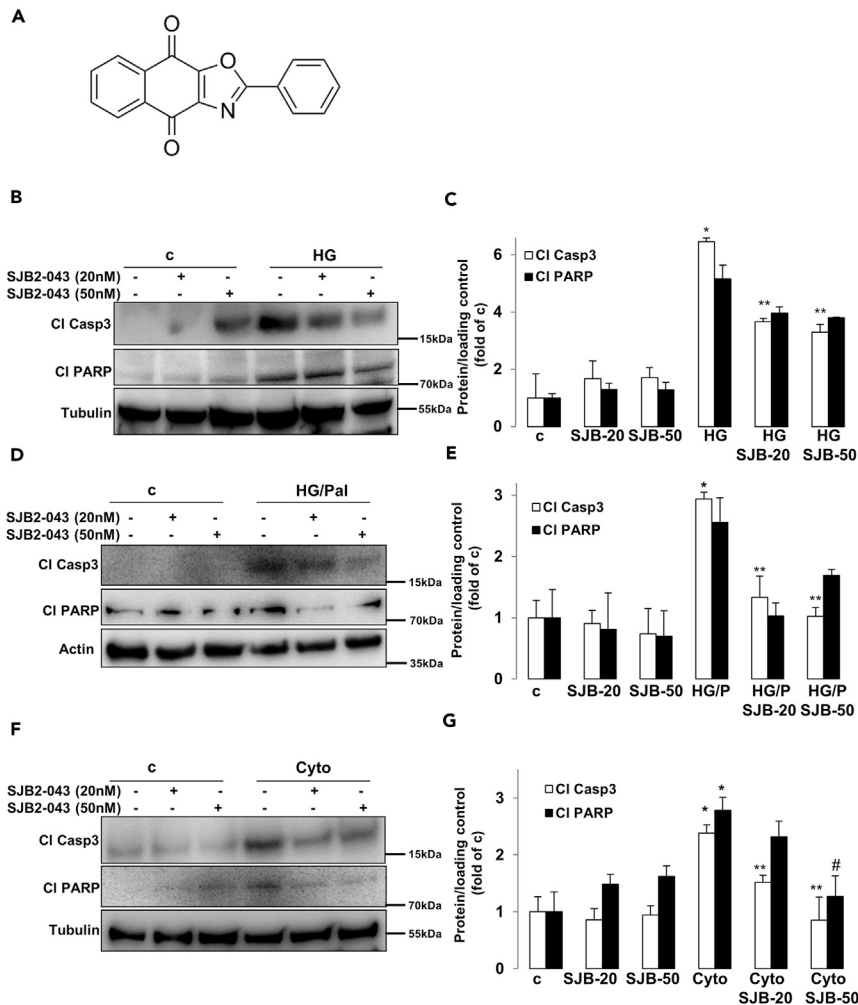


Figure 3. USP1 Inhibitor SJB2-043 Blocks β -Cell Apoptosis Under Diabetic Conditions

(A) Chemical structure of SJB2-043.

(B–G) About 500,000 INS-1E cells/well treated with or without USP1 inhibitor SJB2-043 were exposed to 22.2 mM glucose (HG; B and C), a mixture of 22.2 mM glucose and 0.5 mM palmitate (HG/Pal; D and E), or pro-inflammatory cytokines (2 ng/mL recombinant human IL-1 β , 1000 U/mL TNF- α , and 1000 U/mL IFN- γ ; Cyto; F and G) for 2 days. Representative Western blots and quantitative densitometry analysis of cleaved caspase 3 (CI Casp3) and cleaved PARP (CI PARP) protein levels are shown. Data are pooled from at least three independent cell line experiments except for CI PARP in C (n = 2). Data show means \pm SEM. *p < 0.05 treated compared with control conditions. **p < 0.05 inhibitor-treated compared with treated conditions. #p = 0.05 compared with Cyto (G) alone.

independently by four batches of human islet preparations (Figures 4A–4D). Similar data were obtained using SJB2-043 as approach to target USP1 in isolated human islets (Figures 4E–4H). To confirm protection from apoptosis, *in situ* TUNEL together with insulin double-staining was performed to validate our Western blot data on the level of β -cells. Again, both USP1 inhibitors ML323 and SJB2-043 fully protected human islet β -cells from apoptosis induced by prolonged exposure to elevated glucose/palmitate and to the mixture of cytokines (Figures 4I and 4J), confirming the promising efficacy of USP1 inhibitors in rescuing human β -cells from apoptosis. Although strategies to interfere with the intracellular cell death mechanisms to halt β -cell failure in diabetes are highly promising, they should not compromise the insulin secretory function of pancreatic β -cells. As previously reported, modulation of key endogenous anti-apoptotic proteins in β -cells impairs β -cell function (Luciani et al., 2013). Therefore, we sought to determine whether the chemical blockade of USP1 has any impact on insulin secretion and expression of key β -cell maturation and identity genes. Therefore, we probed the influence of USP1 inhibition on the ability of human islets to secrete insulin in response to glucose. Human islets treated with ML323 and SJB2-043 showed no alteration

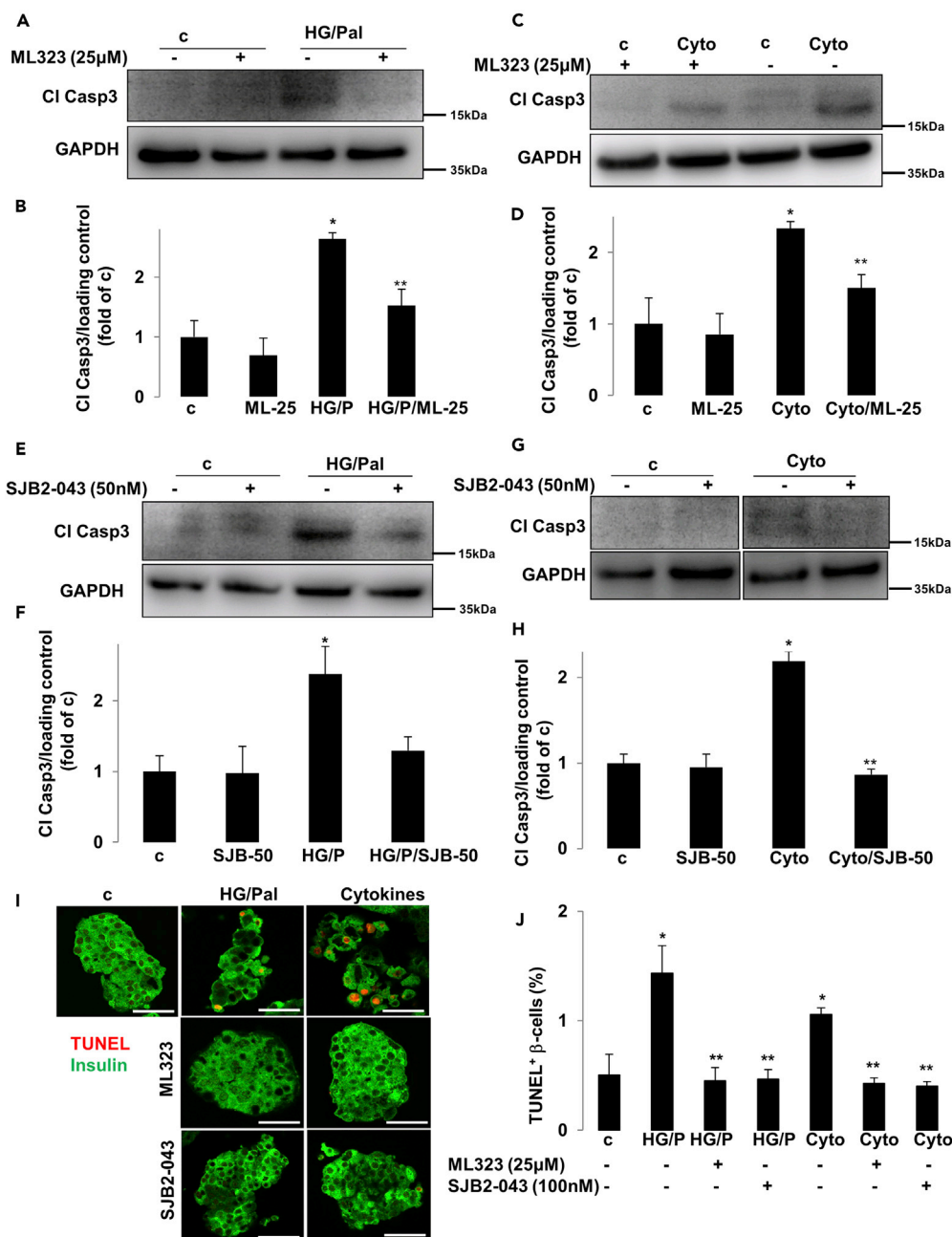


Figure 4. Inhibition of USP1 Promotes β-Cell Survival in Isolated Human Islets

(A–J) Isolated human islets (150–200 islets/dish) treated with or without USP1 inhibitors ML323 or SJB2-043 were exposed to a mixture of 22.2 mM glucose and 0.5 mM palmitate (HG/Pal) (A, B, E, F, I, and J) or to pro-inflammatory cytokines (2 ng/mL recombinant human IL-1β and 1000 U/mL IFN-γ; Cyto; C, D, G–J) for 2 days. Representative Western blots and quantitative densitometry analysis of cleaved caspase 3 (CI Casp3) protein levels are shown. (G) All lanes are from the same gel but were run noncontiguously. (I and J) Human pancreatic islets were fixed, paraffin embedded, and stained for the TUNEL assay and insulin. Representative images (I) and quantitative percentage of TUNEL-positive β-cells (J) are shown. Scale bars represent 50 μm. Data are pooled from at least three human islet preparations. Data show means ± SEM. *p < 0.05 stimuli treated compared with control conditions. **p < 0.05 inhibitor-treated compared with treated conditions.

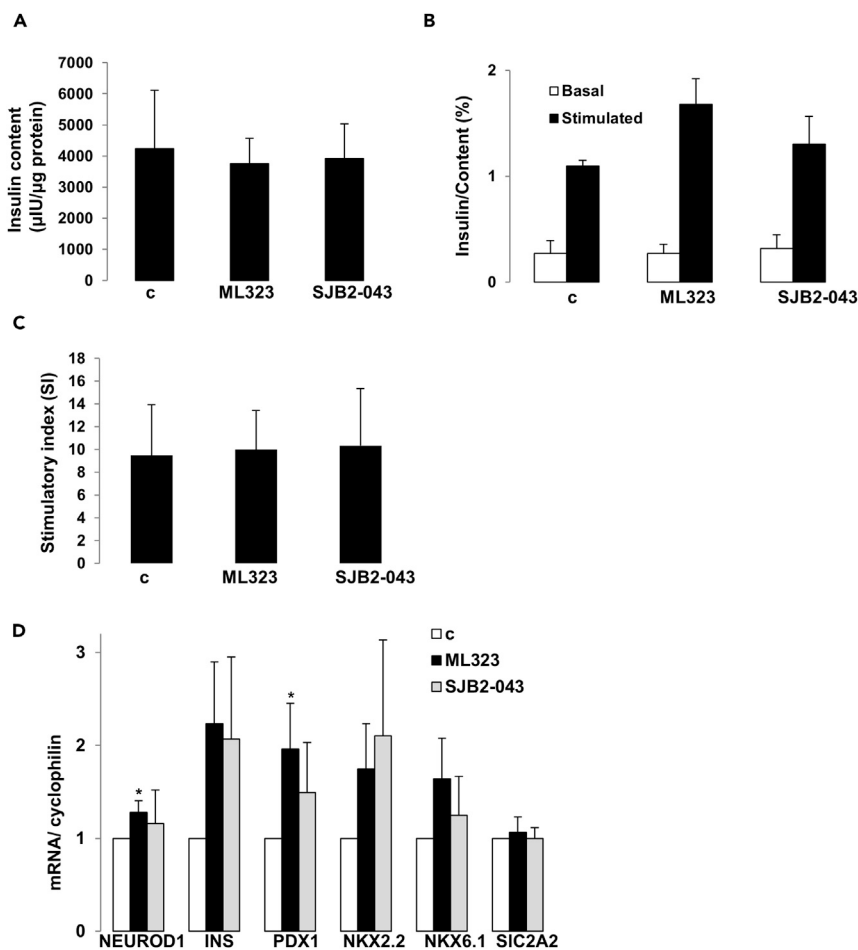


Figure 5. Impact of USP1 Inhibition on Insulin Content, Secretion, and Expression of Functional β -Cell Genes in Isolated Human Islets

(A–D) Isolated human islets were treated with or without USP1 inhibitors ML323 or SJB2-043 for 2 days (30 islets/dish for A–C; 150–200 islets/dish for D). (A) Insulin content analyzed after GSIS and normalized to whole islet protein. (B) Insulin secretion during 1-hr incubation with 2.8 (basal) and 16.7 mM glucose (stimulated), normalized to insulin content. (C) The insulin stimulatory index denotes the ratio of secreted insulin during 1-hr incubation with 16.7 and 2.8 mM glucose. (D) RT-PCR for *NEUROD1*, *INS*, *PDX1*, *NKX2.2*, *NKX6.1*, and *SIC2A2*, normalized to cyclophilin. Tubulin normalization delivered similar results. Pooled data are from four independent experiments from four different human islet donors. Data show means \pm SEM. * $p < 0.05$ compared with control conditions.

in the intracellular insulin content (Figure 5A), and glucose-stimulate insulin secretion (GSIS) was maintained (Figures 5B and 5C), indicating that USP1 inhibition does not affect the human islet insulin secretory function. To determine whether USP1 inhibitors caused a loss of β -cell identity or de-differentiation, expression of functional genes, including insulin (*INS*), key β -cell transcription factors (*PDX1*, *NEUROD1*, *NKX2.2*, and *NKX6.1*), as well as the critical β -cell glucose transporter (*SIC2A2*), were measured by reverse transcription polymerase chain reaction (RT-PCR) in human islets. Our data showed that not only all genes were preserved in USP1 inhibitors-treated human islets cells but also *NEUROD1* and *PDX1* were significantly increased by ML323 (Figure 5D), suggesting full preservation of β -cell function and functional identity genes upon inhibition of USP1 in human islets. Our data show that inhibition of USP1 efficiently blocked human β -cell apoptosis without compromising function.

USP1 Inhibition Suppressed the DNA Damage Response in Pancreatic β -cells

Complex intracellular networks, namely, the DDR, monitor genome integrity and stability by sensing DNA damage and controlling DNA repair pathways and damage tolerance processes (Polo and Jackson, 2011). In principle, if the level of DDR is greater than the cellular capacity, programmed cell death is activated to

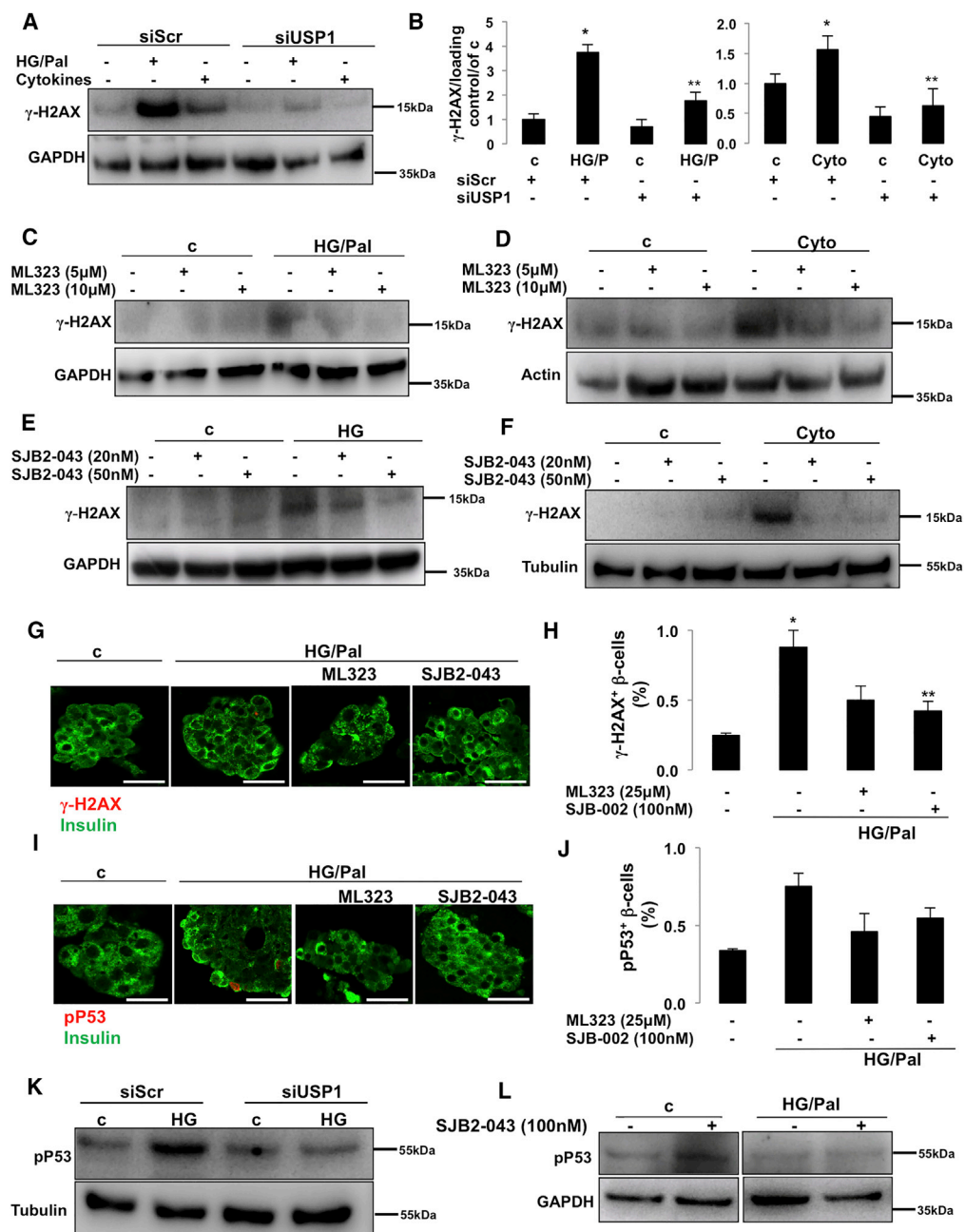


Figure 6. Inhibition of USP1-Suppressed DDR

(A, B, and K) INS-1E cells seeded at 300,000 cells/well were transfected with either control siScr or siUSP1 and treated with a mixture of 22.2 mM glucose and 0.5 mM palmitate (HG/Pal) or pro-inflammatory cytokines (2 ng/mL recombinant human IL-1 β , 1000 U/mL TNF- α , and 1000 U/mL IFN- γ ; Cyto). Representative Western blot (A and K) and quantitative densitometry analysis (B) of γ -H2AX and p-53 proteins are shown.

(C–F) About 500,000 INS-1E cells/well treated with or without USP1 inhibitors ML323 (C and D) or SJB2-043 (E and F) were exposed to a mixture of 22.2 mM glucose and 0.5 mM palmitate (HG/Pal; C), 22.2 mM glucose (HG; E), or pro-inflammatory cytokines (2 ng/mL recombinant human IL-1 β , 1000 U/mL TNF- α , and 1000 U/mL IFN- γ ; Cyto; D and F) for 2 days. Data are pooled from at least three independent cell line experiments. Tubulin loading control in Figure 5F is reused from the same experiment shown in Figure 3F.

(G–J and L) Isolated human islets (150–200 islets/dish) treated with or without USP1 inhibitors ML323 or SJB2-043 were exposed to a mixture of 22.2 mM glucose and 0.5 mM palmitate (HG/Pal) for 2 days. (G–J) Human pancreatic islets were fixed, paraffin embedded, and stained for γ -H2AX (G) or p-p53 (I) and insulin. Representative images (G and I) and

Figure 6. Continued

quantitative percentage of γ -H2AX or p-p53-positive β -cells (H and J) are shown. Scale bars represent 50 μ m. Data are pooled from three human islet preparations except for J (n = 2). (L) Representative Western blot of p-p53 protein is shown. All lanes are from the same gel but were run noncontiguously.

Data show means \pm SEM. *p < 0.05 stimuli treated compared with control conditions. **p < 0.05 inhibitor-treated compared with treated conditions.

prevent cellular mutations and related abnormalities that contribute to tumorigenesis. However, DDR dysregulation leads to multiple pathological settings: extensive impairment of DDR leads to cancer with uncontrolled cell overgrowth, whereas extensive upregulation may precede neurodegenerative and metabolic diseases with specific cell loss (Jackson and Bartek, 2009; Shimizu et al., 2014). Several lines of evidence support the important function of USP1 in DDR processes (Cukras et al., 2016; Nijman et al., 2005; Ogrunc et al., 2016; Sourisseau et al., 2016). As DDR markers are highly elevated in human and rodent diabetic islets/ β -cells *in vitro* and *in vivo* and correlate with β -cell death (Belgardt et al., 2015; Himpe et al., 2016; Nyblom et al., 2009; Oleson et al., 2014, 2016; Tornovsky-Babeay et al., 2014), we sought to determine whether USP1 inhibition would modulate DDR under diabetic conditions. Histone H2AX is a histone H2A variant, which is essential for cell cycle arrest and activation of DNA repair processes upon double-stranded DNA breaks. Upon DNA damage, H2AX is rapidly phosphorylated at Ser139 by PI3K-like kinases, including ataxia telangiectasia mutated (ATM), ataxia telangiectasia and Rad3-related protein (ATR), and DNA-dependent protein kinase (DNA-PK), and its phosphorylation generally referred to as γ -H2AX is universally considered as robust readout of DDR (Yuan et al., 2010). Consistent with previous studies (Belgardt et al., 2015; Himpe et al., 2016; Nyblom et al., 2009; Oleson et al., 2014, 2016; Tornovsky-Babeay et al., 2014), glucolipotoxicity and pro-inflammatory cytokines strongly induced DDR (represented by γ -H2AX formation; Figures 6A and 6B) in INS-1E β -cells. USP1 knockdown significantly blocked γ -H2AX upregulation, correlating with its anti-apoptotic action in response to diabetogenic stimulation (Figures 6A and 6B). Consistently, both USP1 inhibitors ML323 and SJB2-043 markedly reduced γ -H2AX in all tested diabetic conditions (Figures 6C–6F). To confirm β -cell-specific regulation of DDR by USP1 inhibition in human islets, we quantified the number of γ -H2AX-positive β -cells in human islets treated with the diabetogenic milieu in the absence and presence of ML323 and SJB2-043. Glucolipotoxicity induced a number of γ -H2AX positive β -cells, whereas USP1 inhibitors significantly reduced it (Figures 6G and 6H), suggesting the β -cell-specific suppression of γ -H2AX in human islets. Transcription factor p53 is activated in response to several cellular stresses, including DNA damage, and plays a key function in coordinating cell-intrinsic responses to exogenous and endogenous stressors by promoting cell cycle arrest, senescence, and apoptosis (Meek, 2009; Reinhardt and Schumacher, 2012). P53 phosphorylation at serine 15 is the primary event during DDR (phosphorylated by DDR-related kinases ATM and ATR), which promotes both the accumulation and functional activation of p53 and is the surrogate readout of DDR activation (Loughery et al., 2014; Meek, 2009; Meek and Anderson, 2009). To further test the efficacy of USP1 inhibition to suppress DDR, we quantified the number of p-p53 (at Ser15)-positive β -cells in isolated human islets treated with USP1 inhibitors exposed to the diabetic conditions. The number of p-p53-positive β -cells increased in glucose/palmitate-treated human islets, whereas both ML323 and SJB2-043 reduced such p-p53-positive cells (Figures 6I and 6J). Also, chronically elevated glucose-induced p-p53 upregulation was strongly inhibited by USP1 knockdown in INS-1E cells (Figure 6K). In addition, glucose/palmitate-induced p53 phosphorylation was fully blunted in the presence of SJB2-043 (Figure 6L) in human islets, further supporting the attenuation of DDR markers in diabetic β -cells by USP1 inhibition.

USP1 Inhibition Improves Survival and Lowers DDR in Diabetic β -cells

A progressive impairment of β -cell function together with increased β -cell death under diabetic conditions has been clearly documented in human β -cells. To test the potential beneficial effect of USP1 suppression in the human β -cell under conditions of T2D, we performed a proof-of-concept experiment, whereby we inhibited USP1 in two human islet preparations isolated from two patients with T2D. Islets were treated with ML323 and SJB2-043 for 24 hr. Consistent with the improved β -cell survival of human islets under diabetogenic conditions upon USP1 inhibition, isolated T2D islets treated with both USP1 inhibitors showed less apoptotic β -cells, demonstrated in two independent experiments from two different T2D human islet isolations (Figure 7A). In line with our data in INS-1E cells and human islets, both ML323 and SJB2-043 treatment highly reduced the number of γ -H2AX- and p-p53-positive β -cells in human islets consistently in two distinct human T2D islet batches (Figures 7B and 7C). This further confirms the USP1-dependent regulation of DDR under a diabetic environment.

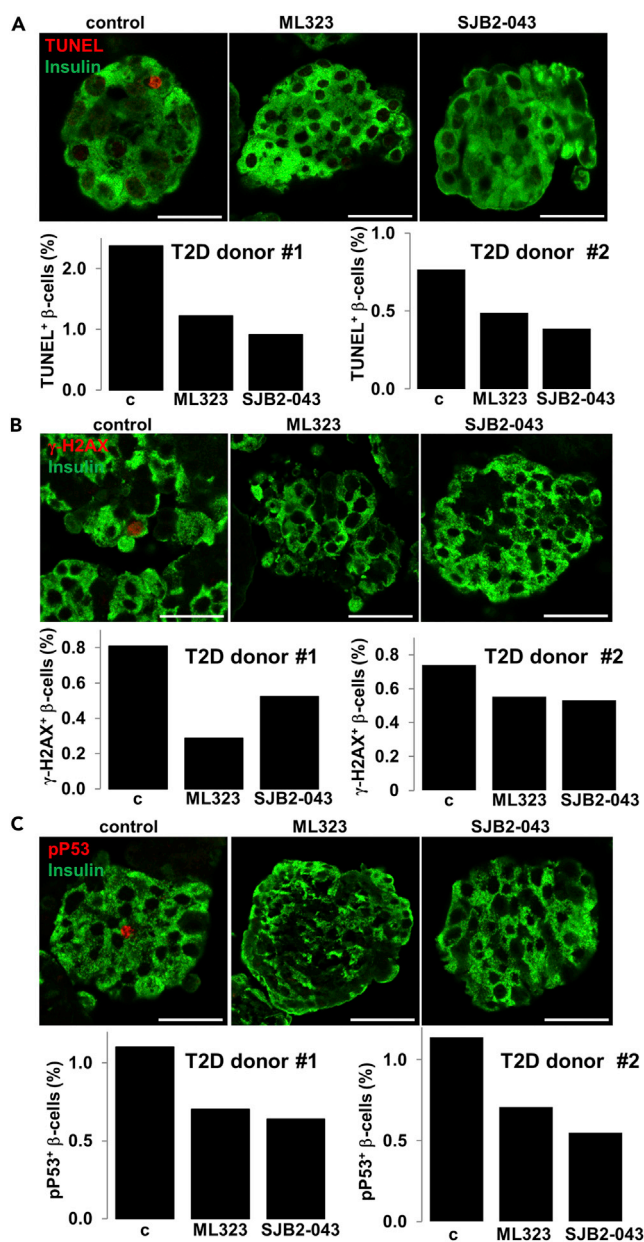


Figure 7. USP1 Inhibitors Reduced β -Cell Apoptosis and DDR in Human T2D Islets

Isolated human islets from two patients with T2D treated with or without USP1 inhibitors ML323 or SJB2-043 for 1 day. (A–C) Human pancreatic islets were fixed, paraffin embedded, and double stained for the TUNEL assay (A), γ -H2AX (B), or p-p53 (C) and insulin. Representative confocal images and individual quantitative percentage of TUNEL, γ -H2AX, or p-p53 positive β -cells are shown from 2 to 4 technical replica/group from two islet donors with confirmed T2D. Scale bars represent 50 μ m. Data are means of TUNEL-, γ -h2AX-, or pp53- and insulin-co-positive β -cells from pooled data of 2–4 different human islet sections spanning the whole islet pellet for each experimental group. About 150–200 islets were plated for each group. The mean number of β -cells scored was 6,050 for each condition for each donor.

DISCUSSION

Loss of insulin-producing pancreatic β -cells results in hyperglycemia and is the hallmark of both T1D and T2D. Identification of key signaling molecules that promote β -cell death in diabetes, together with an understanding of their mechanisms of action, is critical for the disease pathogenesis as well as for novel therapeutic interventions to halt β -cell failure during development and progression of diabetes. This study

provides the first direct evidence that genetic or pharmacological inhibition of the enzyme USP1 protects β -cells from apoptosis under diabetogenic stimulation by attenuating DDR signals.

DDR is a signal transduction pathway, which functions together with other networking pathways known as DNA damage checkpoints (Harrison and Haber, 2006), and its dysregulation is a hallmark of several pathological disorders, such as cancer and neurodegenerative and metabolic diseases (Jackson and Bartek, 2009; Shimizu et al., 2014). Elevated DDR has been observed in pancreatic islets/ β -cells under increased cellular stress and metabolic demand *in vivo* or under diabetic conditions *in vitro*. Surrogate markers of DDR, such as γ -H2AX, p53, and P53BP1, are highly upregulated in primary islets and β -cells in response to oxidative and inflammatory assaults as well as in pancreatic islets from streptozotocin (STZ)-treated diabetic mice, leptin-receptor-deficient *dbdb*, and human T2D islets (Belgardt et al., 2015; Himpe et al., 2016; Nyblom et al., 2009; Oleson et al., 2014, 2016; Tornovsky-Babeay et al., 2014), suggesting that oxidative- or metabolic-mediated double-strand breaks in the DNA and downstream activation of p53 may be a key pathogenic element of β -cell stress under metabolic and inflammatory conditions. This is further supported by the elevated incidence of diabetes in individuals who received irradiation to the pancreas (de Vathaire et al., 2012; Meacham et al., 2009). Furthermore, oxidized DNA and p53 signaling are both highly upregulated in human T2D islets (Sakuraba et al., 2002; Tornovsky-Babeay et al., 2014). Initially, the DDR coordinates a transcriptional program with DNA repair and cell cycle arrest (Ciccio and Elledge, 2010); however, under sustained cellular stresses when DNA damage can no longer be repaired, the DDR initiates apoptosis (Roos and Kaina, 2013). DUBs play an important role in DDR. Although multiple numbers of DUBs are involved in DNA repair and the downstream process, USP1 is the first enzyme characterized as the key player in DDR (Jacq et al., 2013). USP1 is the DUB responsible for deubiquitination of monoubiquitinated FANCD2 (Nijman et al., 2005), an integral component of the Fanconi anemia (FA) DNA repair pathway and PCNA (Kee and D'Andrea, 2012). USP1 and its associated partner USP1-associated factor 1 (UAF1) play an important function in promoting DNA homologous recombination (HR) repair in response to DDR via distinct mechanisms: through FANCD2 deubiquitination (Nijman et al., 2005) or by interacting with RAD51 associated protein 1 (RAD51AP1; Cukras et al., 2016). It is possible that the interactions with these known USP1 targets directly lead to the reduced γ -H2AX described in our study. Also, USP1-dependent regulation of other signaling pathways such as AKT (Zhang et al., 2016; Zhiqiang et al., 2012) or upstream elements of the DDR, such as CHK1, a key kinase involved in DDR and DNA repair, which is also stabilized by USP1 (Guervilly et al., 2011), may affect the DDR output together with γ -H2AX formation (Bozulic et al., 2008; Surucu et al., 2008; Xu et al., 2010). Owing to the complexity of DDR signaling and multi-layer actions of USP1, there may also be dual and time-/concentration-/cell-system-dependent effects on γ -H2AX formation or on DDR in general, as an induction of γ -H2AX upon USP1 inhibition has also been observed (Olazabal-Herrero et al., 2016). Our results suggest that the genetic and pharmacological suppression of USP1 in rodent β -cell and human islets protected the cells from DNA-damage-induced cell death with preserving β -cell insulin secretion and β -cell key maturation genes, proposing the critical function of USP1 in the regulation of β -cell apoptosis under different diabetogenic conditions. However, pathway(s) responsible for the regulation of USP1 as well as the molecular mechanism by which USP1 regulates DDR in β -cells, especially in the diabetic environment, remains unknown and warrants further mechanistic investigations.

Although several USP1 targets, such as FANCD2 and PCNA, have been established in the context of DDR, the identification of novel USP1 substrates in other cellular processes will provide further insights on the action of USP1 in regulating cell survival and stress response. Recently, TANK-binding kinase 1 (TBK1), a key regulator of the innate antiviral immunity and maintenance of immune homeostasis, has been discovered as a novel substrate of USP1 (Yu et al., 2017). Yu et al. showed that USP1 functions as an important cellular enhancer of Toll-like receptor 3/4 (TLR3/4)-, retinoic acid-inducible gene I (RIG-I)-, and cyclic GMP-AMP synthase (cGAS)-induced antiviral signaling by TBK1 deubiquitination and regulation of its stability (Yu et al., 2017). TBK1 has a pleotropic function in the metabolic process, inflammation, and diabetes. Identified as an inflammatory kinase that targets the insulin receptor (Munoz et al., 2009), TBK1 regulates insulin-stimulated glucose uptake in adipocytes (Uhm et al., 2017). TBK1 levels are upregulated in obesity and diabetes, and the inhibition of TBK1 together with another inflammatory IKK-related kinase IKK ϵ by the dual kinase inhibitor amlexanox reduces weight, fatty liver, and inflammation, as well as promotes insulin sensitivity in obese diabetic mice (Reilly et al., 2013) and presents a significant reduction in HbA1c in a subset of patients with T2D (Oral et al., 2017). As diabetogenic conditions, such as elevated palmitic acid, induce β -cell death and dysfunction at least in part through TLR4 signals (Eguchi et al., 2012; Saksida et al., 2012) upstream of TBK1, it is likely that the newly identified USP1-TBK1 axis affects viability, stress

response, and inflammation in β -cells as well as in other metabolically active tissues in metabolic and inflammatory contexts. This remains to be investigated.

Conclusion

Impaired β -cell survival is a key pathogenic element of pancreatic β -cell's insufficiency in both T1D and T2D. Here we demonstrated the anti-apoptotic action of USP1 inhibition through the regulation of DDR in several *in vitro* and *ex vivo* experimental models of diabetes in stressed β -cells in both rodent and human cells. The identification of the previously uncharacterized function of USP1 in the regulation of β -cell apoptosis may have a potential therapeutic relevance for the preservation of functional β -cell mass in diabetes. To warrant this, identification of β -cell-specific USP1 substrates, detailed mechanistic analyses, as well as the *in vivo* preclinical assessment of utility, efficacy, and side effects of currently available USP1 inhibitors are required in the near future.

METHODS

All methods can be found in the accompanying [Transparent Methods supplemental file](#).

SUPPLEMENTAL INFORMATION

Supplemental Information includes Transparent Methods and two figures and can be found with this article online at <https://doi.org/10.1016/j.isci.2018.02.003>.

ACKNOWLEDGMENTS

This work was supported by the German Research Foundation (DFG), the JDRF, and the EFSD/Lilly Fellowship Programme. Human islets were provided through the integrated islet distribution program (IIDP) supported by NIH and JDRF and the ECIT Islet for Basic Research program supported by JDRF (JDRF award 31-2008-413). We thank J. Kerr-Conte and Francois Pattou (European Genomic Institute for Diabetes, Lille) for high-quality human islet isolations and Katrischa Hennekens (University of Bremen) for the excellent technical assistance.

AUTHOR CONTRIBUTIONS

Designed and preformed experiments, analyzed data, and wrote the paper, K.G.; assisted to perform experiments, B.L., K.A., T.Y.; designed and supervised project and wrote the paper, A.A., K.M. All authors critically reviewed the manuscript for important intellectual content and approved the final version to be published.

DECLARATION OF INTERESTS

The authors declare no competing interests.

Received: December 21, 2017

Revised: January 31, 2018

Accepted: February 1, 2018

Published: March 23, 2018

REFERENCES

- Alejandro, E.U., Gregg, B., Blandino-Rosano, M., Cras-Meneur, C., and Bernal-Mizrachi, E. (2015). Natural history of beta-cell adaptation and failure in type 2 diabetes. *Mol. Aspects Med.* 42, 19–41.
- Ardestani, A., Lupse, B., Kido, Y., Leibowitz, G., and Maedler, K. (2018). mTORC1 signaling: a double-edged sword in diabetic beta cells. *Cell Metab.* 27, 314–331.
- Ardestani, A., and Maedler, K. (2018). The Hippo signaling pathway in pancreatic beta-cells: functions and regulations. *Endocr. Rev.* 39, 21–35.
- Ardestani, A., Paroni, F., Azizi, Z., Kaur, S., Khobragade, V., Yuan, T., Frogne, T., Tao, W., Oberholzer, J., Pattou, F., et al. (2014). MST1 is a key regulator of beta cell apoptosis and dysfunction in diabetes. *Nat. Med.* 20, 385–397.
- Belgardt, B.F., Ahmed, K., Spranger, M., Latreille, M., Denzler, R., Kondratiuk, N., von Meyenn, F., Villena, F.N., Herrmanns, K., Bosco, D., et al. (2015). The microRNA-200 family regulates pancreatic beta cell survival in type 2 diabetes. *Nat. Med.* 21, 619–627.
- Bozulic, L., Surucu, B., Hynx, D., and Hemmings, B.A. (2008). PKBalpha/Akt1 acts downstream of DNA-PK in the DNA double-strand break response and promotes survival. *Mol. Cell* 30, 203–213.
- Broca, C., Varin, E., Armanet, M., Tourel-Cuzin, C., Bosco, D., Dalle, S., and Wojtuszczyz, A. (2014). Proteasome dysfunction mediates high glucose-induced apoptosis in rodent beta cells and human islets. *PLoS One* 9, e92066.
- Bugliani, M., Liechti, R., Cheon, H., Suleiman, M., Marselli, L., Kirkpatrick, C., Filipponi, F., Boggi, U., Xenarios, I., Syed, F., et al. (2013). Microarray analysis of isolated human islet transcriptome in type 2 diabetes and the role

of the ubiquitin-proteasome system in pancreatic beta cell dysfunction. *Mol. Cell. Endocrinol.* 367, 1–10.

Butler, A.E., Janson, J., Bonner-Weir, S., Ritzel, R., Rizza, R.A., and Butler, P.C. (2003). Beta-cell deficit and increased beta-cell apoptosis in humans with type 2 diabetes. *Diabetes* 52, 102–110.

Chatenoud, L. (2010). Immune therapy for type 1 diabetes mellitus-what is unique about anti-CD3 antibodies? *Nat. Rev. Endocrinol.* 6, 149–157.

Ciccio, A., and Elledge, S.J. (2010). The DNA damage response: making it safe to play with knives. *Mol. Cell* 40, 179–204.

Cinti, F., Bouchi, R., Kim-Muller, J.Y., Ohmura, Y., Sandoval, P.R., Masini, M., Marselli, L., Suleiman, M., Ratner, L.E., Marchetti, P., et al. (2016). Evidence of beta-cell dedifferentiation in human type 2 diabetes. *J. Clin. Endocrinol. Metab.* 101, 1044–1054.

Costes, S., Gurlo, T., Rivera, J.F., and Butler, P.C. (2014). UCHL1 deficiency exacerbates human islet amyloid polypeptide toxicity in beta-cells: evidence of interplay between the ubiquitin/proteasome system and autophagy. *Autophagy* 10, 1004–1014.

Costes, S., Huang, C.J., Gurlo, T., Daval, M., Matveyenko, A.V., Rizza, R.A., Butler, A.E., and Butler, P.C. (2011). beta-cell dysfunctional ERAD/ubiquitin/proteasome system in type 2 diabetes mediated by islet amyloid polypeptide-induced UCH-L1 deficiency. *Diabetes* 60, 227–238.

Cukras, S., Lee, E., Palumbo, E., Benavidez, P., Moldovan, G.L., and Kee, Y. (2016). The USP1-UAF1 complex interacts with RAD51AP1 to promote homologous recombination repair. *Cell Cycle* 15, 2636–2646.

de Vathaire, F., El-Fayech, C., Ben Ayed, F.F., Haddy, N., Guibout, C., Winter, D., Thomas-Teinturier, C., Veres, C., Jackson, A., Pacquement, H., et al. (2012). Radiation dose to the pancreas and risk of diabetes mellitus in childhood cancer survivors: a retrospective cohort study. *Lancet Oncol.* 13, 1002–1010.

Dexheimer, T.S., Rosenthal, A.S., Liang, Q., Chen, J., Villamil, M.A., Kerns, E.H., Simeonov, A., Jadhav, A., Zhuang, Z., and Maloney, D.J. (2010). Discovery of ML323 as a Novel Inhibitor of the USP1/UAF1 Deubiquitinase Complex. In *Probe Reports from the NIH Molecular Libraries Program (Bethesda (MD))*.

Donath, M.Y., Dalmás, E., Sauter, N.S., and Boni-Schnetzler, M. (2013). Inflammation in obesity and diabetes: islet dysfunction and therapeutic opportunity. *Cell Metab.* 17, 860–872.

Eguchi, K., Manabe, I., Oishi-Tanaka, Y., Ohsugi, M., Kono, N., Ogata, F., Yagi, N., Ohto, U., Kimoto, M., Miyake, K., et al. (2012). Saturated fatty acid and TLR signaling link beta cell dysfunction and islet inflammation. *Cell Metab.* 15, 518–533.

Frescas, D., and Pagano, M. (2008). Deregulated proteolysis by the F-box proteins SKP2 and beta-TrCP: tipping the scales of cancer. *Nat. Rev. Cancer* 8, 438–449.

Garcia-Santisteban, I., Peters, G.J., Giovannetti, E., and Rodriguez, J.A. (2013). USP1 deubiquitinase: cellular functions, regulatory mechanisms and emerging potential as target in cancer therapy. *Mol. Cancer* 12, 91.

Gorasia, D.G., Dudek, N.L., Veith, P.D., Shankar, R., Safavi-Hemami, H., Williamson, N.A., Reynolds, E.C., Hubbard, M.J., and Purcell, A.W. (2015). Pancreatic beta cells are highly susceptible to oxidative and ER stresses during the development of diabetes. *J. Proteome Res.* 14, 688–699.

Grankvist, K., Marklund, S.L., and Taljedal, I.B. (1981). CuZn-superoxide dismutase, Mn-superoxide dismutase, catalase and glutathione peroxidase in pancreatic islets and other tissues in the mouse. *Biochem. J.* 199, 393–398.

Guervilly, J.H., Renaud, E., Takata, M., and Rosselli, F. (2011). USP1 deubiquitinase maintains phosphorylated CHK1 by limiting its DDB1-dependent degradation. *Hum. Mol. Genet.* 20, 2171–2181.

Haataja, L., Gurlo, T., Huang, C.J., and Butler, P.C. (2008). Islet amyloid in type 2 diabetes, and the toxic oligomer hypothesis. *Endocr. Rev.* 29, 303–316.

Harrison, J.C., and Haber, J.E. (2006). Surviving the breakup: the DNA damage checkpoint. *Annu. Rev. Genet.* 40, 209–235.

Hartley, T., Brumell, J., and Volchuk, A. (2009). Emerging roles for the ubiquitin-proteasome system and autophagy in pancreatic beta-cells. *Am. J. Physiol. Endocrinol. Metab.* 296, E1–E10.

Herold, K.C., Usmani-Brown, S., Ghazi, T., Lebastchi, J., Beam, C.A., Bellin, M.D., Ledizet, M., Sosenko, J.M., Krischer, J.P., Palmer, J.P., et al. (2015). Beta cell death and dysfunction during type 1 diabetes development in at-risk individuals. *J. Clin. Invest.* 125, 1163–1173.

Himpe, E., Cunha, D.A., Song, I., Bugliani, M., Marchetti, P., Cnop, M., and Bouwens, L. (2016). Phenylpropionic acid glucoside from rooibos protects pancreatic beta cells against cell death induced by acute injury. *PLoS One* 11, e0157604.

Hofmeister-Brix, A., Lenzen, S., and Baltrusch, S. (2013). The ubiquitin-proteasome system regulates the stability and activity of the glucose sensor glucokinase in pancreatic beta-cells. *Biochem. J.* 456, 173–184.

Huang, C.J., Lin, C.Y., Haataja, L., Gurlo, T., Butler, A.E., Rizza, R.A., and Butler, P.C. (2007). High expression rates of human islet amyloid polypeptide induce endoplasmic reticulum stress mediated beta-cell apoptosis, a characteristic of humans with type 2 but not type 1 diabetes. *Diabetes* 56, 2016–2027.

Jackson, S.P., and Bartek, J. (2009). The DNA-damage response in human biology and disease. *Nature* 461, 1071–1078.

Jacq, X., Kemp, M., Martin, N.M.B., and Jackson, S.P. (2013). Deubiquitylating enzymes and DNA damage response pathways. *Cell Biochem. Biophys.* 67, 25–43.

Jeffery, N., and Harries, L.W. (2016). Beta-cell differentiation status in type 2 diabetes. *Diabetes Obes. Metab.* 18, 1167–1175.

Kaniuk, N.A., Kiraly, M., Bates, H., Vranic, M., Volchuk, A., and Brumell, J.H. (2007). Ubiquitinated-protein aggregates form in pancreatic beta-cells during diabetes-induced oxidative stress and are regulated by autophagy. *Diabetes* 56, 930–939.

Kee, Y., and D'Andrea, A.D. (2012). Molecular pathogenesis and clinical management of Fanconi anemia. *J. Clin. Invest.* 122, 3799–3806.

Kurrer, M.O., Pakala, S.V., Hanson, H.L., and Katz, J.D. (1997). Beta cell apoptosis in T cell-mediated autoimmune diabetes. *Proc. Natl. Acad. Sci. USA* 94, 213–218.

Lenzen, S. (2008). Oxidative stress: the vulnerable beta-cell. *Biochem. Soc. Trans.* 36, 343–347.

Lenzen, S., Drinkgern, J., and Tiedge, M. (1996). Low antioxidant enzyme gene expression in pancreatic islets compared with various other mouse tissues. *Free Radic. Biol. Med.* 20, 463–466.

Liang, Q., Dexheimer, T.S., Zhang, P., Rosenthal, A.S., Villamil, M.A., You, C., Zhang, Q., Chen, J., Ott, C.A., Sun, H., et al. (2014). A selective USP1-UAF1 inhibitor links deubiquitination to DNA damage responses. *Nat. Chem. Biol.* 10, 298–304.

Litwak, S.A., Wali, J.A., Pappas, E.G., Saadi, H., Stanley, W.J., Varanasi, L.C., Kay, T.W., Thomas, H.E., and Gurzov, E.N. (2015). Lipotoxic stress induces pancreatic beta-cell apoptosis through modulation of Bcl-2 proteins by the Ubiquitin-Proteasome system. *J. Diabetes Res.* 2015, 280615.

Loughery, J., Cox, M., Smith, L.M., and Meek, D.W. (2014). Critical role for p53-serine 15 phosphorylation in stimulating transactivation at p53-responsive promoters. *Nucleic Acids Res.* 42, 7666–7680.

Luciani, D.S., White, S.A., Widenmaier, S.B., Saran, V.V., Taghizadeh, F., Hu, X., Allard, M.F., and Johnson, J.D. (2013). Bcl-2 and Bcl-xL suppress glucose signaling in pancreatic beta-cells. *Diabetes* 62, 170–182.

Maedler, K., Sergeev, P., Ris, F., Oberholzer, J., Joller-Jemelka, H.I., Spinas, G.A., Kaiser, N., Halban, P.A., and Donath, M.Y. (2002). Glucose-induced beta-cell production of interleukin-1beta contributes to glucotoxicity in human pancreatic islets. *J. Clin. Invest.* 110, 851–860.

Marroqui, L., Masini, M., Merino, B., Grieco, F.A., Millard, I., Dubois, C., Quesada, I., Marchetti, P., Cnop, M., and Eizirik, D.L. (2015). Pancreatic alpha cells are resistant to metabolic stress-induced apoptosis in type 2 diabetes. *EBioMedicine* 2, 378–385.

Marselli, L., Suleiman, M., Masini, M., Campani, D., Bugliani, M., Syed, F., Martino, L., Focosi, D., Scatena, F., Olimpico, F., et al. (2014). Are we overestimating the loss of beta cells in type 2 diabetes? *Diabetologia* 57, 362–365.

Masini, M., Bugliani, M., Lupi, R., del Guerra, S., Boggi, U., Filippini, F., Marselli, L., Masiello, P.,

- and Marchetti, P. (2009). Autophagy in human type 2 diabetes pancreatic beta cells. *Diabetologia* 52, 1083–1086.
- Mathis, D., Vence, L., and Benoist, C. (2001). beta-Cell death during progression to diabetes. *Nature* 414, 792–798.
- Meacham, L.R., Sklar, C.A., Li, S., Liu, Q., Gimpel, N., Yasui, Y., Whitton, J.A., Stovall, M., Robison, L.L., and Oeffinger, K.C. (2009). Diabetes mellitus in long-term survivors of childhood cancer. Increased risk associated with radiation therapy: a report for the childhood cancer survivor study. *Arch. Intern. Med.* 169, 1381–1388.
- Meek, D.W. (2009). Tumour suppression by p53: a role for the DNA damage response? *Nat. Rev. Cancer* 9, 714–723.
- Meek, D.W., and Anderson, C.W. (2009). Posttranslational modification of p53: cooperative integrators of function. *Cold Spring Harb. Perspect. Biol.* 1, a000950.
- Meier, J.J., Bhushan, A., Butler, A.E., Rizza, R.A., and Butler, P.C. (2005). Sustained beta cell apoptosis in patients with long-standing type 1 diabetes: indirect evidence for islet regeneration? *Diabetologia* 48, 2221–2228.
- Mistry, H., Hsieh, G., Buhrlage, S.J., Huang, M., Park, E., Cuny, G.D., Galinsky, I., Stone, R.M., Gray, N.S., D'Andrea, A.D., et al. (2013). Small-molecule inhibitors of USP1 target ID1 degradation in leukemic cells. *Mol. Cancer Ther.* 12, 2651–2662.
- Munoz, M.C., Giani, J.F., Mayer, M.A., Toblli, J.E., Turyn, D., and Dominici, F.P. (2009). TANK-binding kinase 1 mediates phosphorylation of insulin receptor at serine residue 994: a potential link between inflammation and insulin resistance. *J. Endocrinol.* 201, 185–197.
- Nijman, S.M., Huang, T.T., Dirac, A.M., Brummelkamp, T.R., Kerkhoven, R.M., D'Andrea, A.D., and Bernards, R. (2005). The deubiquitinating enzyme USP1 regulates the Fanconi anemia pathway. *Mol. Cell* 17, 331–339.
- Nyblom, H.K., Bugliani, M., Fung, E., Boggi, U., Zubarev, R., Marchetti, P., and Bergsten, P. (2009). Apoptotic, regenerative, and immune-related signaling in human islets from type 2 diabetes individuals. *J. Proteome Res.* 8, 5650–5656.
- Ogrunc, M., Martinez-Zamudio, R.I., Sadoun, P.B., Dore, G., Schwerer, H., Pasero, P., Lemaître, J.M., Dejean, A., and Bischof, O. (2016). USP1 regulates cellular senescence by controlling genomic integrity. *Cell Rep.* 15, 1401–1411.
- Olazabal-Herrero, A., Garcia-Santisteban, I., and Rodriguez, J.A. (2016). Mutations in the 'Fingers' subdomain of the deubiquitinase USP1 modulate its function and activity. *FEBS J.* 283, 929–946.
- Oleson, B.J., Broniowska, K.A., Naatz, A., Hogg, N., Tarakanova, V.L., and Corbett, J.A. (2016). Nitric oxide suppresses beta-cell apoptosis by inhibiting the DNA damage response. *Mol. Cell Biol.* 36, 2067–2077.
- Oleson, B.J., Broniowska, K.A., Schreiber, K.H., Tarakanova, V.L., and Corbett, J.A. (2014). Nitric oxide induces ataxia telangiectasia mutated (ATM) protein-dependent gammaH2AX protein formation in pancreatic beta cells. *J. Biol. Chem.* 289, 11454–11464.
- Oral, E.A., Reilly, S.M., Gomez, A.V., Meral, R., Butz, L., Ajluni, N., Chenevert, T.L., Korytnaya, E., Neidert, A.H., Hench, R., et al. (2017). Inhibition of IKKvarepsilon and TBK1 improves glucose control in a subset of patients with type 2 diabetes. *Cell Metab.* 26, 157–170.e7.
- Poitout, V., and Robertson, R.P. (2008). Glucolipototoxicity: fuel excess and beta-cell dysfunction. *Endocr. Rev.* 29, 351–366.
- Polo, S.E., and Jackson, S.P. (2011). Dynamics of DNA damage response proteins at DNA breaks: a focus on protein modifications. *Genes Dev.* 25, 409–433.
- Rahier, J., Guiot, Y., Goebbels, R.M., Sempoux, C., and Henquin, J.C. (2008). Pancreatic beta-cell mass in European subjects with type 2 diabetes. *Diabetes Obes. Metab.* 10 (Suppl 4), 32–42.
- Reilly, S.M., Chiang, S.H., Decker, S.J., Chang, L., Uhm, M., Larsen, M.J., Rubin, J.R., Mowers, J., White, N.M., Hochberg, I., et al. (2013). An inhibitor of the protein kinases TBK1 and IKK-varepsilon improves obesity-related metabolic dysfunctions in mice. *Nat. Med.* 19, 313–321.
- Reinhardt, H.C., and Schumacher, B. (2012). The p53 network: cellular and systemic DNA damage responses in aging and cancer. *Trends Genet.* 28, 128–136.
- Rhodes, C.J. (2005). Type 2 diabetes—a matter of beta-cell life and death? *Science* 307, 380–384.
- Ritzel, R.A., Butler, A.E., Rizza, R.A., Veldhuis, J.D., and Butler, P.C. (2006). Relationship between beta-cell mass and fasting blood glucose concentration in humans. *Diabetes Care* 29, 717–718.
- Robertson, R.P., Harmon, J., Tran, P.O., and Poitout, V. (2004). Beta-cell glucose toxicity, lipotoxicity, and chronic oxidative stress in type 2 diabetes. *Diabetes* 53 (Suppl 1), S119–S124.
- Roos, W.P., and Kaina, B. (2013). DNA damage-induced cell death: from specific DNA lesions to the DNA damage response and apoptosis. *Cancer Lett.* 332, 237–248.
- Saksida, T., Stosic-Grujicic, S., Timotijevic, G., Sandler, S., and Stojanovic, I. (2012). Macrophage migration inhibitory factor deficiency protects pancreatic islets from palmitic acid-induced apoptosis. *Immunol. Cell Biol.* 90, 688–698.
- Sakuraba, H., Mizukami, H., Yagihashi, N., Wada, R., Hanyu, C., and Yagihashi, S. (2002). Reduced beta-cell mass and expression of oxidative stress-related DNA damage in the islet of Japanese Type II diabetic patients. *Diabetologia* 45, 85–96.
- Schmidt, M., and Finley, D. (2014). Regulation of proteasome activity in health and disease. *Biochim. Biophys. Acta* 1843, 13–25.
- Shimizu, I., Yoshida, Y., Suda, M., and Minamino, T. (2014). DNA damage response and metabolic disease. *Cell Metab.* 20, 967–977.
- Sourisseau, T., Helissey, C., Lefebvre, C., Ponnailles, F., Malka-Mahieu, H., Olausen, K.A., Andre, F., Vagner, S., and Soria, J.C. (2016). Translational regulation of the mRNA encoding the ubiquitin peptidase USP1 involved in the DNA damage response as a determinant of Cisplatin resistance. *Cell Cycle* 15, 295–302.
- Surucu, B., Bozusic, L., Hynx, D., Parcellier, A., and Hemmings, B.A. (2008). In vivo analysis of protein kinase B (PKB)/Akt regulation in DNA-PKcs-null mice reveals a role for PKB/Akt in DNA damage response and tumorigenesis. *J. Biol. Chem.* 283, 30025–30033.
- Talchai, C., Xuan, S., Lin, H.V., Sussel, L., and Accili, D. (2012). Pancreatic beta cell dedifferentiation as a mechanism of diabetic beta cell failure. *Cell* 150, 1223–1234.
- Tiedge, M., Lortz, S., Drinkgern, J., and Lenzen, S. (1997). Relation between antioxidant enzyme gene expression and antioxidative defense status of insulin-producing cells. *Diabetes* 46, 1733–1742.
- Tiwari, S., Roel, C., Tanwir, M., Wills, R., Perianayagam, N., Wang, P., and Fiaschi-Taesch, N.M. (2016). Definition of a Skp2-c-Myc pathway to expand human beta-cells. *Sci. Rep.* 6, 28461.
- Tomita, T. (2010). Immunocytochemical localisation of caspase-3 in pancreatic islets from type 2 diabetic subjects. *Pathology* 42, 432–437.
- Tornovsky-Babeay, S., Dadon, D., Ziv, O., Tzipilevich, E., Kadosh, T., Schyr-Ben Haroush, R., Hija, A., Stolovich-Rain, M., Furth-Lavi, J., Granot, Z., et al. (2014). Type 2 diabetes and congenital hyperinsulinism cause DNA double-strand breaks and p53 activity in beta cells. *Cell Metab.* 19, 109–121.
- Uhm, M., Bazuine, M., Zhao, P., Chiang, S.H., Xiong, T., Karunanithi, S., Chang, L., and Saltiel, A.R. (2017). Phosphorylation of the exocyst protein Exo84 by TBK1 promotes insulin-stimulated GLUT4 trafficking. *Sci. Signal.* 10, eaah5085.
- Vetere, A., Choudhary, A., Burns, S.M., and Wagner, B.K. (2014). Targeting the pancreatic beta-cell to treat diabetes. *Nat. Rev. Drug Discov.* 13, 278–289.
- Xu, N., Hagarat, N., Black, E.J., Scott, M.T., Hochegger, H., and Gillespie, D.A. (2010). Akt/PKB suppresses DNA damage processing and checkpoint activation in late G2. *J. Cell Biol.* 190, 297–305.
- Yu, Z., Song, H., Jia, M., Zhang, J., Wang, W., Li, Q., Zhang, L., and Zhao, W. (2017). USP1-UAF1 deubiquitinase complex stabilizes TBK1 and enhances antiviral responses. *J. Exp. Med.* 214, 3553–3563.
- Yuan, J., Adamski, R., and Chen, J. (2010). Focus on histone variant H2AX: to be or not to be. *FEBS Lett.* 584, 3717–3724.
- Yuan, T., Gorrepati, K.D., Maedler, K., and Ardestani, A. (2016a). Loss of Merlin/NF2 protects pancreatic beta-cells from apoptosis by inhibiting LATS2. *Cell Death Dis.* 7, e2107.

Yuan, T., Rafizadeh, S., Azizi, Z., Lupse, B., Gorrepati, K.D., Awal, S., Oberholzer, J., Maedler, K., and Ardestani, A. (2016b). Proliferative and antiapoptotic action of exogenously introduced YAP in pancreatic beta cells. *JCI Insight* 1, e86326.

Yuan, T., Rafizadeh, S., Gorrepati, K.D., Lupse, B., Oberholzer, J., Maedler, K., and Ardestani,

A. (2017). Reciprocal regulation of mTOR complexes in pancreatic islets from humans with type 2 diabetes. *Diabetologia* 60, 668–678.

Zhang, X., Lu, X., Akhter, S., Georgescu, M.M., and Legerski, R.J. (2016). FANCI is a negative regulator of Akt activation. *Cell Cycle* 15, 1134–1143.

Zheng, Q., Huang, T., Zhang, L., Zhou, Y., Luo, H., Xu, H., and Wang, X. (2016). Dysregulation of

ubiquitin-proteasome system in neurodegenerative diseases. *Front. Aging Neurosci.* 8, 303.

Zhiqiang, Z., Qinghui, Y., Yongqiang, Z., Jian, Z., Xin, Z., Haiying, M., and Yuepeng, G. (2012). USP1 regulates AKT phosphorylation by modulating the stability of PHLPP1 in lung cancer cells. *J. Cancer Res. Clin. Oncol.* 138, 1231–1238.

Acknowledgements

“Gratitude is when memory is stored in the heart and not in the mind.” As per this adorable quote, my heart overflows with joy to acknowledge all the wonderful people who set their footprints and strengthened my hope during the pursual of this highly valued academic degree 'Doctor of Philosophy', which is absolutely a dream come true in my life.

First of all, I would love to express my deepest gratitude to one of the invincible woman in science, my dear **Kathrin Maedler**, who opened the door of opportunity to face the scientific research world and to get trained as a researcher in her laboratory. I thank her for inspiring me in multiple ways from the beginning of my PhD journey, her selfless efforts on refining many students (including myself) through her scientific intelligence and brilliance, and to 'go the extra mile' is highly admirable.

I am highly delighted to thank my dear mentor and excellent PhD advisor, **Amin Ardestani**, for trusting me to work on his igniting projects and for shaping me by inculcating his great ideas and scientific strategies in order to bear fruits and produce promising results. I also thank him for being patient with me all these years and for his constant motivation throughout this unpredictable research path, without him this thesis wouldn't be possible.

I feel more privileged to thank one of the great Harvard catalyst **Cristina Aguayo-Mazzucato**, for being the external expert in reviewing my thesis. And I am grateful for investing her valuable time for this review process. And I am equally thankful and grateful to dear **Olivia Masseck** for her acceptance to be a part in the assessment committee. I honestly express my hearty thanks to all the committee members including **Christian Arend, Nick Heise and Amal Mathew** for considering me in their priority list and for their precious time.

I feel very happy to thank dear **Ting**, one of the wonderful reference in the lab, who shared her project work and set the road for me to move forward and complete the LATS project. I am thankful to dear **Shruti** for her dedication and hardwork which added more insight and shaped the LATS paper. I express my hearty thanks to all the co-authors of neratinib paper and LATS paper for sharing their work with me and for all their great contribution and support.

I am very thankful to all the previous members of the lab **Payal, Zahra, Anke, Katharina, Michael, Niels, Janina, Lei, Delsi and Sahar**. And I am very thankful to **Wei** for all his scientific help and great advise whenever required and for all the wonderful memory he gave during his presence in the lab. I am also thankful to **Jenny**, who taught me to handle the animal experiments at the initial days of my PhD.

I take this wonderful opportunity to thank one of the most precious woman in my life, my beloved sister **Durga** (a sister from another mother), whose presence in the lab always comforted me and gave me more hope.

During the final phase of my PhD, I earned amazing friends who stood with me at the most difficult times. I feel highly encouraged to have the friendship of **Blaz**, with whom I was growing to enrich myself in the knowledge of science. I thank him for all his needful help at times of trouble. I thank **Katrischa** for all her excellent technical support and for solving all the problems at the needful times. I thank **Shirin** for her very big smile and for all her encouragement. I would like to thank **Murali** and **Huan** for making the environment very light and cheerful. I thank **Mona** and **Kshitija** for sharing the office with me and for all their beautiful hearts.

The best part of my PhD is supervising and working with many masters and bachelor students, my special thanks to all the lab rotation and master thesis students- **Anasua, Hazem, Arundathi, Bhavishya, Anna, Alexandra, Marina and Jae** for all their support.

I am humbled to thank all my God given friends and families in this beautiful country. I am forever grateful to my dear beloved spiritual parents **Prem uncle & Cordil aunty** for leading me in the righteous path and strengthening my Faith, beloved **Carlson & Josh** for their motivation, my beloved host parents **Angelika & Achim** for standing with me in all my ups and downs in Bremen. I thank my beloved **Joy mam, Chithra akka, Joseph uncle & his team, Tharani sis, Prasad anna and Miruthu** for their great support during the most painful phase of my PhD. I thank my treasurable family in India, my **loving mom & dad** and precious brothers **Goutham & Karnesh** for being my backbone and also for giving me more freedom to pursue my dream academic career abroad. Due to space constraints, I couldn't mention all the names in detail, however, I am really grateful to all the ODMC, Good news church and HIPM prayer conference family members for all their earnest prayers and friendly love. Above all, I thank my Omniscient God for his immense grace in providence, protection and promotion, glory belongs to him alone.